DESIGN AND DEVELOPMENT OF *BAMBUSA TULDA* REINFORCED BIO-COMPOSITES FOR STRUCTURAL APPLICATIONS

A Thesis Submitted in

Partial Fulfillment of the Requirements

for the Degree of

DOCTOR OF PHILOSOPHY

By

ABIR SAHA

(Roll No.196103002)

DEPARTMENT OF MECHANICAL ENGINEERING

INDIAN INSTITUTE OF TECHNOLOGY GUWAHATI

GUWAHATI (ASSAM)-781039

JULY 2024

TH-3447_196103002

© Indian Institute of Technology Guwahati (IITG), Guwahati, 2024

TH-3447_196103002

Dedicated to my
beloved father Mr. Prabir Kumar Saha,
and
mother Mrs. Malaya Saha.

TH-3447_196103002

Certificate

This is to certify that the thesis entitled "**Design and Development Of *Bambusa tulda* reinforced Bio-composites for Structural Applications**" being submitted by **Mr. Abir Saha** to the Indian Institute of Technology, Guwahati, for the award of the degree of Doctor of Philosophy in Mechanical Engineering is a record of original bonafide research work carried out by him under my supervision and guidance. The thesis work, in my opinion, has reached the requisite standard fulfilling the requirements for the degree of Doctor of Philosophy.

The results contained in this thesis have not been submitted in part or full to any other University or Institute for the award of any degree or diploma.

Dr. Poonam Kumari

Associate Professor

Department of Mechanical Engineering

Indian Institute of Technology Guwahati

Guwahati - 781039

TH-3447_196103002

Declaration

I, Abir Saha (Roll no: 196103002) declare that the present written submission is my thoughts in my own words. I have adequately cited and referenced the original sources, where other's ideas have been involved. I also declare that I have adhered to all principles of academic honesty and integrity and have neither fabricated nor falsified any idea/data/fact/source in my submission. I understand that any violation of the above will be cause for disciplinary action by the Institute and can also evoke penal action from the sources which have thus not been properly cited or from whom proper permission has not been taken when needed.

(Abir Saha)

Date: Roll No. 196103002

TH-3447_196103002

Brief Biodata of the Author

The author, Abir Saha, was born in the town Haripal situated in West Bengal State, India. He graduated with B.Tech with Honours in Mechanical Engineering from Guru Ghasidas Vishwavidyalaya (A Central University), Bilaspur, Chhattisgarh in the year 2017. Subsequently, in 2017, he secured admission for his M.Tech degree in Design and Manufacturing (Mechanical Engineering) at the National Institute of Technology Silchar (NITS), Assam, based on his performance in the GATE (Graduate Aptitude Test in Engineering) Mechanical Engineering paper. Again after qualifying the GATE in 2019, he joined the Ph.D. program at the Department of Mechanical Engineering, IIT Guwahati in July 2019. The research work is carried out during the period July 2019 to July 2024. The author's research focuses on composite materials, green composites, natural materials, natural fiber, smart materials and structures, sustainable design, and multi-criteria decision-making techniques. The author has also been selected for a prestigious paid research internship at Polytechnique Montréal, Université de Montréal, Canada durinh his PhD. This four-month program, running from January 2024 to May 2024, is highly competitive and selects only 25 candidates worldwide.

TH-3447_196103002

List of Publications from the Thesis

List of Publications in International Journals

1. Saha, A. and Kumari, P., 2022. Functional fibers from *Bambusa tulda* (Northeast Indian species) and their potential for reinforcing biocomposites. *Materials Today Communications*, 31, p.103800. **DOI:** 10.1016/j.mtcomm.2022.103800

2. Saha, A. and Kumari, P., 2023. Effect of alkaline treatment on physical, structural, mechanical and thermal properties of *Bambusa tulda* (Northeast Indian species) based sustainable green composites. *Polymer Composites*, 44(4), pp.2449-2473. **DOI:** 10.1002/pc.27256

3. Saha, A., Kulkarni, N.D., Kumar, M. and Kumari, P., 2023. The structural, dielectric, and dynamic properties of NaOH-treated *Bambusa tulda* reinforced biocomposites—an experimental investigation. *Biomass Conversion and Biorefinery*, pp.1-20. **DOI:** 10.1007/s13399-023-04709-5

4. Saha, A., Kulkarni, N.D., Kumari, P.,2003. Development of Bambusa tulda-reinforced different biopolymer matrix green composites and MCDM-based sustainable material selection for automobile applications. *Environment, Development and Sustainability.* **DOI:** 10.1007/s10668-023-04327-1

5. Saha, A., Kulkarni, N.D. and Kumari, P., 2024. Development of Bambusa tulda fiber-micro particle reinforced hybrid green composite: A sustainable solution for tomorrow's challenges in construction and building engineering.*Construction and Building Materials*, 441, p.137486. **DOI:** 10.1016/j.conbuildmat.2024.137486

TH-3447_196103002

International Conference

1. Saha. A., Kumari, P., 2022. Extraction, and Characterization of composite using functional fibers from *Bambusa tulda*. *North-East Research Conclave- 2022*, May 20-22, 2022 at IIT Guwahati, Guwahati,India.

2. Saha. A., Kumari, P., 2022. Sustinable development of bio composite using functional fiber from *Bambusa tulda*. *8th Asian Conference on Mechanics of Functional Materials and Structures (ACMFMS-2022)*, December 11-14, 2022 at IIT Guwahati, Guwahati,India.

3. Saha. A., Kumari, P., 2023. Development of Sustainable Light Weight Green Composites Derived from *Bambusa tulda* Fiber and Cashew-nut Shell-based Biopolymer. *11th International Conference on Materials for Advanced Technologies (ICMAT-2023)*, June 26-30, 2023 at SUNTEC, Singapore.

4. Saha. A., Kumari, P., 2023. Development of *Bambusa tulda* reinforced different bio-polymer matrix green composites *International Conference on Materials for Energy and Sustainable Development (MESD-2023)*, October 27-29,2023 at JNU, New Delhi, India.

TH-3447_196103002

Acknowledgements

First and foremost, I want to express my sincere gratitude toward my Ph.D. supervisor, Dr. Poonam Kumari, for providing me an opportunity to work under her supervision. I am grateful to her for her consistent guidance, motivation, patience, kindness and family support as well, over these years. She has always made available herself for discussions besides her busy schedules. Her enthusiasm, sublime work ethics, analytical abilities, and never-say-die attitude towards research and life as well, has natured my scientific skills and also inspired me immensely to work hard. I am proud to have her as my Ph.D. supervisor. Thank you, Ma'am, for all your help, advice, and support.

I want to thank my doctoral committee member, Prof. K. S. R. Krishna Murthy, Dr. Nelson Muthu , and Prof. Arbind K. Singh, for their encouragement, insightful comments, and suggestions which have helped me to refine and widen my research from various perspectives. My sincere gratitude also goes to the Head of Department of Mechanical Engineering, Prof. K. S. R. Krishna Murthy, for providing all the resources needed for my research. I also thankful to all faculty and staff members of the Mechanical Engineering department who help me whenever I needed. Without their help, it would not have been possible to conduct my research. It is an honor for me to thank the Indian Institute of Technology Guwahati for giving me such an excellent opportunity for undergoing my research.

I gratefully acknowledge the Science and Engineering Research Board, India for providing financial support through grant SB/WEA04/2019 to support this research work. I would like to thanks Science and Engineering Research Board, India for providing International Travel Scheme (ITS) to attend International Conference on Materials for Advanced Technologies (ICMAT)-2023 (Grant reference-ITS/2023/001375) during my Ph.D. I am also thankful to the Ministry of Education,

TH-3447_196103002

Government of India for providing me financial support during my Ph.D. at IIT Guwahati.

I want to thank my seniors, Dr. Susanta Behera, Dr. Agyapal Singh, Dr. Sharnish Kar, Dr. Sathish Kumar R., Dr. Mukesh Kumar and Dr. Viwek Kumar for their mentorship related to make things done and hand-holding whenever I got stuck during the research. I must mention Mr. Nikhil Dilip Kulkarni, my fellow researcher, whose continuous support and suggestions have enriched my knowledge in various fields and made my PhD journey smoother. I should also mention about Anshika Bagla, Vaibhav, Abhimanyu and Vaishnavi for their timely help, suggestions, and encouragements. It was fun to work with the PG students whose contributions showed new dimension to this research. I am indebted to my colleagues and friends Santosh Kumar, Vijay Meena, Rockey Kumar, Siddharth Senapati, Suraj and Sahil who made this journey along with me creating a memorable campus life.

My special gratitude goes to my family for their role in my life. I offer my regards to my loving parents, Mr. Prabir Kumar Saha and Mrs. Malaya Saha, whose love, teachings, sacrifices, and blessings brought me this far. I am thankful to my younger brother Mr. Subir Saha for instances taking my share of responsibilities. My parents and brother are the backbone of my happiness, and I dedicate my thesis to them.

Finally, I thank God for always being with me.

Abir Saha

TH-3447_196103002

Abstract

Traditional materials like metals, ceramics, and polymers cannot provide the unique combination of qualities needed to match advancements in modern technologies, leading to a focus on composites. Due to environmental concerns and the disadvantages of synthetic fibers, research is increasingly focused on natural fibers to develop sustainable, biodegradable composites that are suitable for automotive, aerospace, and construction because of their excellent strength-to-weight ratio. Using bamboo-based biocomposites as an example of eco-friendly and sustainable material development, the present study focused on designing and developing eco-friendly and sustainable biomaterials. This study investigates the physical, mechanical, structural, and thermal properties of *Bambusa tulda* fiber and its reinforced green composites. Initial investigations were conducted on fibers extracted from the inner, middle, and outer parts of bamboo culms, evaluating their physical, chemical, mechanical, and thermal properties. Physical and tensile properties of the fibers were analyzed using Weibull's statistical approach. The investigation revealed that technical fibers extracted from the outer part (external technical fibers) of the bamboo culm had higher cellulose content (58.13 ± 3.51%), higher crystallinity index (60.142%), greater tensile strength (365.014 ± 50.441 MPa), modulus (14.098 ± 1.763 GPa), lower moisture absorption capacity, and higher thermal stability than fibers from the middle and inner parts of the bamboo. The extracted external technical fibers were then chemically treated with different concentrations of sodium hydroxide (NaOH). Various characterization processes were used to examine the effects of chemical treatment. Single-fiber tensile testing, fiber pull-out testing, X-ray diffraction (XRD), Fourier transform infrared spectroscopy (FTIR), thermogravimetric analysis (TGA), and atomic force microscopy were performed to examine the impact of these treatments. The investigation found that fibers treated with 6% NaOH exhibited a tensile strength of 526.452 ± 17.509 MPa and a tensile modulus of 24.055 GPa,

TH-3447_196103002

both higher than those of untreated fibers. These treated fibers also had higher cellulose content and greater surface roughness, which improved interfacial interaction with the polymer matrix. Furthermore, green composite samples were fabricated with various fiber weight fractions (10%, 20%, 30%, and 40%). As compared to untreated fiber composites, 30% fiber-loaded composites exhibited maximum tensile strength, tensile modulus, and flexural strength of 94.56 ± 5.56 MPa, 5.11 ± 0.266 GPa, and 97.8 ± 5.11 MPa, respectively. The effect of chemical treatments on the mechanical properties of biocomposites was investigated using composites with a 30% fiber weight fraction and different NaOH treatments. Composites with 30% fiber weight fraction, 6% NaOH treatment showed better tensile strength (132.916 MPa), tensile modulus (6.983 GPa), flexural strength (154.8 MPa), modulus (8.243 GPa), and impact strength (44.06 kJ/m^2), with reduced moisture absorption compared to untreated fiber reinfored composites. Additionally, the effect of different polymer matrices on the thermo-mechanical and physical properties of the composites were analyzed. The best material among the developed composites was selected using a multi-criteria decision-making (MCDM) technique, VIKOR. Bamboo microparticles and bamboo fibers were hybridized to produce bamboo fiber-reinforced biocomposites to improve their properties, and their thermomechanical properties were analyzed. The developed hybrid composites showed a maximum tensile strength of 163.17 ± 6.44 MPa, a flexural strength of 144.26 ± 4.44 MPa, and an impact strength of 64.52±5.97 kJ/m^2. These values are higher than those for non-hybrid composites by 12.72%, 19.79%, and 12.07%, respectively. These findings highlight the potential of these developed composites for advanced structural engineering applications across various industries, including automotive, aerospace, packaging, electronics, sports, medical devices, and construction.

Keywords: Natural Fiber, Bamboo Fiber, Bio-composite, Green Composite, Sustainable Material, Mechanical Properties.

TH-3447_196103002

Contents

TH-3447_196103002

TH-3447_196103002

TH-3447_196103002

TH-3447_196103002

TH-3447_196103002

TH-3447_196103002

TH-3447_196103002

List of Figures

TH-3447_196103002

TH-3447_196103002

TH-3447_196103002

TH-3447_196103002

TH-3447_196103002

TH-3447_196103002

List of Tables

TH-3447_196103002

TH-3447_196103002

List of Abbreviations

AFM = Atomic force microscopy
ATR = Attenuated total reflectance
BF= Bamboo fiber
BFBC= Bamboo fiber bio-composite
BFHC= Bamboo fiber hybrid composite
BMP= Bamboo Micro Particle
CAGR= Compound annual growth rate
CNSL= Cashew nutshell liquid
DMA = Dynamic mechanical analysis
ETF= External technical fiber
FE-SEM= Field emission scanning electron microscopy
FRP= Fiber reinforced polymer
FTIR = Fourier transform infrared spectroscopy
ITF= Internal technical fiber
IFSS= Interfacial shear stress
MADM= Multi-attribute decision making
MTF= Middle technical fiber
NaOH= Sodium hydroxide
NFC= Natural fiber composites
NFRC= Natural fiber reinforced composites
PLA= Polylactic acid
PP= Polypropylene
TGA = Thermo-gravimetric analysis
Tg= Glass transition temperature
USD= United States Dollar
UTM = Universal testing machine
VIKOR= VIekriterijumsko KOmpromisno Rangiranje
XPS = X-ray photoelectron spectroscopy
XRD = X-ray diffraction

TH-3447_196103002

List of ASTM Standards Used for Different Testings

ASTM standard used	Dimension	Testing properties
ASTM-D-570-98	(20×20×3 mm^3)	Water absorption test
ASTM-D-638-3	(160×14×3 mm^3)	Tensile Test
ASTM-D-790-3	(130×14×3 mm^3)	3-point bending test
ASTM-D-785	(20×20×3 mm^3)	Hardness test
ASTM-D-792-13	(20×20×3 mm^3)	Density and void content of composites
ASTM D 2320-98	(20×20×3 mm^3)	Density measurement of bamboo fiber
ASTM-D 3175-04	(Powder sample)	Ash content in fiber
ASTM D-3822-07	Single fiber sample	Single fiber tensile testing
ASTM-D-6110	(64×12.7×3.2 mm^3)	Charpy Impact test
ASTM E871-82	(Powder sample)	Moister content
ASTM-E-1876-15	(60×20×3 mm^3)	Natural Frequency analysis
ASTM-G-160-12	(50×50×3 mm^3)	Biodegradability test

TH-3447_196103002

List of Machines Used for Different Testings

Atomic force microscopy-(Infinity Bio, Model: MFP-3D, Maker: OXFORD Instruments)
Dynamic mechanical analyser-(Anton Paar, Maker: Physica MCR, Model: 702)
FTIR spectrometer-(PerkinElmer, Model: Spectrum-2, Singapore)
Hot oven-(IKON, Model: IK-109, India)
Impact testing machine-(IT-30, Maker: FIE, India)
LCR meter-(HIOKI, Model: IM3536)
Muffle furnace-(YOMO, Model: MF – 5510 D, India)
Rockwell hardness tester-(maker: FIE, India)
Sigma field emission microscopy-(Make: Zeiss, Germany)
Sputter coater-(model: BALTEC-SCD-005, USA)
Stereomicroscope-(Model: SMZ25, Nikon, Japan)
Tensile testing machine-(Shimadzu, model: AGX-V, Japan)
Tensile testing machine-(Zwick Roell, Model: Z005TN)
Thermogravimetric analyser-(Perkin Elmer Instrument, model: STA 800, USA)
Weighing balance-(Sartorius, Model: Cubis®, Germany)
XPS machine-(ULVAC-PHI, INC; MODEL:04-900)
XRD machine-(BRUKER, model: D8 advance, United States)

TH-3447_196103002

Chapter 1

INTRODUCTION

1.1 PREFACE

Alternative environmentally friendly materials, like natural fiber composites, have gained popularity as a result of global concern over fossil fuel depletion, plastic waste, and the increasing carbon footprints of products. Petrochemicals derived from fossil fuels are used in the manufacture of most plastics [1]. In 2021, global plastic consumption was valued at USD 568.9 billion and is expected to grow annually by 3.2% for the next seven years [2]. Even though plastics are inexpensive and have desirable long-lasting properties, they accumulate as waste in landfills and oceans after they reach the end of their useful lives. Environment scientists predict that by 2050, there will be approximately 12,000 million tons of plastic waste in landfills worldwide. It is estimated that 400 million tons of plastic waste are generated annually, almost half of which comes from packaging. Approximately 150 million tons of the 400 million tons end up in oceans around the world [3]. There is a possibility that marine organisms can consume these microplastics, which may contaminate the food supply. It is evident from the discussion above that petroleum-based plastics and synthetic materials are harmful to the environment when used to develop polymeric materials or polymer composites [4]. It is therefore imperative to use sustainable materials that are renewable, biodegradable and eco-friendly. This has led to the development of environmentally compatible solutions, such as biocomposites [5]. Biocomposites have excellent properties like- recyclability, biodegradability, strength, lightweight and cost efficiency, making them an attractive research area. Generally, biocomposites are made of bio-based polymers and natural fibers, which are derived from renewable natural resources, and can be used to replace traditional non-renewable

TH-3447_196103002

plastics [6]. During the forecast period of 2017-2023, bio-based composites demand is expected to grow at a compound annual growth rate (CARG) of 11.2%. According to this data, the global biocomposites industry is expected to have a large market [7].

Natural fibers, such as banana, jute, coir, bamboo, hemp, pineapple leaf, flax, kenaf, ramie, and sisal, are extracted from different parts of plants—stems, seeds, leaves, or agricultural wastes [8]. These fibers serve as highly effective reinforcements in biobased thermoset or thermoplastic polymer matrices. Bamboo fiber, in particular, offers numerous advantages over other plant fibers, including higher mechanical strength, stiffness, rapid growth rate, and high absorption of atmospheric carbon dioxide. In comparison to other natural fibers, bamboo fiber has a lower density [9]. Bamboo, with its significantly faster growth rate compared to other wood types and natural fibers, can reach maturity within three years of being planted. This rapid growth enables the mass production of bamboo-based biocomposites with reduced impact on biodiversity. Such a characteristic allows bamboo-based biocomposites to exhibit superior specific properties. The bamboo family comprises more than 1000 species and 70 genera, all of which can naturally thrive in various climates, particularly in Asia and South America [10]. Each bamboo species possesses a distinct composition, leading to variations in thermo-mechanical properties [11]. Therefore, it is crucial to analyze different bamboo species separately. One notably abundant bamboo in the northeastern part of India, especially in the Assam region, is *Bambusa tulda*.

The primary focus of the present thesis is on the design and development of biocomposites using bamboo from North-East India (*Bambusa tulda*), specifically tailored for various structural applications with a concurrent emphasis on mitigating adverse effects on the ecosystem.The present thesis includes: (a) classified extraction of bamboo fiber from *Bambusa tulda* and investigation of their potential for reinforcing biocomposites, (b) alkalization of extracted bamboo fiber with different NaOH concentrations, (c) development of bamboo-based biocomposites with different weight fractions of fiber and with both treated and untreated fiber, (d) investigation of the effect of different epoxy matrices on the properties of bio and green composites, their suitable application for automobile interior application and (e) hybridization of bamboo-based biocomposites with bamboo micro particles and their futuristic structural engineering applications.

TH-3447_196103002

1.2 NATURAL FIBER

Natural fibers are formed through geological processes or extracted from the bodies of plants or animals. Example of some natural fiber is- pineapple leaf fiber, hemp, flax, sisal, jute, kenaf, bamboo etc [12]. These fibers find applications as components in composite materials, influencing the properties through the orientation of the fibers. Additionally, natural fibers can be consolidated into sheets to produce paper or felt. Emergent ecological attentiveness throughout the world has elicited a paradigm shift towards designing materials well-suited with the environment. These environmental apprehensions have forced governments and private organizations to invest millions of dollars in the research and development of the use of natural cellulosic fibres as a viable alternative to synthetic fiber based polymer composites and to produce environmentally gentle composite materials [13]. Properties such as light weight, cost, availability and environmental friendliness make these fibers perfect replacement to conventional or synthetic fibers. The main constituents of natural fibers are cellulose, hemicellulose, lignin, pectin and wax [14].

Cellulose: Cellulose is the basic framework constituent of all natural fibers. The natural polymer cellulose composed of carbon, hydrogen and oxygen which by degrading process produce glucose. All the glucose units in cellulose molecules linked by long chains. Cellulose's crystallinity controls the properties of fibers which is determined by hydrogen bonding in it. The properties like strength, stiffness and stability is provided by this component [15].

Hemicelluloses: These are polysaccharides which are relatively short and are bonded together in the form of chains. Cellulose micro fibrils are firmly associated with hemicelluloses and embedded the cellulose in a matrix. Hemicellulose generally contains glucose, glucuronic acid, mannose, xylose etc. and it causes absorption of moisture, thermal degradation and biodegradation of the fiber. The nature of hemicellulose is hydrophilic and their molecular weight is comparatively lower than that of cellulose [16].

Lignin: It is a hydrocarbon polymer and it adds rigidity to the fiber. Non-reversible elimination of water from sugar causes the formation of lignin. UV degradation in plants can be eliminated by controlling lignin content. Chemical adhesiveness within the fibers is not possible without the

TH-3447_196103002

presence of lignin [17].

Pectin: Presence of pectin adds flexibility to plants it contains heteropolysaccharides. Major quantity of pectin is present in bast fibers. Strength of a fiber mainly depends on pectin content within the fiber.

Wax: The plant waxes are combinations of long chains of aliphatic hydrocarbons. The ingredients it contains are ketones, fatty acids, aldehydes, primary and secondary alcohols [18].

Now a days natural fibers are used in numerous applications. **Fig. 1.1** represents the various application of the natural fiber [19].

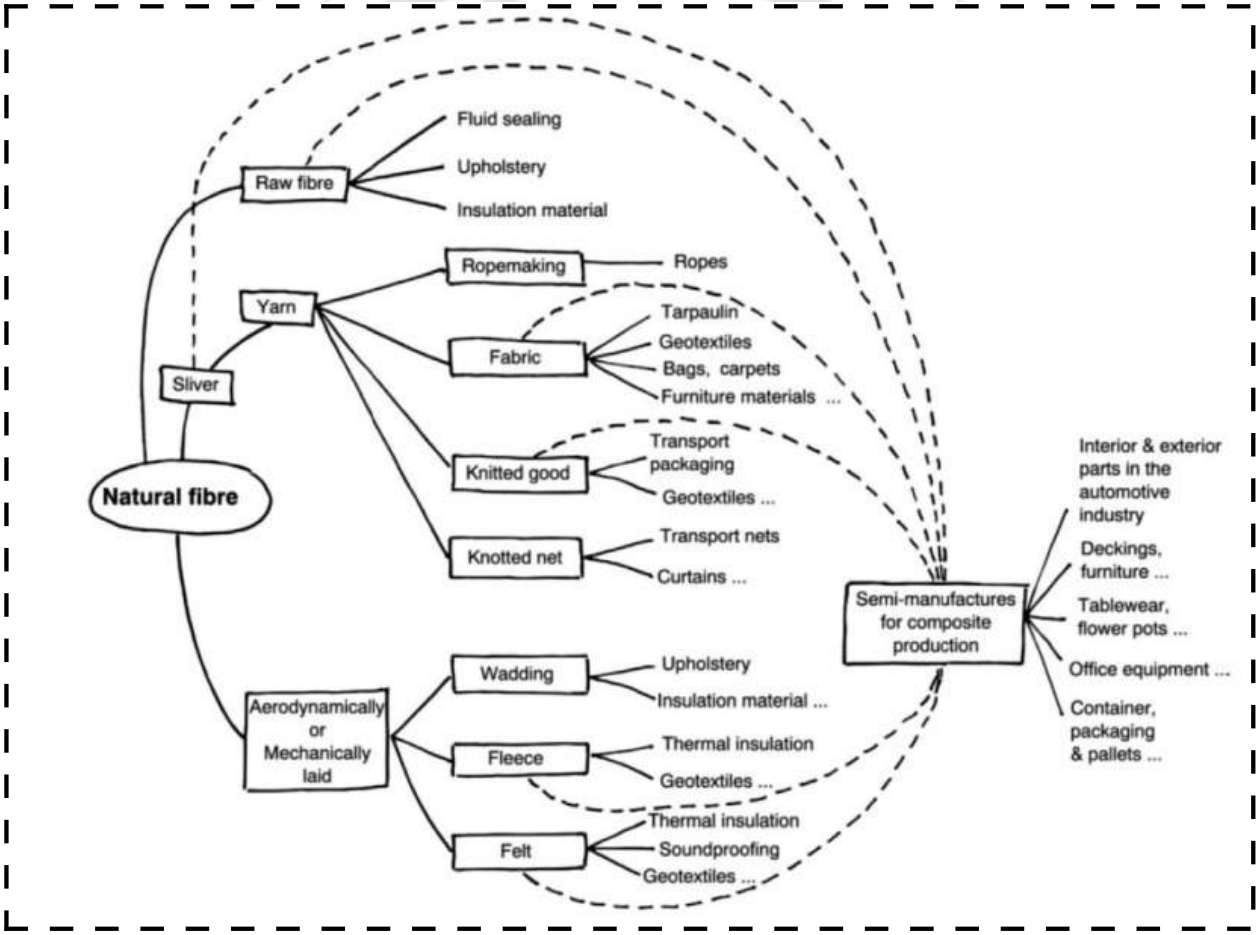

Fig. 1.1: Different applications of natural fibers [38].

1.3 FEATURE OF BAMBOO AND BAMBOO FIBER

Bamboo is a hollow culm belonging to the grass family. Being a perennial plant, it can grow up to 40 m in a torrential rain climatic condition. It has two different areas called nodes and internodes

TH-3447_196103002

along the length. The distance between nodes varies depends on the bamboo species [20]. Among natural fiber plants, bamboo has attracted considerable attention in recent years as a sustainable structural material for different applications (building construction, housing, flooring, alternative fillers, automotive, and furniture) [21] because it has low density, good mechanical properties, and low cost. In very recently it has been reported that curtains made from bamboo can absorb electromagnetic radiation (like- X-ray, infrared etc.) of various wavelengths. This thing helps to reduce the harmfulness of electromagnetic radiation to the human body [22].

The bamboo is growing in various countries of the world. More than 1450 species of bamboo coming from 70 different genera can be found in different climatic zones - from cold mountains to warm tropical regions. The bamboo growing region has been divided into different region accordingly: Asia-Pacific bamboo region, European and North American bamboo region and African bamboo region. Among these, the Asia-pacific is the largest bamboo growing region in terms of bamboo production and bamboo variation in the world. About 65% of the world bamboo production is produced by this region. In the other hand, American and African region only has 28% and 7% part of the total production [23]. In Asia, the large area of bamboo production has been occupied by six major counties. They are- India, China, Japan, Korea, Vietnam, Malaysia and others. The huge awareness of bamboo plantation in China has increased the global bamboo population by 30%. The below **Table 1.1** [24] show the different countries of the bamboo region.

Table 1.1: Bamboo region along with the counties [22].

Sl. No.	Bamboo regions	Countries
1.	Asia-Pacific region	India, China, Korea, Japan, Vietnam, Malaysia, Bangladesh, Sri Lanka, Thailand and Australia.
2.	American region	Columbia, Brazil, Mexico, Costa Rica and some European counties.
3.	African region	Mozambique and Eastern Sudan.

Bamboo fiber is a natural fiber extracted from bamboo plants. It is a sustainable and eco-friendly

TH-3447_196103002

material known for its versatility and various applications. The process of obtaining bamboo fiber involves harvesting bamboo, breaking it down into pulp, and then mechanically or chemically processing it to create the fibers. Here are some key characteristics and uses of bamboo fiber:

Sustainability: Bamboo is a rapidly renewable resource, making bamboo fiber an eco-friendly alternative to traditional fibers [25].

Biodegradability: Bamboo fibers are biodegradable, contributing to environmentally friendly end-of-life disposal.

High growth rate: The growth rate of bamboo is very high. Sime bamboo species can grow 90cm/day. Moreover, where wood takes about ten years to reach its maturity, bamboo matures in just 6-8 months [10].

Low carbon footprint: Due to small harvesting cycle and rapid growth rate of bamboo it has low carbon footprint.

Superior mechanical properties: Bamboo fiber, with its relatively higher cellulose content, exhibits superior thermo-mechanical properties compared to other natural fibers [26].

Softness: Bamboo fibers are soft and smooth, providing a comfortable and gentle feel against the skin.

Breathability: Bamboo has natural moisture-wicking and breathable properties, making bamboo fiber garments suitable for warm weather [27].

Antibacterial: Bamboo has natural antibacterial properties, reducing the growth of bacteria on the fiber [28].

The percentage compositions of bamboo fibers vary based on factors such as bamboo age, region, and environmental conditions. Consequently, the percentages of cellulose, lignin, hemicellulose, and ash in bamboo fibers differ. Notably, approximately 90% of bamboo's total weight consists of fibers, while the remaining 10% comprises tannins, pigments, ash, fat, protein, and pectin [29]. These components are situated in the cell cavity of specialized organelles and play crucial roles in bamboo's physiological activity.

TH-3447_196103002

1.4 BAMBOO ANATOMY

Bamboo is a prominent member of the grass family Poaceae. Its culm (or stem), as illustrated in **Fig. 1.2**, is cylindrical, hollow, and divided into nodes and internodes. At the nodes, a diaphragm (septa) forms, dividing the culm transversely. The primary mechanical function of the septa is to prevent Brazier buckling, which is initiated by ovalization of the cross-section during bending [30]. Unlike wood, bamboo does not exhibit secondary growth, which restricts geometric adaptation and increases the need for structural optimization at the material level [31]. For a physics-based prediction of the mechanical behavior of bamboo material, its characterization in terms of its multiscale hierarchical composition is a key prerequisite for micromechanics modeling. **Fig. 1.3**, adapted from a recent manuscript by Wegst et al. [32] , illustrates the typical hierarchical organization of bamboo culm material. Each hierarchical scale can be characterized by suitable microimaging technologies.

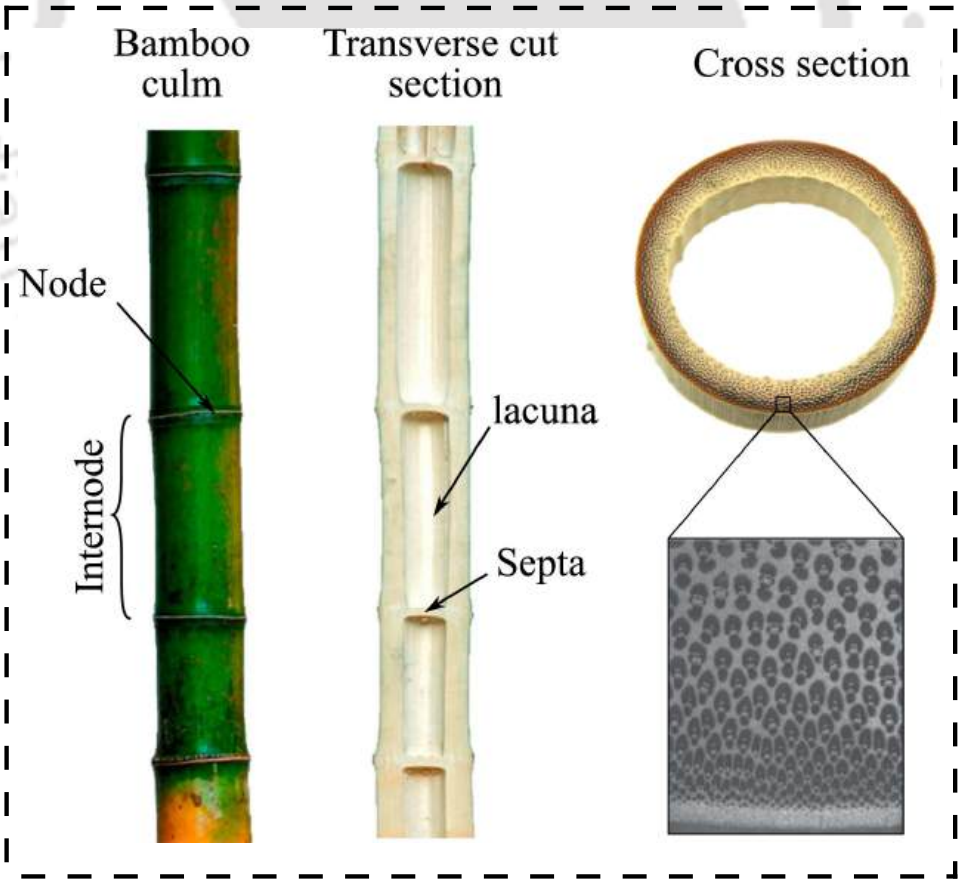

Fig. 1.2: Macroscale anatomy of a bamboo culm [28].

TH-3447_196103002

In the following, a brief description of the heterogeneous microstructures found at each hierarchical scale is provided, illustrated with corresponding imaging data taken from the literature. Additionally, the selection of the elastic and failure properties of the base materials—cellulose, hemicellulose, and lignin—stemming from mechanisms at the nano- and atomic scale is explained.

1.4.1 Macroscale: Cross Section

The macroscopic observation level corresponds to a length scale ranging from centimetres to several millimetres. At this scale, the bamboo cross-section is characterized by vascular bundle tissues, with their main axis aligned parallel to the longitudinal direction of the stem. These bundles are embedded in a matrix composed of parenchyma tissue. As illustrated in **Fig. 1.2**, the density of vascular bundles increases radially across the circular cross-section. This distribution of bundles can be quantified using scanning electron microscopy (SEM). **Fig. 1.4** (b) shows a representative micro image that illustrates the radial grading of vascular bundles, as provided by Mannan et al. [33].

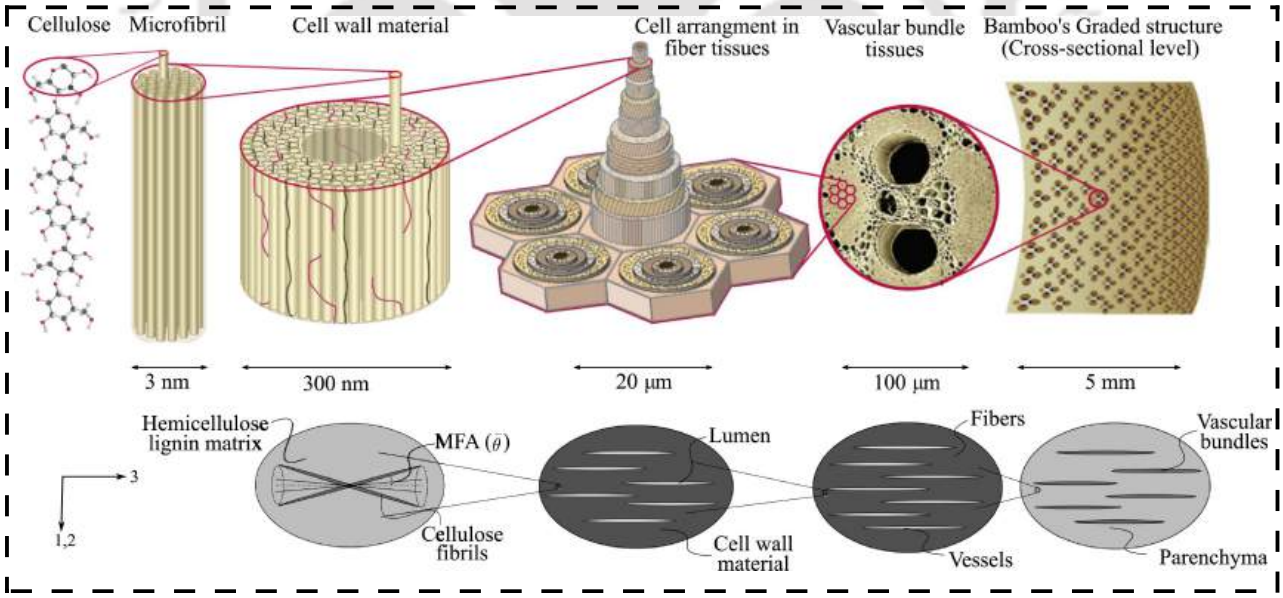

Fig. 1.3: Hierarchical structure of bamboo and its micromechanical representation [30].

1.4.2 Mesoscale: Functional Regions

A vascular bundle has a diameter of approximately 100 μm. It consists of xylem and phloem tissues surrounded by a sclerenchyma fiber sheath. Xylems and phloems are responsible for the

TH-3447_196103002

transportation of nutrients and water within the plant. Support is provided to the xylem and phloem vessels by sclerenchyma fibers. The volumetric contribution and morphology of fibers and vessels in vascular bundles can be determined from SEM images at a suitable scale. An example of a SEM image is shown in **Fig. 1.4** (b), provided by Dixon and Gibson [34]. The sclerenchyma cells in the fibers are long hollow tubes oriented in the stem direction, with a characteristic length scale on the order of 10–20 μm. These cells have thick cell walls surrounding lumens with polygonal or circular cross sections. The thickness of the cell walls in the sclerenchyma cells varies radially across the cross-section. These characteristics of the sclerenchyma fibers can be quantified using SEM images, such as those in **Fig. 1.5** (a) and (b) provided by Dixon and Gibson [34].

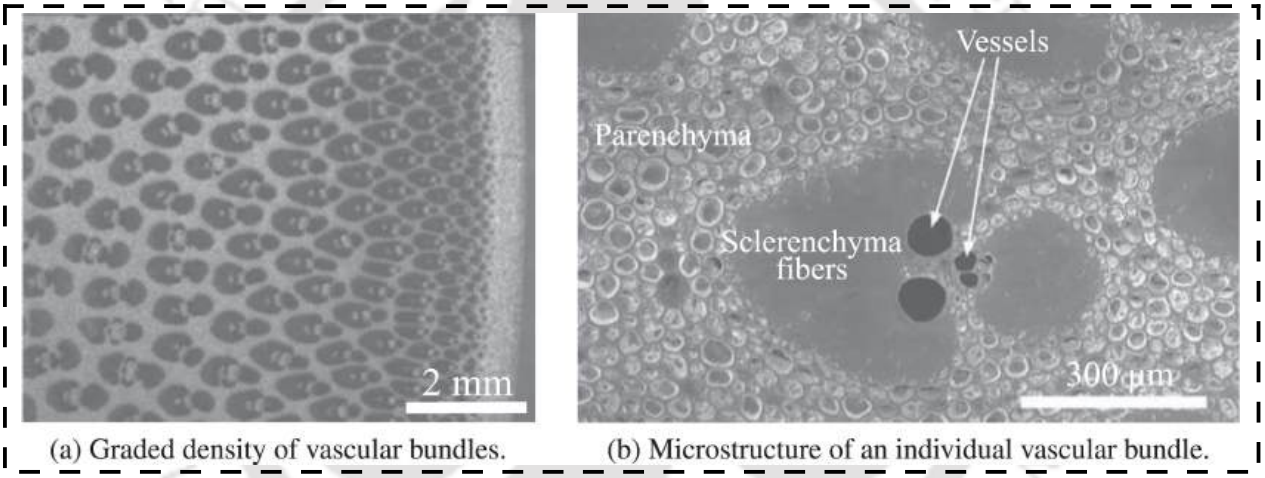

Fig. 1.4: SEM images depicting the radial gradation within the bamboo cross section and the typical structure of a vascular bundle [31].

The parenchyma cells form the base of the stem cross-section and exhibit polyhedral geometry. They consist of thin cell walls filled with living protoplasm that contains water and various molecules. The typical length scale of parenchyma cells is 5–10 μm [35]. **Fig. 1.6** (a) and (b) show SEM images of transverse and longitudinal cuts through parenchyma tissue taken by Mannan et al. [33]. The morphology and volume fractions of different phases in all mesoscale regions can be determined using these images.

1.4.3 Microscale: Cell Walls and Their Components

The cell wall material corresponds to an observation scale of 100–300 nm. Both the parenchyma and sclerenchyma cells are composed of cellulose fibers embedded in a non-cellulosic matrix of

TH-3447_196103002

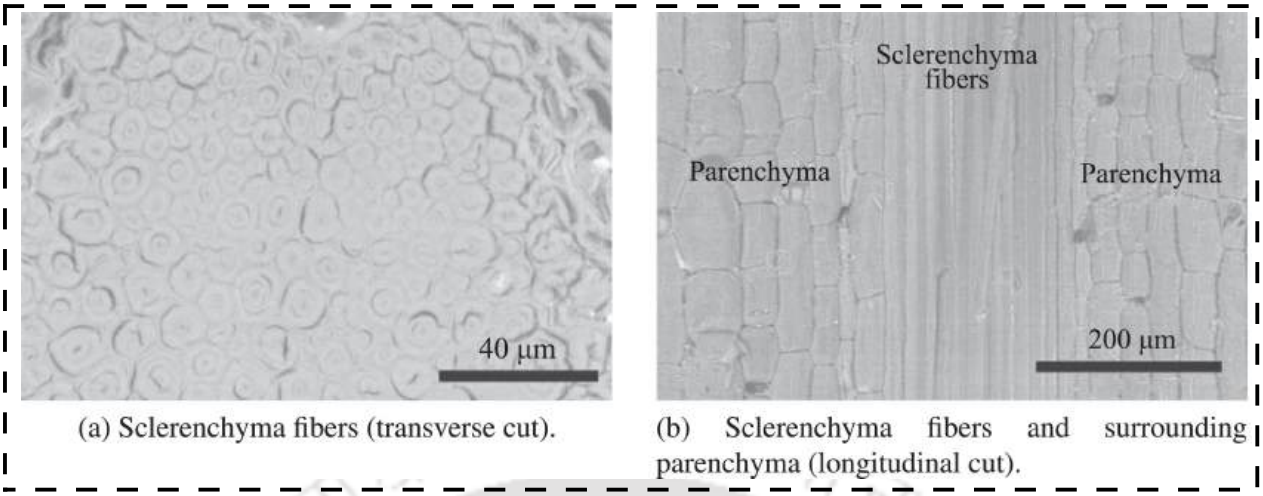

(a) Sclerenchyma fibers (transverse cut).

(b) Sclerenchyma fibers and surrounding parenchyma (longitudinal cut).

Fig. 1.5: SEM images showing thick cell and long sclerenchyma fibers surrounded by parenchyma matrix tissue [32].

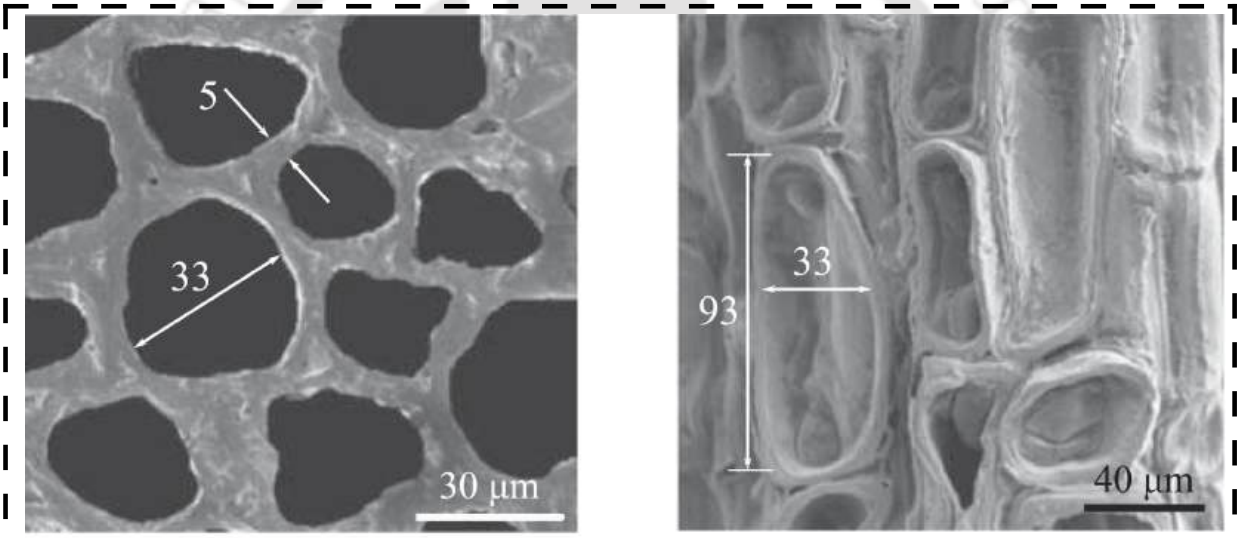

(a) Parenchyma cells (transverse cut).

(b) Parenchyma cells (longitudinal cut).

Fig. 1.6: SEM images showing the internal structure of parenchyma cells [33].

hemicellulose and lignin. In the cell wall material, cellulose fibrils are helically wound with an average microfibril angle (MFA) to the cell axis, denoted by $\overline{\theta}$. **Fig. 1.7** (a) presents micro-images of cell walls of parenchyma produced via ultraviolet (UV) microscopy by Suzuki and Itoh [36], where the color intensity reflects the lignin concentration in the cell wall region. **Fig. 1.7** (b) depicts transmission electron microscopy (TEM) images showing the multi-layered cell wall structure in a matured sclerenchyma fiber, from a paper by Gritsch and Murphy [37]. The cell wall structures in the different regions can be characterized using these images. The non-cellulosic host matrix for cellulose microfibrils is primarily composed of hemicellulose and lignin. The typical length scale of

TH-3447_196103002

the hemicellulose-lignin matrix is 8–20 nm. Lignin and hemicellulose also serve as hydrophilic sites within the cell wall material, and their properties depend on moisture content [38, 39].

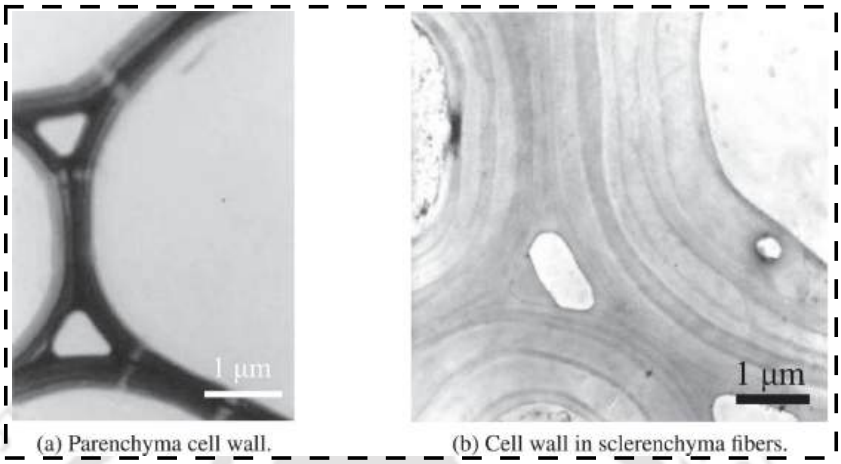

Fig. 1.7: Cell wall characterization: (a) Cell wall in parenchyma region observed with UV microscopy reported by Suzuki and Itoh [36]. (b) TEM image of layered cell wall in matured sclerenchyma fibers [37].

1.5 EXTRACTION OF BAMBOO FIBER

While bamboo fibers are sourced from bamboo trees, their extraction methods lead to two categorizations based on processes [40]: (a) Original bamboo fiber, directly obtained through mechanical and physical means without any chemical additives. This variant is often referred to as "Original," "Pure bamboo," or "Natural bamboo." (b) Bamboo pulp fiber, also known as bamboo viscose fiber or regenerated cellulose bamboo fiber, involves the extraction of bamboo fibers with the assistance of chemical additives.

The extraction of bamboo fibers involves two main processes—mechanical and chemical processing. Both processes start with bamboo strips splitting, and the choice between mechanical or chemical methods depends on the intended usage and the stress the bamboo fibers will endure. The chemical process entails alkali hydrolysis (NaOH) to yield cellulose fibers, followed by multi-phase bleaching through the passage of alkali-treated cellulose fibers with carbon disulfide. This chemical method is favored by many manufacturers due to its efficiency and shorter duration [41].

In contrast, the mechanical process involves treating initially crushed bamboo with enzymes, resulting in the formation of a spongy mass. The individual fibers are then obtained with the

TH-3447_196103002

assistance of a mechanical comb. Despite being less cost-effective compared to the chemical process, this method is more environmentally friendly [42]. The extraction of fibers can be conveniently categorized into rough or fine bamboo based on the preparation technique [43]. Rough bamboo fibers undergo preparation through cutting, boiling, and separation, followed by fermenting the bamboo with enzymes. On the other hand, fine bamboo involves boiling, fermenting with enzymes, washing, bleaching through acid treatment, and finally soaking in oil, followed by air-drying. The outlined procedures are depicted in **Fig. 1.8** [44]. An inherent advantage of the mechanical process for fiber extraction over the chemical process lies in the superior environmental characteristics of the extracted fiber .

Fig. 1.8: Extraction of rough and fine bamboo fiber [42].

1.5.1 Mechanical Extraction Technique

This approach encompasses various processes, including steam explosion, retting, crushing, grinding, and milling bamboo to extract fibers tailored for specific applications, particularly in composite reinforcements.

TH-3447_196103002

Steam explosion method: Steam explosion, a low-energy consumption process initiated in 1962, is employed to separate bamboo plant cell walls and produce pulp, primarily serving the pulp industry. Although effective in isolating lignin from the plant's surface, this method yields dark and rigid fibers [45]. Complete lignin removal is deemed impossible through steam explosion alone; however, machine mixing allows the extraction of bamboo fiber cotton (BFC) with lignin as a remnant [46].

Studies indicate that BFC-reinforced composites exhibit significantly higher tensile strength compared to those with bamboo fiber alone. In a specific procedure, bamboo is repeatedly cut, overheated, and treated to safeguard cell walls from fracture. Steam, released and repeated for ash removal, causes lignin remnants to condense on fiber surfaces, reducing adhesion between resin and fibers [47].

The steam explosion softens bamboo fibers by cracking cell walls, facilitating extraction. Crushing the softened cell wall reduces shear resistance and allows partial lignin decomposition [48]. Ultrasonic washing removes lignin, and subsequent isocyanate treatment eliminates unexpended cells. Tensile strength analysis reveals that steam-explosion-extracted fibers outperform isocyanate-treated ones due to weak interfaces between soft cells and fibers, impacting composite strength. Consequently, there's a need for alternative treatment techniques enhancing adhesion between bamboo fiber and the formed matrix [49].

Retting process: This method involves peeling the cylindrical section of the culm to obtain strips. Before peeling, bamboo bark is removed. The strips are then soaked in water for at least 3 days, compressed, and trimmed with a sharp-edged knife. The scraping process significantly influences fiber quality, minimizing fiber breakage along the length. Another approach involves cutting raw bamboo into longitudinal fragments without removing the bamboo epidermis and node, with no scraping or combing [50].

In this method, bamboo strips are rinsed with water, while culms undergo a 2-month water fermentation at room temperature before effective aerobic and anaerobic retting separates the bundles from the culm. Studies show that the extracted fiber bundle consists of a single fiber with variable length [51].

Crushing process: To extract bamboo fibers, the initial step involved using a roller crusher to cut raw bamboo into small pieces. Subsequently, these pieces were extracted into coarse fibers using a pin roller. The coarse fibers underwent boiling at 90 °C for 10 hours in a dehydrator to remove fat before being dried in a rotary dryer [52]. However, a drawback of this process is the production of short fibers that tend to become powdery with excessive mechanical processing [53].

Grinding process: Grinding involves cutting the bamboo culm without nodes into strips, followed by soaking them in water for 24 hours [54]. After wetting, the strips are manually cut into smaller pieces using a sharp knife. An extruder can be employed to obtain wide strips, while longer strips can be achieved by cutting bamboo into small chips, with the grinding process taking approximately 30 minutes [55].

Typically done with a high-speed blender, this ensures that bamboo fibers are of smaller sizes, later separable with sieves of various sizes and apertures. An alternative drying method involves using an oven for 72 hours at 105°C. Employing a high tensile load during grinding yields longer fibers and increases transverse length. This grinding procedure has been employed to extract fibers, enabling effective study of the morphological and rheological behavior of bamboo fiber composites . The same grinding system has also been utilized in producing dried bamboo strands and studying Nano clay [56].

Rolling mill process: This method entails cutting the bamboo culm into smaller pieces, typically 1 mm thick, by removing nodes. The strips are soaked in water for 1 hour, facilitating fiber separation under very low speed and pressure.

Subsequently, the rolled strips are soaked for an additional 30 minutes, and the fibers are sliced into small pieces using a sharp knife or razor blade. These fibers, ranging from 220 to 270 mm in size, are sun-dried for a maximum of 2 weeks [20]. An alternative approach involves compressing bamboo strips between two pairs of steel cylinders, allowing fiber extraction without soaking in water. Typically, the slicing process involves water soaking to soften lignin, and the fibers can be passed through a roller to reduce their bonding strength. Fibers extracted through this process usually range from 30 to 60 cm in length [57].

TH-3447_196103002

1.5.2 Chemical Extraction Technique

This process involves reducing or eliminating the lignin content of elementary fibers through alkali or acid retting, chemical retting, Chemical Assisted Natural (CAN), or degumming. This treatment also significantly affects other components of the bamboo microstructure, including hemicellulose, pectin, and hemicellulose. The chemical procedures employed in different studies are discussed in the following section.

Simultaneous extraction and degumming: Researchers have employed a combination of chemicals and enzymes for fiber extraction, followed by the addition of a degumming process to achieve finer and softer fibers. This involves removing gummy and pectin content from decorticated bamboo strips [58]. It's important to highlight that enzymes play a crucial role in degrading the gummy material within the middle lamella and cell wall, facilitating a highly effective separation of cellulose fibers.

Alkali or acid retting process: This processing method involves bamboo stripping and subsequent heating in a stainless-steel vessel with a 1.5 M NaOH solution at 70 °C for 5 hours. After heat treatment, the alkaline-treated bamboo strips are pressed using steel to separate the fibers [59]. Notably, this extraction process minimizes fiber damage. Another approach involves sizing bamboo into smaller chips, soaking them in 1 M NaOH for 2 hours at 70°C, stimulating cellulose and noncellulose parts to enhance bamboo fiber separation. This procedure, repeatable under controlled pressure, allows fiber extraction in pulp form. However, a drawback is the development of larger fiber bundles with continued extraction.

In a separate study, bamboo strips soaked in 1 M NaOH for 72 hours were subjected to fiber extraction with trifluoroacetic acid (TAA) solutions. Lignin obtained dissolved completely in both NaOH and TAA. The study concluded that lignin remained in the middle lamella when soaked in NaOH but could be substantially removed with TTA, highlighting that alkaline solutions offer superior interfacial bonding for fiber composites compared to methods like degumming or mechanical extraction [60].

Chemical retting process: The chemical-assisted natural retting process has been identified

TH-3447_196103002

as effective for water and lignin removal from bamboo fibers. In this method, bamboo culms are thinly sliced longitudinally and manually separated into fibers. They are then immersed in a 1-3% $Zn(NO_3)_2$ solution at a 1:20 liquor-to-bamboo ratio, maintaining a temperature of 40°C at neutral pH for 16 hours and subsequently boiling in water for 1 hour. The process, conducted in a Bio-Oxygen Demand incubator, ensures more efficient lignin removal compared to alkaline or acid retting, although resulting in high bamboo fiber moisture content.

In a different study [61], bamboo culms are sliced into 2-cm chips, roasted at 150°C for 30 minutes, soaked in water for 24 hours at 60°C, air-dried, and rolled on a flat surface to remove impurities. This procedure is repeated, and the fiber bundles are soaked and cooked in various solutions, including 0.5% NaOH, 2% $Na_5P_3O_{10}$, 2% Na_2SO_3, and 2% NaSi, before acid treatment with 0.5% diethylenetriamine pentacetic acid and 0.04% xylanase acid. After hot water washing, the bamboo fibers undergo further cooking, bleaching, refinement with 0.5% H_2SO_4 acid, and emulsification for 5 days. The study concludes that the resulting bamboo fiber has a small orientation angle, making it suitable for exterior macrofibrils and an excellent reinforcement compared to fibers from cotton, ramie, and flax [62].

1.5.3 Combined Mechanical and Chemical Extraction Process

This method combines mechanical extraction, employing compression molding methods (CMM) and roller molding methods (RMM), with chemical extraction through alkali and acid solutions [63]. In CMM, bamboo strips are pressurized in a bed of alkaline solutions using a load of 10 tons at both ends to extract fibers. Key factors for quality fibers include bed thickness and compression time. RMM involves flattening bamboo strips using two fixed rollers or one rotating end while the other is fixed. Chemical and mechanical processes facilitate quick separation into various sizes of bamboo fibers. Essential factors for RMM are compression mound size and roller diameter, determining the amount of extractable fiber.

In another study, fibers were extracted using only a roller. Nodes of the bamboo culm were removed, and internodes were sliced longitudinally to create strips. These strips were soaked in NaOH solutions (1%, 2%, and 3%) at 70°C for 10 hours. The mechanical properties of fibers

TH-3447_196103002

soaked in 1% NaOH were superior. Using a roller looser, alkali-treated strips were extracted, and the resulting small fibers were dried in an oven at 105 °C for 24 hours [64].

1.6 DIFFERENT SURFACE AND FIBER TREATMENT PROCESSES OF BAMBOO FIBER

The natural fibers have very had inter-facial interaction with polymer matrix. The surface and fiber treatment are the most suitable process to increase the inter-facial bonding between natural fiber and polymer matrix. This section is presenting a discussion about different surface modification techniques:

1.6.1 Salinization Treatment

In this method, the fibers are immersed in a 3:2 alcohol-water solution containing a silane-based adhesion promoter for 2 hours at a pH of approximately 4. Subsequently, they are rinsed in water and dried in an oven. Organosilanes, a primary category of coupling agents, play a crucial role in bonding polymers to mineral fibers. During salinization, the functional group in the coupling agent initiates a reaction with the polymer, either through copolymerization or the formation of an interpenetrating network (IPN) [65].

1.6.2 Acetylation Treatment

This method entails introducing an acetyl functional group into an organic compound. The primary purpose of acetylation is to cover the hydroxyl (OH) groups of fibers, responsible for their hydrophilic nature, with molecules possessing greater hydrophobic characteristics. In the acetylation process, fibers are immersed in glacial acetic acid for 1 hour, followed by immersion in a mixture of acetic anhydride and a few drops of concentrated sulfuric acid for a short duration. Subsequently, the fibers are filtered, washed, and dried in a ventilated oven [66].

1.6.3 Benzoylation Treatment

Benzoylation of fibers enhances fiber–matrix adhesion, increasing composite strength, reducing water absorption, and improving thermal stability. The process begins with alkaline pretreatment to activate the hydroxyl groups of cellulose and lignin in the fiber. Subsequently, the fiber is

TH-3447_196103002

suspended in a solution containing 10% NaOH and benzoyl chloride for 15 minutes. The treated fibers are then soaked in ethanol for 1 hour to remove benzoyl chloride, followed by washing with water and drying in an oven at 80°C for 24 hours [67].

1.6.4 Maleization Treatment

Maleated coupling agents are commonly employed to reinforce composites incorporating fillers and fiber reinforcements. The use of maleic anhydride is widespread in modifying both the fiber surface and the polypropylene (PP) matrix to achieve exceptional interfacial bonding and mechanical properties in composites. The reaction mechanism involves heating the copolymer to approximately 170°C before fiber treatment, followed by the esterification of cellulose fiber. This treatment increases the surface energy of cellulose fibers, bringing it closer to the surface energy of the matrix [66]. Consequently, this results in improved wettability and higher interfacial adhesion of the fiber.

1.6.5 Isocyanate Treatment

In this treatment process, fibers treated with sodium hydroxide are washed and dried. Subsequently, the fibers are immersed in carbon tetrachloride (CCl_4), a catalyst is introduced, and the mixture is thoroughly stirred. The reaction can persist for an extended period at a temperature slightly above room temperature, with continuous stirring. The fibers are then purified through refluxing and, ultimately, washed with distilled water before being oven-dried at 100°C [68]. The isocyanate group reacts with the hydroxyl group on the fiber surface, enhancing the interface adhesion with the polymer matrix [65].

1.6.6 Peroxide Treatment

In this surface treatment method, fibers are immersed in a solution of dicumyl (or benzoyl) peroxide in acetone for approximately thirty minutes, followed by draining and drying. Studies have demonstrated noteworthy enhancements in the mechanical characteristics of natural fibers, particularly in terms of strength and stiffness, leading to improved mechanical properties of the resulting composite [69].

TH-3447_196103002

1.6.7 Enzymatic Treatment

The utilization of enzyme-based techniques in fiber treatment is gaining prominence and becoming increasingly important. Currently, the use of enzymes for modifying natural fibers is experiencing rapid growth. One significant factor contributing to the adoption of this technology is the cost-effectiveness and environmentally friendly nature of enzymes. The reactions catalyzed by enzymes are highly specific, leading to focused and precise performance. Enzymatic treatments are typically conducted through experiments lasting 90 minutes under constant agitation (80 rpm) at the optimum temperature in a standard water bath. The enzymes are then deactivated by heating at 90 °C for 10 minutes. To eliminate traces of enzymes and buffer reagents, the fibers are washed with warm water, and the samples are subsequently dried at 80°C for 5 hours and stored in polyethylene bags [70].

1.6.8 Corona, cold plasma Treatment

Both corona discharge and cold plasma treatments are physical processes employed for surface oxidation activation. This method alters the surface energy of cellulose fibers [71]. Different plasma gases can be utilized to achieve various surface modifications. Surface cross-linking can be introduced, the surface energy may be increased or decreased, and reactive free radicals and groups can be generated.

1.7 NATURAL FIBER REINFORCED POLYMER COMPOSITES (NFRCs)

Natural fiber composites are materials formed by combining natural fibers with a matrix material, often a polymer, to create a composite material with enhanced properties. These composites leverage the unique characteristics of natural fibers, such as jute, hemp, flax, sisal, bamboo, and others, to reinforce and improve the performance of the composite. The matrix material, typically a polymer like polypropylene or epoxy, binds the fibers together, providing structural integrity. Polymer matrix may also derive from natural resources like vegetables oil, fruits shell, starch, cellulose, and proteins etc. to develop green composite for various sustainable applications. It provided great strength and stiffness, along with anisotropic in nature, resistance to corrosion, wear resistance and

TH-3447_196103002

fatigue resistance [72]. NFRPCs having greater advantageous over other conventional and synthetic composites materials like high strength to weight ratio, required stiffness to weight ratio, lower cost, lighter weight, lower density per unit volume, noncorrosive, high fracture toughness, high fatigue strength, nontoxicity, nonmagnetic properties, outstanding chemical and moisture resistance, better thermal and impact resistance, eco-friendly with nature, biodegradable and biocompatibility [73].

Previous studies have emphasized that the performance of Natural Fiber Reinforced Polymer Composites (NFRPCs) relies on factors such as chemical composition, physical and mechanical properties, cell dimensions, fiber structure, and the interaction between fiber and matrix. Improving the mechanical properties of NFRPCs is contingent on factors like fiber orientation, fiber strength, physical characteristics of the fiber, and interfacial adhesion properties. Strengthening the base structures, i.e., the natural fibers, enhances the stiffness of the polymer matrix, leading to overall improvement [16].

NFRPCs face challenges such as moisture, which can disrupt the composite structure and hinder bonding and mechanical properties. Additionally, the distinct chemical structures of reinforcement and matrix materials can result in weaker interfacial bonding and ineffective stress transfer during NFRPC interfaces [74]. To address these challenges, chemical modification and hybridization of natural fibers emerge as crucial and effective methods to enhance mechanical performance and foster stronger interfacial interactions between fibers and polymer matrices.

1.7.1 Different Fabrication Process of NFRCs

Biocomposites, or natural fiber composites, are materials made by combining natural fibers with a matrix material, often a polymer, to create a composite with improved properties. The manufacturing processes for biocomposites can vary, and several methods are commonly employed. The some of common fabrication method is presented below [75, 76, 77]:

1. **Compression Molding**

   • **Process:** Natural fibers and the matrix material are mixed and then compressed in a mold under heat and pressure.

TH-3447_196103002

- **Application:** Suitable for producing biocomposite products with relatively simple shapes.

2. **Injection Molding:**

   - **Process:** Molten polymer is injected into a mold containing natural fibers. The mixture solidifies, forming the final product.

   - **Application:** Used for manufacturing complex shapes and detailed components.

3. **Extrusion**

   - **Process:** Molten polymer and natural fibers are forced through a die to create a continuous profile. The profile can be cut into specific lengths.

   - **Application:** Continuous profiles for various applications, such as decking or structural components.

4. **Resin Transfer Molding (RTM)**

   - **Process:** Liquid resin is injected into a closed mold containing natural fibers. The resin impregnates the fibers, and the composite cures.

   - **Application:** Suitable for producing large, complex parts with high fiber content.

5. **Hand Lay-Up**

   - **Process:** Natural fibers and resin are manually laid up layer by layer in a mold.

   - **Application:** Commonly used for prototyping and small-scale production of simple shapes.

6. **Pultrusion**

   - **Process:** Continuous fibers are pulled through a resin bath and then through a heated die where curing takes place. The cured profile is then cut to the desired length.

   - **Application:** Continuous profiles with high fiber volume fraction for structural applications.

7. **Sheet Molding Compound (SMC)**

TH-3447_196103002

- **Process:** Natural fibers are pre-impregnated with resin and then compressed between two heated mold halves.
- **Application:** Suitable for large, flat components with relatively high production volumes.

8. **Hand Lay-Up (Spray-Up)**
   - **Process:** Natural fibers and resin are sprayed onto a mold surface.
   - **Application:** Used for large, low-cost components such as boat hulls and automotive parts.

The choice of manufacturing process depends on factors such as the desired properties of the final product, the complexity of the shape, production volume, and cost considerations.

1.7.2 Application of NFRCs

Natural fiber composites find applications across various industries due to their unique properties and environmentally friendly characteristics. Some common applications are presented below [14, 78, 79, 80]:

1. **Automotive Industry:**
   - *Interior Components:* Natural fiber composites can be used in the production of interior components such as door panels, dashboards, and seat backs. They provide a lightweight alternative to traditional materials, contributing to fuel efficiency.
   - *Exterior Components:* Some automotive manufacturers use natural fiber composites for non-structural exterior components like body panels. These composites can be an eco-friendly alternative to traditional materials.

2. **Construction and Building Materials:**
   - *Structural Components:* Natural fiber composites can be incorporated into structural elements like beams and columns in construction. They offer good strength-to-weight ratio and can be used in various building applications.
   - *Insulation Materials:* NFCs are used in the production of insulation materials for buildings. These composites can provide effective thermal and acoustic insulation.

TH-3447_196103002

3. **Aerospace Industry:**

   - *Interior Components:* Similar to the automotive industry, natural fiber composites can be used in the aerospace sector for interior components, helping to reduce overall weight and improve fuel efficiency.

4. **Packaging Industry:**

   - *Biodegradable Packaging:* Natural fiber composites can be utilized in the production of biodegradable packaging materials, offering a sustainable alternative to traditional plastics.

5. **Consumer Goods:**

   - *Furniture:* NFCs can be used in the manufacturing of furniture, providing a lightweight and environmentally friendly alternative to traditional materials.
   - *Sporting Goods:* Natural fiber composites are employed in the production of sports equipment such as bicycle frames, tennis rackets, and snowboards due to their lightweight and high strength properties.

6. **Electronics Industry:**

   - *Casing and Housings:* Natural fiber composites can be used in the production of casings and housings for electronic devices. They offer a balance between strength, weight, and environmental impact.

7. **Marine Industry:**

   - *Boat Components:* NFCs can be used in the construction of boat components such as hulls and decks. They offer good resistance to moisture and can be a lightweight alternative to traditional marine materials.

8. **Renewable Energy:**

TH-3447_196103002

- *Wind Turbine Blades:* Natural fiber composites can be employed in the manufacturing of wind turbine blades. Their lightweight nature can contribute to increased energy efficiency.

9. **Medical Devices:**

   - *Prosthetics and Orthopedic Devices:* NFCs can be used in the production of prosthetics and orthopedic devices, providing a lightweight and potentially more comfortable alternative.

10. **Infrastructure:**

    - *Bridge Components:* Natural fiber composites can be used in the construction of bridge components, offering a lightweight and durable alternative to traditional materials.

As industries seek sustainable and eco-friendly alternatives to traditional materials, the use of natural fiber composites continues to grow, with ongoing research and development expanding their range of applications.

1.8 GENERAL OBJECTIVE OF THE PRESENT WORK

The objective of this research is to develop and characterize bamboo fiber-reinforced bio-composites, aiming to advance sustainable engineering applications. The study focuses on extracting fibers from different parts of the *Bambusa tulda* culm, evaluating the effects of alkali treatment, and exploring the properties of bio-composites reinforced with bamboo fibers and hybrid bamboo materials. By enhancing the mechanical, thermal, and physical characteristics of these bio-composites, the research targets potential applications in the automotive industry, contributing to global sustainability efforts by providing eco-friendly and renewable material alternatives. Ultimately, this research aspires to significantly impact the field of sustainable materials by thoroughly understanding bamboo fiber-reinforced bio-composites. By addressing key challenges in material extraction, treatment, and characterization, the study aims to develop lightweight, durable, and eco-friendly

TH-3447_196103002

materials that align with global sustainability goals, reduce carbon emissions, and developing bio-economic opportunities in the burgeoning bio-composites industry.

1.9 ORGANISATION OF THE THESIS

The complete work presented in the thesis has been organized into eight chapters. An overview of the contents of all eight chapters are presented below:

Chapter 1 is devoted to a concise introduction of natural fibers, specifically bamboo fiber, discussing their global distribution, inherent features, and its anatomy. The chapter further describes the extraction process, chemical treatment process, and development process of natural fiber-reinforced polymer composites. Additionally, it touches upon the application of natural fiber-reinforced composites.

Chapter 2 contains an introductory part with composite materials, encompassing the history, classification, and characteristics of composite materials. It delves into bio and green composites. The chapter also content extensive literature review and outlines the proposed objectives of the current work. The review covers various aspects, including different types of bamboo fiber, classified extraction methods, chemical treatment processes, the development of bamboo-based bio-composites, the influence of diverse matrix materials on bio-composites, and bamboo fiber-reinforced hybrid bio-composites. Additionally, the chapter addresses research gaps identified in the literature, as well as the motivation and objectives of the present research work.

Chapter 3 focuses on the systematic extraction of Bambusa tulda fiber from bamboo culm, exploring its physio-chemical, thermal, and mechanical properties. The physical characterization involves examining the structural morphology through SEM, measuring density, and conducting chemical analysis to determine the fiber's composition. Structural characterization includes XRD and FTIR analysis, while mechanical properties are assessed through single fiber tensile testing. Thermal behavior is investigated using thermogravimetric analysis. Additionally, the extracted fiber's potential as a reinforcement material in bio-composites is evaluated through a comparative study with other natural fibers extracted from literature.

In **Chapter 4**, the influence of chemical treatment using various NaOH concentrations on the

TH-3447_196103002

physical, chemical, and mechanical attributes of bamboo fiber is explored. The comparison between treated and untreated fibers involves assessing density, identifying functional groups within the fiber, conducting XRD analysis, XPS analysis, single fiber tensile testing, measuring surface roughness, evaluating interfacial shear strength, and examining thermal stability.

In **Chapter 5**, bio-composites are developed with different weight fraction and differently treated and untreated fiber. Apart from that, the different physical, structural, mechanical, thermal, and dielectric characterization of developed bio-composites are also presented in this chapter.

Chapter 6, presents effect of different matrix materials on *bamusa tulda* reinforced bio-composites. The effect has been analysis in terms of physical, thermal and mechanical properties. Additionally, this chapter presents a VIKOR-based MADM method for selecting and optimizing bio-composites for automobile interiors applications.

Chapter 7, investigates the effect of bamboo micro particles on different thermo-mechanical and physical properties of bamboo fiber reinforced bio-composites.Furthermore a comparative study with different hybird composite has been presented. Moreover, this chapter includes a comparative analysis of various hybrid composites drawn from the literature.

Finally, the major conclusions of the present work, contribution of the present thesis and suggestions for future research are summarized in **Chapter 8**.

1.10 SUMMERY

This chapter provides information about the introduction of composite materials, their history, applicability, and sustainability. A brief overview of natural fibers and bamboo fiber is also presented. The different fiber extraction processes, surface modification processes of fibers, different development processes of natural fiber-reinforced biocomposites, their suitable applications are discussed. The organization of the thesis is also found in this chapter. The next chapter describes about classification and history of composite materials. An extensive literature review on different species of bamboo fiber, their extraction, chemical treatment, development processes of biocomposites, and different characterization techniques is also found in next chapter. Furthermore, the literature gaps, and objective of the present work are also presented in the **Chapter 2**.

TH-3447_196103002

Chapter 2

LITERATURE REVIEW

2.1 INTRODUCTION

The Chapter **1** provides a concise overview of natural fibers, particularly bamboo fiber, covering their global distribution, inherent features, extraction methods, chemical treatment processes, and the developmental process of natural fiber-reinforced polymer composites. This chapter presenting the classification and history of composite materials and literature review for the present study. For a systematic study, review has been divided into six sections which provide information related to the issues and concerns to be considered in the thesis. **Fig. 2.1** represents the different section of the literature review.

In this chapter, a classification and history of composite materials are provided in **Section 2.2**.A brief discussion about green and bio composites are described in **Section 2.3**. An extensive literature review is provided in **Section 2.4**. The extraction process, specifically the classified extraction, is thoroughly discussed along with the related literature in **Section 2.5**. A comprehensive examination of past literature pertaining to the chemical treatment of bamboo fiber is presented in **Section 2.6**. **Section 2.7** offers a succinct overview of the literature concerning the development and characterization of bamboo-based bio-composites. The analysis of the literature on the impact of different matrix materials on the properties of bio-composites is presented in **Section 2.8**. Furthermore, **Section 2.9** encompasses the literature on hybrid bamboo fiber composites.The literature's identified research gaps are outlined in **Section 2.10**. The motivation behind the current work is detailed in **Section 2.11**.**Section 2.12** is providing research question. **Section 2.13** outlines the objectives of the present thesis. **Section 2.14** presents the novelity of the present work

TH-3447_196103002

and the chapter concludes with a conclusion section discussed in **Section 2.15**.

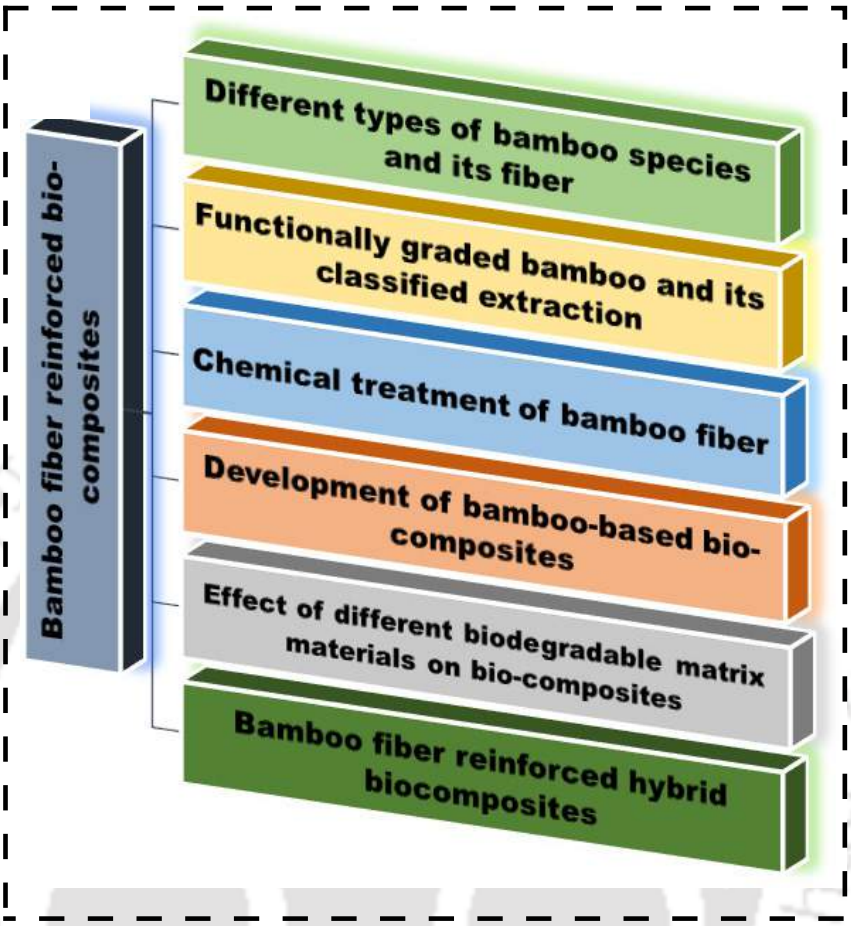

Fig. 2.1: Classification of literature review

2.2 COMPOSITE MATERIAL

A composite material is a structural material which consists of two or more constituent phases which are not soluble in each other and combined at the macroscopic level. Generally, there are two phases in a composite material, one is the matrix phase and another is the reinforcing phase [81]. Two different phases have different purposes. The purpose of the reinforcement phase is to carry the load which is applied to the composite structure and matrix material works as binding material. It helps to distribute the load uniformly throughout the reinforcing material, not only that it protects the fiber from an outside environmental effect like a chemical reaction, moister, etc [82]. Generally, two types of reinforcement materials are there one is fiber (it may be long fiber or it may be short fiber) and another one is particulate. Fibers are again two types one is synthetic

TH-3447_196103002

fiber(man-made) like- carbon fiber, glass fiber, etc. and another is a natural fiber like jute fiber, bamboo fiber, hemp fiber, pineapple leaf fiber etc current research leads to the development of natural fiber-natural particulate reinforced composite [83].

2.2.1 History of Composite Material

Development of composite material from ancient times to present is explained below:

Ancient Times: Composite materials, inherent in nature's design, manifest in living organisms such as seaweeds, bamboo, wood, and even human bones. The historical use of reinforced polymeric materials dates back to around 4000-2000 B.C. in Babylonia, where the populace employed materials comprising reinforced bitumen or pitch. In the regions of Egypt and Mesopotamia around 3000 B.C., historical evidence suggests the construction of river boats from bundles of papyrus reed embedded in a bitumen matrix. A remarkable early instance of filament winding processes emerged in Egypt around 2500 B.C. during the era of mummification. In this practice, meticulously treated deceased bodies were enveloped in linen tapes, subsequently impregnated with a natural resin, resulting in the creation of a rigid cocoon. The utilization of lac, known to India and China for millennia, finds mention in the Vedas written around 1000 B.C. In India, lac resin was employed as a filler for sword hafts and in the production of whetstones by combining shellac with fine sand—an early precursor to the contemporary composite grinding wheel. By 500 B.C., the Greeks had advanced composite technology in shipbuilding, constructing triremes with three banks of oars. These vessels featured keels of exceptional length, surpassing what could be achieved with a single length of timber. Thus, the roots of composite technology trace back to ancient times, illustrating its enduring presence in human history [84].

1200's: The inception of the first composite bows occurred approximately in 1200 AD. The Mongols innovatively crafted these bows by combining wood, bamboo, horns, and cattle tendons, complemented by the use of pine resin in the bow-making process. Renowned for their formidable capabilities, these bows remained among the most dreaded weapons until the 14th century.

1800's: The roots of modern polymer science can be traced back to Henri Braconnot's pioneering work in the 1830s. Collaborating with Christian Schönbein and others, Henri explored derivatives

TH-3447_196103002

of the natural polymer cellulose, leading to the development of novel semi-synthetic materials such as celluloid and cellulose acetate. The term "polymer" was officially coined in 1833 by Jöns Jakob Berzelius, although his contributions to polymer science in the contemporary sense were limited. In the 1840s, Friedrich Ludersdorf and Nathaniel Hayward independently discovered that the addition of sulfur to raw natural rubber (polyisoprene) prevented the material from becoming sticky. Charles Goodyear obtained a U.S. patent in 1844 for vulcanizing natural rubber with sulfur and heat, a process that had been patented by Thomas Hancock in the UK the previous year. Vulcanization strengthened natural rubber, preventing it from melting with heat while retaining flexibility. This breakthrough enabled the practical production of waterproofed articles and paved the way for the widespread manufacturing of rubberized materials. Vulcanized rubber stands out as the earliest commercially successful outcome of polymer research. In 1884, Hilaire de Chardonnet established the first artificial fiber plant, producing regenerated cellulose or viscose rayon as a silk substitute. However, this material was highly flammable [85].

1900's: The year 1907 witnessed a groundbreaking moment with Leo Baekeland's invention of the first synthetic plastic—a thermosetting phenol–formaldehyde resin known as Bakelite. This marked a significant leap in the realm of polymer innovation. The properties such as non-conductivity and heat-resistant made Bakelite as the most widely used composite in industrial and consumer good applications. Materials like vinyl, polystyrene, phenolic came into the existence in this period, reinforcement was needed to provide strength and stiffness.

1930's: The most important phase in the composite history which saw the rise of new form of resins which have been using till date came into the existence. Owens Corning started the usage of glass fiber and introduced fiber reinforced polymer industry. Development of unsaturated polyesters and some important epoxies become available.

1940's: The production of fiber reinforced polymers took place during World War 2, scientists learned many things about fiber glass during this period. For the first time hull type boats were developed during this time. The year 1947 saw the development of composite body automobile and led to the development of 1953 Corvette. Fiber glass was used to build this type of car. Different types of methods like sheet molding compound and bulk molding compound turned out to be

TH-3447_196103002

emergent form of moldings for many industries.

1960's: Introduction and development of carbon fibers which were used to improve the strength to weight ratio of thermosets which led to the usage in different kinds of fields like aerospace, consumer goods, and automotive started.

1990's and 2000's: By 1995, composite materials became the most useful materials in manufacturing and construction fields. Replacement for the conventional materials took place in this period. Every manufacturer saw the rise of composite in many fields and later it became a part of daily human needs. Development of high strength composite and continued development of finish technology like PVD expanded the applications in automotive industries [86].

Present: There has been huge research going on from the government, industries and manufacturers in the field of composites. Aerospace and Marine industries are looking for innovative methods to produce highly effective composite materials. Natural fibers came into existence which has got excellent strength to weight ration and highly cost effective which can replace synthetic fibres completely. The development of Hybrid composite materials that is the combination of two or more fillers in a single matrix which has got better properties than conventional composite materials [87, 88]. The content from Ashby's article has been partially replicated in **Fig. 2.2**.

It is estimated that the global composites market will reach US$ 130.8 billion by 2024 at a CAGR (Compound Annual Growth Rate) of 7.8%, while the Indian composites market is projected to reach US$ 2.0 billion by end of 2021 with a forecasted CAGR of 14.1% [89]. As of 2019-2020, India consumes about 0.3 kilograms of composites per capita compared with 2.5 kilograms in China and 11 kilograms in the US. The data indicates that the composite industry in India has a large market potential [90].

2.2.2 Classification of Composite Material

Depending upon the type of reinforcement and matrix material, composite materials are classified into different categories.

1. According to the type of matrix material, composite material can be classified as:

    - Metal Matrix Composites

TH-3447_196103002

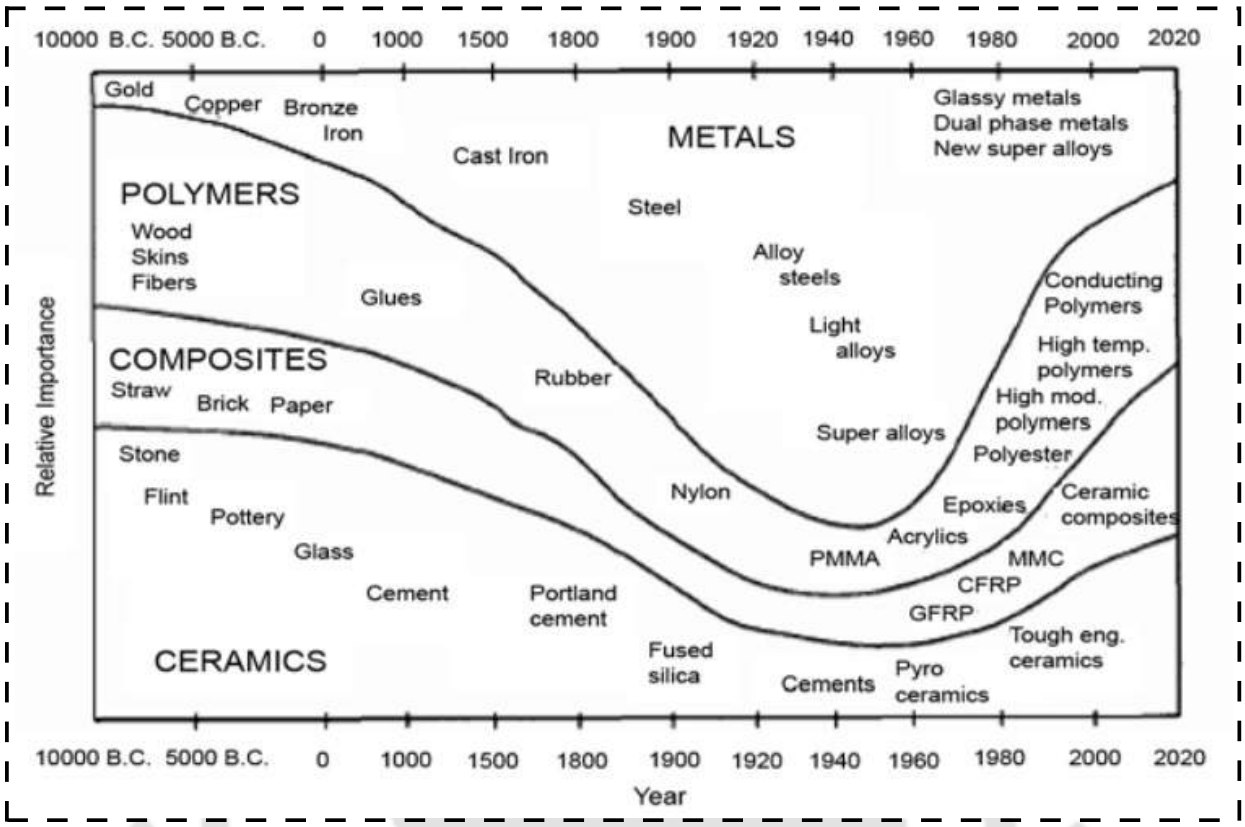

Fig. 2.2: Relative importance of material development through history [86].

- Ceramic Matrix Composites
- Polymer Matrix Composites

2. According to the type of reinforcing the material, composite material can be classified as:
   - Fiber Reinforced Composites
   - Particulate Reinforced Composites
3. Hybrid composite

Metal Matrix Composites: Metal matrix composites typically utilize a ductile metal as the matrix material, proving particularly advantageous in applications requiring elevated temperatures. Compared to polymer and ceramic composites, metal matrix composites exhibit significantly higher thermal conductivity. They are nonflammable and exhibit excellent resistance to the impact of organic fluids. However, the cost of these composites is higher than that of polymer and ceramic matrix composites. Commonly employed matrix materials in metal matrix composites include alloys

TH-3447_196103002

of Ti, Al, Be, Ag, and Cu. While these materials offer enhanced functionality, certain combinations of composites may exhibit reactivity at higher temperatures, leading to material degradation. This challenge can be addressed through the application of a suitable coating to the dispersed material or by altering the combination of matrix and reinforcement. Metal matrix composites find extensive use in aerospace and structural applications [91].

Ceramic Matrix Composites: Despite possessing outstanding physical and mechanical properties, Ceramic matrix composites face limitations in their application due to their inherent brittleness. The restricted usage in certain areas, particularly in automobile and structural applications, is further influenced by the relatively low fracture toughness of these composites. To address these challenges, innovative combinations of ceramic composites have been developed, incorporating ceramic particulates or platelets to enhance the fracture toughness of the ceramic matrix. This enhancement opens up a broader spectrum of applications. An additional advantage of ceramic matrix composites lies in their ability to resist material deterioration even at elevated temperatures. Commonly utilized matrix materials in these composites include C, $Al_2 2O_3$, and mullite [92].

Polymer Matrix Composites: Polymer matrix composites find extensive use in diverse fields such as engineering, construction, automobile industries, and agricultural buildings. Their widespread application can be attributed to several advantages, including specific strength, the anisotropic nature of the composite, stiffness, wear resistance, and fatigue resistance. These qualities position polymer matrix composites as ideal substitutes for various materials. Their affordability, material strength, and ease of fabrication contribute to their prevalence as the most commonly used composites. The field of polymer matrix composites has witnessed substantial investment, research, and development, leading to continuous advancements. Recent progress in polymer matrix composites has expanded their applications to include the construction of bridges, tunnels, turbine blades, storage vessels, as well as fire and blast walls [93].

Fiber Reinforced Composite: Reinforcement of fibers into the matrix phase bring about significant improvements to the mechanical properties of the composite with added advantages like lightweight, increase in strength to weight ratio and dimensional stabilities [94]. Length of the fiber, their orientation relative to other fibers, the concentration of fibers and distribution have a

TH-3447_196103002

significant effect on the mechanical properties of the fiber reinforced composite. The necessity of the critical length of the fiber plays a dominant role in strengthening and stiffening of the composite. The most frequently used fibers are glass, carbon, aramid and many natural fibers [95]. The common point in all these fibers is ideally their less density and provides the matrix required strength and stiffness [96].

Particulate Reinforced Composite: Particle-reinforced composites can be categorized into two subtypes: large particle composites and dispersion-strengthened composites. In large particle composites, the term 'large' signifies that the interactions between particles and the matrix cannot be analyzed on an atomic or molecular level. The particulates exhibit significantly higher strength and stiffness than the matrix phase. Achieving an even distribution of particles within the matrix enhances reinforcement effectiveness, leading to overall improvements in composite properties. On the other hand, dispersion-strengthened composites involve strengthening at an atomic level. The particles in these composites are relatively smaller, typically within a diameter range of 0.01 to 0.1 µm [97]. The mechanism of strengthening in dispersion-strengthened composites is akin to precipitation hardening. Notably, the strength of these composites can be maintained even at elevated temperatures and over extended periods, as the dispersed particles remain unreactive with the matrix phase [98].

Hybrid Composite Material: The integration of two or more distinct types of reinforcement materials into a unified matrix has given rise to the emergence of hybrid composite materials. These composites exhibit enhanced mechanical properties compared to those containing a single type of fiber in the matrix. The development of hybrid composite materials aims to strike a balance between cost and performance [99]. The properties of hybrid composite materials are contingent upon factors such as fiber content, fiber length, bonding strength between the matrix and fiber, and the arrangement of fibers. Diligent design of hybrid composites enables the attainment of a harmonious blend of properties. The selection of fibers and matrix for hybrid composite materials depends on the intended purpose of hybridization, working conditions, and specific requirements imposed on the material. While the concept of hybrid systems for improving material properties is well-established in engineering design, the advent of high-performance natural fibers has spurred

TH-3447_196103002

innovative material designs, including hybrid composites. Combining two or more different fibers with varying lengths and diameters in a single matrix offers more advantages than utilizing a single type of fiber in the matrix [100]. A hybrid composite material can involve a combination of synthetic and natural fibers, natural and natural fibers, or synthetic and natural fibers. Notably, the hybridization of natural and synthetic fibers in a single matrix represents a sophisticated and cost-effective composite material with excellent properties.

2.3 BIOCOMPOSITES AND GREEN COMPOSITES

A biocomposite refers to a composite material comprising a matrix (resin) and natural fiber reinforcement. The escalating environmental concerns and the cost associated with synthetic fibers have spurred the adoption of natural fibers as reinforcements in polymeric composites. The matrix phase is composed of polymers derived from both renewable and nonrenewable resources. This matrix serves a critical role in safeguarding the fibers against environmental degradation and mechanical damage, ensuring cohesion among the fibers, and efficiently transferring loads. Biofibers, derived from biological sources like crops (such as cotton, flax, or hemp), recycled wood, waste paper, crop processing byproducts, or regenerated cellulose fiber (viscose/rayon), constitute the primary components of biocomposites [12]. The burgeoning interest in biocomposites spans industrial applications (including automobiles, railway coaches, aerospace, military applications, construction, and packaging) and fundamental research, driven by their numerous advantages such as renewability, cost-effectiveness, recyclability, and biodegradability. Biocomposites can be employed independently or as a complement to traditional materials, including carbon fiber. Proponents of biocomposites assert that their utilization enhances health and safety during production, results in lighter weight materials, imparts a visually appealing aspect reminiscent of wood, and offers superior environmental credentials. The rapid growth of interest in biocomposites underscores their potential contributions to sustainable practices and applications across various industries [73].

Green Composite: Green composites, a subgroup of biocomposites, consist of natural fibers combined with biodegradable resins. These composites earn their "green" designation due to their environmentally friendly and sustainable qualities. Their biodegradable nature allows for easy dis-

TH-3447_196103002

posal without causing harm to the environment. Typically durable, green composites are primarily utilized to extend the life cycle of products that would otherwise have a short lifespan [101].

2.4 LITERATURE REVIEW ON DIFFERENT TYPES OF BAMBOO SPECIES AND ITS FIBER

The exploration of bamboo and its versatile fibers has garnered increasing attention within the realm of literature, reflecting a growing fascination with sustainable materials and eco-friendly alternatives. This literature review delves into the extensive body of work dedicated to various bamboo species and their fibers, shedding light on their unique properties, applications, and ecological significance. As a renewable resource with remarkable strength and flexibility, bamboo has emerged as a promising alternative to traditional materials in diverse industries, ranging from construction to textiles. This comprehensive survey navigates through the wealth of research, examining the distinctive characteristics of different bamboo species and their fibers, while also highlighting the pivotal role they play in fostering sustainability and environmental conservation.

The bamboo family consists of more than 1000 species and 70 genera, all of which can grow naturally in different climates, particularly in Asia and South America [102]. Liu et al. [103] extracted bamboo fibers from *Phyllostachys Pubescens* through the chemical extraction process. The fiber from *Dendrocalamopsis oldhami* bamboo was extracted by Cao et al. [104] by using the boiling technique. Experimental investigations have been performed on *Bambusa heterostachya*, *Gigantochloa scrtechinii*, *Gigantochloa levis*, *Dendrocalamus asper* and *Dendrocalamus pendulus* by Zakikhani et al. [105] Across the world, researchers are investigating the sustainability of bamboo fibers by considering local and abundant bamboo species which have high cellulose content. *Gigantochloa levis* [106], *Guadua angustifolia* [107], *Phyllostachys Heterocycla* [108], *Gigantochloa scortechinii* [109], *Dendrocalamus latiflorus* [110], *Macana bamboo* [111] and *Bambusa vulgaris* [112] are some of the bamboo species that are well explored for fiber extraction.

Apart from the aforementioned species, various other bamboo varieties found in different parts of the world include *Bambusa vulgaris* [113], *Dendrocalamus giganteus* [114], *Dendrocalamus latiflorus* [115], *Phyllostachys makinoi* [116], *Phyllostachys pubescens* [117],*Bambusa blumeana* [118],

TH-3447_196103002

Bambusa tuldoides [119], *Gigantochloa brang*, *Gigantochloa wrayi* [120], *Phyllostachys bambusoides*, and *Phyllostachys nigra* [121]. These species are utilized either as a source of fiber or as biomass, contributing to the diverse applications of bamboo in various industries.

Several bamboo species native to India include *Dendrocalamus asper*, and *Cephalostachyum pergracile*, predominantly found in the northern regions. In the southern part of India, *Ochlandra spp.* and *Melocanna baccifera* thrive, while the northeastern part is home to *Bambusa nutans*, *Dendrocalamus strictus*, and *Bambusa tulda* [122]. This geographical distribution highlights the rich diversity of bamboo species across different regions of India. The major constituents of bamboo fibers are cellulose, hemicellulose, lignin, extractive, ash and moisture content. Constituents in bamboo fibers have a significant impact on their thermomechanical properties. Species-to-species, these constituents' proportions may differ, resulting in different thermo-mechanical properties. As such, identifying and characterizing bamboo species are essential for fiber extraction. The *Bambusa tulda* is one of the bamboo species found in the northeast parts (Assam region) of India, that has not been explored. However, this bamboo is used for developing local products and supporting the construction industries.

2.5 LITERATURE REVIEW ON FUNCTIONALLY GRADED BAMBOO AND ITS CLASSIFIED EXTRACTION

Bamboo is an innately functional material, exhibiting variations in structural and constituent properties from the inner part to the outer part in the radial direction, which contributes to its variation in mechanical and physical properties. The mechanical properties and microstructure of the bamboo in the transverse direction were studied by Amada and Untao [61]. In their study, it was observed that the fiber distribution was denser in the outer section of the bamboo culm compared to the inner section. Ray et al. [123] reviled that not only numbers and diameters of bamboo fiber but also the quality and strength of bamboo fibers are varied from inner part to outer part of the bamboo culm. The variation of tenisle strength for the bamboo fiber is presented in **Fig. 2.3**. Shao et al. [124] investigated the tensile properties of the bamboo blocks and also calculated the fiber's volume fraction in a block. It was reported that the outer parts of the culm

TH-3447_196103002

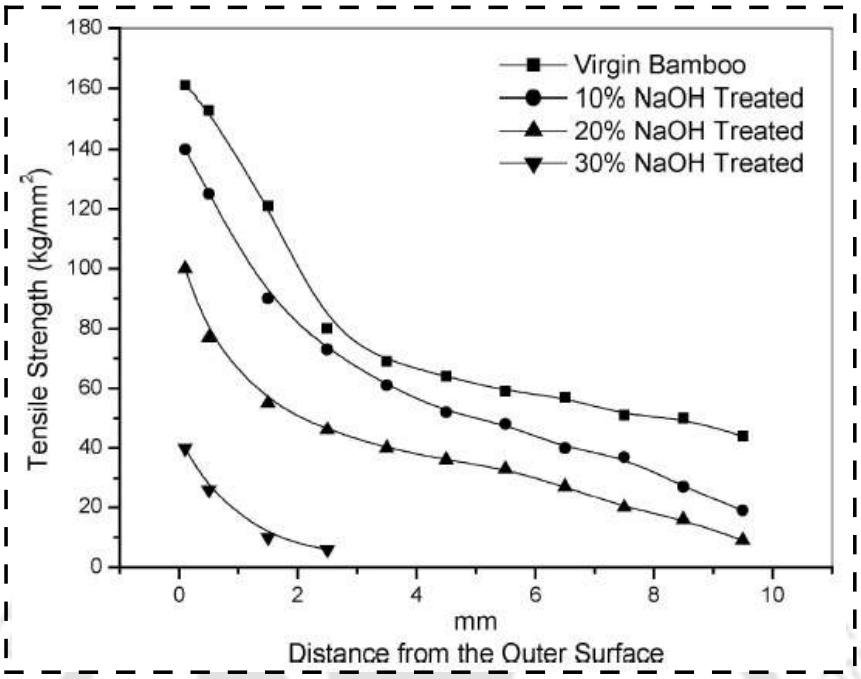

Fig. 2.3: Variation of tenisle strength for the bamboo fiber extracted from different bamboo surface [103].

have higher tensile strength and higher vascular bundle than the inner parts. Moreover, Zakikhani et al. [20] found that vascular bundles were embedded in parenchyma tissue. Bamboo culms are reinforced by vascular bundles and microfibrils. Dixon and Gibson [34] investigated Moso bamboo in the light of structural mechanics and reported that the load-bearing capacity of bamboo strips extracted from the outer part of the bamboo culm is higher than the inner part. The interlaminar fracture toughness properties of bamboo strips have been investigated by H. Chen et al.[125].The authors also reported the higher fracture toughness behaviour of external strips. The study of Chen et al. [126] investigated the Mode I interlaminar fracture toughness of bamboo with varying proportions of fiber cells (FCs) and parenchyma cells (PCs). Utilizing in situ SEM, it reveals that the middle region, with balanced FCs and PCs, exhibits the highest fracture toughness due to intrinsic mechanisms involving plastic zone size and crack kinking, and extrinsic mechanisms related to fiber bridging. This research addresses critical gaps in understanding bamboo's fracture toughness, essential for optimizing its use in structural applications. Further, M. Chen et al. [127] examined the flexural strength and ductility of bamboo strips. Similar to previous reports, the external strips showed higher flexural strength and ductility. Wang and Shao [108] has given

TH-3447_196103002

empirical formulation for variation of fiber volume fraction from the interior to the exterior side. The extraction of strip from bamboo clum has been presented in **Fig. 2.4**. Zhan et al. [128] examined the moisture diffusion properties of bamboo, essential for understanding its growth, development, and optimizing manufacturing processes. Testing bamboo in different locations reveals that its graded hierarchical structure significantly influences moisture transportation efficiency. The study suggests adaptation strategies in bamboo growth and provides insights for optimizing bamboo-based product manufacturing technology.

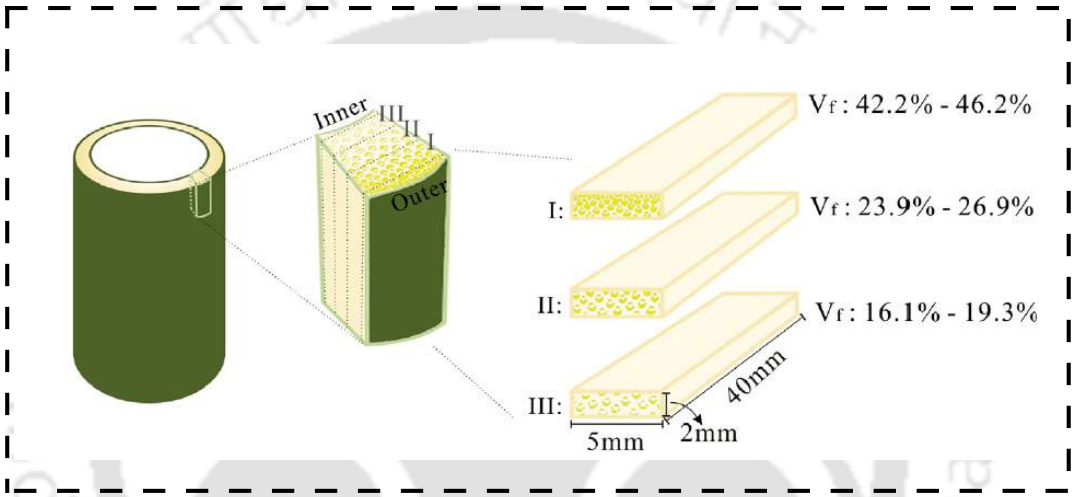

Fig. 2.4: Extraction of bamboo strip from bamboo clum [88].

Azadeh et al. [129] investigates the static and dynamic flexural behavior of bamboo as a functionally graded material. It determines the Static Flexural Modulus (SFM) for untreated bamboo and assesses the impact of heat on the Dynamic Flexural Modulus (DFM). The static flexural tests reveal variations in Modulus of Elasticity (MOE) with fiber density, while the dynamic flexural tests show a minor effect of heat treatment on DFM. The non-destructive impulse excitation technique is proposed for assessing DFM in heat-treated specimens. Overall, the study provides insights into the mechanical properties of bamboo strips extracted from different radius of the bamboo clum.

It is well known that bamboo strips extracted from the external parts of the bamboo culms have better mechanical properties than internal strips, but the variation of the physical, mechanical, thermal, and microstructural properties of extracted fiber from the external to internal parts of the bamboo culm is still limited. Moreover, their potential as a reinforcing agent for bio-composite is

TH-3447_196103002

also need to be explored.

2.6 LITERATURE REVIEW ON CHEMICAL TREATMENT OF BAMBOO FIBER

The chemical treatment of bamboo fiber is a crucial aspect in enhancing its properties and making it suitable for various applications. Bamboo, a versatile and sustainable natural fiber, has gained significant attention in recent years due to its eco-friendly and renewable nature. To fully exploit its potential, researchers have explored different chemical treatments to modify its structure and improve its performance in terms of strength, durability, and functionality. One common chemical treatment involves the use of alkali solutions, such as sodium hydroxide (NaOH), to remove impurities, hemicellulose, and lignin from bamboo fibers. Alkali treatment not only cleanses the fibers but also increases their crystallinity, resulting in improved mechanical properties and make better interfacial interaction with polymer matrix [130]. This process has been extensively studied to understand its effects on bamboo fiber and optimize the treatment conditions.

Das and Chakraborty [131] treated Bengal's *Bamboosa Balcua* bamboo fibers with various NaOH concentrations (10%, 15%, 20%). They found that 15% NaOH increased the crystalline index, improving fiber properties. Higher concentrations, however, decreased crystallinity due to lignin-induced brittleness. FTIR confirmed reduced lignin after alkali treatment, resulting in increased elongation during tensile testing. Thereafter, Das and Chakraborty [132] explored the impact of chemical treatment on bamboo fiber's thermal and dynamic mechanical properties. The DSC curve revealed a 15% reduction in moisture absorption, enhancing bonding with polymer matrices. Additionally, the treated fibers exhibited a noteworthy increase in storage modulus and glass transition temperature. However, the study observed a simultaneous significant decrease in the loss modulus value. Subsequently, Das and Chakraborty [133] examined the impact of chemical treatment on the physical and mechanical properties of bamboo fiber. The bamboo treated with 15% NaOH exhibited the highest tensile properties, revealing a 34.6% increase in tensile strength compared to untreated bamboo fiber. However, additional increments in chemical treatment resulted in a decrease in these properties. Kushwaha and Kumar [134] investigated different treatments on bamboo fiber,

TH-3447_196103002

concluding mercerization as the most effective for enhancing mechanical properties. They further studied the optimal concentration of NaOH solution, revealing that a 5% concentration provided the maximum mechanical properties and improved water resistance [135]. Liu et al. [25] examined the effects of different concentrations of NaOH on fiber crystalline and structural properties.6% NaOH concentration shows highest crystalline index and thermal stability. Further improvement in NaOH treatment concentration shows decrement in cellulose content as well as themrmal and structural proprieties. Manalo et al. [59] conducted alkali treatment of bamboo fiber using 4%, 6%, and 8% NaOH solutions. They determined that the optimal chemical treatment for strengthening the mechanical properties of bamboo fiber is with a 6% NaOH solution. Chang et al. [136] explored hot compressed water treatment of Moso bamboo fibers, reporting increased tensile strength, elastic modulus, and elongation before break for fibers treated at 140°C. The study suggested a positive impact of maleic anhydride addition on mechanical properties, providing a novel approach for hemicellulose removal from bamboo fiber surfaces for the bio-refinery industry. Chen [125] investigated the microstructure and mechanical properties of individual bamboo fibers after alkali treatment with varying NaOH concentrations (6%, 8%, 10%, 15%, and 25%). Characterization included electron microscopy, spectroscopy, X-ray diffraction, and tensile strength tests. Alkali treatment resulted in more surface wrinkles and pores, transforming microfibril aggregates and cellulose structure. Fiber diameter, lumen, and cross-sectional area decreased, causing cracks in the cell wall. Tensile strength and modulus of elasticity decreased, with NaOH concentration affecting MOE more than tensile strength. However, elongation at break significantly increased, indicating potential for textile applications. Higher NaOH concentrations shifted fibers from brittleness to ductility. Khan et al. [137] treated the bamboo fiber with different NaOH solutions and investigated their different mechanical properties. The chemical treatment reduce the fiber diameter and increase the tensile strength. The 6% NaOH-treated fiber showed the most desirable interfacial shear strength. More then the optimal treatment concentration the strength and stiffness of the fiber decreased. Later on, Buson et al. [138] explored alkalinization and acetylation treatments on bamboo fibers to enhance adhesion in polymer composites. Acetylated fibers exhibited lower water absorption, improved thermal stability, decreased crystallinity, and increased surface roughness

TH-3447_196103002

for better fiber/matrix adhesion. However, acetylation reduced the fiber's mechanical strength to 19,820 MPa, compared to 27,670 MPa for natural fibers and 31,730 MPa for alkaline-treated fibers. Tong et al. [139] examined the impact of alkaline treatment on Malaysian bamboo fibers. Alkaline treatment enhanced fiber morphology and physico-chemical properties, as revealed by FTIR, TGA, and SEM analysis. Treated fibers exhibited a 45.6% increase in tensile strength and a 72% increase in modulus compared to untreated fibers. The surface roughness was notably reduced. FTIR and TGA indicated gradual removal of lignin and hemicellulose. These findings suggest that locally sourced bamboo fibers are promising as reinforcement agents in composite materials. This study of Chen et al. [140] aimed to assess the wettability and thermal properties of individual bamboo fibers post-alkali treatment with varying sodium hydroxide (NaOH) concentrations. Atomic force microscopy revealed increased surface roughness. Lower NaOH concentrations enhanced wettability, but higher concentrations (15% and 25%) reduced it. Thermogravimetric analysis indicated improved thermal stability at low NaOH concentrations, while higher concentrations compromised thermal stability, shifting decomposition temperatures to higher values. Zhang et al. [141] treated Moso bamboo with 2, 6 and 10% NaOH concentrations and the thermomechanical properties of the fiber investigated. The chemical treatment affected positively on the properties of fiber. **Fig. 2.5** presents the typical stress-strain curves of treated and untreated fiber. The study of Chen et al. [142] explored the impact of alkali treatment on bamboo parenchyma cells and fibers. Treatment at concentrations above 10% led to parenchyma cell collapse and fiber separation. Starch extraction occurred at 2% NaOH. Alkali treatment removed lignin and hemicellulose from fibers but only lignin from parenchyma cells. Cellulose transformation observed in both cell types. Parenchyma cells exhibited lower thermal stability than fibers, and alkali treatment more significantly affected the thermal stability of parenchyma cells than fibers. Wu et al. [143] compared the effects of alkali treatment on bamboo fibers and parenchyma cells. Both were mechanically separated from the same bamboo and treated with 5% alkali solution at different times and temperatures. The microstructure, chemical composition, crystallinity, and thermal stability were analyzed. Alkali treatment temperature had a greater impact on chemical composition and crystallinity than treatment time. Increasing temperature removed hemicellulose and lignin, impacting crystallinity.

TH-3447_196103002

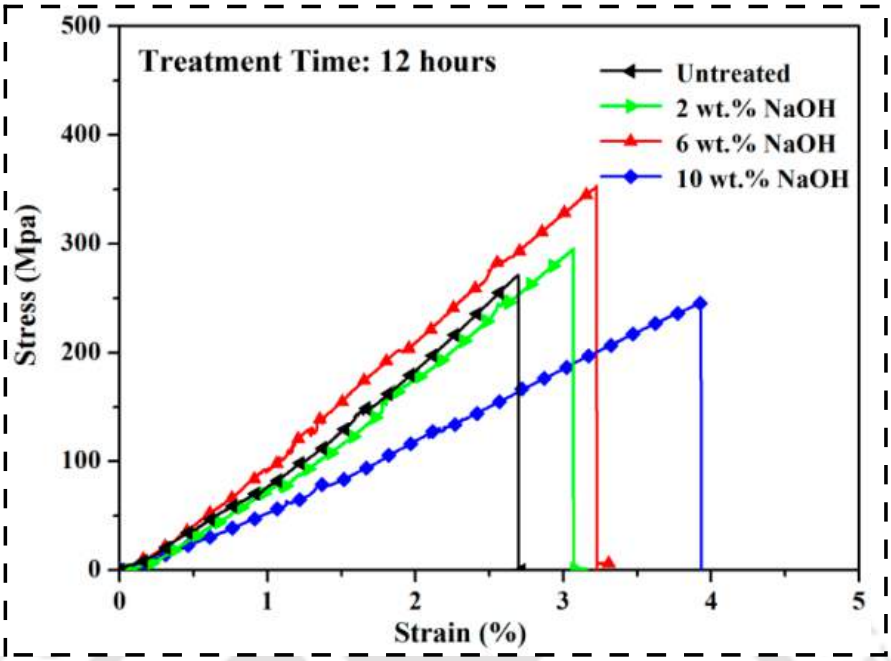

Fig. 2.5: Typical stress –strain curve for different chemical treated bamboo fiber [122].

In conclusion, the literature on the chemical treatment of bamboo fiber underscores its significance in enhancing the fiber's properties for diverse applications. Researchers have explored various chemical treatments, such as alkali solutions, acetylation, and coupling agents, to modify the bamboo fiber's composition and structure. These treatments have been found to influence not only the mechanical and thermal properties of bamboo fibers but also their morphological characteristics. However, the optimization of treatment conditions remains a key focus for achieving the desired balance between improved properties and potential drawbacks. Some study has been reported by different authors on different bamboo fiber regarding their NaOH treatment but how the concentration of chemical treatment affecting the physical, structural, mechanical and thermal properties of bamboo fiber is still limited.

2.7 LITERATURE REVIEW ON DEVELOPMENT OF BAMBOO BASED BIOCOMPOSITES

In comparison to other natural fiber composites, bamboo fiber composites have superior thermo-mechanical properties and are easy to obtain. These factors contributed to the 59.3 billion USD bamboo market in 2021, which will continue to grow at a CAGR of 4.5% until 2030 [144]. Re-

TH-3447_196103002

searchers around the world investigated the thermo-mechanical properties of different bamboo fiber and their reinforced composites.

H.E. Glen et al. [145] marked a groundbreaking moment in 1950 by introducing bamboo fiber as a reinforcing material in conjunction with Portland cement. Subsequently, Mehra et al. [146] delved into the examination of flexural and shear properties in an existing Portland cement bamboo composite. Fang and Mehra [147] investigated the influence of fiber volume fraction on the strength and ductility of the cemented composite. A significant development occurred in 1983 when Guthrie and Torley [148] patented the design and creation of a low-cost composite building material crafted from short bamboo fiber and Portland cement. Mansur and Aziz [149] conducted experimental studies on the mechanical properties of a woven bamboo mesh fiber-reinforced cement composite. In 1997, Chen et al. [150] achieved a milestone by introducing the first bamboo fiber-reinforced polymer composite, with polypropylene polymer serving as the matrix material. Mi et al. [151] secured a patent for a bamboo fiber-reinforced polypropylene composite, highlighting the augmentation of tensile strength, modulus, and elongation before the break value resulting from the addition of bamboo fiber to the polypropylene matrix.

The major development of bamboo based polymer composite has been observed in three specific region which is as per the bamboo avalibility region, the region are- development in asia-pacific region, american region and african region. The region wise literature on development of different bamboo based composites has been presented below:

2.7.1 Development in Asia Specific Region

Several distinct bamboo species are found in the Asian region, with significant advancements in bamboo composites primarily noted in India, China, Japan, South Korea, and Malaysia. The following sections provide a detailed overview of literature on the development of polymer composites in each respective region.

Development in India- Rajulu et al. [152] developed a bamboo short fiber-reinforced composite using Araldite as the matrix material, exploring various fiber lengths for mechanical testing. The study indicated an optimal tensile load for a 30 mm fiber length, with a subsequent decline in

TH-3447_196103002

load-bearing capacity as fiber length increased. Later on, the same researchers advanced their work by creating a continuous fiber-reinforced polymer composite, reporting improved tensile strength and load-bearing capacity compared to the earlier short fiber composite [153]. A notable advantage of natural fiber-reinforced composites is their lightweight nature. Rajulu et al. [154] characterize their composite through specific gravity tests. This revealed a reduction in specific gravity and void content, emphasizing the composite's lightweight properties and improved bonding strength between bamboo fiber and epoxy resin. Saxena and Gowri [155] utilized bamboo fiber from Madhya Pradesh, India to develop bamboo fiber-reinforced epoxy and polypropylene composites. Surface treatment with polyestermide polyol enhanced mechanical strength and water resistance, demonstrating improved fiber-matrix bonding. Further, Das and Chakraborty [133] explored the impact of chemical treatment on composite mechanical properties. Alkali treatment significantly influenced tensile strength, modulus, flexural strength, modulus, and impact strength. Continuing their research, Das and Chakraborty [156] extended the study to include a different matrix material, Resol matrix, reporting lesser mechanical properties but greater strength before break value compared to the previous polyester resin. The study emphasized the crucial role of both reinforcing material and matrix material in determining composite properties. Krishnaprasad et al. [157] focused on microfibrils extracted from bamboo fiber to develop bamboo microfibril-reinforced polyhydroxy butyrate (PHB) composites, reporting increased impact and tensile strength with bamboo microfibril loading. Gupta [158] developed a bamboo-based epoxy composite, exploring the effect of fiber loading on water content and chemical resistance. The study found decreased chemical resistance with increased fiber content. Kumari et al. [159] explored the effect of chemical treatment on polyester-bamboo composites, noting improvements in thermo-mechanical properties and reduced water absorption after alkali treatment. The study highlighted the cost-effectiveness and eco-friendliness of the developed composite.

Development in China- China is one of the major producer of bamboo and bamboo based composite. Wang et al. [160] investigated the impact of moisture content and bamboo micro-fiber size on the mechanical properties of PVC composites reinforced with Makino bamboo fibers. The study revealed a density-moisture absorption correlation and identified an optimal bamboo filler per-

TH-3447_196103002

centage for enhanced tensile and flexural properties. Phuong et al. [161] studied recycled bamboo fiber-reinforced polypropylene composite, using Makino bamboo from China. Chemical treatments, particularly alkali treatment, improved fiber structure and thermo-mechanical properties, while acetylation enhanced compatibility between bamboo fiber and matrix, resulting in superior mechanical properties. The morphology of treated and untreated fiber has been presented in **Fig. 2.6** The

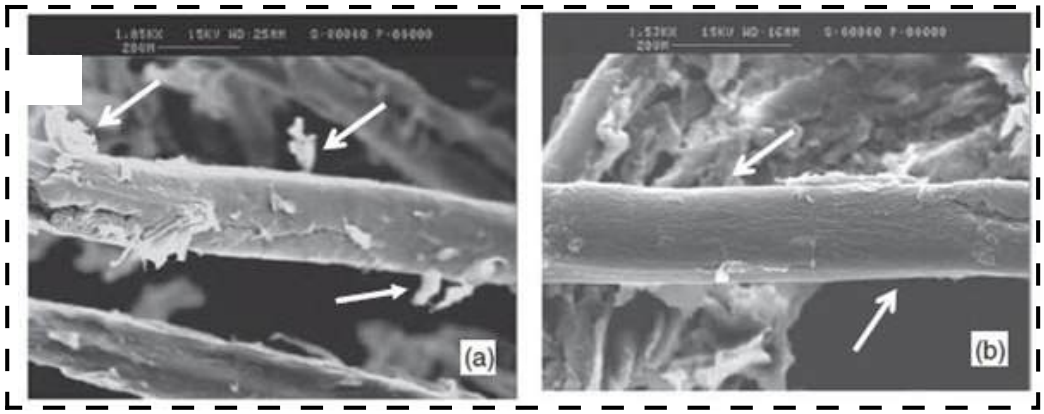

Fig. 2.6: (a) Bamboo fiber surface before and (b) after the chemical treatment [142].

hydrophilic nature of lignocellulose fibers posed challenges in fiber-matrix bonding and composite durability. Hung et al. [162] investigated Makino bamboo fiber-reinforced high-density polyethylene composites, finding that chemical treatment notably enhanced retention properties and decay resistance during natural weathering. Wang and Ying [163] proposed a method for a uniform Makino bamboo fiber-reinforced polypropylene composite, incorporating alkali-treated and untreated bamboo fibers with a silane coupling agent. The study demonstrated improved mechanical properties and reduced water absorption in the alkali-treated bamboo fiber-reinforced composite, indicating the success of the enhancement process. Yu et al. [53] innovated a process for bamboo fiber-reinforced composite with an oriented bamboo fiber mat, achieving significant mechanical property improvements without chemical treatment. Zhu et al. [164] evaluated the physical and mechanical properties of these composites after outdoor exposure, indicating good dimension stability performance despite gradual decreases in mechanical values. Xie et al. [165] explored three bamboo species for fiber extraction, creating composites with varying densities. A density of 1200 kg/m^3 showed superior mechanical properties, better dimension stability, and lower water absorption. The

TH-3447_196103002

study concluded that bamboo fiber-reinforced composite properties were highly influenced by the bamboo species. Chunhong et al. [166] fabricated non-woven bamboo fiber-reinforced polypropylene composites via compression molding. Alkali-silane treated fibers were identified as optimal, minimizing void content and moisture absorption. Chemical treatment of fibers proved beneficial in hindering water diffusion and preventing moisture damage. Huang and Young [167] investigated hygral, mechanical, and interfacial strength of continuous bamboo-reinforced epoxy composites. The study concluded that moisture negatively affecting the mechanical properties of the composite. Zhang et al. [106] examined the relationships among internal structure, chemical composition, and hygroscopic properties of bamboo fiber-reinforced composite (BFRC). Compression molding altered internal cellulose structure, reducing water absorption capacity and making BFRC less hygroscopic. Rao et al. [168] introduced a novel technique to develop bamboo-fiber reinforced polymer composites with varying concentrations of phenol-formaldehyde for outdoor use. Higher resin concentrations improved water resistance and shear strength but reduced compressive strength. A 20% resin concentration was deemed optimal for cost-effective outdoor applications. Wang et al. [169] fabricated a homogeneous bamboo fiber-reinforced polypropylene composite by modifying bamboo fibers with 3-aminopropyltriethoxysilane (APTES). APTES modification improved mechanical and water resistance properties, highlighting its advantages for enhancing interfacial adhesion. However, APTES was noted to have a negative impact on thermal properties.

Development in Japan- In Japan, researchers and industry professionals have explored the use of bamboo fibers as a reinforcement in polymer composites to enhance the mechanical properties of the materials. These composites can offer advantages such as high strength, low weight, and eco-friendliness. The development of bamboo fiber composites aligns with the country's efforts to promote sustainable and innovative materials. Kim et al. [170] developed a bio-composite using Moso bamboo fiber and vinyl ester resin. Bamboo fibers were extracted through various methods, with alkali extraction demonstrating superior single fiber tensile strength and greater fiber-matrix contact angle. Chemical treatment using sodium hydroxide decreased fiber tensile properties but increased interfacial shear strength, enhancing fiber-matrix bonding and overall composite mechanical properties. Wang et al. [171] applied an impregnation modification process to *Neosinacallamus*

TH-3447_196103002

affinis bamboo, incorporating nano-$CaCO_3$ particles for enhanced surface roughness. Modified bamboo showed significant improvements in single fiber tensile strength, young's modulus, and elongation before break. Subsequently, the study investigated the effects of fiber dipping time and concentration, determining optimal conditions for maximum tensile strength, modulus of elasticity, and elongation before break. Later Wang et al. [172] compared two fiber modification techniques, blending modification (BM) and impregnation modification (IM). IM exhibited superior mechanical properties in bamboo fiber composites. The interfacial interaction was further explored in 2019, with IM-treated bamboo fibers used to develop composites with high-density polyethylene (HDPE). Among three manufacturing processes (hot pressing, extrusion, and injection molding), injection molding showed the highest mechanical properties, concluding it as the most effective process for IM-modified bamboo fiber and HDPE composites.

Development in Korea- The development of bamboo fiber composites aligns with global efforts towards sustainability and eco-friendly alternatives in various industries. South Korea, as a technologically advanced country, has likely been involved in research and applications of bamboo fiber composites in sectors such as construction, automotive, and consumer goods. Ma and Joo [173] utilized South Korean bamboo and PLA to create a composite through the film-stacking process. To enhance the interaction between fibers and matrix, three treatment methods were employed: direct silane coupling (DC), silane coupling during UV irradiation (CDU), and silane coupling after plasma treatment (CAP). XRD analysis revealed that DC treatment increased the crystalline region, while CAP and CDU treatments augmented the amorphous region of bamboo fibers. The interfacial shear strength improved by 44.2%, 87.4%, and 64.2% with DC, CAP, and CDU treatments, respectively. Tensile strength in composites with DC, CAP, and CDU-treated fibers increased by 43.7%, 71.1%, and 60.7%. Silane coupling after plasma treatment was identified as the most effective technique for enhancing bamboo-composite properties. Later, Kang and Kim [49] developed a Korean bamboo-reinforced PLA composite, exploring thermo-mechanical properties. Alkali treatment increased fiber ductility, brightness, and thinness. Delignified bamboo-reinforced PLA composites exhibited superior flexural and tensile strength compared to untreated bamboo composites. Thermal properties were influenced by treatment; alkali-treated composites showed an

TH-3447_196103002

increase in initial decomposition temperature but a decrease in maximum decomposition temperature. Silane treatment induced surface modification of bamboo fibers, enhancing bonding strength with the matrix and overall thermo-mechanical properties.

Development in Malaysia- Malaysia has been actively involved in the exploration and development of bamboo composites. Malaysia, with its abundant bamboo resources, has recognized the potential of bamboo in various applications, including the production of composite materials for construction, furniture, and other industries. Researchers and industries in Malaysia have been studying the use of bamboo fibers and particles as reinforcement in composite materials. These composites can offer advantages such as strength, durability, and sustainability. Malaysia's interest in bamboo composites aligns with the broader global movement towards eco-friendly and renewable materials. Tong et al. [139] studied Malaysian bamboo fiber composites, extracting fibers through roller milling and hand layup. A 24-hour treatment with 8% NaOH solution enhanced mechanical properties, yielding a 45.6% increase in tensile strength and a 72% increase in modulus. Excessive NaOH concentrations adversely affected properties, indicating lignin and hemicellulose removal. The findings suggest the viability of local bamboo fibers for effective reinforcement in composite production. Chin et al. [174] investigated the mechanical and thermal properties of Malaysian bamboo fiber-reinforced polymer composites. Chemical treatment and physical milling were employed on bamboo fibers, integrated with three thermosetting polymers. Optimal tensile and bending properties were achieved in the 40% fiber-reinforced epoxy composite, suggesting the proposed preparation method as a valuable guide for robust bamboo fiber composites, potentially applicable for external strengthening of buildings and structures. Furthermore, Hassan et al. [112] explored the influence of fiber soaking and drying time on the mechanical properties of bamboo-epoxy composites. With a predefined NaOH concentration, optimal tensile properties were achieved with 3.99 hours of soaking time and 72 hours of drying time.Composites utilizing this treated fiber demonstrated enhanced characteristics when compared to untreatment methods.

TH-3447_196103002

2.7.2 Development in American Region

The development and uses of bamboo fiber composites in the Americas, particularly in North and South America, has been limited compared to regions like Asia. However, interest in sustainable and eco-friendly materials has been growing globally, and there has been increasing attention to bamboo as a renewable resource. Porras and Marañon [175] developed biodegradable composite using woven bamboo fiber and PLA from Colombia, showing impressive mechanical properties (86MPa tensile, 154MPa bending, 13.44 kJ/m^2 impact strength) via film stacking compression molding. Scanning electron microscopy indicated good bonding, with identified failure modes as structural delamination and matrix cracking. The laminates exhibited excellent energy absorption and high elongation before break, suggesting suitability for engineering structures. Later, Sánchez et al. [176] developed agglomerated panels with vegetable resin and *Guadua* bamboo fiber through manual molding, finding the composite feasible for medium and low-load non-structural applications. In 2019, delignification with cold plasma and alkaline treatments enhanced mechanical properties and reduced water absorption. Furthermore, Lima [177] studied the impact of a coupling agent on mitigating mechanical property loss during the natural aging process. Inácio [178] assessed the aging effects on thermal and mechanical behavior in Brazilian bamboo composites. The addition of bamboo fiber improved fatigue life, tensile and flexural strength, with aging causing a reduction in tensile strength, flexural strength, and fatigue life. Thermogravimetric analysis indicated increased degradation temperatures with the addition of fiber and further increases due to aging.

2.7.3 Development in African Region

The use of bamboo composites in Africa has been gaining attention due to the continent's abundant bamboo resources and the growing interest in sustainable and eco-friendly materials. Africa's diverse climates and ecosystems offer favorable conditions for bamboo growth, presenting opportunities for the development of bamboo-based composites. Bamboo composites in Africa may find applications in construction, furniture, and various industries. Researchers and organizations in countries with significant bamboo resources, such as Ethiopia, Ghana, and Cameroon, have been exploring the potential of bamboo composites for economic and environmental benefits. Akindapo

TH-3447_196103002

et al. [179] developed sustainable protective shields using Nigerian bamboo fiber and polyester resin composites. Bamboo fibers were treated with NaOH, and composites were formed with varying weight percentages. The most promising composite (40% bqamboo fiber loaded composite) exhibited excellent mechanical properties, low water absorption, and thermal stability. The findings highlight the potential of treated bamboo fiber-polyester composites for sustainable applications in security and defense equipment. Mebratie et al. [180] explored the mechanical properties of oil-treated Ethiopian Highland bamboo fiber/polyester composites. The oil treatment aimed to enhance flexibility, resulting in higher tensile and flexural strengths. Oil-treated composites outperformed untreated ones, showing improved characteristics, with increased strain and reduced breakage due to enhanced strand flexibility from lubrication. Daramola et al. [181] developed high-density polyethylene (HDPE) composites by compressing short bamboo fiber (BF) reinforced with 0.5 M NaOH-treated BF. Various weight fractions (2-10 wt.%) were melt-compounded with HDPE. Mechanical properties improved up to 4 wt.% BF, while water absorption increased with higher fiber content. Morphological analysis indicated homogeneous BF dispersion at lower weight fractions, with agglomeration at higher fractions. The study concludes that treated bamboo fibers effectively reinforce HDPE.

The current literature on bamboo-based biocomposites highlights a significant gap in research pertaining to the optimization of processing techniques and the scalability of production. While some studies have explored the mechanical and environmental advantages of bamboo-based biocomposites, there is limited research on the systematic development of cost-effective and scalable manufacturing methods based on Northeast Indian bamboo. Additionally, there is a lack of comprehensive investigations into the influence of varying bamboo species, processing parameters on the final properties of the biocomposites. Addressing this literature gap is essential for unlocking the full potential of bamboo-based biocomposites, enabling sustainable and widespread adoption in various applications.

TH-3447_196103002

2.8 LITERATURE REVIEW ON EFFECT OF DIFFERENT BIODEGRADABLE MATRIX MATERIALS ON BIO-COMPOSITES

In the earlier period (before 2017), researchers predominantly dedicated their efforts to crafting natural fiber-reinforced composites with high strength. However, around mid-2017, there was a noticeable shift in focus towards the development of green composites or biodegradable composites. The escalating carbon footprint resulting from plastic waste and concerns about depleting fossil fuels have heightened interest in alternative environmentally friendly materials. In previously documented literature, the development of polymeric materials or polymer composites using petroleum-based polymers and synthetic materials is acknowledged to be environmentally harmful. Consequently, there is an imperative need to utilize bio-based polymers and bio-based reinforcement materials for the formulation of sustainable materials. Liuyun et al. [182] integrated bamboo fiber into a nano-hydroxyapatite-PLGA composite, producing biodegradable composites with varying bamboo fractions (0%, 5%, 10%, 20%) through a solution mixing method. Investigating mechanical properties, interfacial structure, and crystallization behavior, the bamboo-hydroxyapatite-PLGA composite displayed superior thermo-mechanical properties to the bamboo-PLGA composite. The addition of 5% bamboo fiber showed optimal mechanical properties, indicating the bamboo-hydroxyapatite-PLGA composite's potential superiority over the nano-hydroxyapatite-PLGA composite for biomedical applications. Fang Wang et al. [183] developed bamboo fiber-reinforced green composites using hot-pressing with polylactic acid as the matrix and varying fiber volume fractions (30%, 40%, 50%). Tensile testing revealed increased strength and reduced elongation with higher fiber volume. Chemical treatment improved tensile strength by 38.6% and elongation by 34.4%, though the modulus decreased by 15.7%. **Fig. 2.7** presents the XRD graph of treated and untreated fiber reinforced polylactic acid. Later Wang et al. [184] investigated the effect of chemical treatment on crystallization index and chemical composition of fibers. It was reported that due to chemical treatment the crystallization index of the bamboo fibers were increased which affected positively on the ductility of biocomposite. Thereafter, Yang et al. [185] investigated the dynamic mechanical (DMA) and thermal properties of these composites. A decrement in glass transition temperature was reported with the increment of fibers volume fraction. TGA results exposed that the degra-

TH-3447_196103002

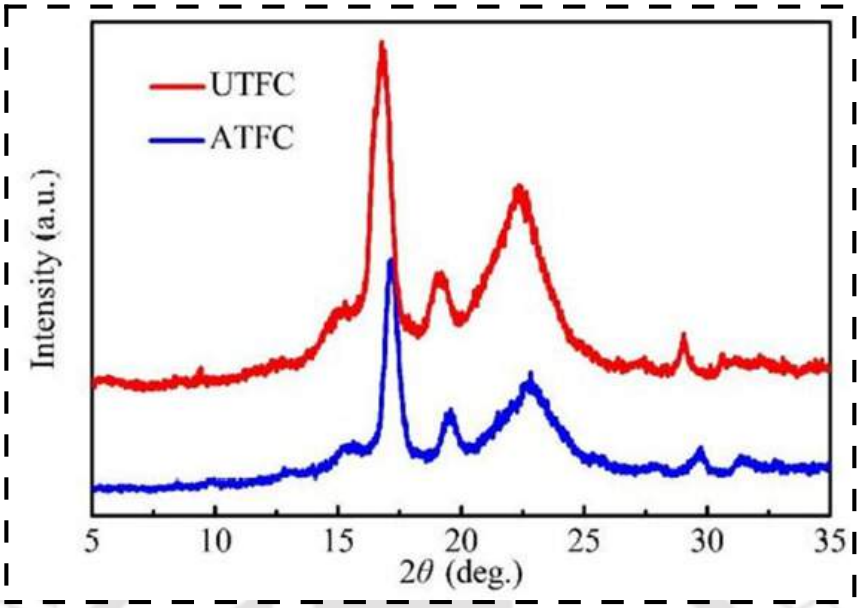

Fig. 2.7: XRD pattern of treated and untreated bamboo fibers [164].

dation temperature of the composite increased with increasing the fiber content. The detailed analysis concluded that the bamboo fibers have a positive effect on thermo-mechanical properties of the epoxy composite and providing feasibility to using bamboo fiber-reinforced composites for medium and low structural application. Long et al. [186] developed bio degradable short bamboo fiber reinforced PLA composite. To increase the fiber-matrix interaction, the fibers were treated with alkine solution and MAPP was added with matrix material. Addition of 5% MAPP was showed maximum tensile strength (33.73 MPa), flexural strength (47.18 MPa) and impact strength (3.15 kJ/m^2). There after, Long et al. [187] added polyethylene glycol with the matrix material to increase the mechanical properties of the composite. Addition of polyethylene glycol shown greater crystalline index with compared to previously prepared composites. The maximum tensile, flexural and impact strength of 65.46 MPa, 97.94 MPa and 3.25 kJ/m^2, respectively were reported for present composites which were 94.07%, 107.58% and 3.17% greater in tensile strength, flexural strength and impact strength respectively. Yang et al. [188] examined the biodegradable characteristics and impact of degradation on the mechanical properties of a previously prepared bamboo fiber composite. Soil burial degradation and microbial degradation tests were conducted. The degradation process led to a deterioration in the mechanical properties of the composite, along with a

TH-3447_196103002

decrease in thermal stability. Interestingly, the crystallinity of the PP component increased during degradation. Zindani et al. [189] developed bio-composites using cashew nutshell liquid-based biopolymer and *Punica granatum* fiber. The developed bio-composites show permissible mechanical and structural properties. The maximum tensile and flexural strength has been reported as 84 MPa and 166 MPa, whereas the maximum tensile and flexural modulus has been reported as 4.75 GPa and 8.15 GPa. Sanchez et al. [111] developed vegetable-based polyurethane polymer bamboo composites. The developed composite shows a maximum tensile strength of 70.94 ± 8.35 MPa, a maximum modulus of 9166 ± 125 MPa and a density of 0.97 gm/cm^3 can be used for advanced engineering and semi-structural application. Cortat et al. [190] developed sustainable composites using nutshell residue with polypropylene (PP). The sustainable green composites were with 5, 10, 15, 20, 25 and 30% of reinforcement by wt. Further author characterized the prepared samples by performing different physical, mechanical and thermal testing. The maximum tensile strength and tensile modulus have been recorded as 30 MPa and 2401 MPa, respectively. Loganathan et al. [191] investigated the physical-mechanical and flammability properties of Cyrtostachys renda Fibers Reinforced Phenolic Resin Bio-composites. The developed composites experimentally investigated the properties in terms of tensile, flexural, impact, and water absorption. Kumar et al. [192] developed bio-composites using kenaf/pineapple fiber and Formulite bio-epoxy. The bio-content of the epoxy was 34%. The developed composite shows a maximum strength of 86.47 MPa in tensile and 116.43 MPa in flexural. The impact strength of the composites has been reported as 33.87 kJ/mm^2. The author concludes that the developed composites can be used in semi-structural engineering applications.

The existing literature on biodegradable biocomposites reveals a noteworthy gap in understanding the long-term structural integrity and environmental impact of these materials. While numerous studies have investigated the initial biodegradability and mechanical properties of such biocomposites, there is a scarcity of research focusing on the comprehensive evaluation of their degradation over time. Additionally, the influence of diverse environmental conditions on the biodegradation process and the subsequent effects on material properties remains an underexplored aspect. Moreover, the majority of bio-composites in the literature are based on thermoplastic polymer matrixes.

TH-3447_196103002

As per the author's knowledge, very little literature exists on thermoset biopolymers-based composites. Bridging this literature gap is crucial for advancing sustainable materials development and ensuring a thorough comprehension of the lifecycle and eco-friendly attributes of biodegradable biocomposites.

2.9 LITERATURE REVIEW ON BAMBOO FIBER REINFORCED HYBRID BIOCOMPOSITES

Hybrid bamboo composites refer to materials that combine bamboo fibers with other reinforcing materials to create a composite material with enhanced properties. These composites leverage the strengths of bamboo, a natural and sustainable resource, along with the unique characteristics of other materials. The combination of bamboo fibers with polymers, other natural fibers, or even traditional reinforcing agents like glass fibers or any others natural fiber/particles can lead to improved mechanical, thermal, and structural performance.

Thwe et al. [193] created a durable bamboo-glass fiber hybrid composite to enhance hygrothermal aging resistance. The study compared bamboo fiber reinforced polypropylene (BFRP) and bamboo-glass fiber reinforced polypropylene (BGRP) composites, finding improved fatigue resistance in BGRP. Aging at 75°C significantly impacted tensile strength. In the other hand, coupling agents mitigated degradation. Han et al. [194] developed HDPE/bamboo composites with varying nanoclay and maleated polyethylene (MAPE) by melt compounding. The effect of compounding characteristics, clay dispersion and HDPE crystallization, on mechanical properties of composites has been analysied. MAPE was crucial for clay exfoliation in HDPE/bamboo systems, enhancing tensile strength, bending modulus, and strength. However, the addition of clay reduced overall mechanical properties, requiring further study on pre-coating fibers for enhanced synergy. Okubo et al. [195] innovated hybrid biocomposites, blending biodegradable poly(lactic acid) with microfibrillated cellulose (MFC) and bamboo fiber bundles. The hierarchical reinforcement system enhances properties, with 1 wt% well-dispersed MFC significantly improving fracture energy by almost 200%. The fracture morphology around bamboo fiber bundles also undergoes a significant change in hybrid bamboo/MFC/PLA composites. Later, Cuicui Wang et al. [196] enhanced

TH-3447_196103002

composite mechanical properties by surface-modifying bamboo fibers with nano calcium carbonate particles. Composites, using untreated, blending modified, and impregnation modified fibers with high-density polyethylene, exhibited increased flexural and impact properties. Impregnation modification showed greater effectiveness, with a 44.19% improvement over untreated fibers. However, no significant enhancement was observed in impact strength and flexural modulus.

Chee et al. [197] prepared Bamboo/kenaf-reinforced epoxy hybrid composites using hand layup, were studied for their thermal and thermo-oxidative stabilities at different bamboo and kenaf fiber ratios. Results showed improved stability with higher bamboo content. Further, Qianting Wang et al. [198] enhanced bamboo-polypropylene composite by incorporating graphene oxide with short bamboo fiber. The addition improved interfacial strength, resulting in a 12.6% increase in tensile strength and a 23.7% increase in flexural strength with 0.1% graphene oxide. Gouda et al. [199] added graphene nano partials with bamboo microparticles and investigated the synergetic effect of these two particles on the thermo-mechanical properties of hybrid composites. Cement bypass dust (CBPD) and cenosphere fly ash were used as fillers by Gupta [200] in bidirectional bamboo fiber-reinforced polymer composites. Two sets of composites, one with untreated bamboo fibers and the other with alkali-treated fibers, were fabricated with varying filler compositions. Chemical resistance and water absorption properties were studied, indicating that filled composites exhibited good resistance to acids, solvents, and alkalis, along with improved water resistance compared to neat composites. These composites hold potential for diverse industrial and civil engineering applications. Adediran et al. [201] developed bamboo fiber-coconut shell husk reinforced polyvinyl chloride composite. Bamboo fibers (BF) treated with NaOH and particulate coconut shell (PCS) were incorporated into polyvinyl chloride (PVC) to enhance properties for ceiling boards and insulating pipes. Compression molding resulted in composites with improved strength, modulus, and wear resistance, with optimal performance at 2 wt% PCS and 15 wt% BF. The combination of 0–30 wt% BF and 2 wt% PCS demonstrated the best overall property enhancement. Ramu et al. [202] added groundnut shell, copper particle and MWCNT filler separately into bamboo fiber epoxy composites. The author reported impressive results in thermos mechanical and physical properties with groundnut shell and carbon nanotube filler reinforced hybrid bamboo composites.

TH-3447_196103002

Furthermore, Ramu et al. [203] reported significant increases after filler addition to hybrid composites with rice husk and bamboo fiber mat. Sarmin et al. [204] added olive biomass into bamboo fiber reinforced epoxy-based bio-composites to develop a cost-effective and sustainable composite material with superior thermos-mechanical properties. Alam et al. [205] added egg shell as a reinforcing particle into bamboo fiber reinforced hybrid polyester laminated composites. Hybridization in reinforcement increased the tensile and flexural properties of the composites positively. Kumar et al. [206] developed composites with bamboo fiber and SiO_2 particles. The author analyzed the positive effect of SiO_2 addition on bamboo fiber reinforced composites. Chakkour et al. [207] developed montmorillonite and eggshell /bamboo fiber reinforced biocomposites for reducing the moister aging of composites. Results indicate improved water absorption, thickness swelling, and mechanical properties at a 3wt% filler content. The composites exhibit enhanced strengths under ambient conditions, though slight improvement is observed in wet conditions.

In conclusion, the literature review on bamboo fiber-reinforced hybrid composites reveals a diverse range of studies focused on enhancing the mechanical, thermal, and physical properties of these sustainable materials. Researchers have investigated a wide array of hybridization approaches, exploring diverse reinforcing materials in conjunction with bamboo fibers. These materials include ceramic particles, natural fibers, and a combination of both natural and synthetic particles. The studies demonstrate that fiber and micro particle hybridization contribute to improved interfacial adhesion, leading to enhanced mechanical properties. Furthermore, efforts have been made to understand the impact of environmental factors, such as natural weathering and aging, on the long-term durability of hybrid bamboo composites. While challenges like delamination and matrix cracking have been identified, the overall findings emphasize the potential of bamboo fiber-reinforced hybrid composites for sustainable applications in diverse industries, offering a compelling alternative to traditional materials. However, the effect of adding bamboo micro particles into bamboo fiber reinforced bio composite is still limited. Future research should continue to address optimization strategies, explore additional treatment methods of bamboo particles, and thermo-mechanical properties aspect of these composites for broader implementation in various structural engineering and construction applications.

TH-3447_196103002

2.10 RESEARCH GAPS

Based on the above literature, the following research gaps has been identified:

- In the majority of the existing literature, bamboo fibers sourced from China and northeastern Asia have been predominantly utilized by researchers. While a few studies have introduced bamboo of Indian origin, it's noteworthy that the northeastern region of India, particularly Assam, boasts a diverse and abundant range of bamboo resources. There is very limited work available on bamboo and bamboo fiber available at this region.
- Most of the literature performed extraction of bamboo fiber from any part of the bamboo clum. The bamboo is a naturally functionally graded materials and its properties changes from inner to outer section of the culm. So, classified extraction and comparative characterization of bamboo fiber from different section of bamboo clum in radial direction is still a major research gap.
- To increase mechanical properties of fiber and interfacial bonding strength between fiber and matrix materials chemical treatment with constant alkaline solution (5%) is present in literature. Very few research is presented by controlling the effect of concentration of NaOH solution. There is a need to investigate the effect of NaOH concentrations on thermo-mechancial and physical properties of the bamboo fiber to set the optimal value of NaOH concentration.
- From the literature it has been observed that most of the papers presented with non-degradable polymer matrix. Very few was working on degradable polymer matrix. And most of these degradable polymer matrix are thermoplastic. The effect of biodegradable thermosetting matrix material need to be studied.
- Further, bamboo based materials can be used for electronic parts, for this purpose, its physical, mechanical and dielectric properties need to be exploded.
- There is very limited studies available on FTIR and XRD characterization of bamboo fiber composites.

TH-3447_196103002

- Several micro and nano-particles have been added to bamboo fiber reinforced bio-composites to improve their thermo-mechanical properties, but the effect of bamboo micro particles on bamboo fiber reinforced bio-composites are still limited.

2.11 MOTIVATION

The research on bamboo fiber-reinforced bio-composites is motivated by several factors. First, it aligns with global sustainability efforts, as bamboo is a rapidly renewable resource that can replace less sustainable materials like plastic and metals, contributing to eco-friendly alternatives. Additionally, bamboo's low environmental impact and biodegradability can help reduce carbon emissions and pollution, making it an environmentally friendly choice. Furthermore, this research offers economic opportunities in the rapidly growing bio-composites industry, potentially creating jobs and business growth. Bamboo's excellent strength-to-weight ratios make it suitable for reinforcement, leading to lightweight and durable materials. Finally, there is a growing market demand for sustainable materials, making bamboo fiber-reinforced bio-composites a valuable solution. In conclusion, this research has the potential to address sustainability challenges, drive innovation, and positively impact the environment and society, making it a motivating endeavor for those committed to eco-friendly solutions.

2.12 RESEARCH QUESTIONS

The major research questions for the present thesis are as follows:

1. How do the material properties of fibers extract from different radial parts (inner, middle, and outer) of the Bambusa tulda bamboo culm differ, and what are the implications of these differences in the performance of bamboo-based bio-composites?

2. What is the effect of varying concentrations of NaOH solution on the mechanical, thermal, and dielectric properties of bamboo fibers and the resulting bio-composites?

3. How do different weight percentages of bamboo fiber and NaOH concentrations influence the thermal, dielectric, static, and dynamic mechanical properties of bio-composites, and how

TH-3447_196103002

suitable are these composites for automobile interior and different structural applications?

2.13 OBJECTIVES OF THE PRESENT WORK

Based on the current literature survey, the following research objectives are proposed for the present research work:

1. To extract fiber from three different parts (inner, middle and outer part of the bamboo culm in the radial direction) of *Bambusa tulda* by using suitable fiber extraction process. To conduct complete material characterization by performing SEM, FTIR, XRD, TGA, UTM tesing.
2. To study the effect of NaOH solution concentration (2, 4, 6, 8, 10 % w/v ratio) on the fibers and composites.
3. To investigate the effect of various weight percentage of fiber as well as NaOH concentrations on thermal, dielectric, static and dynamic mechanical properties of developed bamboo based bio-composite.
4. To develop bio-composites with bamboo fiber as reinforcement material and different bio-polymer as matrix materials and study their physical, thermal and mechanical characteristics for automobile interior applications.
5. To develop hybrid bio-composites with bamboo fiber and bamboo micro particles as duel reinforcement phase. Further, study and compare their different structural and mechanical properties.

2.14 RESEARCH NOVELTY

The novelty of the proposed research lies in several key areas:

1. Firstly, the extraction and comprehensive material characterization of fibers from different radial parts of Bambusa tulda using advanced techniques (SEM, FTIR, XRD, TGA, UTM) provide unprecedented insights into their properties.

TH-3447_196103002

2. Secondly, the systematic study of NaOH solution concentration effects on fibers and composites addresses a gap in the understanding of chemical treatment optimization.

3. Thirdly, the investigation of the influence of fiber weight percentages and NaOH concentrations on thermal, dielectric, static, and dynamic mechanical properties of bamboo-based bio-composites is a novel approach.

4. Fourthly, developing bio-composites with bamboo fibers and various biopolymers specifically for automobile interior applications emphasizes practical innovation and sustainability.

5. Finally, developing and comparing hybrid bio-composites with dual reinforcement phases (bamboo fibers and micro particles) introduces a unique perspective on enhancing structural and mechanical properties. This multifaceted research significantly advances the field of bamboo-based bio-composites for structural application.

2.15 CONCLUSION

This chapter provides a comprehensive literature review covering various aspects, including different types of bamboo fiber, the classification of bamboo fiber extraction, chemical treatment of the fiber, development of diverse bamboo-based biocomposites, the impact of various matrix materials on biocomposites, and the exploration of bamboo-based hybrid biocomposites. Through an exhaustive literature survey, research gaps were identified, motivating the undertaking of the current study. The survey also played a crucial role in defining the research objectives. The chapter concludes with an overview of the thesis structure. The subsequent chapter (**Chapter 3**) initiates with a focused exploration of bamboo fiber extraction from *Bambusa tulda*, and concluded with their potentiality analysis for reinforcing bio-composites.

TH-3447_196103002

Chapter 3

Classified Extraction of *Bambusa tulda* Fiber for Bio-Composite Reinforcement

3.1 INTRODUCTION

Bamboo is an inherently functional material, exhibiting variations in structural and constituent properties from the inner part to the outer part in the radial direction. These variations contribute to its diverse mechanical and physical properties. In this chapter, for the first time, bamboo fibers are extracted from three different parts (i.e. inner, middle, and outer parts of the culm in the radial direction) of *Bambusa tulda*. *Bambusa tulda* is one of the bamboo species highly available in the northeastern part of India, especially in the Assam region. The different materials used for this study are presented in **Sec. 3.2.1**. The fibers are extracted using the retting process. The detailed classified extraction process is presented in **Sec. 3.2.2**. Furthermore, the extracted fiber is characterized by performing structural morphology analysis using FESEM (Field Emission Scanning Electron Microscopy) images, chemical composition analysis by measuring different constituents of bamboo fiber. Extracted fibers are further analyzed for density, crystallinity index, crystalline size, and thermogravimetric analysis (TGA). The tensile properties, such as tensile strength, tensile modulus (Young's modulus), and elongation before break value for the extracted fiber from different regions, are measured, and their statistical analysis is performed using the Weibull distribution. **Sec. 3.3** presents the detailed characterization of the extracted fiber. The investigation revealed that the technical fiber extracted from the outer part (external technical fiber) of the bamboo culm has a higher cellulose content (58.13 ± 3.51%), higher crystallinity index (60.142%), greater

TH-3447_196103002

tensile strength (365.014 ± 50.441 MPa), modulus (14.098 ± 1.763 GPa), low moisture absorption capacity, and higher thermal stability than fibers from the middle and inner parts of the bamboo. Additionally, a comparative study of Bambusa tulda fiber with other previously reported fibers is done and presented in **Sec. 3.4**. The comparative study shows the great potential of external technical fiber (ETF) as reinforcing materials for biocomposites. This study will help develop *Bambusa tulda*-based sustainable bio-composites for futuristic applications.

3.2 Material and Methods

3.2.1 Materials

The bamboo culms in the age group of 3.5 to 5 years of species Bambusa tulda were purchased from the local Nursery at Guwahati. The benzene (C_6H_6) (95% pure), ethanol (C_2H_5OH) (99.9% pure) and sodium hydroxide pellet (NaOH) were procured from Sigma-Aldrich, India. Sulfuric acid (H_2SO_4) (98% pure), Barium chloride ($BaCl_2$), filter paper and litmus paper were purchased from Merck Life Science Private Limited, India.

3.2.2 Extraction of Bamboo Fiber

Bamboo green culms of 350 to 400 mm length (diameter of 60 to 65mm) were selected for cleaning and the knots were removed with the help of a knot cleaning machine (Freshly harvested, green culms have high moisture content, which gradually decreases as they dry. This drying process, known as seasoning, can lead to shrinkage and increased brittleness. Green culms are heavier due to the high-water content. As they dry, they become lighter.It is easier to extract fiber from green culm rather than dry culm). Thereafter, the cylindrical culm was split into four pieces using a splitting machine. The thickness of the cut culm was measured as 14 ± 2 mm. Then with the help of a planner machine, the epidermal (most inner layer) and endodermal (most outer layer) of the bamboo was removed and billets were made. The average thickness of the billet was maintained as 12 ± 1 mm and length as 350 ± 10 mm. Thereafter each billet was cut vertically into 3 equal thickness strips. The thickness of each strip was maintained at 4 ± 0.5 mm. Strips are taken from the outermost, middlemost and innermost part of the culm and are known as external strip, middle

TH-3447_196103002

strip, and internal strip, respectively. The strips were soaked in distilled water for 3 days and fibers were peeled with the help of a sharp knife and comb. The extracted fibers were placed into a hot air oven for 4 hrs at 80 °C. This fiber extraction process is named as retting process [208]. In the previous study, the retting method was found to be the most appropriate process for continuous (long) fiber extraction [102]. The fiber extracted from external, middle and internal strips were named as external technical fiber (ETF), middle technical fiber (MTF) and internal technical fiber (ITF). The average length of the extracted fiber was measured as 300 ± 7 mm. **Fig. 3.1** (a), (b), (c) and (d) show the selected bamboo clum, cross-sectional view and strip classification of bamboo culm, water submerged bamboo strips and extracted technical fiber, respectively.

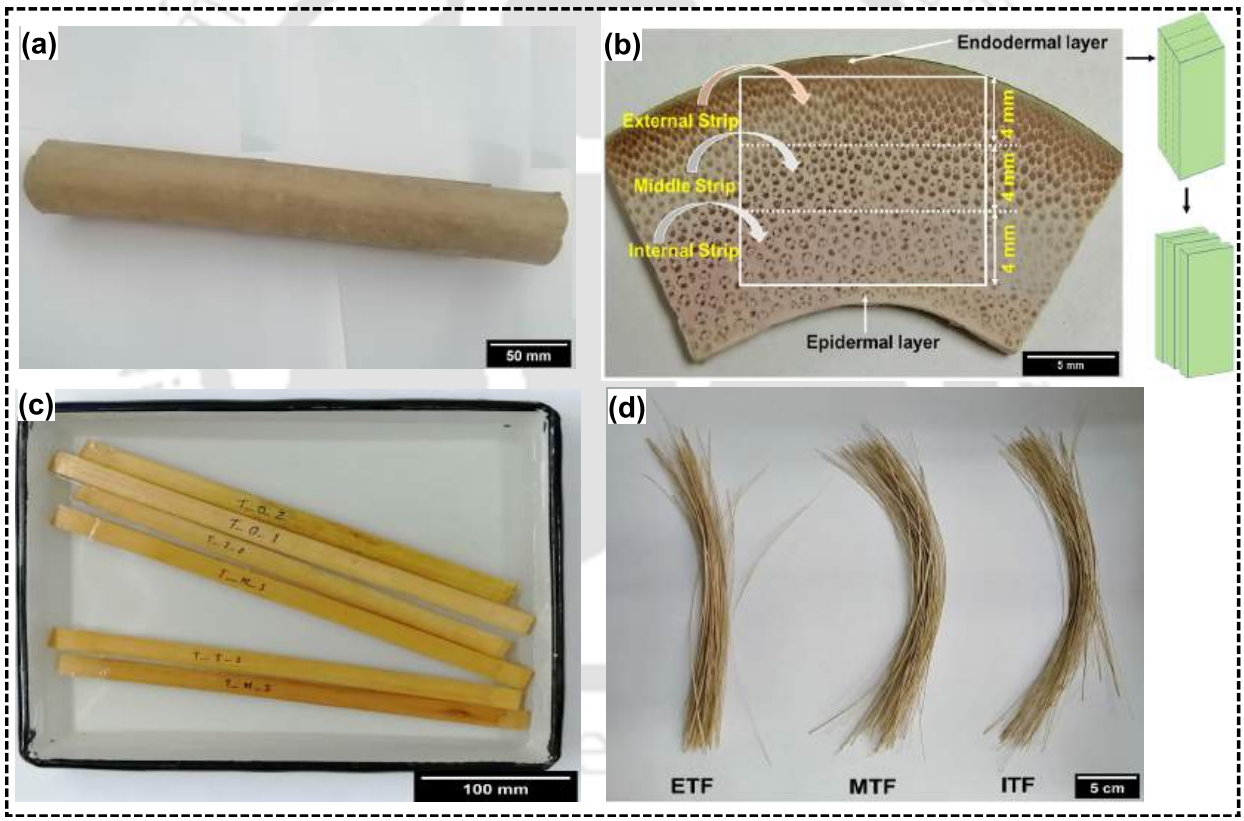

Fig. 3.1: (a) bamboo clum, (b) cross-sectional view and strip classification of bamboo culm, (c) water submerged bamboo strips and (d) extracted technical fibers.

3.2.3 Characterization of Fiber

A detailed analysis of the extracted fiber has been carried out in order to understand its physical, mechanical, thermal, and structural characteristics. In this section, detailed results are presented.

TH-3447_196103002

3.2.3.1 Structural Characterization

The structural morphology of all three types of fiber (internal, middle and external) was examined with the help of Sigma field emission microscopy (Make: Zeiss, Germany). As the natural fibers are non-conductive or less conductive [209], to increase the conductivity of the samples thin film of gold was coated. The Sputter coater (model: BALTEC-SCD-005, USA) is used for very thin gold coating on the fiber samples. To investigate the diameter of the original single fiber, the FESEM image was analyzed with the help of ImageJ software (open-source software). The diameters of randomly selected twenty-five original single fiber from each group were measured and statistical analysis was done with the help of Minitab 17 software (student version).

3.2.3.2 Diameter of Technical Fiber

The diameters of technical fiber were determined by randomly selecting twenty-five fibers from each group and examined under a stereomicroscope (Model: SMZ25, Nikon, Japan). The diameter of each technical fiber was measured at five different places of the fiber and the mean value has been reported.

3.2.3.3 Chemical Composition of Fiber

The chemical composition of the fiber played a vital role in the physical and mechanical properties of the fiber. The general chemical composition of natural fiber is cellulose, hemicellulose, lignin, extractive, ash and moisture [24]. The extracted fiber from three different regions (outer, middle and inner part of the bamboo culm) were ground into powder as used as a sample of chemical composition. The moisture content of fiber was obtained by putting 1 gm of ground fiber into a hot oven (IKON, Model: IK-109, India) at 105 ± 5 °C till constant weight was achieved [210]. The moisture content of the samples (W_1) was calculated through the weight difference of the samples as per **Eq.3.1**. Ash content (W_2) of oven-dried samples were determined by heating samples at a muffle furnace (YOMO, Model: MF – 5510 D, India) at 580 ± 20 °C for 4hrs as per **Eq.3.2** [211].

Other components like- extractive, hemicellulose, lignin and cellulose content were determined by the process described in the literature S. Li et al. [212] and A. Verma et al. [213] The flow process

TH-3447_196103002

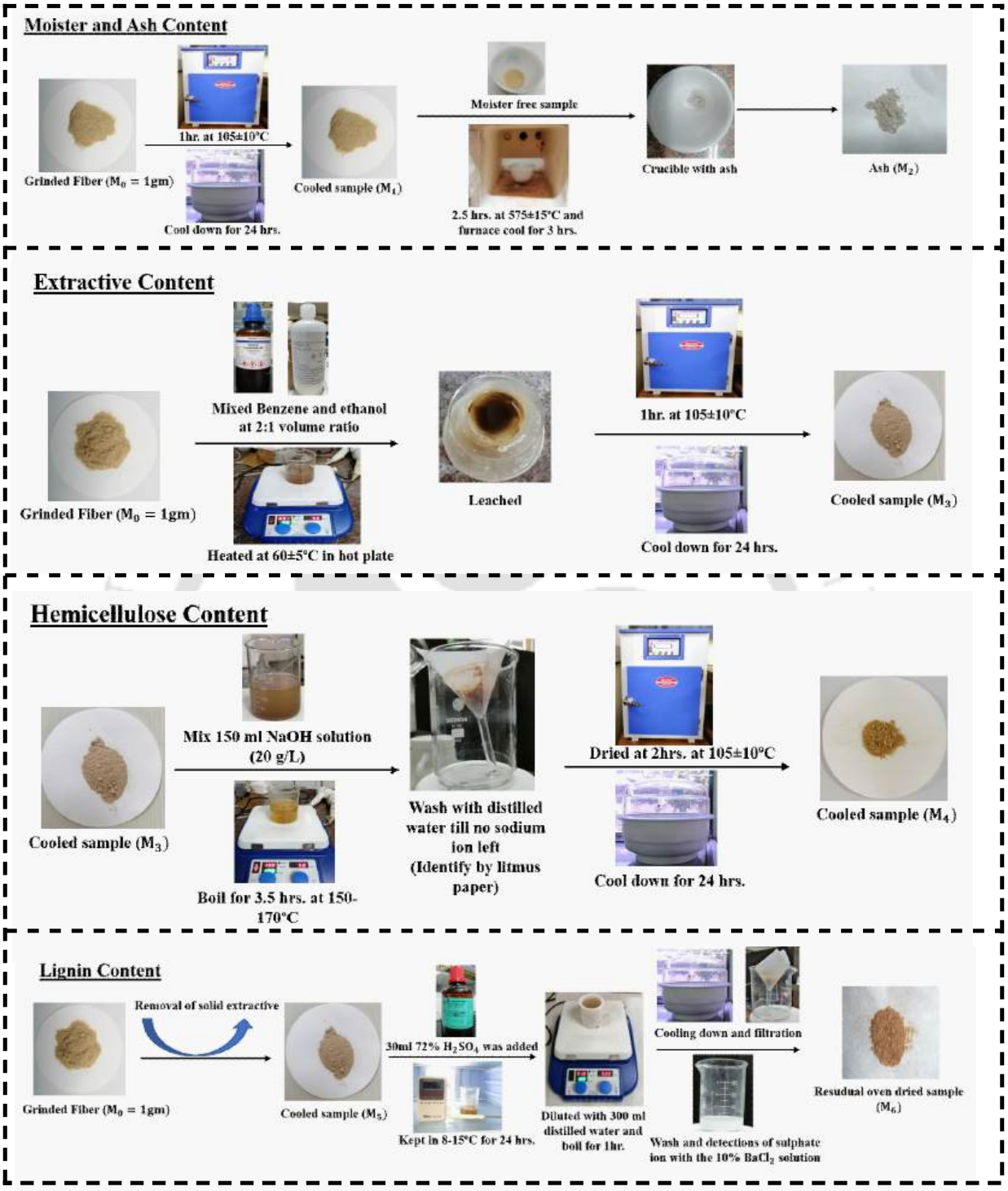

Fig. 3.2: Flow diagram of the chemical composition analysis.

has been presented in **Fig. 3.2**. The following equations **Eq.3.3**, **Eq.3.4**, **Eq.3.5** and **Eq.3.6** are used to find extractive percentage (W_3), hemicellulose (W_4), lignin (W_5) and cellulose (W_6) weight

TH-3447_196103002

fraction, respectively.

$$W_1 = \frac{M_0 - M_1}{M_0} \times 100\% \tag{3.1}$$

$$W_2 = \frac{M_2}{M_0} \times 100\% \tag{3.2}$$

$$W_3 = \frac{M_1 - M_3}{M_0} \times 100\% \tag{3.3}$$

$$W_4 = \frac{M_3 - M_4}{M_0} \times 100\% \tag{3.4}$$

$$W_5 = \frac{M_6}{M_0} \times 100\% \tag{3.5}$$

$$W_6 = 100 - (W_1 + W_2 + W_3 + W_4 + W_5) \tag{3.6}$$

Where M_0 is the initial mass, M_1= measured mass after moisture is removed, M_2= mass of ash, M_3= mass after removal of extractive, M_4= mass after removal of hemicellulose and M_6 is the mass of lignin residue of grounded fiber.

3.2.3.4 Density of Fiber

The density of the extracted fiber from the different regions (internal, middle and external) of bamboo culm was determined with the help of a Pycnometer as solid and toluene as the liquid medium. The samples and results were prepared as per ASTM D 2320-98 [214]. The extracted fiber was chopped and dried in a hot air oven at 70 °C for 4 hrs to remove moisture content. The density of the fiber bundles is calculated by **Eq.3.7**.

$$\rho_{fiber} = \frac{(m_3 - m_1)}{(m_2 - m_1) - (m_4 - m_3)} \rho_{liq} \tag{3.7}$$

where, ρ_{fiber} is the density of fiber,ρ_{liq} is the density of liquid used (here it is toluene,0.8623 gm/cm^3 at 25°C). m_1 is the mass of pycnometer at empty condition, m_2 is the mass of pycnometer filled with toluene, m_3 is the pycnometer's mass filled with chopped bamboo fiber and m_4 is the mass of the pycnometer filled with both toluene and chopped fiber. The electronic precise weighing balance of Sartorius (Model: Cubis®, Germany) with an accuracy of ±0.1mg was used to measure the weight of the sample. Five bundles from each sample have been taken for density measurement and the average density is reported with standard deviation.

TH-3447_196103002

3.2.3.5 XRD Analysis

A powder X-ray diffraction (XRD) analysis was performed using BRUKER (model: D8 advance, United States) to determine the crystallographic information of classified extracted bamboo fiber under Cu-Kα radiation ($\lambda = 1.542\mathring{A}$) operated at 30kv/15mA. The intensity count has been recorded between 2θ= 10 to 60 ° with a speed of 2 °/min and step size of 0.02 °. The crystallinity index of the fiber samples was determined with the help of the Ruland-Vonk method as per **Eq.3.8** and the crystalline size of the fiber samples was determined with the help of Scherrer's formula as per **Eq.3.9** [215].

$$Cr\% = \frac{(A_T - A_{Am})}{A_T} \times 100\% \tag{3.8}$$

$$CS = \frac{K \times \lambda}{\beta \times Cos\theta} \tag{3.9}$$

where A_T is the total area under the XRD graph, and A_{Am} is the area of the amorphous zone. where K, β, λ and θ are denoted as Scherrer's constant, full-width half maximum of the peak, the wavelength of radiation and Bragg angle, respectively.

3.2.3.6 FTIR Analysis

A Fourier transform infrared spectroscopy (FTIR) was carried out on different extracted fiber to determine the presence of the functional group. The FTIR experiment was performed in Attenuated Total Reflection (ATR) mode with the help of the PerkinElmer (Model: Spectrum-2, Singapore) spectrometer. FTIR spectra were recorded between 4000 cm^{-1} to 400 cm^{-1} with a resolution scan of 2 cm^{-1}. For this experimental work, each sample was scanned 12 times and an integrated graph has been presented as the final result. To prepare the sample of FTIR, the bamboo fiber extracted from different radii has been ground into powder and mixed with KBr (Potassium Bromide) with a weight ratio of 1:150 (10 mg of ground bamboo fiber was mixed with 1500 mg of KBr) and compressed in a circular mould to form pellet for the experiment [216]. The FTIR analysis helps to identify the constituents of natural fibers, such as cellulose, hemicellulose, lignin, and wax. This understanding aids in interpreting the results of tensile testing of the fibers. Additionally, it allows for the explanation of mass losses at different temperatures for natural fibers.

TH-3447_196103002

3.2.3.7 Mechanical Testing

Tensile properties (tensile strength, modulus, and elongation before break) of extracted technical fiber was measured by tensile testing. Shimadzu Tensile testing machine was used (model: AGX-V, Japan) with a load cell of 1 kN (minimum load applying capacity of 0.001 N) for tensile testing. Twenty-five samples of each group (external, middle and internal extracted) of fiber were tested by following ASTM D-3822-07 [89] standard. The gauge length of 40 mm and a crosshead speed of 0.5 mm/min (engineering strain rate of 0.0002083 S^{-1}) was considered for testing. The environmental condition of testing was 25°C temperature and 65% relative humidity. Due to the presence of deviation in the testing result, the statistical analysis of the results was performed with the help Weibull model in Minitab 17 software (student version). **Eq.3.10** presents the basic model of Weibull distribution [90]. Where m is the shape parameter and η is the scale parameter.

$$F_x = 1 - e^{-\left(\frac{x}{\eta}\right)^m} \tag{3.10}$$

3.2.3.8 Water Absorption Test

Natural fibers are hydrophilic. The moisture content of fiber plays a vital role in the processing and performance of bio-composite. The water absorption test of the fiber was performed by soaking it into distilled water at room temperature (25°C) with an RH value of 65% for different durations (300 seconds to 7200 seconds with equal time intervals). Finally, the water absorption percentage was calculated with the help of **Eq.3.11**. Five fiber samples of each group were tested and the average value was reported.

$$M_W = \frac{W_t - W_d}{W_d} \times 100\% \tag{3.11}$$

where M_W = moisture content,W_t= weight of fiber sample at time t, W_d= weight of dry fiber sample.

3.2.3.9 Thermogravimetric Analysis

For high-temperature applications, the thermogravimetric analysis (TGA) of the substance is very important. TGA analysis of the extracted fiber was performed with the help of the Perkin Elmer

TH-3447_196103002

Instrument (model: STA 800, USA). 5 mg to 8 mg of ground fiber samples were heated from room temperature (25°C) to 600°C with a heating rate of 10°C/min in a nitrogen atmosphere and weight loss curves have been recorded. The study chose TGA over DSC due to its focus on thermal stability and compositional analysis, as TGA better addresses thermal degradation and stability of composite materials. While DSC provides insights into phase transitions, incorporating both TGA and DSC in future studies could offer a more comprehensive thermal analysis.

3.3 RESULTS AND DISCUSSIONS

3.3.1 Structural Morphology of Bamboo Fiber

The structural morphology is very important to understand the internal structure of natural fiber and it helps to determine its potentiality as a reinforcing material in any bio-composites [192]. The morphology of technical fiber has been observed with 500 times magnification and presented in **Fig. 3.3** (a), (b) and (c). Like other natural fiber, the technical fibers are composed of many single fibers or elementary fibers (sometimes it is also called microfibril). The growth direction of these single fiber is parallel to the length of technical fiber or bundle fiber. The major component of a single fiber is cellulose. This cellulose made the skeleton of the cell wall and non-cellulose components like- hemicellulose, lignin etc act as filling material for these skeletons [217]. The cellulose skeleton provides elasticity and strength to the bamboo fibers. Whereas non-cellulosic compounds, lignin act as the binding material of these microfibrils. This non-cellulosic material helps the fiber to distribute the externally applied load homogeneously throughout the fiber body [218]. It is observed that the numbers of single fibers were more for ETF and they were smaller in diameter and distributed densely. Whereas for MTF and ITF the single fiber's distribution density gradually decrease compared to ETF. Not only density but also diameter of single fiber, is varied from ETF to ITF. To understand the diameter distribution of a single fiber, the diameter of 25 single fibers from each technical fiber has been measured with the help of ImageJ software and statistical analysis has been performed. **Fig. 3.3** (d), (e) and (f) showed Weibull distribution of single fiber diameter inside ETF, MTF and ITF, respectively. The statistical parameters for the diameter of single fibers in different technical fibers are presented in **Table 3.1**.

TH-3447_196103002

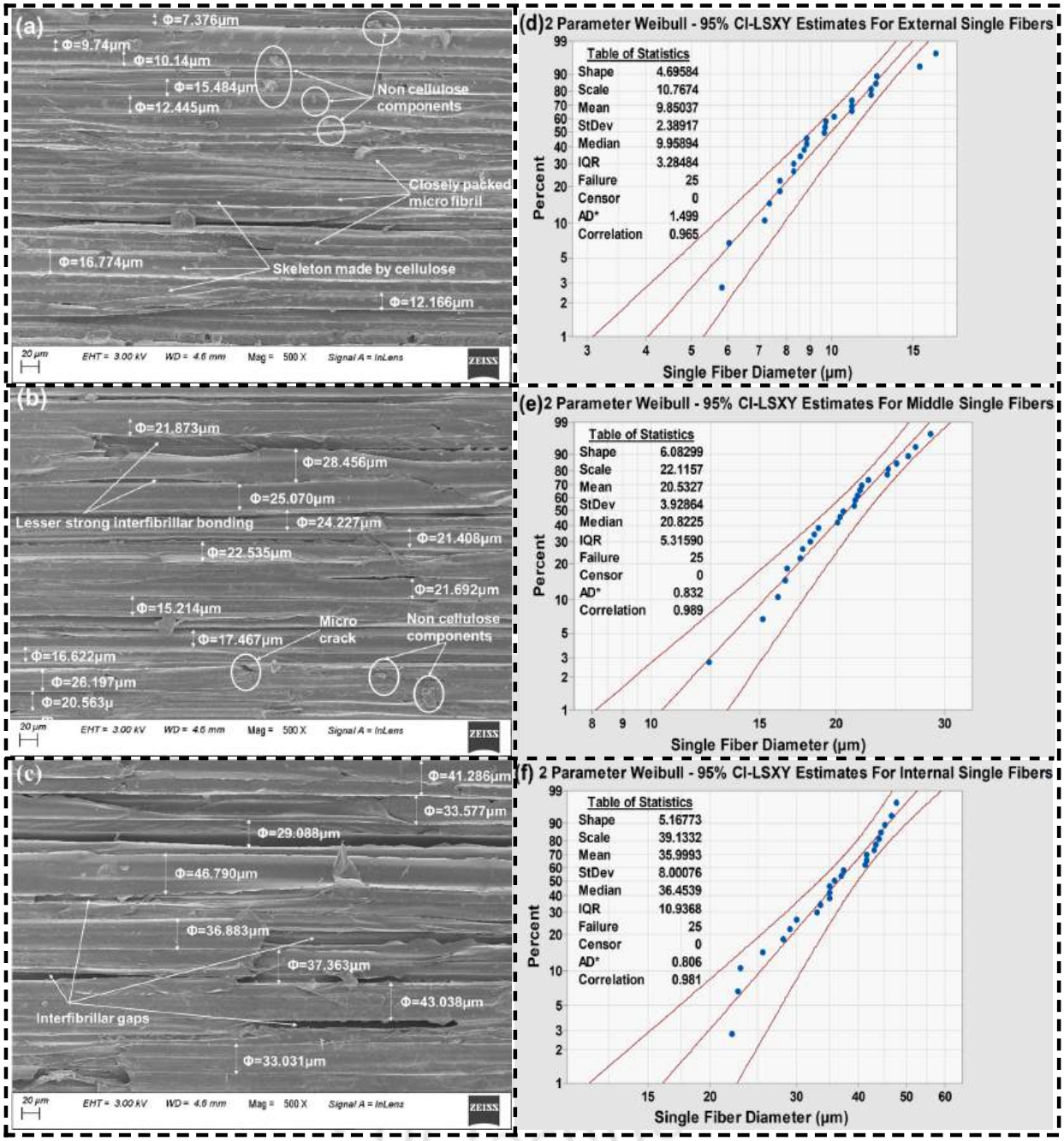

Fig. 3.3: SEM image of (a) ETF, (b) MTF and (c) ITF, Weibull distribution for single fiber diameter in (d) ETF, (e) MTF and (f) ITF.

Table 3.1: Statistical parameters for diameters of single fibers in different technical fibers

Fiber Type	Shape	Scale	Mean	Median	St. Dev	IQR	Co-relation
ETF (micron)	4.695	10.767	9.850	9.958	2.389	3.284	0.965
MTF (micron)	6.082	22.115	20.532	20.822	3.828	5.315	0.989
ITF (micron)	5.167	39.133	35.999	36.453	8.000	10.936	0.981

TH-3447_196103002

In bamboo, the diameter of a single fiber and its distribution density gradually vary from the exterior to the interior, making it a functionally graded material [218]. For Mechanical or manual extraction of fiber it is difficult to remove all parenchyma cells from the fiber. But it could be removed after chemical treatment of fiber. The higher value of single fiber distribution density makes the technical fiber stronger. So, for any bio-composite, ETF is a more suitable reinforcement material compared to MTF and ITF.

3.3.2 Diameter of Technical Fiber

Technical fiber diameter is a very important parameter for the design and development of fiber-reinforced composites. The diameter of the extracted fiber sample was measured with the help of a stereomicroscope. **Fig. 3.4** (a) (b) and (c) shows the diameter of technical fiber extracted from the internal, middle and external parts of the bamboo culm. It is observed that the average diameter of ETF, MTF and ITF are 689.575 ± 12.678; 642.492 ± 13.562 and 616.445 ± 5.024 µm, respectively. It can be seen that ETF is thicker than MTF and ITF. The diameter of technical fiber is affected by arrangement, tightness and number of single fibers present in it. The arrangement of the vascular bundle inside the bamboo is also a major factor and it influences the technical fiber's diameter [89].

The external technical fiber contains closely packed single fibers and efficiently arranged vascular bundles.Therefore, the separation of fiber bundles from one to another was difficult and it results in higher technical fiber diameter. However, it was easier to separate the internal technical fibers, which resulted in smaller diameters. Smaller pore size with larger technical fiber diameter may lead to better fiber wettability. Further, it may form better fiber-matrix interfacial bonding which leads to better mechanical properties [89]. In the present case, ETF shows its characteristics and thus it is a more appropriate reinforcing material compared to the other two types of extracted fibers.

3.3.3 Density of Fiber

The density of ETF, MTF and ITF have been measured as 0.9174 ± 0.0268 gm/cm^3, 0.8305 ± 0.0207 gm/cm^3 and 0.6968 ± 0.0213 gm/cm^3, respectively. The density of ETF is quite higher than the density of ITF and MTF. It may be due to the presence of higher single fiber density inside ETF bundles. A similar type of density variation has also been reported in previous research with bamboo

TH-3447_196103002

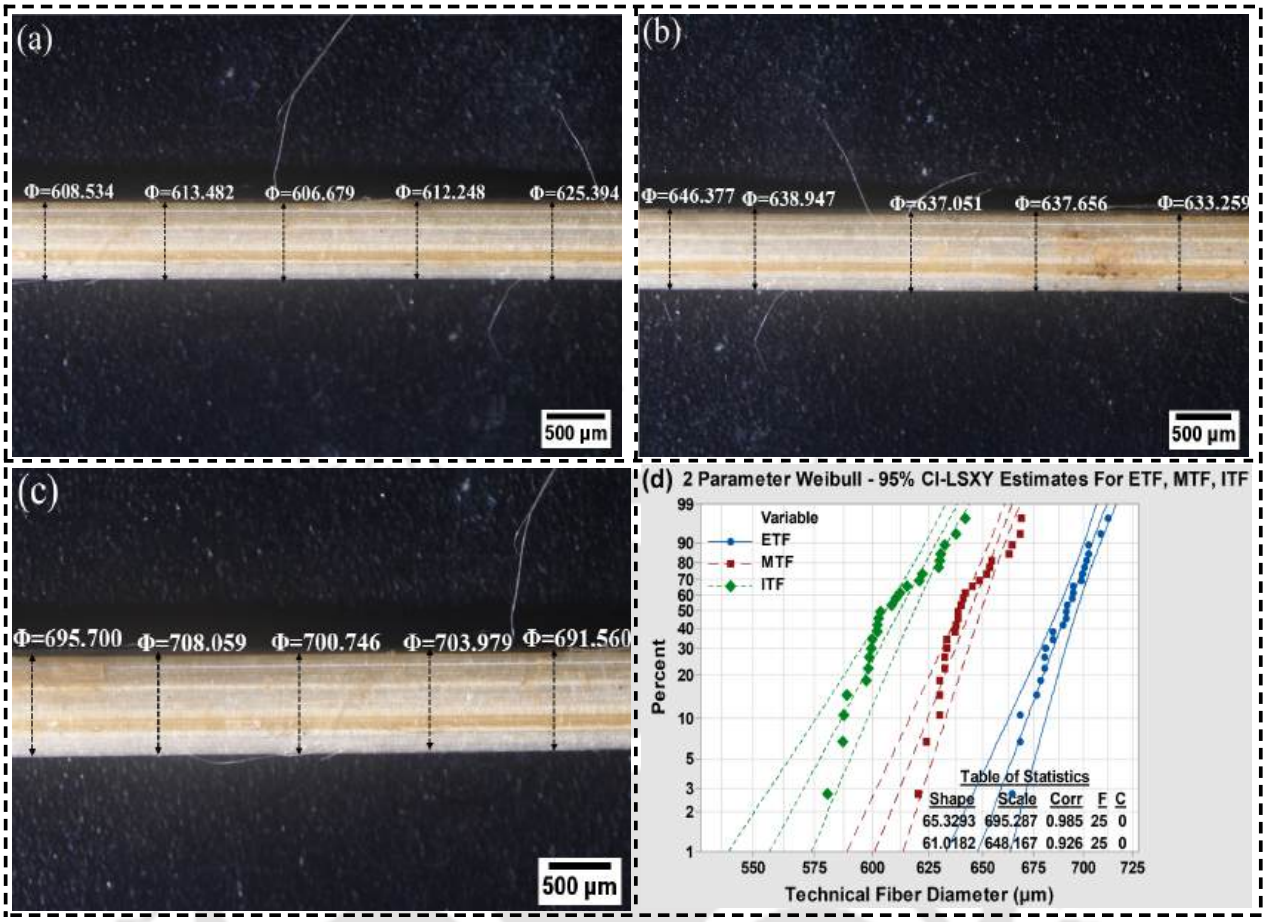

Fig. 3.4: Diameter of technical fiber (a) ITF, (b) MTF, (c) ETF, and (d) Weibull distribution for technical fiber diameters.

culm [34]. The density of the reinforcing material played a vital role in the development of polymer-based bio-composite. The general density of thermosetting polymers is in the range of 1.1 to 1.3 gm/cm^3 [219]. At the time of the composite fabrication process, if the density of reinforcing fiber is much lower than the matrix, then due to bouncy the fiber may float on the upper surface of the composite plate. If the density of the fiber is much higher than the polymer matrix then it may sink to the lower surface of the developed polymer plate. This may lead to the development of defective composite plates [220, 221]. Due to the change in viscosity of the material and its penetration into asperities as well as the porous surface of the fiber, the apparent density of the fiber changes when it is subjected to high pressure and temperature [89, 220]. The density of ETF tulda fiber is lesser than Chilean bamboo, Korea (1.1 gm/cm^3) [49], *Bambusa Oldhami*, China (1.08 gm/cm^3) [175], and Moso bamboo, China (0.93 gm/cm^3) [222], whereas higher than Guadua bamboo, Colombia (0.6 gm/cm^3) [223], *Neosinocalamus affinis*, china (0.72 gm/cm^3) [167] and *Phyllostachys pubescens*,

TH-3447_196103002

china (0.751 gm/cm^3) [106]. Therefore, the comparative study revealed that external technical fiber (ETF) can be used as a reinforcing material potentially for the development of bio-composites with low density.

3.3.4 Chemical Composition

The structure and mechanical properties of the natural fiber are directly dependent on the chemical composition of the fiber. In the present study, the ETF has shown 58.13 ± 3.51% of cellulose content, which is 6.49% and 16.11% higher than MTF and ITF. The cellulose content provides fiber strength, stiffness and crystallinity [224]. So, higher cellulose content may provide the ETF with higher tensile strength and tensile modulus compared to MTF and ITF. The lignin act as the binding material of the microfibril and provides the fiber with a higher load-bearing capacity and protects the fiber from moisture and biological attack [223]. The ETF shows 18.39 ± 1.15% lignin content. This value is 12.39% and 35.39% higher than MTF and ITF. The hemicellulose act as cementing material of the cellulose skeleton. It is also one of the amorphas materials present in the fiber [167]. The ETF shows 14.76 ± 2.97% hemicellulose content, which is 24.46% and 40.95% lower than MTF and ITF. The higher moisture and extractive content results in less interfacial bonding between fiber and polymer matrix [104, 224]. It has been observed that for the ETF, both moisture and extractive contents are lower compared to MTF and ETF. The graphical representation of the chemical composition of all three types of technical fibers are presented in **Fig. 3.5** and a comparative study for chemical composition with other previously reported bamboo fibers has been presented in **Table 3.2**.

3.3.5 XRD Analysis

The X-ray diffraction of ground fiber has been performed and the diffraction curve has been presented in **Fig. 3.6**. It has been observed that all three types of technical fiber show three peaks (one sharp and two broads). For ETF these picks are at 2θ= 15.68°, 22.24° and 34.92° whereas for MTF and ITF these 2θ values are 15.53°, 22.2°, 34.86° and 15.46°, 22.18°, 34.72°, respectively. The peak around 2θ= 15°, 16°, 22° and 34° are corresponding to the crystalline plane (1 $\bar{1}$ 0), (1 1 0), (0 0 2) and (0 4 0) respectively [103, 226]. The Peaks for (1 $\bar{1}$ 0) and (1 1 0) planes are

TH-3447_196103002

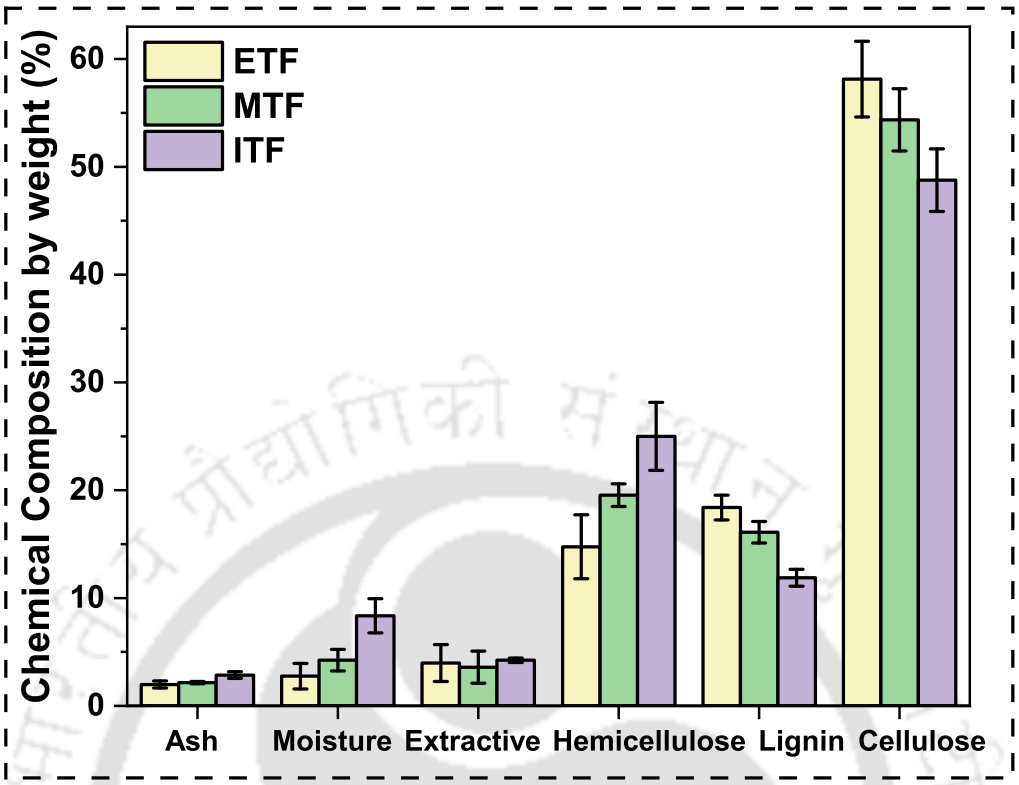

Fig. 3.5: Chemical composition in technical fibers.

Table 3.2: Comparative study for chemical composition of ETF with other previously reported bamboo fiber.

Bamboo Specimen	Cellulose (%)	Hemicellulose (%)	Lignin (%)	Extractive (%)	Ash (%)	Moisture (%)	Reference
Bambusa tulda (ETF)	58.13± 3.51	14.76± 2.97	18.39± 1.15	3.97± 1.20	1.98± 0.33	2.75± 1.18	Present study
Bambusa heterostachya	54.61	6.85	20.85	10.69	3.45	3.55	[224]
Moso (China)	66.7	11.0	19.0	1.8	0.3	1.8	[167]
Bambusa emeiensis	72.6	11.1	9.5	3.4	2.2	1.2	[224]
Guaduaangustifolia Kunth	58.63	13.37	26.45	–	–	–	[223]
Phyllostachys pubescens	40.1	32.9	26.6	3.1	1.2	–	[225]
Neosinocalamus affinis	74.1	21.46	0.72	1.38	–	–	[171]
Dendrocalamopsis oldhmami	45.0	26.1	23.1	3.9	1.5	–	[104]
Phyllostachys Pubescens	43.41	23.96	24.25	–	–	–	[136]

TH-3447_196103002

overlapped [227]. The reason behind the peak at 15.68°, 16.6° and 22.24° are due to the presence of cellulose Iβ (native cellulose) inside the bio fiber [228]. Due to the presence of amorphous material inside the technical fibers a broad amorphous peak has been observed at around 2θ=18 to 19° for all three types of extracted fibers. As per the recommendation of Lila et al.[90], due to the smaller crystalline size of cellulose, the Ruland-Vond method has been adopted to find out the crystalline index of technical fiber rather than the Segal method [89]. The 'Origin 2021b (student version)' software was used to find the area of the curves and graphical analysis.

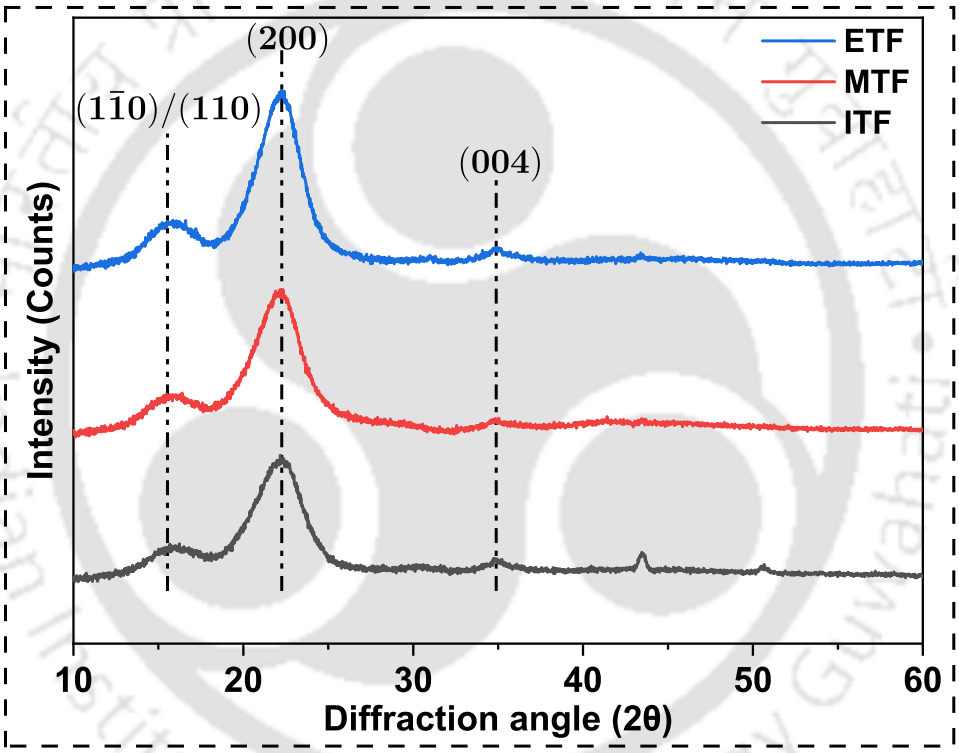

Fig. 3.6: XRD pattern of technical fibers.

The crystallinity of the ETF has been found as 60.142% whereas for MTF and ITF this crystallinity value has been calculated as about 55.613% and 48.842% respectively. The crystallinity index of ETF is 4.529% and 11.3% higher than MTF and ITF respectively. The crystallinity value of ETF is higher than *Guaduaangustifolia Kunth* (58.63%) [171], *Phyllostachys Heterocycla* (51.28%) [125], *Neosinocalamus affinis* (53.42%) [223] and *Gigantochlea scotechini* (49.92%) [167] bamboo fiber but lesser than *Bambusa heterostachya* (62.5%) [110], *Phyllostachys Pubescens* (67.5%) [224] and Moso bamboo fiber (61.51%) [108]. From the XRD curve, the crystalline size of the ETF was

TH-3447_196103002

found as 2.578 ± 0.337 nm which was 2.40% and 5.85% higher than MTF (2.516 ± 0.379nm) and ITF (2.427 ± 0.3436nm). The bigger crystalline size is attributed to lower moisture absorption and chemical reactivity [228].

The bigger crystalline size and better crystallinity index exhibit rich cellulose contents in ETF, which may lead to less moisture absorption and better mechanical properties of developed bio-composites.

3.3.6 FTIR Analysis

The obtained FTIR spectra in ATR mode for ETF, MTF and ITF are shown in **Fig. 3.7**. The peak at 3344 cm^{-1} is due to the stretching vibration of the hydrogen bond of O-H (hydroxyl) groups

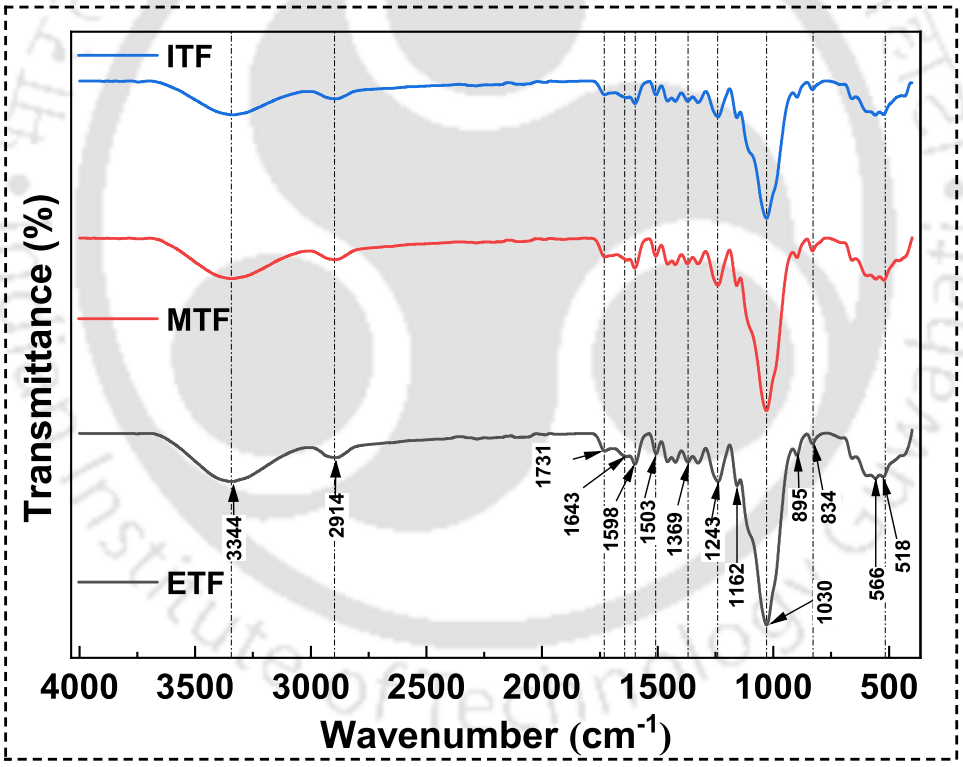

Fig. 3.7: FTIR spectra of technical fibers.

present in cellulose, hemicellulose and lignin. The presence of this hydroxyl group signifies that the fiber is hydrophilic. There are many numbers of hydroxyl groups present in cellulose that can interact with water or moisture by making hydrogen bonds. But interaction depends on the types of cellulose and its degree of crystallinity. On the other hand, the hydroxyl groups present in the amorphous phase are easily accessible to make a hydrogen bond with water [228]. The other peaks

TH-3447_196103002

for the assigned transmission band of FTIR spectrum have been tabulated in **Table 3.3**. The difference in functional group may lead fiber to different properties [89]. The FTIR analysis reveals that all three types of extracted technical fiber possess the same functional groups and the same type of chemical components (cellulose, hemicellulose, lignin, extractive and moisture).

Table 3.3: Assignment of transmittance bands in FTIR spectra.

Wave number (cm^{-1})	Assignment	References
3344	Stretching vibration of O-H groups present in Cellulose, hemicellulose and lignin	[229]
2914	Stretching vibration of C-H group of Cellulose and lignin	[230]
1731	C=O group's Stretching vibration of hemicellulose	[230]
1643	Water absorption	[110]
1598	Vibration of C=C bond in aromatic group of lignin	[216]
1503	C-O bonding vibration of lignin	[216]
1462	C-H and C-O bond stretching and bending vibration of lignin	[215]
141	Bending vibration of -CH2 group of cellulose and lignin	[231]
1369	Bending vibration of C-H2 bond present in cellulose and hemicellulose	[215]
1320	Due to bending vibration of C-H bond in cellulose	[231]
1243	Stretching vibration of C=O bond present in extractive and lignin	[232]
1162	Carbonyl groups present in hemicellulose	[232]
1030	C-C/C-O bond stretching vibration of cellulose	[215]
895	bending vibration of C-H group of cellulose	[233]
663	Vibration of O-H groups of cellulose	[221]
566	Vibration of p-hydroxyphenyl of propene in lignin molecule	[233]

3.3.7 Mechanical Properties Analysis

The extracted bamboo fiber was tested with the help of a static tensile machine under the same conditions. The fiber was grouped into 3 series, with 25 fiber specimens from each group (ETF, MTF and ITF), so a total number of 75 specimens were tested for this work. **Fig. 3.8** (a), (b) and (c) are the obtained stress-strain curves of ETF, MTF and ITF groups. It can be seen from the stress-strain curve that stress increases quasi-linearly as strain increases to its maximum and a sudden rupture is observed when stress reaches its maximum value. This behaviour of fracture is attributed to the brittle nature of the bamboo fiber, which is quite similar to other lignocellulose fibers [167]. The ETF showed a higher tensile strength value (365.014 ± 50.441 MPa) than MTF (250.147 ± 39.552 MPa) and ITF (147.925 ± 41.108 MPa). This may be due to the presence of higher cellulose content in EFT (about 6.49 and 16.11% higher than MTF and ITF respectively).

TH-3447_196103002

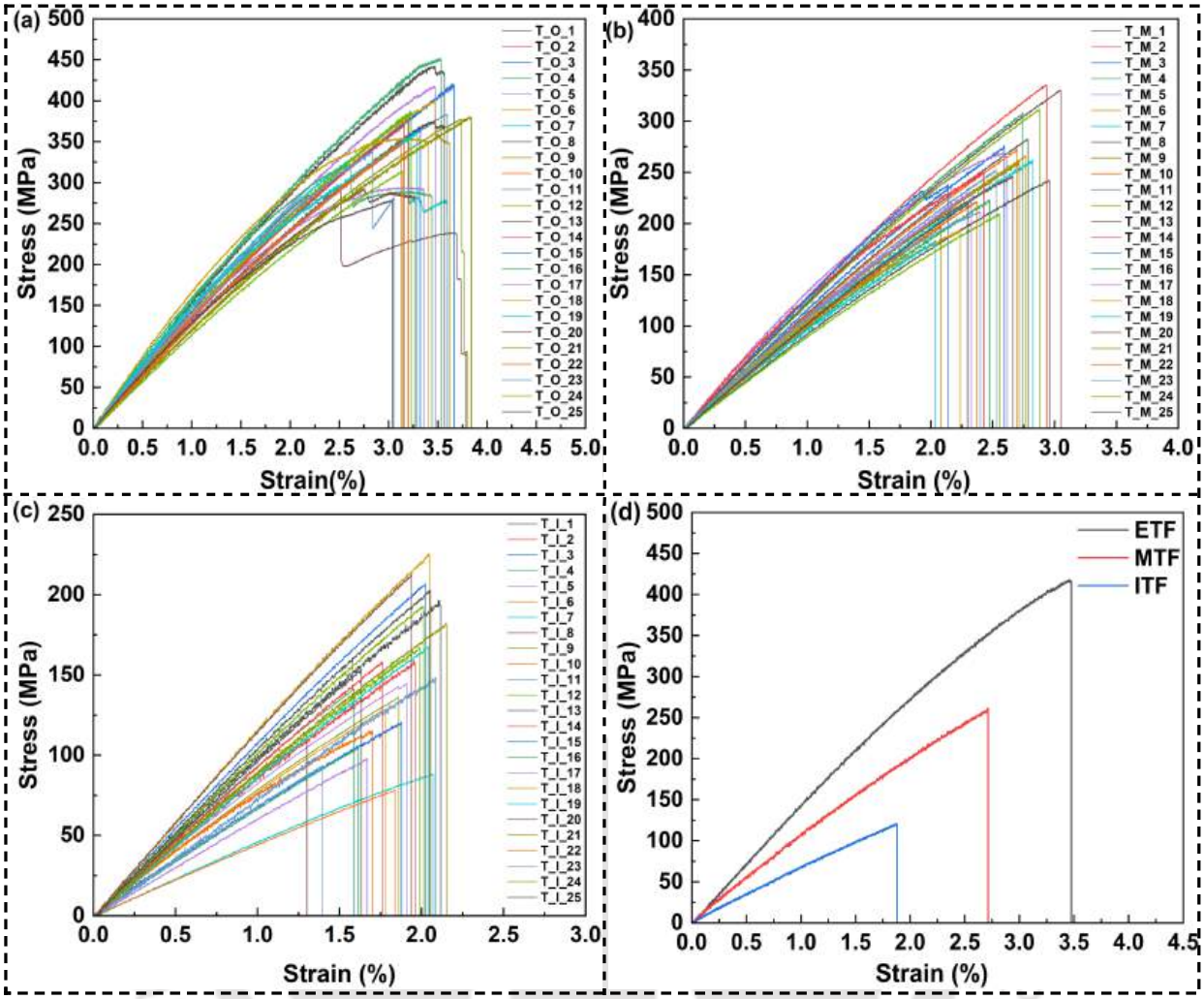

Fig. 3.8: Stress-strain curve for (a) ETF, (b) MTF, (c) ITF and (d) comparative stress-strain curve.

In addition, it could also be seen in the SEM image that the ETF microfibrils are tightly packed together which provides continuous solid structure and higher strength value. The ETF showed a tensile modulus value of 14.098 ± 1.763 GPa which is 24.35% and 41.52% higher than MTF and ITF. The higher tensile modulus of ETF is attributed to the greater crystallinity index of the fiber. The ETF has also higher lignin content (which acts as an adhesive material within bamboo microfibril), as a result of which the cellulose and hemicellulose components are tightly bound and showed greater strength and stiffness [171]. It is also observed that ETF has a higher value of elongation before break than MTF and ITF. As a result, ETF absorbs more energy before they fail than MTF and ITF. Several factors may affect the elongation before break value, such as microfibril angle and gauge length etc.[234]. **Fig. 3.8** (d) represents a comparative stress-strain diagram of

TH-3447_196103002

technical fiber.

The statistical analysis of mechanical properties was conducted with the help of Minitab version 17 commercial software (student version) using three and two-parameter Weibull law to determine suitable distribution. The two parameters' Weibull value was found much closer to the experimental mean values of the samples. So, two parameters Weibull was treated as most suitable for the analysis, a similar analogy was reported by Lila et al.[89] with Munja fiber and Amroune et al.[233] with date palm fiber. The two parameters Weibull distribution results for strength, strain at failure, and young's modulus of ETF, MTF, and ITF are shown in **Fig. 3.9** (a to f) and **Fig. 3.10** (a to d). The parameters of the Weibull modulus (shape factor) and Weibull scale were determined by using the least-squares estimation technique (LS). Statistical parameters of mechanical properties for *Bambusa tulda* are presented in **Table 3.4**. Moreover, it is evident that all the investigational data is spread around the line and fitted correctly. The Weibull distribution reveals a better correlation with a correlation factor (R^2) value of around 0.958 to 0.992.

The present results are compared with relative literature in **Table 3.5**. The present comparison shows that some of the bamboo varieties, like- *Dendrocalamus latiflorus*, Macana bamboo, *Phyllostachys heterocycla*, *Phyllostachys pubescens*, *Dendrocalamus asper*, *Gigantochloa levis* have higher strength and modulus than present bamboo (*Bambusa tulda*), whereas *Gigantochlea scotechini*, *Bambusa vulgaris*, *Gigantochloa scortechinii*, *Gigantochloa levis*, *Bambusa heterostachya* have lower strength than tulda. *Bambusa tulda* also exhibits higher values of elongation before the break compared to other previously reported bamboo fiber, except for *Phyllostachys pubescens* and *Phyllostachys heterocycla*. *Bambusa tulda* fibers with moderate tensile strength and modulus and higher elongation before break can serve as reinforcement for composites used in low to medium-load structural applications.

3.3.8 Moisture Absorption Behaviour

The result of the moisture absorption test is shown in **Fig. 3.11**. It can be seen from **Fig. 3.11** that ETF absorb less water as compared to MTF and ITF. At approximately 5400 seconds, all the samples start achieving saturation and after 7200 seconds, the moisture content of ITF, MTF

TH-3447_196103002

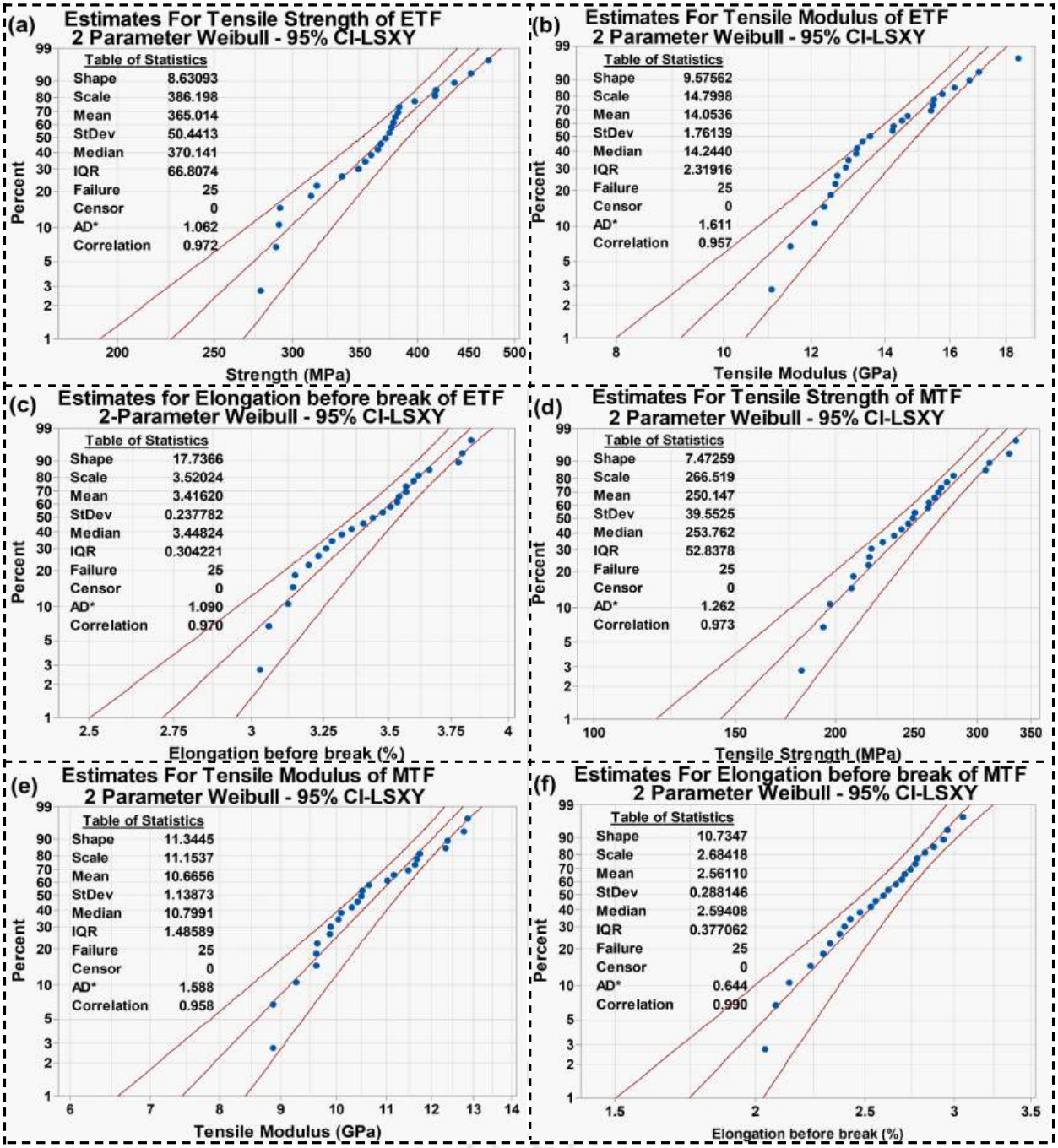

Fig. 3.9: Weibull distribution for (a) tensile strength, (b) tensile modulus, (c) elongation before the break, of ETF and (d) tensile strength, (e) tensile modulus, (f) elongation before the break, of MTF.

and MTF became 94.299 ± 2.67%, 85.677 ± 5.029% and 74.994 ± 4.88%, respectively. The higher moisture absorption behavior of natural fibers can be attributed to several interconnected factors. Firstly, natural fibers contain hydroxyl (–OH) groups in their cellulose structure, which have a strong affinity for water molecules, making the fibers highly hydrophilic [236]. Additionally, natural

TH-3447_196103002

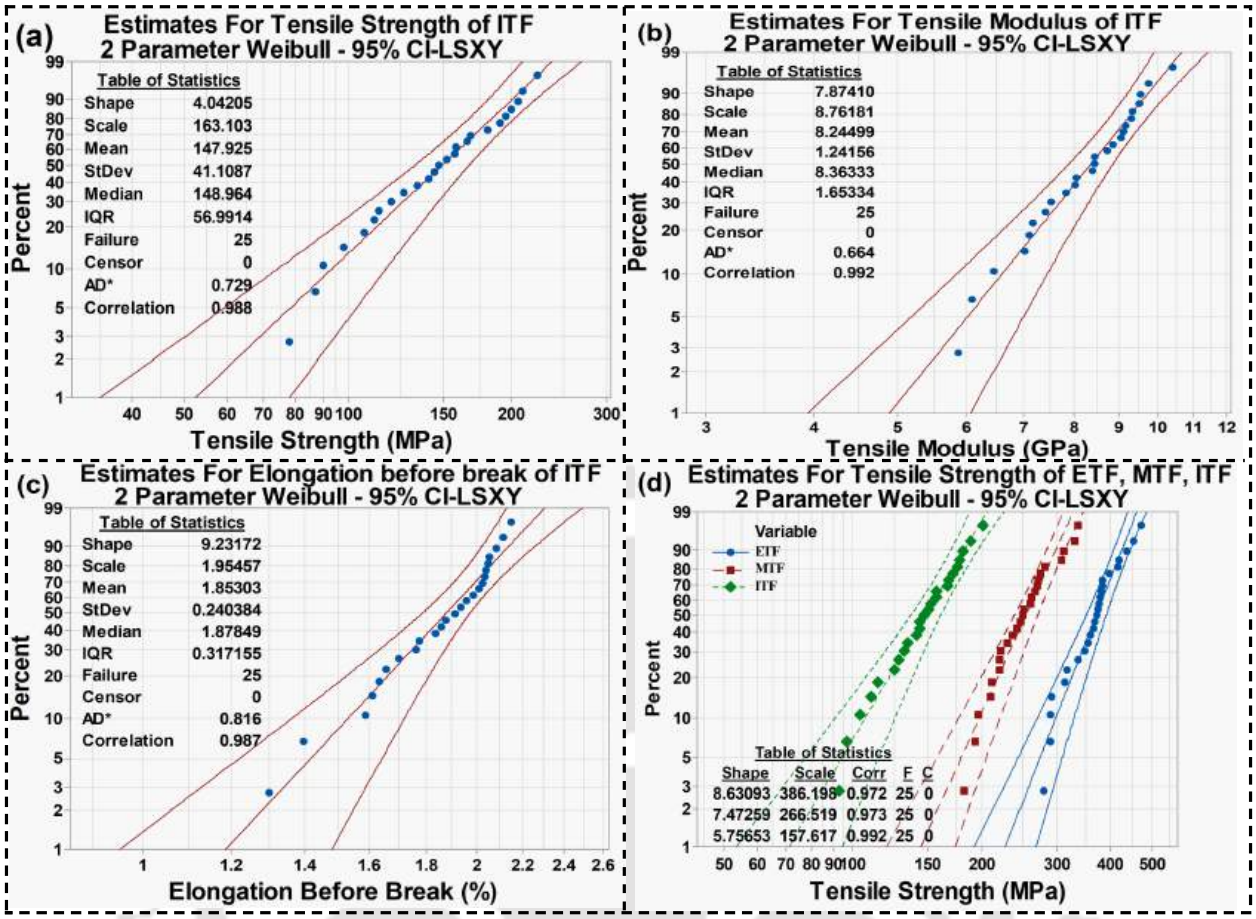

Fig. 3.10: Weibull distribution for (a) tensile strength, (b) tensile modulus, (c) elongation before the break, of ITF and (d) comparative stress distribution diagram of technical fibers.

Table 3.4: Statistical parameters of mechanical properties for *Bambusa tulda* fibers.

Fiber	Properties	Shape	Scale	St. Dev	Mean	Median	IQR	Co-relation
ETF	Strength (Mpa)	8.630	386.198	50.441	365.014	370.141	66.8074	0.972
	Modulus (GPa)	9.575	14.799	1.761	14.053	14.244	2.319	0.957
	Strain (%)	17.736	3.520	0.2377	3.416	3.448	0.304	0.970
MTF	Strength (MPa)	7.472	266.519	39.552	250.147	253.762	52.837	0.973
	Modulus (GPa)	11.344	11.153	1.138	10.665	10.799	1.485	0.958
	Strain (%)	10.734	2.684	0.288	2.561	2.594	0.377	0.990
ITF	Strength (MPa)	4.042	163.103	41.108	147.925	148.964	56.9914	0.988
	Modulus (GPa)	7.874	8.761	1.241	8.244	8.363	1.653	0.992
	Strain (%)	9.231	1.954	0.240	1.853	1.878	0.317	0.987

fibers are often more porous than synthetic fibers, with pores and capillaries within the fiber structure providing additional sites for water absorption. The surface of natural fibers is typically rougher compared to synthetic fibers, increasing the surface area available for moisture absorption [237]. Moreover, besides cellulose, natural fibers contain other components like hemicellulose and

TH-3447_196103002

Table 3.5: Comparative study for mechanical properties of ETF with others previously reported bamboo fiber.

Bamboo Species	Tensile Strength (MPa)	Tensile Modulus (GPa)	Elongation before break (%)	Reference
Bambusa tulda	365.014 ± 50.441	14.098 ± 1.818	3.416 ± 0.237	Present study
Gigantochlea scotechini	140 ± 56.753	11.45 ± 2.495	3.02 ± 0.60	[171]
Dendrocalamus latiflorus	430 ± 41.17	25.62 ± 1.64	2.00 ± 0.27	[235]
Macana bamboo	583 ± 48	25.513 ± 3.760	2.099 ± 0.19	[111]
Bambusa vulgaris	138.88 ± 1.23	4.96 ± 0.23	2.70 ± 0.45	[112]
Gigantochloa scortechinii	276.472 ± 59.42	33.41 ± 6.86	1.15 ± 0.56	[109]
Phyllostachys Heterocycla	496.52 ± 92.08	15.85 ± 5.62	5.56 ± 2.66	[108]
Guadua angustifolia	513 ± 69	55 ± 5	1.18 ± 0.19	[107]
Gigantochloa levis	262 ± 75	9.8 ± 1.6	2.7 ± 0.7	[106]
Phyllostachys pubescens	717.53 ± 188.67	43.34 ± 8.66	2.03 ± 0.56	[167]
Dendrocalamus pendulus	293.47 ± 65.44	13.942 ± 1.66	2.7	[105]
Dendrocalamus asper	916.49 ± 98.2	39.444 ± 8.36	2.72	[105]
Gigantochloa levis	750.66 ± 85.08	23.634 ± 4.43	2.47	[105]
Gigantochloa scrtechinii	374 ± 40.11	31.260 ± 6.95	2.29	[105]
Bambusa heterostachya	199.25	–	–	[137]
Neosinocalamus affinis	792.022 ± 208.02	26.73 ± 3.20	2.88 ± 0.18	[171]
Moso, China	192 ± 73.67	–	–	[234]
Phyllostachys Pubescens	916	13.6	12.6	[103]

pectin, which are more hydrophilic and contribute to higher moisture absorption [238]. The presence of other hydrophilic components, such as proteins and lignin, in certain natural fibers further enhances their moisture absorption capabilities. In summary, the intrinsic hydrophilic nature of the fiber's chemical structure, combined with its physical characteristics such as porosity and surface roughness, leads to higher moisture absorption in natural fibers [239].

A higher value of water absorption not only leads to degradation of its mechanical property but is also responsible for weaker fiber-matrix interfacial bonding of bio-composites [110]. Higher moisture content in fibers can significantly influence the mechanical and thermal properties of composites in several ways. Moisture can act as a plasticizer, reducing the interfacial bonding between the fibers and the matrix, which leads to a decrease in tensile strength and stiffness of the composite. Additionally, absorbed moisture can cause fibers to swell, leading to internal stresses and potential deformation in the composite material, affecting its dimensional stability and overall integrity. The presence of moisture can also accelerate fatigue damage, resulting in reduced

TH-3447_196103002

fatigue life and increased susceptibility to crack propagation under cyclic loading. Furthermore, moisture can catalyze the degradation of the polymer matrix and fiber-matrix interface at elevated temperatures, leading to a reduction in thermal stability. Moisture absorption can lower the glass transition temperature of the composite, affecting its performance at higher temperatures; the material may become more flexible and less rigid at lower temperatures than intended. Increased moisture content can also alter the thermal conductivity of the composite. Since water has a higher thermal conductivity than many polymers, this might lead to changes in the heat transfer characteristics of the composite. In summary, higher moisture content in fibers can negatively impact the mechanical strength, stiffness, dimensional stability, fatigue resistance, thermal stability, and thermal properties of composites, often leading to reduced overall performance and reliability [240]. ETF shows a lower water absorption value than the other two types of extracted fiber, hence it has greater potential to be used as a reinforcing material for bio-composite.

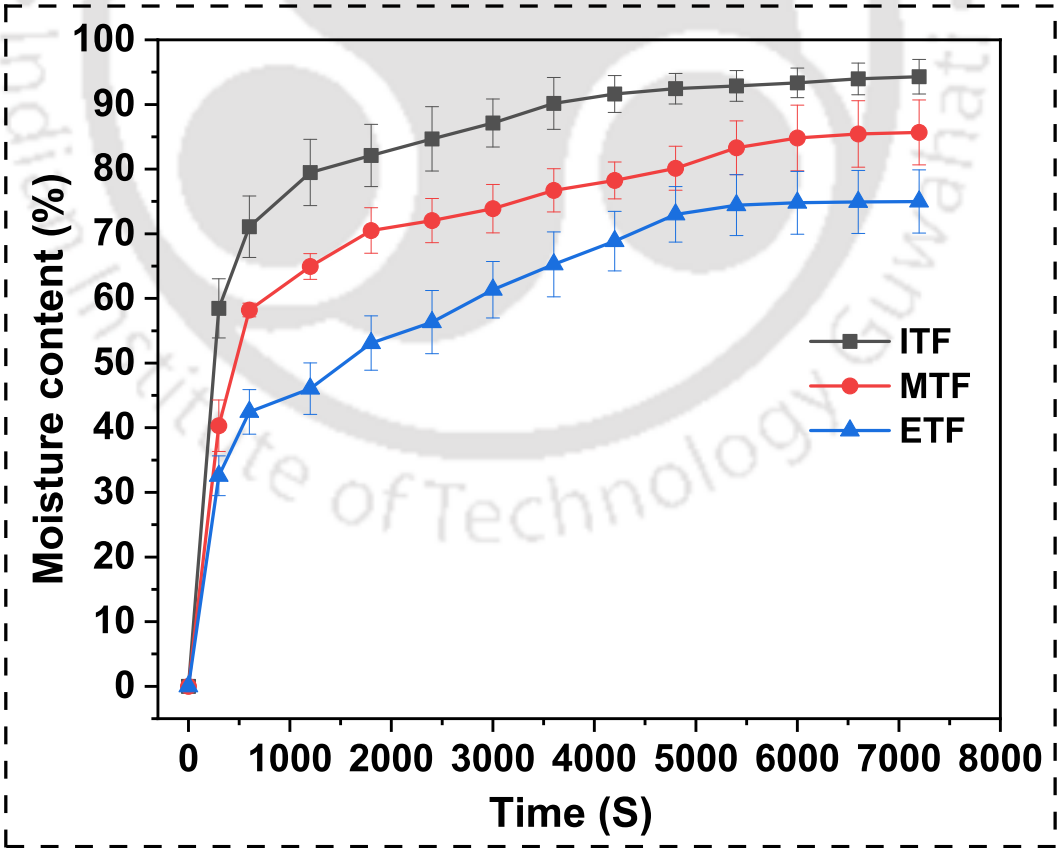

Fig. 3.11: Moisture absorption behaviour of technical fibers.

TH-3447_196103002

3.3.9 Thermogravimetry Analysis

Thermal stability is considered to be one of the major parameters for natural fiber functioning as reinforcement in bio-composite materials [241, 242]. The thermogravimetry analysis of extracted fiber has been done and presented in **Fig. 3.12**.

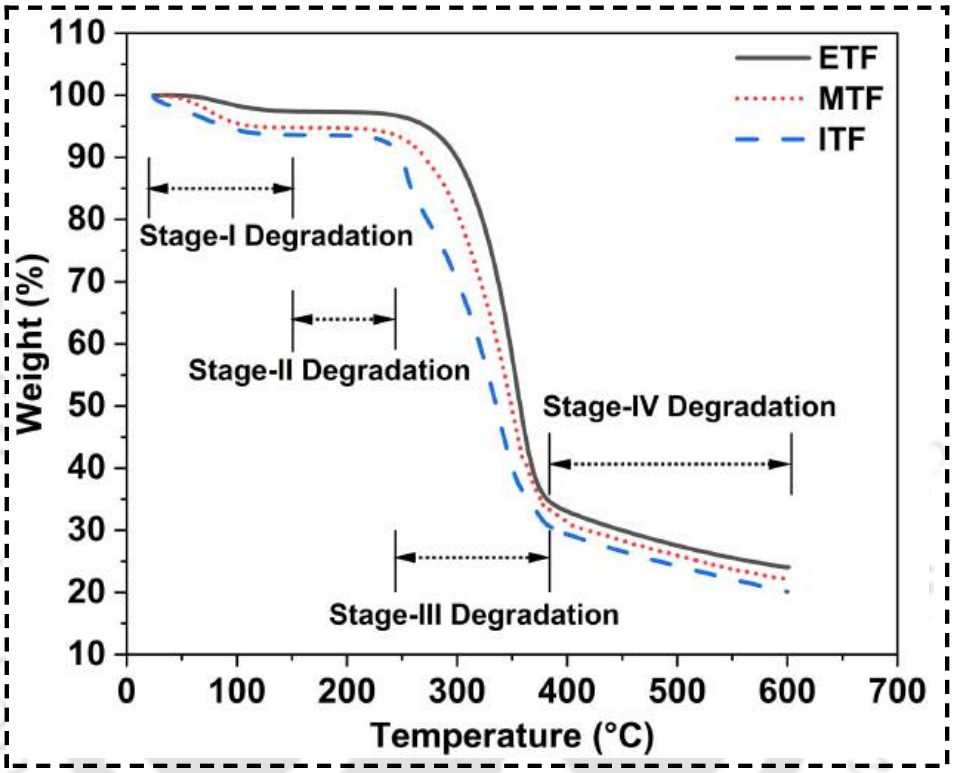

Fig. 3.12: Thermogravimetric analysis of technical fibers.

The TG curves revealed that all three types of fiber lose their mass in the four-stage process. Temperatures go from 24°C to 150°C in the first stage of mass degradation. Which indicated that moisture evaporation was taking place [221]. The next stage is the dismissal of hemicelluloses, extractive, and the small amount of cellulose of fiber from 150°C to 252°C [216]. Here major mass degradation (around 60-64%) takes place as the temperature goes from 240°C to 381°C, leading to the thermal degradation of cellulosic elements [89]. The fourth stage of degradation is in the range of 381°C to 600°C, which leads to thermal degradation of lignin and high crystalline cellulose [243]. The weight percentage of degradation for all three types of technical fiber were presented in **Table 3.6**. In stage-I, ITF shows more degradation, which could be due to the presence of a greater moisture level in bio fiber. The ETF shows a higher T_{50} (50% weight loss at T temperature) value

TH-3447_196103002

(about 356.63°C) and higher MRDT (maximum rate of degradation temperature) value. It may happen due to the higher crystalline index of cellulose [189]. ETF also has more residue mass than ITF and MTF.

Table 3.6: Comparative study for mechanical properties of ETF with others previously reported bamboo fiber.

Fiber Type	Stage-I mass loss (%)	Stage-II mass loss (%)	Stage-III mass loss (%)	Stage-IV mass loss (%)	T_{50} (°C)	MRDT (°C)	Residue mass (%)
ITF	6.36	5.52	64.95	35.11	344.44	338.94	20.11
MTF	5.19	1.98	63.76	34.78	348.75	348.75	21.96
ETF	2.56	1.01	63.59	31.49	356.63	354.91	24.05

3.4 COMPARATIVE STUDY WITH DIFFERENT NATURAL FIBERS

Table 3.7 provides a comparative analysis of the mechanical properties of Bambusa tulda (ETF) with various other previously reported bamboo and natural fibers, including key parameters such as density (ρ), cellulose content, moisture content, tensile modulus, tensile strength, crystallinity index (CI), thermal stability, and references. Bambusa tulda (ETF) from the present study has a moderate density (0.917 gm/cm^3), cellulose content (58.13%), and moisture content (2.75%). It exhibits a tensile modulus of 14.098 GPa, tensile strength of 365.014 MPa, a crystallinity index of 60.142%, and thermal stability at 234.651°C. Munja Fiber displays a higher tensile modulus (62 GPa) and tensile strength (970 MPa) compared to Bambusa tulda (ETF). Corchorus (Jute) has a high density (1.46 gm/cm^3), tensile modulus (19.5 GPa), tensile strength (473 MPa), and thermal stability (240°C). Flax stands out with an extremely high tensile modulus (400-938 GPa) and tensile strength (61.4-128 MPa), though its thermal stability data is missing. Hemp shows a high tensile modulus (70 GPa) and tensile strength (690 MPa), with a thermal stability of 225°C. Kenaf offers a wide range for tensile modulus (9-53 GPa) and tensile strength (350-930 MPa). This table highlights the diversity in mechanical properties among different natural fibers, illustrating how Bambusa tulda (ETF) compares with others and emphasizing the potential of various fibers for specific engineering applications.

TH-3447_196103002

TH-3447_196103002

Table 3.7: Comparative study for mechanical properties of ETF with others previously reported bamboo fiber.

Fiber	ρ (gm/cm^3)	Cellulose (%)	Moisture (%)	Tensile Modulus (GPa)	Tensile Strength (MPa)	CI (%)	Thermal Stability (^{o}C)	References
Bambusa tulda (ETF)	0.917	58.13	2.75	14.098	365.014	60.142	234.651	Present study
Munja Fiber	1.423	–	–	62	970	77.58	201.45	[89]
Punica granatum	1.237	–	–	14.38	327	–	–	[189]
Corchorus (Jute)	1.46	61	12.6	19.5	473	71.39	240	[244]
Flax	1.5	85	10	400-938	61.4-128	70	–	[245]
Coir	1.1-1.5	43	–	4-6	175	57	–	[246]
Hemp	1.5	70.2	10.8	70	690	87.87	225	[247]
Kenaf	1.2-1.45	56.4	–	9-53	350-930	40	–	[248]
Portia tree	1.412	70.2	10.83	20.57	557.82	48.17	245.2	[249]
Aloe vera	1.33	67.4	5.8	42.29	805.5	56.5	225	[250]
Mulberry	–	37.38	–	–	–	58.8	210	[251]
Red banana	0.99	72.90	9.36	12.41	440	62.1	120	[252]
Coccinia grandis	1.517	63.22	9.14	26.515	424.242	46.09	105	[253]
Side cordifolia	1.33	69.5	8.51	42.84	703.95	56.92	80.5	[254]
Areca palm leaf	1.09	57.49	9.35	9.39	364.66	–	110	[255]
Raw ARBFs	1.234	67.32	10.21	1.8	19.37	72.47	230	[256]

ρ= density; CI= crystalline index

3.5 SUMMARY

In this study, bamboo fiber has been successfully extracted from the internal, middle, and outer segments of the bamboo culm of *Bambusa tulda*. The diameter of a single fiber has been observed using FESEM (Field emission scanning electron microscopy). The diameter of the technical fiber has been measured using stereo-optical microscopy. The density and chemical composition of the extracted fiber have been determined. The crystallinity index and crystalline size of the fiber have been observed with the help of XRD (X-Ray diffraction analyzer).Furthermore, mechanical and thermal analyses have been performed using a Single Fiber Tensile Testing Machine and a thermo-gravimetric analyzer. The study explores the potential of these fibers as reinforcing materials in bio-composites, and the following conclusions have been drawn from the experimental investigation:

(i) The SEM image reveals that external technical fibers (ETF) comprise finer single fibers than middle and internal technical fibers, making ETF more compact and stronger.

(ii) The FTIR results indicated similar kinds of chemical bonding in all three types of technical fibers

(iii) The chemical composition analysis revealed that external technical fibers (ETF) had higher lignin and cellulose content, along with lower moisture, extractive, and hemicellulose content compared to middle and internal technical fibers (MTF) and (ITF).

(iv) The higher cellulose content in ETF led to a higher crystalline index compared to MTF and ITF.

(v) The ETF exhibit a larger crystal size than ITF and MTF. The increased crystalline size of ETFs contributes to their reduced water absorption properties and enhanced chemical stability.

(vi) Due to higher crystalline index and crystalline size of ETF, it exhibited higher thermal stability.

(vii) In the comparative analysis among ETF, MTF, and ITF, it is evident that ETF exhibits superior potential as reinforcing materials for biocomposites.

TH-3447_196103002

Chapter 4

Effect of NaOH Treatment Concentrations on Bamboo Fiber

4.1 INTRODUCTION

In many studies, bamboo fibers have been used as reinforcement materials in polymer matrices, and it has been found that their interface bonding with the matrix materials is poor. The most commonly used process for improving interface interaction is alkalizing of bamboo fiber with NaOH solutions. From the previous section it has been observed that the fiber extracted from the external part of the *Bambusa tulda* culm is suitable for reinforcing bio-composites. In this section those fibers are chemically treated with different concentrations of sodium hydroxide.The chemical treatment of fiber has been done with different NaOH concentrations of 2%, 4%, 6%, 8%, and 10% w/v (for 2% NaOH solution, the solution has been made with 2g of NaOH pellet mixed with 100 ml of distilled water). The effect of chemical treatment has been investigated by performing different physical, chemical, thermal and mechanical characterization process. The section **Sec. 4.2.1** describes about the materials used in the study. The **Sec. 4.2.2** and **Sec. 4.2.3** present the fiber extraction process and chemical treatment process of the extracted fiber. The impact of chemical treatment on density, chemical composition, crystalline properties, tensile properties, interfacial properties, and thermal degradation behavior is detailed in **Sec. 4.3**. The chemical treatment of fiber affected positively on different properties of bamboo fiber.The investigation revealed that the 6% NaOH-treated fiber showed better thermo-mechanical and interfacial properties. Relative to the untreated fiber (BF_0), the fiber treated with 6% NaOH (BF_6) demonstrated a 42.09% increase in tensile strength and a 75.71% increase in modulus. The chemical treatment enhances

TH-3447_196103002

fiber surface roughness, consequently boosting the interfacial bonding strength between the bio-epoxy and the fiber. Nevertheless, treatments exceeding a 6% NaOH concentration resulted in the removal of cellulose from fiber surfaces, leading to a reduction in both crystallinity index and mechanical properties of the fiber.

4.2 MATERIALS AND EXPERIMENTAL METHODS

4.2.1 Materials

Local bamboo (Bambusa tulda), age group 3 to 4 years, was procured from a local nursery in Guwahati. The sodium hydroxide pellet (NaOH) and acetone were purchased from Merck Life Science Private Limited, India.

4.2.2 Fiber Extraction

THe bamboo fiber has been extracted from bamboo clum by using retting process. the detained process has been mentioned in **Sec.3.2.2**. The only extracted external technical fiber are used here for chemcial treatment of fiber. **Fig. 4.1** represents a schematic process diagram of the fiber extraction.

4.2.3 Chemical Treatment of Fiber

The chemical treatment of fiber has been done with different NaOH concentrations (2%, 4%, 6%, 8%, and 10% w/v). The solution of NaOH (i.e for preparing 2% NaOH solution 2g of NaOH pellet was mixed with 100 ml of distilled water) was made by using distilled water with the NaOH pellets at room temperature and put on a magnetic stirrer for 5 to 8 mins at 750 rpm for preparing a homogeneous mixture [216]. Thereafter the fibers were put into the solution and the beaker was placed on a magnetic stirrer at 48°C with 430 rpm for 8hrs [257]. After 8hrs. duration, the fibers were taken out of the NaOH solution and washed with distilled water and acetone. This washing removed lower-molecular-weight biopolymers and impurities (such as lignin, hemicellulose, wax and fat).Finally, the treated fiber was put into an oven for 24 hrs at 65°C. A schematic diagram of the chemical treatment process has been presented in **Fig. 4.2**. The fiber treated with 2, 4, 6, 8 and 10% NaOH concentration has been nominated as BF_2, BF_4, BF_6, BF_8 and BF_10, respectively.

TH-3447_196103002

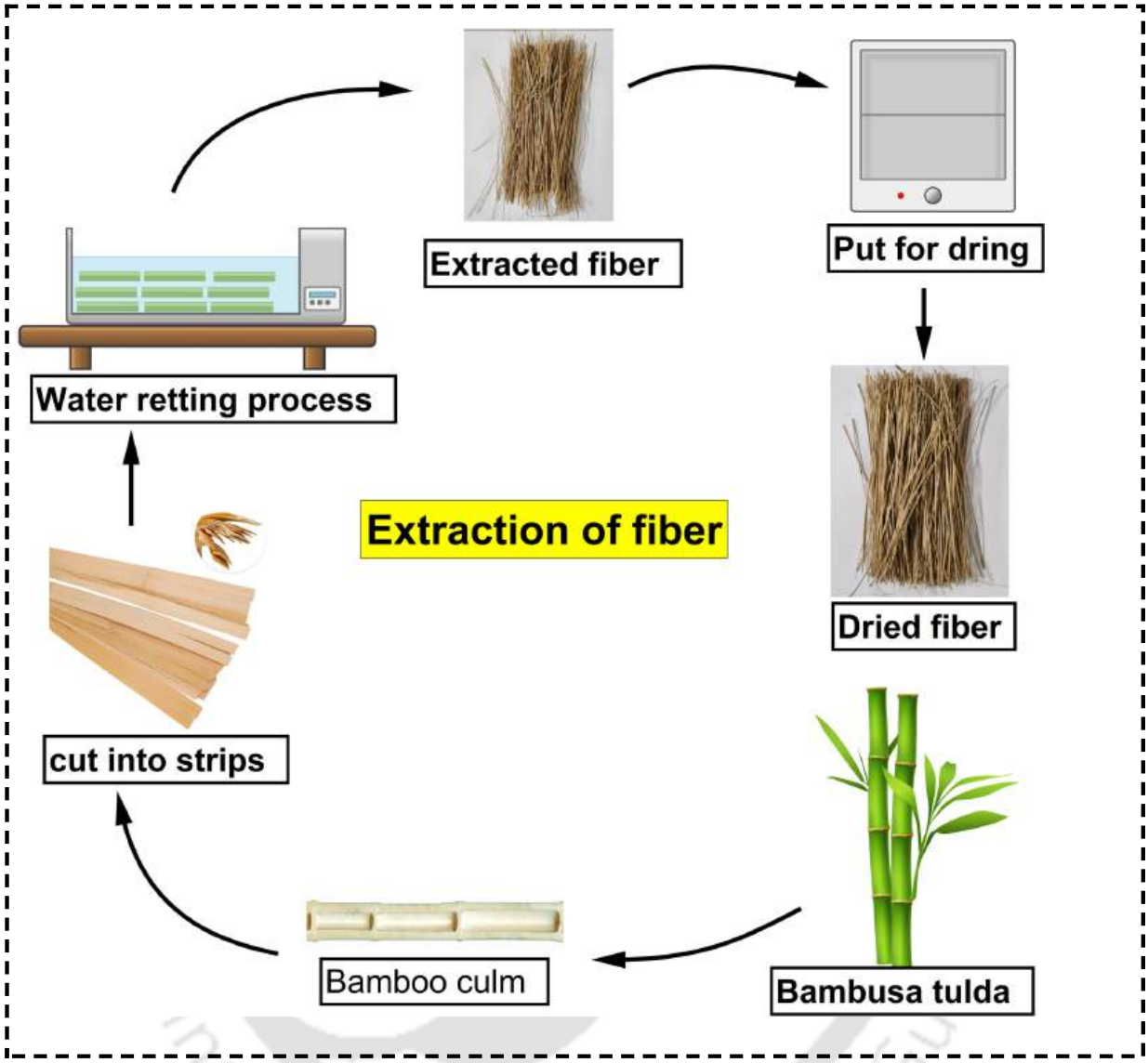

Fig. 4.1: Fiber extraction process.

The surface modification mechanism for bamboo fiber through NaOH treatment may be completed in a two-step reaction. During step-I; The NaOH molecule severance into Na^+ (Sodium cations) and OH- (hydroxide anions). Thereafter when the bamboo fiber has been put into this solution, Na^+ ions may graft hypothetically into the cellulose part of the bamboo fiber. The reaction produced modified cellulose, which may be more crystalline and thermally stable than previous cellulose [216].

4.2.4 Characterization of Fiber

This section provides a comprehensive exploration of the impact of chemical treatment on the physical, mechanical, structural, and thermal properties of the fiber, with detailed findings are

TH-3447_196103002

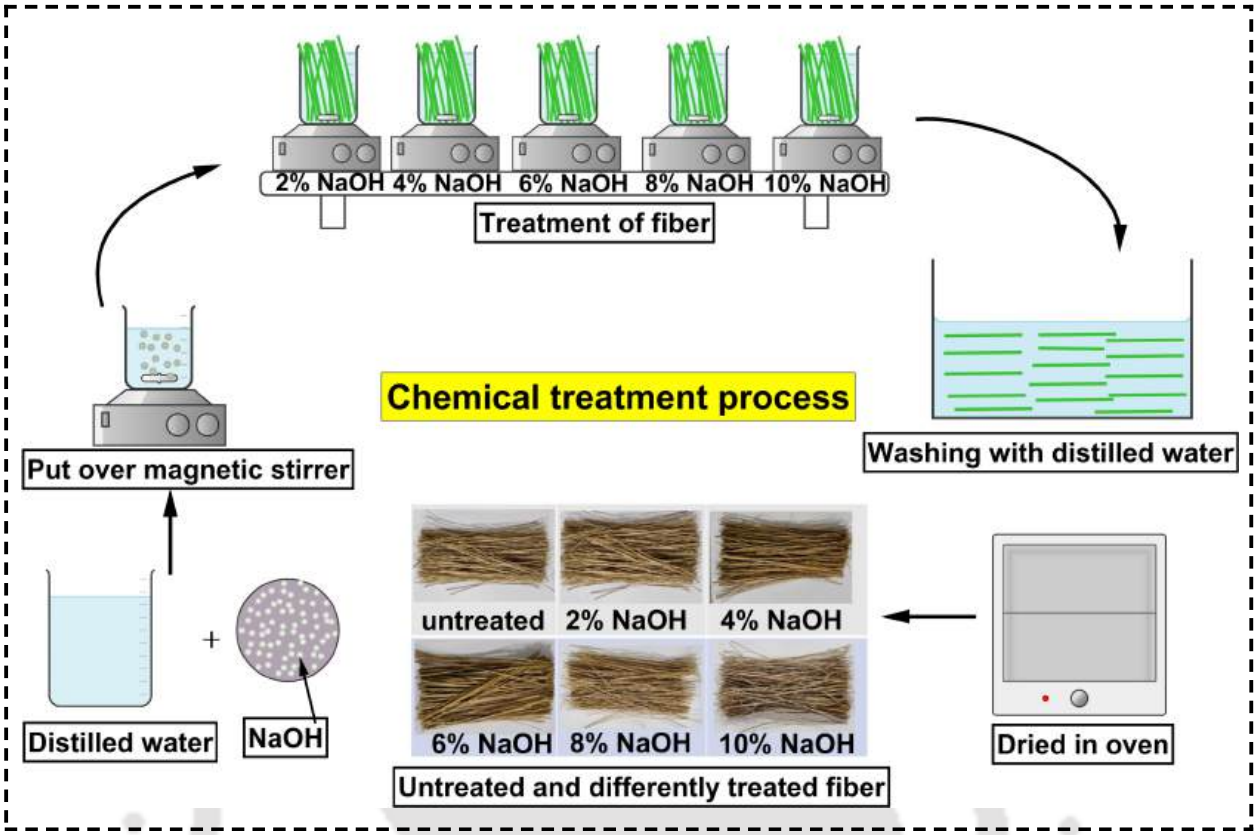

Fig. 4.2: Chemical treatment of fiber.

presented for analysis.

4.2.4.1 Physical Characterization of Fiber

The effect of chemical treatment on mass loss, fiber's diameter and density have been investigated. The mass loss and density of the differently treated fiber has been measured by using equation **Eq.4.1** and **Eq.4.2**, respectively [258].

$$W_{loss} = \frac{W_{bt} - W_{at}}{W_{bt}} \times 100\% \tag{4.1}$$

$$\rho_{fiber} = \frac{(m_3 - m_1)}{(m_2 - m_1) - (m_4 - m_3)} \rho_{liq} \tag{4.2}$$

Where ρ_{liq} is density of liquid (for the present experiment used liquid is toluene; 0.862 gm/cm^3 at room temperature) and ρ_{fiber} is density of fiber. m_1, m_2 and m_3 are the mass of an empty pycnometer, pycnometer filled with toluene, and pycnometer filled with chopped bamboo fiber

TH-3447_196103002

respectively. m_4 represented the mass of pycnometer when filled with toluene and chopped fiber.

A stereomicroscope (Model: Nikon: SMZ25, Japan) was used to measure the diameter of ten random fibers from each group, and the average result is represented with standard deviation.

4.2.4.2 FTIR Analysis

Fourier transform infrared spectroscopy (FTIR) was used to determine how chemical treatment affects bamboo fiber functional groups. The sample for FTIR has been prepared by mixing the ground fiber with potassium bromide (KBr) at a weight ratio of 1:150 [257]. The investigation has been carried out with a PerkinElmer FTIR machine in ATR mode between the range of 400 cm^{-1} to 4000 cm^{-1} with a scanning speed of 2 cm^{-1}.

4.2.4.3 XRD Analysis

The crystallinity index and crystalline size of bamboo fiber were investigated by performing an X-ray diffraction analysis. The analysis has been performed with the help of BRUKER (model: D8 advance; USA) under Cu-Kα radiation operated at 15mA/30kv ($\lambda = 1.542$Å). The XRD intensity has been recorded between 2θ values of 10° to 60° with a step size of 0.02° and a scanning speed of 2°/min. To find out the crystallinity index the Ruland-Vonk method was used **Eq.4.3** and the crystalline size has been calculated by using Scherrer's formula **Eq.4.4** [226].

$$Cr\% = \frac{(A_T - A_{Am})}{A_T} \times 100\% \tag{4.3}$$

where A_T is the total area under the XRD graph, and A_{Am} is the area of the amorphous zone.

$$CS = \frac{K \times \lambda}{\beta \times Cos\theta} \tag{4.4}$$

where K, β, λ and θ are denoted as Scherrer's constant, full-width half maximum of the peak, the wavelength of radiation and Bragg angle, respectively.

4.2.4.4 X-ray Photoelectron Spectroscopy (XPS)

X-ray Photoelectron Spectroscopy (XPS) (ULVAC-PHI, INC; MODEL:04-900) has been used to study the influence of NaOH treatment on compound and chemical bonding. The test equipment

TH-3447_196103002

has an X-ray source of Al-Kα. Surveys and high-resolution scans were conducted at 100 eV pass energy with 1 eV step and 50 eV pass energy with 0.05 eV step, respectively.

4.2.4.5 Tensile Testing

A Shimadzu tensile testing machine (model: AGX-V, Japan) with a 1 kN load cell was used to test the tensile strength of fiber. The samples have been prepared according to the ASTM D-3822-07 [259] standard, with 40 mm gauge lengths and 0.5 mm/min crosshead speeds. Ten samples from each group were tested at room temperature 25^{o}C with 65% RH value.

4.2.4.6 Atomic Force Microscopy (AFM)

The surface roughness and topology of the treated and untreated fiber have been observed with the help of Infinity Bio (Model: MFP-3D, Maker: OXFORD Instruments) microscopy machine in non-contact mode. A range of 10×10 μm^2 area was scanned and the image has been analysed with the help of Gwyddion software. Gwyddion is an open-source software package used for the analysis of data obtained from scanning probe microscopy (SPM) techniques, such as atomic force microscopy (AFM) and scanning tunnelling microscopy (STM). One of its features includes the estimation of surface area.The flowchart of the process is presented in **Fig. 4.3**. The steps of the process is described below:

(i) **Data Acquisition:** Gwyddion begins with acquiring the topographic data from the SPM techniques. The data is typically in the form of a height matrix, where each element corresponds to the height of a specific point on the surface.

(ii) **Surface Reconstruction:** The software reconstructs the surface based on the height matrix. This involves creating a mesh grid of the surface, with each point corresponding to a height value from the matrix.

(iii) **Triangulation:** Gwyddion uses a triangulation method to divide the surface into small triangles. Each point on the height matrix is considered a vertex, and neighboring points are connected to form a series of triangles.

TH-3447_196103002

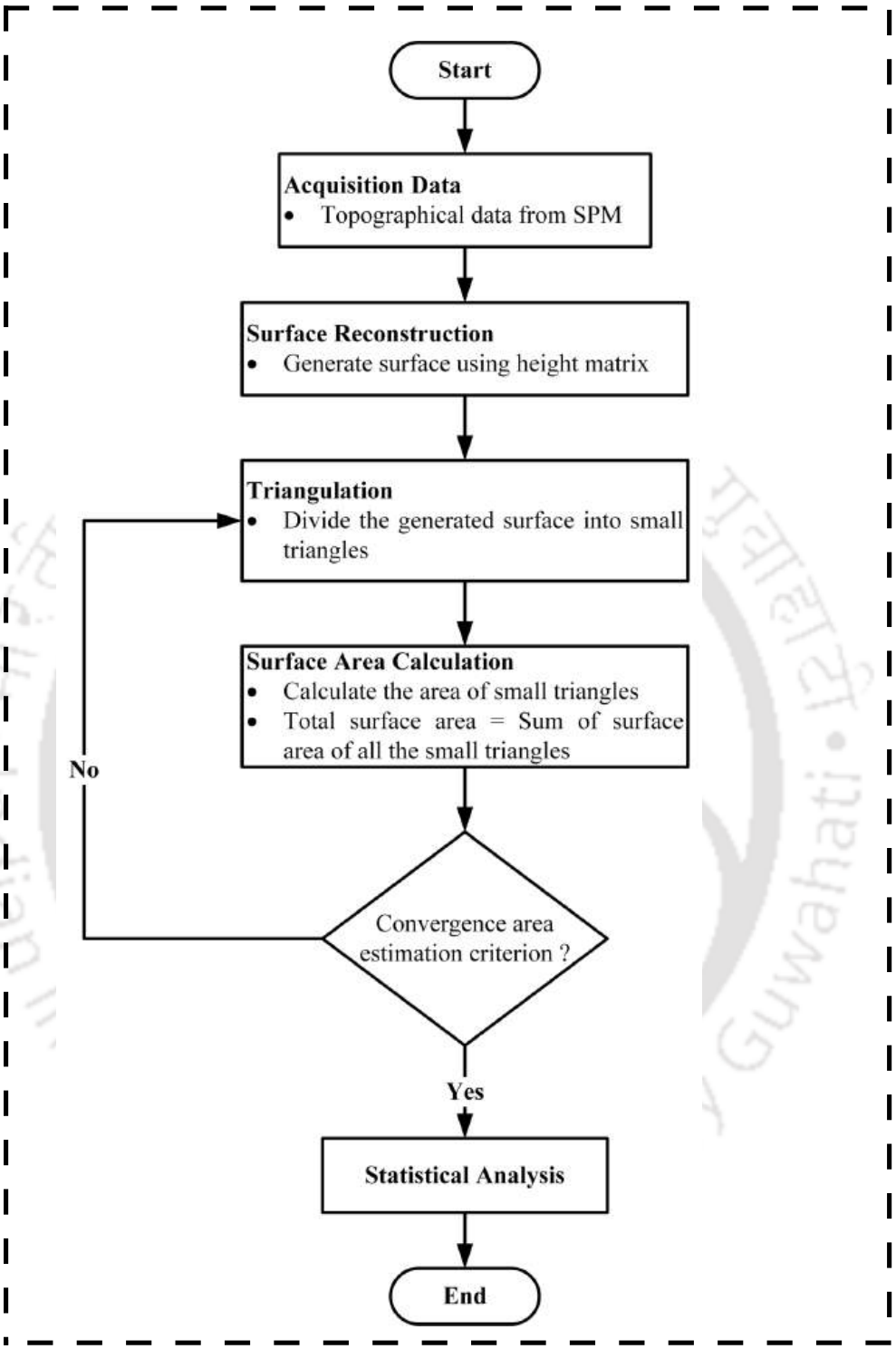

Fig. 4.3: Flowchart for AFM technique.

(iv) **Surface Area Calculation:** The surface area is calculated by summing the areas of these small triangles. The area of each triangle is computed using the coordinates of its vertices. The total surface area is the sum of the areas of all the triangles.

TH-3447_196103002

(v) **Convergent of Surface Area Estimation:** The software performed triangulation repeatedly, with each iteration producing progressively smaller triangles. After several iterations, the area estimation value stabilized, even as the triangles continued to decrease in size. This stable value, corresponding to a specific triangle size, is identified as the convergent triangle size, and all further estimations are conducted using this size.

(vi) **Statistical Analysis:** Gwyddion provides statistical tools to analyze the distribution of heights and the calculated surface areas. This helps in understanding the roughness and texture of the surface.

Gwyddion employs a well-established triangulation method to estimate surface area from SPM data, providing reliable and reproducible results. The level of accuracy is highly dependent on the quality and resolution of the input data, as well as the precision of the SPM instrument used. Comparatively, Gwyddion's methodologies are robust, though users should always consider the potential sources of error inherent in their specific datasets and measurement techniques.

4.2.4.7 Interfacial Shear Strength (IFSS)

Single fiber pull-out testing is a crucial technique used in composite material research to evaluate the interfacial properties between a fiber and the matrix material. This test provides insights into the fiber-matrix adhesion, which is essential for understanding the mechanical behavior and performance of composite materials. The effect of chemical treatment on interfacial shear strength has been investigated by performing fiber pull-out tests. The primary objective of single fiber pull-out testing is to measure the interfacial shear strength (IFSS) between the fiber and the matrix [260]. This helps in assessing the quality of the bond and predicting the overall performance of the composite under mechanical stress. The following steps are followed for making the sample for single fiber pullout testing [261].

(i) **Preparation:** A single fiber is embedded in a matrix material (typically a resin) with a controlled embedment length (3.5mm, total length of the single fiber is 50mm). The matrix is then cured to form a solid composite.

TH-3447_196103002

(ii) **Mounting:** The composite specimen is mounted in a testing apparatus where the matrix is fixed, and the fiber is clamped.

(iii) **Testing:** The fiber is pulled out of the matrix at a controlled rate using a tensile testing machine. The pulling speed was fixed as 0.3mm/min. The force required to pull the fiber out is recorded [262] .

(iv) **Data Collection:** The force-displacement data is collected throughout the test. The peak force observed just before the fiber is completely pulled out is used to calculate the interfacial shear strength.

A Zwick Roell (Z005TN) tensile testing machine was used to pull the embedded fiber. The interfacial shear strength has been calculated as the Greszczuk equation; **Eq.4.5** [167].

$$\tau = \frac{F}{\pi \times d \times L} \tag{4.5}$$

Where τ is the interfacial shear strength, F is the maximum pull-out force; d is the diameter of fiber and L is the length of fiber embedded into epoxy. **Fig. 4.4** represents the schematic of test sample for single fiber testing of bamboo fiber.

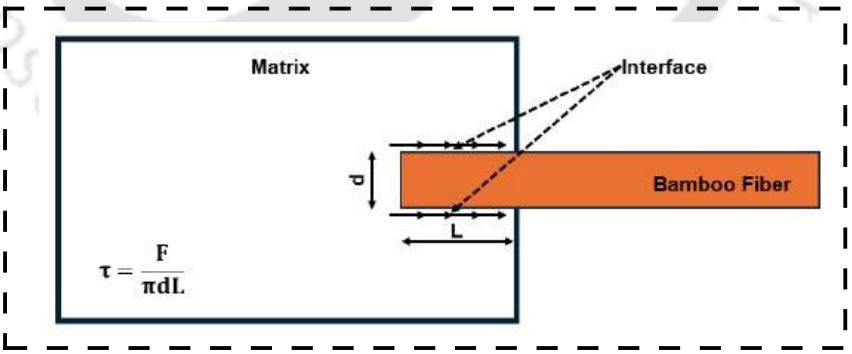

Fig. 4.4: Schematic of Single fiber pullout sample for bamboo fiber.

4.2.4.8 Thermogravimetric Analysis (TGA)

Thermogravimetric analysis (TGA) has been conducted on different fiber samples by using a Perkin Elmer Instrument (model: STA-800; USA) that maintained a constant heating rate of 10°C/ minute

TH-3447_196103002

in the range of 25°C to 600°C in an N_2 gas environment. The thermal activation of the treated and untreated fiber has been analysed by using the Broido equation, **Eq.4.6**.

$$\ln\left[\ln\left(\frac{1}{y}\right)\right] = -\left(\frac{E_a}{R}\right)\left[\left(\frac{1}{T} + K\right)\right] \tag{4.6}$$

4.2.4.9 Field Emission Scanning Electron Microscopic Analysis

The effect of chemical treatment on surface morphology has been analysed with the help of a Zeiss (model: Sigma) was used. The gold coating has been done on fiber samples with the help of a sputter coater (model: BALTEC-SCD-005, USA).

4.3 RESULTS AND DISCSSION

4.3.1 Physical Characterization of Fiber

A directly proportional mass loss of bamboo fiber has been observed with NaOH solution concentration. As a result of the 2% NaOH solution concentration, mass loss was observed to be 6.424%, whereas, at 6 and 10% NaOH solution concentration, mass loss was reported to be 21.452% and 33.64%. **Fig. 4.5** represents the mass loss value of fiber with different NaOH concentrations. A continuous decrement trend has been recorded with the diameter of technical fiber diameter of the bamboo when NaOH concentration increased. The average diameter of untreated fiber has been observed as 690.04 ± 12.45 μm whereas for 6% and 10% treatment concentrations this diameter has been reported as 575.45 ± 11.23 μm and 507.62 ± 10.41 μm. Increasing NaOH concentration led to a continuous increment in bamboo fiber density up to 6% but the further increment in NaOH concentration led to a decrement in density value. A study by Cai et al. [263] reveals that fibers contain non-cellulose substance polysaccharides that are low-molecular-weight and form amorphous, random, and breached structures; removing these nanocellulose components could result in a higher fiber density. If the concentration of NaOH is greater than 6%, this analogy does not apply because when the treatment with non-cellulose components is done with a high alkaline concentration, the cellulose component of the fiber may also be damaged and removed, causing a sudden drop in density [216]. **Fig. 4.5** represents the density with different NaOH concentrations.

TH-3447_196103002

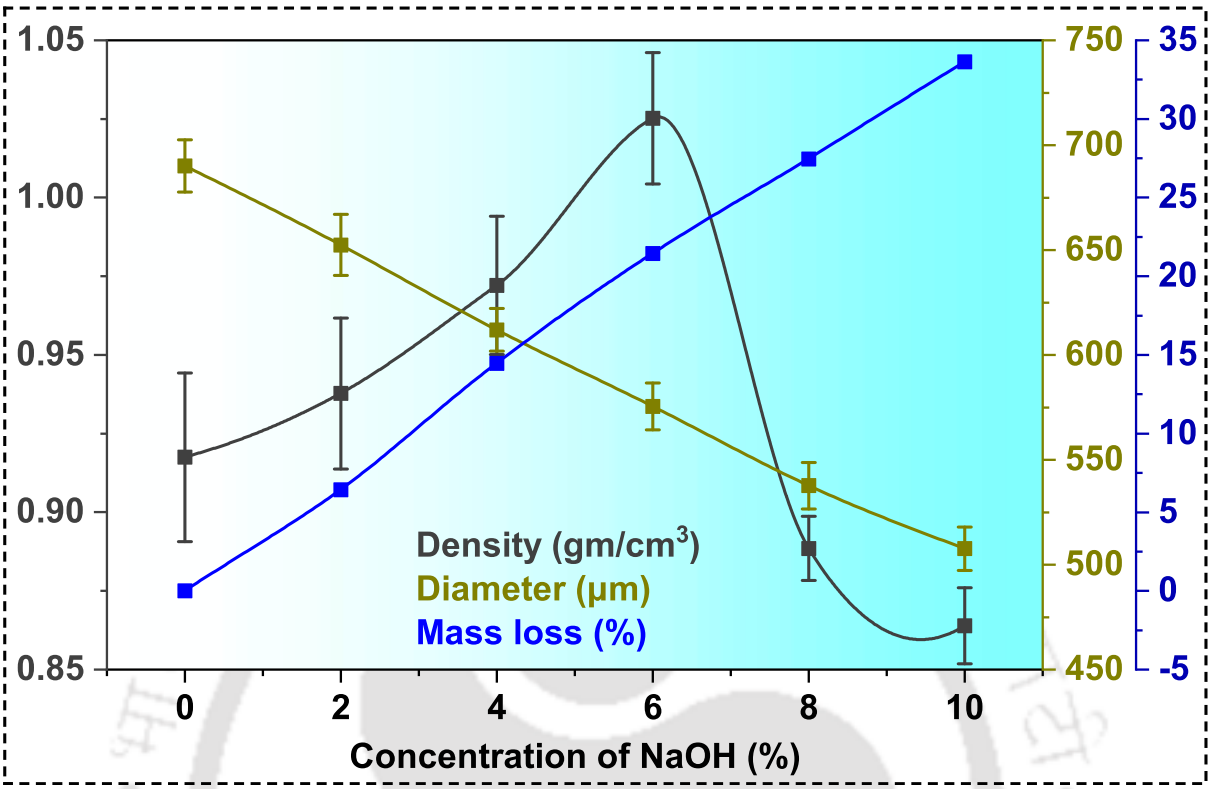

Fig. 4.5: Variation of physical properties of bamboo fiber with NaOH treatment concentration.

4.3.2 Chemical and Structural Characterization of Fiber

The effect of chemical treatment with different NaOH concentrations on functional groups of bamboo fiber has been characterized by performing FTIR analysis and presented in **Fig. 4.6**. An absorption band has been observed near about 3344 cm^{-1} for all types of treated and untreated bamboo fiber due to O-H groups' stretching vibration presented in lignin, hemicellulose and cellulose components. The stretching vibrations of C-H groups in lignin and cellulose have produced another band at 2914 cm^{-1} wave numbers for all samples. A spike has been observed at 1731 cm^{-1} wave numbers due to vibration of stretching types of C=O group presented in hemicellulose [257]. However, this spike did not appear after chemical treatment the fiber. This may be evidence that hemicellulose is being removed from fiber after treatment. The peak at 1598 m^{-1} and 1503 cm^{-1} of untreated fiber are due to the bending vibration of the C=C and C-O bond from lignin [159]. In treated fiber, these two peaks are absent, indicating that the lignin has been removed after chemical treatment. In addition to these two peaks but also peaks at 1369 cm^{-1} (presenting bending

TH-3447_196103002

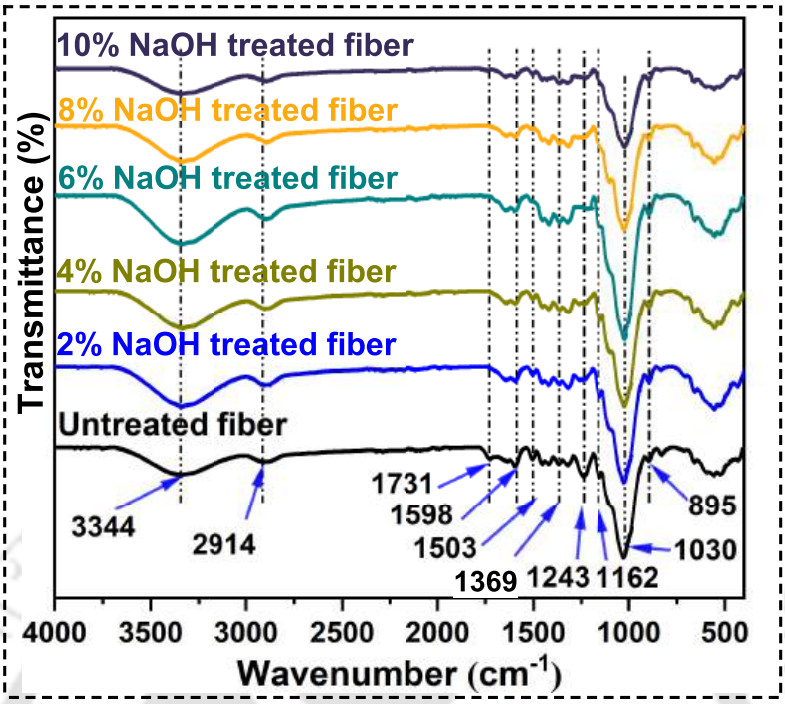

Fig. 4.6: FTIR spectra for treated and untreated bamboo fiber.

vibration of -CH_2 groups of hemicellulose) and 1243 cm^{-1} (presenting stretching vibration of C=O groups of hemicellulose) are also absent after chemical treatments; indicating successful removal of hemicellulose, extractive and lignin. In untreated fiber, a spike at 1162 cm^{-1} exists due to the presence of carbonyl groups in hemicellulose; this spike is absent in treated fiber as well, indicating that lignin has been removed. The absence of some of the peaks at 895 cm^{-1} (bending vibration of C-H bond of cellulose) and 1320 cm^{-1}(due to C-H bond's bending vibration of cellulose) [264] in 8% and 10% NaOH-treated fiber indicates that some percentage of cellulose has been removed along with some non-cellulose components from fiber. For the entire spectrums, multiple absorption peaks were observed, indicating bamboo fiber has undergone multiple changes and has been removed of non-cellulosic components (like- lignin; hemicellulose; extractive) at different NaOH concentrations.

The powder XRD has been performed on treated and untreated ground bamboo fiber and the diffraction curve has been shown in **Fig. 4.7** (a). For all treated and untreated fibers crystalline peaks are observed at around 2θ= 15.53°, 22.2° and 34.8°; corresponding to the crystalline plane (1 1 0); (0 0 2) and (0 4 0) [226]. The reason behind these peaks is the presence of β-cellulose

TH-3447_196103002

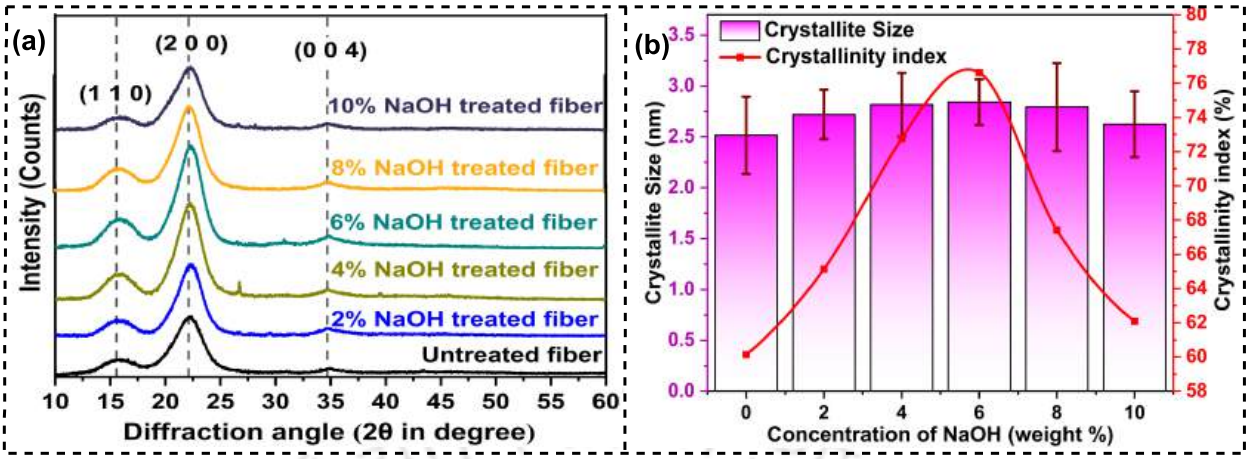

Fig. 4.7: (a) XRD pattern, (d) variation of crystallinity and crystalline size with NaOH concentration.

inside the bamboo fiber. An amorphous peak is also observed at 2θ= 18-19° from the crystallographic pattern of treated and untreated fiber; which is due to the presence of amorphous material inside the fiber [215]. The crystallinity index of different fiber has been found by following the Ruland-Vonk method [89] and presented in **Fig. 4.7** (b). Crystallinity refers to the proportion of the bamboo fiber material that is in a crystalline form as opposed to an amorphous form [265]. Higher crystallinity generally enhances the thermal stability and mechanical strength of bamboo fibers. This is because the ordered structure of crystalline regions provides resistance to thermal deformation and improves load-bearing capacity. Therefore, a high degree of crystallinity in bamboo fibers contributes to their ability to maintain structural integrity under thermal and mechanical stress, making them suitable for applications requiring durable and heat-resistant materials [266]. Crystalline size, or crystallite size, indicates the dimensions of the individual crystalline regions within the bamboo fibers [267]. Smaller crystallite sizes can lead to an increase in the material's toughness and impact resistance. This is due to the grain boundary strengthening effect, where smaller grains provide more barriers to dislocation movement, enhancing the material's mechanical properties. In the context of thermomechanical performance, smaller crystallite sizes can improve the fiber's ability to withstand mechanical deformation and thermal cycling, thereby enhancing the overall durability and performance of the bamboo fibers in demanding conditions. Not only that higher crystalline size is also referred to lesser moisture absorption and less chemically reactive

TH-3447_196103002

[268]. Whereas the crystallinity index (CI) is a quantitative measure of the relative amount of crystalline material within the bamboo fibers. It is crucial for predicting the thermomechanical behavior of the fibers [269]. A higher crystallinity index implies a greater proportion of crystalline regions, which generally correlates with improved thermal stability and mechanical strength. This index helps in assessing the quality and performance potential of the bamboo fibers, enabling better optimization of their properties for specific applications. For instance, fibers with a higher CI would be preferable for use in environments where high mechanical strength and thermal stability are essential [270].The crystallinity index and crystalline size of fiber increased with the increment of NaOH concentration up to 6%, but when the concentration of NaOH was increased to more than 6%, the crystallinity index and crystalline size started to decrease. The untreated fiber has been reported with a crystalline index of 60.142% and crystalline size of 2.516 ± 0.379 nm; whereas the maximum crystalline index and crystalline size have been reported for 6% NaOH treated fiber as 76.62% and 2.841 ± 0.224 nm, respectively. As a result of chemical treatment, molecular rearrangements may occur, resulting in modification of cellulose, which shows a better crystalline size and crystallinity index [228]. However, when NaOH concentrations exceed 6%, crystalline cellulose is removed along with amorphous components resulting in decrement of crystalline index.

4.3.3 Effect of Chemical Treatment on the Surface Element of Fiber

Treated and untreated bamboo fiber's surface elements have been analysed with X-ray photoelectron spectroscopy (XPS). The wide scan spectrum of XPS for untreated and treated fiber is presented in **Fig. 4.8**.

In **Fig. 4.8** three major peaks are observed for all treated and untreated bamboo fiber. The peak near 286 eV and 534 eV is an indication of the presence of a large amount of C and O elements on the fiber's surface [264]. A weak peak at 401 eV is associated with the presence of nitrogen (N) in a very small amount on the fiber surface. The elemental composition percentage present in different fiber is presented in **Table 4.1**.

According to the elemental composition table, the O/C ratio has continuously decreased (up to 6% of concentration) after chemical treatment. The elimination of hemicellulose from the ligno-

TH-3447_196103002

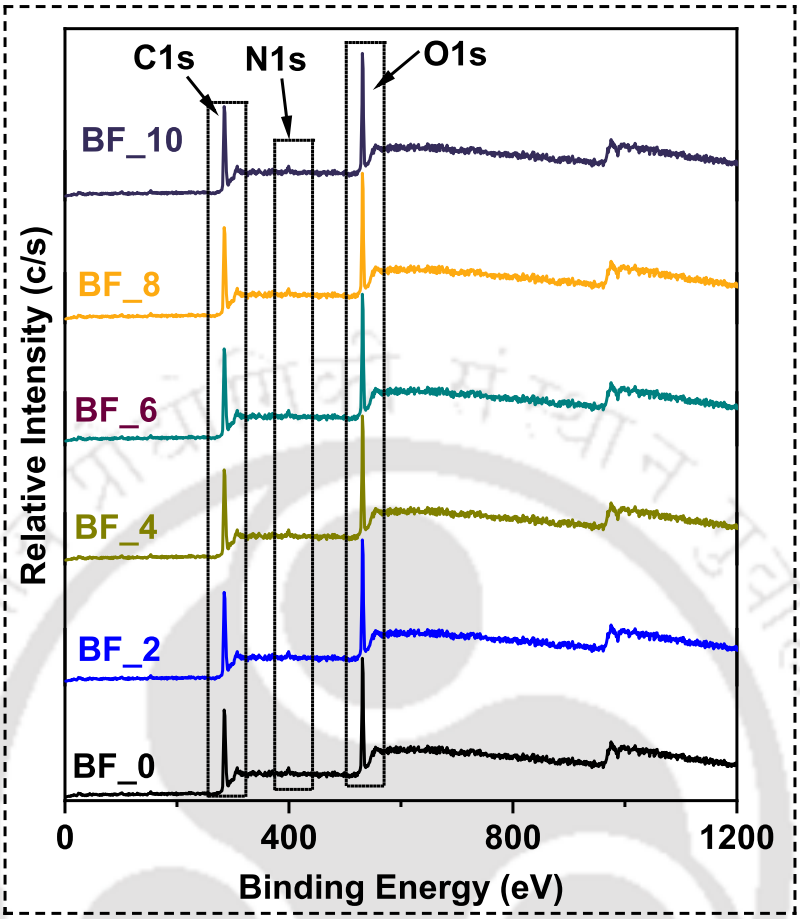

Fig. 4.8: XPS spectra of different treated and untreated bamboo fiber.

cellulose fiber is what causes this deterioration. Moreover, the hydrophilicity of natural fibers is directly related to the O/C ratio. After chemical treatment, a reduced O/C ratio indicates that the fiber has turned hydrophobic. However, when NaOH concentration exceeds 6% (for 8% and 10% concentrations), the cellulose part of the fiber also degrades along with the hemicellulose part, resulting in hydrophilic fibers. In order to understand the functional groups, present in treated and untreated bamboo fiber, the C1s signals were further analysed. The C1s peak was fitted and deconvolved into four primary peaks using Origin software. These four peaks reflect the four different types of carbons that can be found in both untreated and treated bamboo fiber. The C1 peak is observed at 284.15 eV corresponding to -C-C and -C-H bonds, which are present in hydrocarbon compounds of lignin and fatty acid [271].The C2 peak at 285.83 eV is corresponding to -C-O of cellulose and hemicellulose. The peak at 287.49 eV is corresponding to the -C=O bond of acetals, aldehydes or ketones of bamboo fiber (C3) and the fourth one (C4) has been observed

TH-3447_196103002

Table 4.1: Element contents of different bamboo fiber.

Samples	C1s	O1s	Na1s	Si2P	N1s	O/C
BF_0	67.44	0.26	0.09	0.97	1.24	0.449
BF_2	67.87	29.99	0.23	0.94	0.97	0.442
BF_4	68.01	29.33	0.55	0.91	1.20	0.431
BF_6	68.42	28.75	0.66	0.84	1.33	0.420
BF_8	68.07	28.94	0.54	0.98	1.47	0.425
BF_10	67.25	29.66	0.44	1.11	1.54	0.441

at 288.79 eV corresponds to the bonding of carbon atoms with carbonyl or non-carbonyl oxygen atoms [272]. In general, C1 and C4 components are mainly derived from lignin and extractives present in bamboo fiber, whereas C2 and C4 components are derived from carbohydrates. **Fig. 4.9** displays the deconvoluted graphs of the C1s signals and **Table 4.2** displays the locations of each peak and their corresponding percentages. **Fig. 4.9** and **Table 4.2** indicate that following NaOH treatment up to 6% concentration, the C1 percentage decreases constantly. The relative content of C1 refers to the relative percentage of lignin in lignocellulose fiber [136]. The NaOH treatment up to 6% concentration successfully removes the lignin, resulting in a continuous decrease in the C1 values. In addition, the treatment with NaOH concentrations greater than 6% (both with 8% and 10% NaOH) removed cellulose from the fiber and resulted in an increase in C1 values. There is a decrease in the area under C2 peak, indicating a decrement in hemicellulose over cellulose as a result of treatment. C3 peak area indicates overall carbonyl functional group presence. Up to 6% concentration, an incremental trend was observed for areas of these C3 peaks. Nonetheless, the content of the carbonyl polymer might be eliminated by a significant NaOH concentration. In light of this, a diminishing tendency has been noticed for the concentrations of NaOH at 8 and 10%. The C4 peak is the indication of the presence of extractive and hemicellulose in the bio-fiber [136]. The percentage of C4 content shows a decremental trend with NaOH concentration. Essentially, this involves continuously applying NaOH to bamboo fiber to remove hemicellulose and extractive components.

TH-3447_196103002

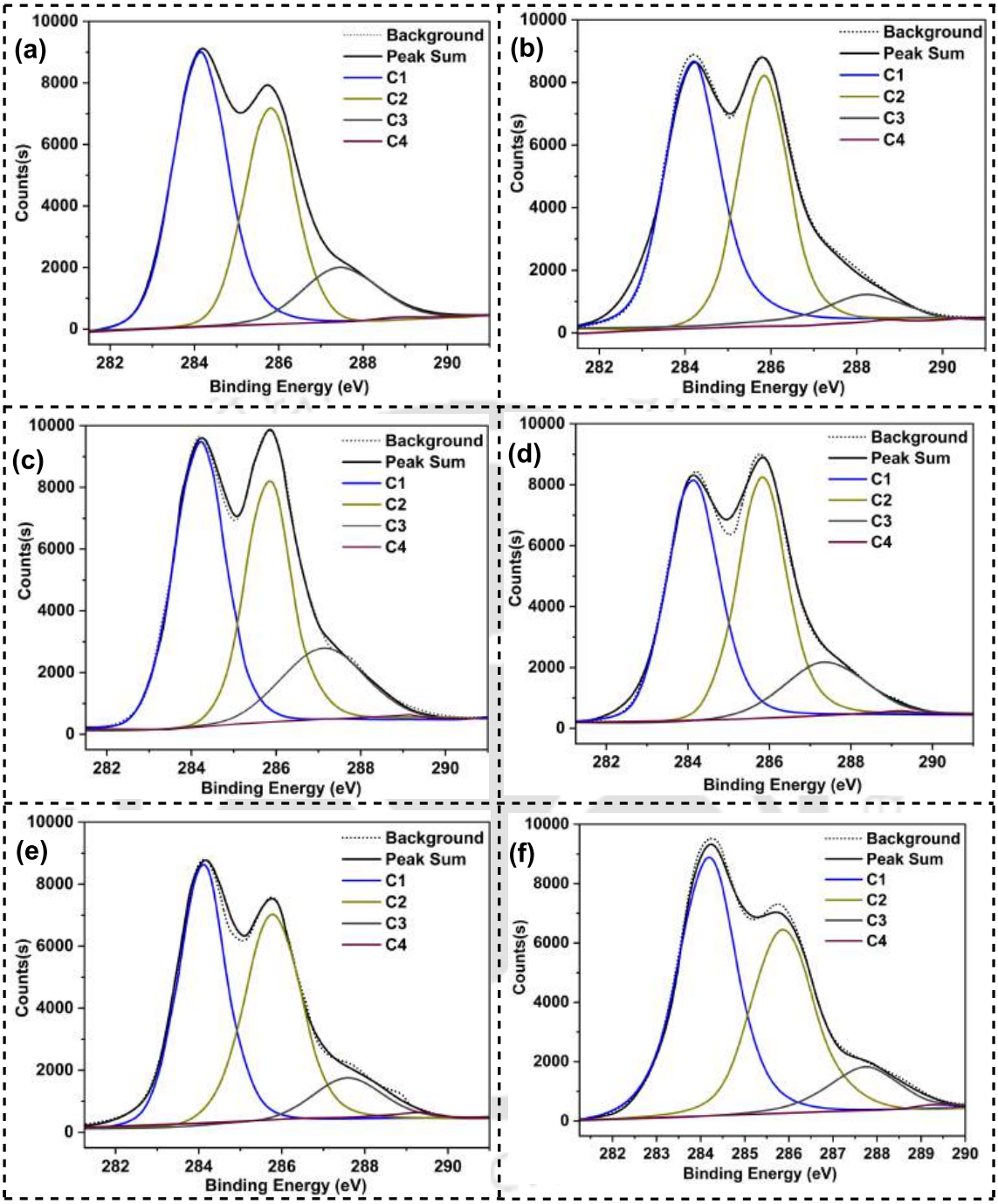

Fig. 4.9: XPS spectra of deconvoluted peak of C1s for (a)B_N_0, (b)B_N_2,(c)B_N_4,(d)B_N_6,(e) B_N_8, (f)B_N_10.

4.3.4 Mechanical Characterization of Fiber

The tensile properties of different fibers have been tested using a static tensile test machine, and their stress-strain curves are shown in **Fig. 4.10** (a). Like other lignocellulose fiber (like- munja, coir, hemp, sisal, hemp, kenaf, aloe vera, palm leaf etc) [67, 89, 245, 250, 255, 273] both treated and

TH-3447_196103002

Table 4.2: Percentage of Carbon and peak position of deconvoluted graphs of different types of bamboo fiber.

Samples	Rel. content. (%)				Peak position (eV)			
	C1	C2	C3	C4	C1	C2	C3	C4
BF_0	49.58	38.56	11.86	0.82	284.10	285.81	287.46	288.84
BF_2	47.89	36.45	14.88	0.78	284.21	285.83	287.30	288.98
BF_4	47.26	34.25	17.79	0.7	284.24	285.84	287.13	289.01
BF_6	45.41	35.16	18.8	0.63	284.11	285.81	287.35	289.22
BF_8	46.82	43.04	9.56	0.58	284.10	285.77	287.59	289.36
BF_10	51.58	37.44	10.29	0.69	284.17	285.86	287.74	289.21

untreated fiber exhibit a quasilinear increment of stress as strain increases until the stress reaches its maximum value and then sudden rupture is observed when stress reaches to its maximum value. **Fig. 4.10** (b) illustrates the effects of NaOH concentration on tensile strength, tensile modulus, and elongation at the break value of the fiber. As NaOH solution concentrations are increased up to 6%, the fiber's tensile strength and tensile modulus values increased continuously. When NaOH concentration exceeds 6%, tensile strength and modulus value begin to decline. The maximum tensile strength and tensile modulus were reported with 6% NaOH-treated bamboo fiber with the numeric value of 526.452 ± 17.509 MPa and 24.055 GPa, respectively. It has been confirmed from XRD result that due to chemical treatment, the crystallinity index of the fiber has been increased. Crystallinity is the measurement of the degree of structural order of the molecules in a material. An increase in crystallinity indicates that the atoms or molecules inside materials are arranged in a more regular and periodic pattern; which can help to transmit stress and load from one atom to another atom more easily, resulting in greater tensile strength and Young's modulus of fiber. Moreover, treatment shows continuous decrement in elongation at break value. As the microfibrils are pulled apart, the fiber can elongate by squeezing the impurities. But after chemical treatment, these impurities have been removed and shown lower elongation at break value. A similar type of decrement trend has been also reported by Chin et al. [174] for Gigantochlea scotechini bamboo.

The effect of chemical treatment on interfacial shear strength has been investigated by performing a single fiber pull-out test. As NaOH concentrations increased up to 6%, the interfacial shear

TH-3447_196103002

strength (IFSS) value of the fiber increased; however, as NaOH concentrations increased beyond 6%, the IFSS value slowly decreased. **Fig. 4.10** (c) represents the IFSS value for different NaOH-concentrated fiber. By chemical treatment of fiber, the surface roughness and effective area have been increased, which makes reinforcement-matrix stress transmission more efficient; therefore, the IFSS value has increased. When the concentration of the treatment exceeds 6%, however, this theory will not be applicable. More than 6% treatment resulted in decrease in crystallinity and the removal of cellulose from the fiber; resulting in weaker reinforcement and low IFSS value. Furthermore, very high roughness values also may increase the fiber's stress concentration factor, which may also be responsible for the decline in IFSS as well as tensile strength value.

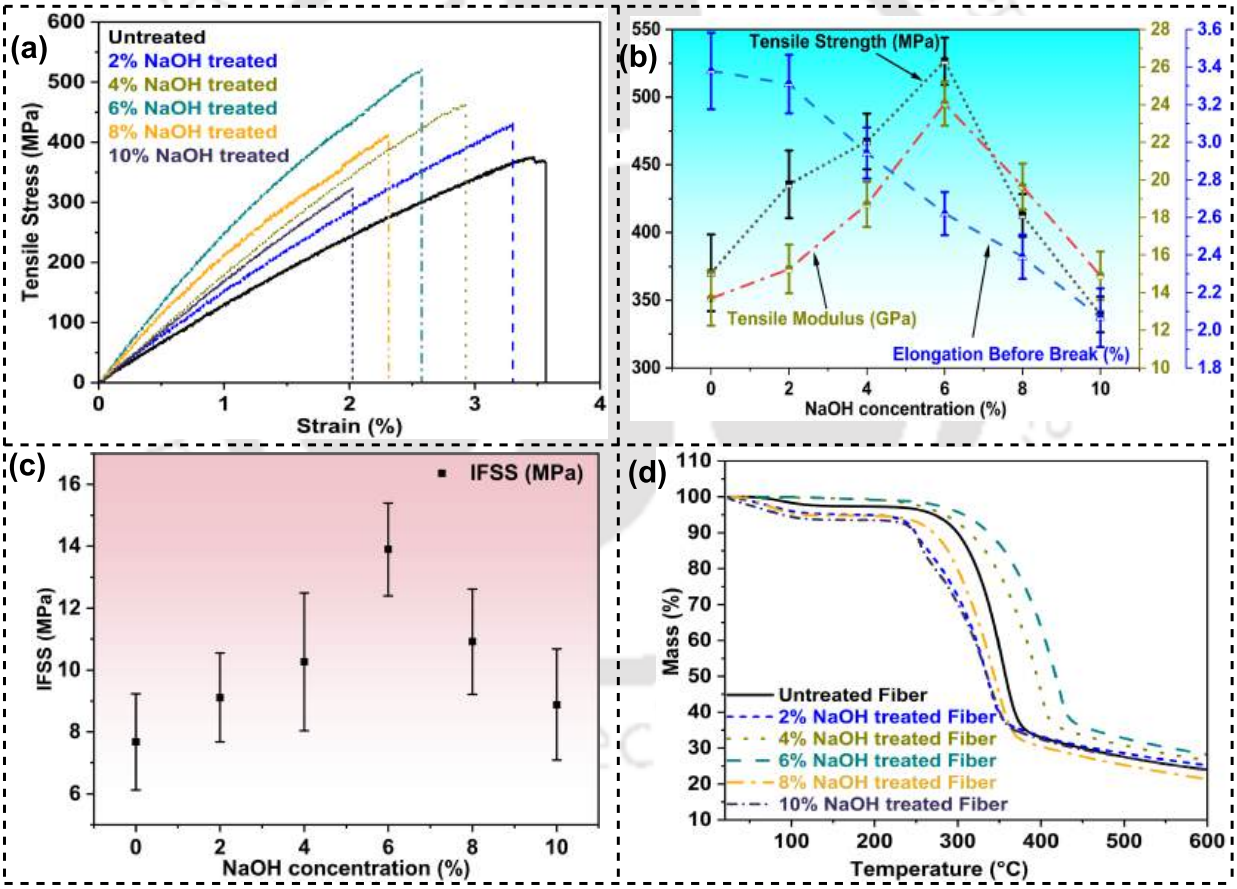

Fig. 4.10: (a) Tensile stress-strain curve for fibers, (b) variation of tensile properties, (c) IFSS value of fibers, (d) Thermogram of differently treated fiber.

TH-3447_196103002

4.3.5 Thermal Characterization of Fiber

In order to interpret the thermal stability of the fiber, thermogravimetric analysis has been performed on both the treated and untreated fibers. The thermograms of the fibers are presented in **Fig. 4.10** (d). Generally, all types of fiber showed four-stage thermal degradation as described by by Chin et al. [174]. Up to 6% concentrated NaOH treatment show an increment in the thermal stability of the fibers. This result can be correlated with the XRD results. The crystallinity index and crystalline size of the fiber increase as a result of chemical treatment; a higher crystallinity index corresponds to higher thermal stability and a higher crystalline size corresponds to lower moisture absorption. Due to lower moisture absorption, the thermal mass degradation is also decreased in the range of 25°C to 150°C. But chemical treatment beyond 6% NaOH concentration resulted in a lower crystallinity index as well as lower thermal stability. The maximum residual mass has been observed for 6% NaOH-treated fiber with a numeric value of 28.38%, while the minimum value has been reported for 10% NaOH-treated fiber with a numeric value of 21.41%. The thermal activation energy of the treated and untreated fiber has been identified and presented in **Fig. 4.11**.

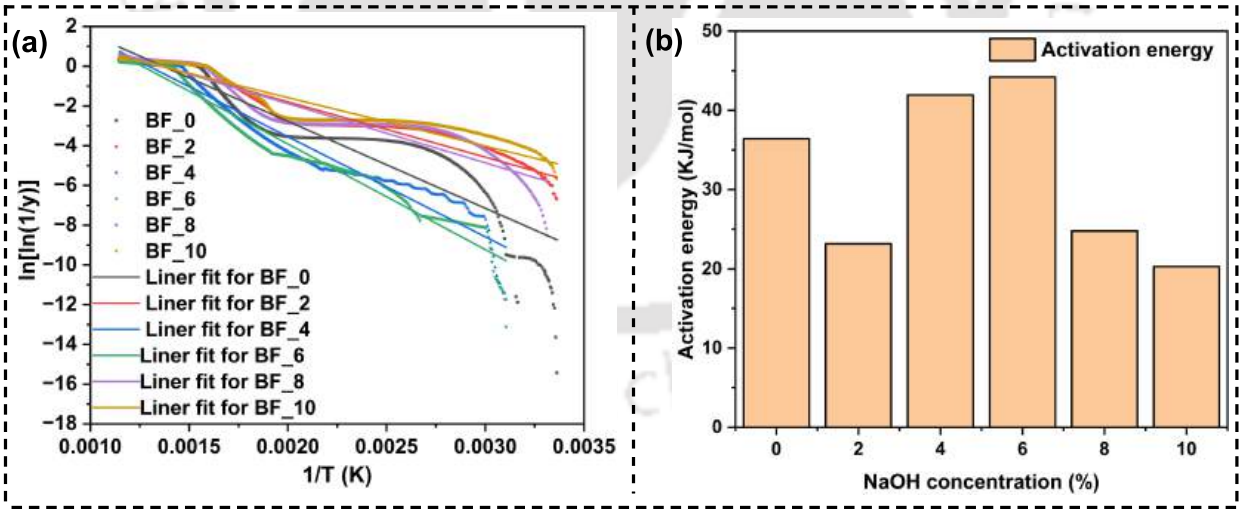

Fig. 4.11: (a) Thermal activation energy graph with straight line fitting; (b) variation of thermal activation energy with NaOH concentration for different treated and untreated fiber.

With the chemical treatment, the activation energy of the fiber has been increased. For untreated fiber the thermal activation energy has been recorded as 36.422 kJ/mol. The maximum activation energy has been recorded for BF_6 types of bamboo fiber with a numeric value of 44.204 kJ/mol.

TH-3447_196103002

Table 4.3: Thermal degradation properties of treated and untreated fiber.

Fiber type	Stage-I mass loss (%)	Stage-II mass loss (%)	Stage-III mass loss (%)	Stage-IV mass loss (%)	Residual mass (%)	Activation energy (kJ/mol)
BF_0	2.565	5.529	63.433	31.855	24.050	36.422
BF_2	4.826	5.933	61.176	27.372	25.243	23.162
BF_4	0.419	1.876	36.761	56.870	26.653	41.941
BF_6	0.448	0.895	23.887	62.384	28.254	44.204
BF_8	5.187	9.572	62.762	33.022	21.392	24.710
BF_10	6.357	4.505	62.042	29.783	23.831	20.300

The details of mass loss and activation energy of all treated and untreated fiber have been tabulated in **Table 4.3**.

4.3.6 Effect of Different Chemical Treatment on Surface Roughness of Fiber

Due to chemical treatment, the surface of the fiber has been modified and roughness has been increased. The RMS surface roughness for different treated fiber has been presented in **Fig. 4.12** (a). Due to increment in roughness, effective area of fiber has been also increased. To calculate the

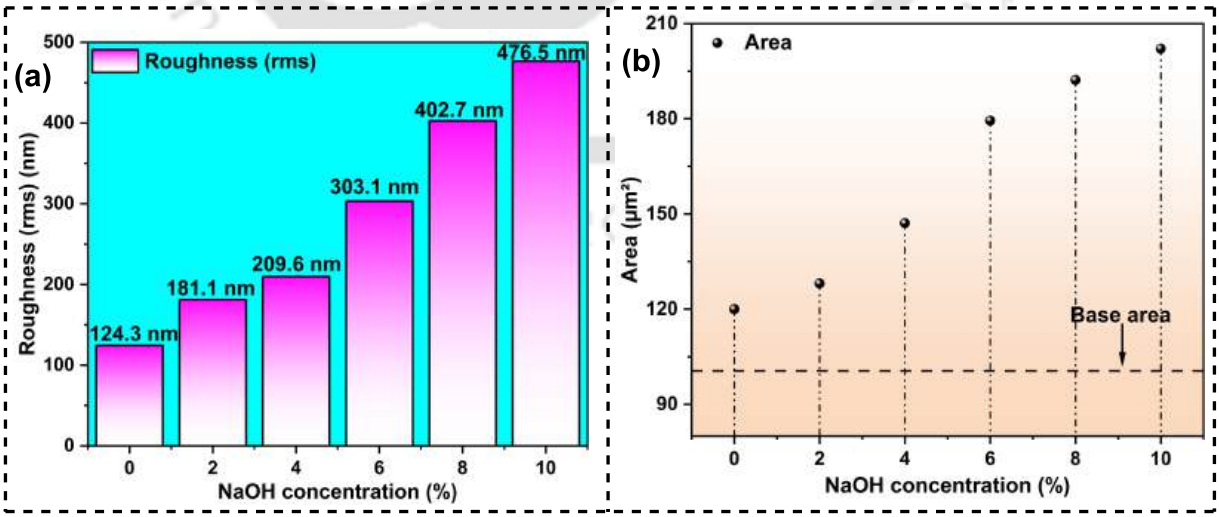

Fig. 4.12: (a) RMS roughness value, (b) effect area of fiber for different treatment concentration.

surface area of fibers from AFM morphology images, Gwyddion software has been used. **Fig. 4.12**

TH-3447_196103002

(b) represents the variation of the effective area of fiber with NaOH concentration. It has been observed that when the roughness increases, the effective area of the fiber rises as well. For the base area of 100 μm^2; the effective area has been calculated as the lower value of 120 μm^2 for untreated fiber and a higher value of 202.1 μm^2 for 10% NaOH treated fiber. Due to chemical treatment impurities and other nanocellulose compounds are removed. This removal increases the surface roughness as well as effective area of the fiber. **Fig. 4.13** represented the 2D and 3D images of AFM morphology for different fibers.

4.3.7 Morphological Analysis of Bamboo Fiber

Fig. 4.14 represents the surface morphology of treated and untreated fiber. Polysaccharides (such as pectin, lignin, and hemicellulose) as well as parenchyma cells and waxes were observed on the untreated fiber surface in **Fig. 4.14** (a) [6, 192, 274]. In most cases, the polysaccharides are weakly attached to the fiber surface. Whereas for treated fiber; these impurities are absent. Furthermore, by removing these impurities, the surface roughness of the fiber has also increased. Additionally, the chemical treatment caused fibrillation on the surface of the fibers, which can be seen clearly in **Fig. 4.14** (b) and (c). When polysaccharide elements were removed, fibrillation was created, resulting in interfibrillar spaces. As a result of these interfibrillar spaces, when biopolymer is added to this fiber, the resin anchors to the fibers, which helps the bio epoxy to transmit charges from the biopolymer to the bamboo fiber when the load is applied; this may increase the strength of the final biocomposites. **Fig. 4.14** (d) is the fiber treated with 6% NaOH solution. From **Fig. 4.14** (e) and (f), it can be seen that the over-concentration of NaOH (more than 6%) destroyed the fiber surface, which may result in a very weak interfacial bond between fibers and matrix and a lower mechanical strength for the developed composite. The single fiber pulled-out samples have been investigated by scanning electron microscopy to understand the interfacial interaction between bamboo fiber and bio-epoxy. From previous reports, diffusion bonding, chemical bonding, and mechanical bonding have been identified as the most common interfacial bonding mechanisms between bio-fiber and polymer matrix [275]. These three types of bonding are also observed in present samples. **Fig. 4.15** (a) (c) and (e) are SEM images of different bonding. Whereas **Fig. 4.15**

TH-3447_196103002

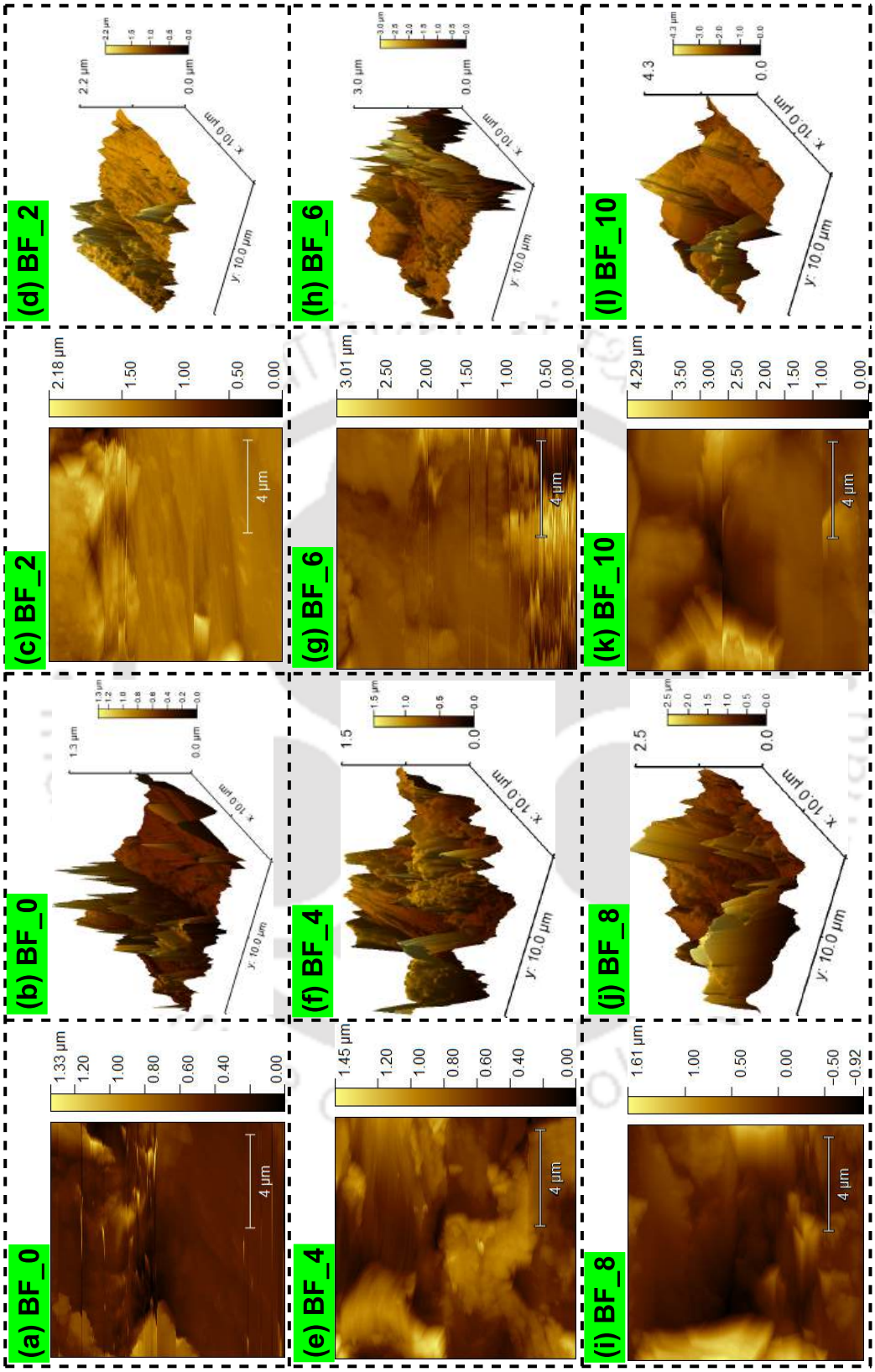

Fig. 4.13: Topological map (a), (c), (e), (g), (i), (K) and 3D AFM image (b), (d), (f), (h), (j) and (l) of different fiber.

TH-3447_196103002

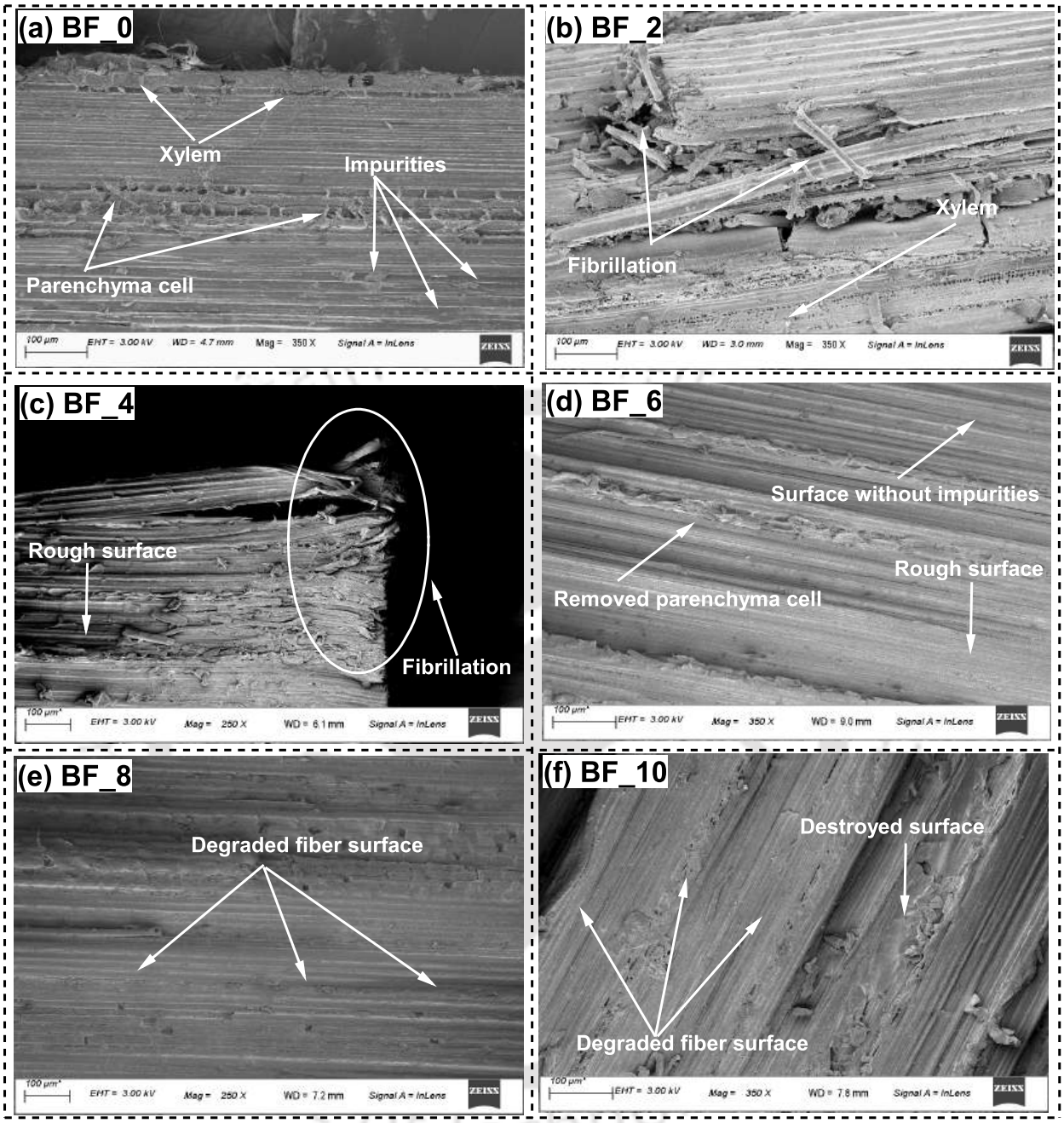

Fig. 4.14: SEM Image of different treated and untreated bamboo fiber.

(b), (d) and (f) are the schematic understanding of the bonding. Diffusion bonding has been observed to be the most common bonding for untreated bamboo fiber.Due to van-der-Waals force or hydrogen bonding, intimate intermolecular interactions occur, resulting in diffusion bonding. From the SEM image of untreated fiber; it has been observed that the fiber's surface is covered with many waxy,pectin and parenchyma cells. As a result, hydroxyl groups may not be able to

TH-3447_196103002

react with the polymer matrix properly [26]. This results in fiber debonding from the matrix at low load. With treated bamboo fiber most of the observed bonding is either chemical bonding or mechanical bonding. Chemisorption reactions have happened between treated bamboo fiber and matrix; this leads to the formation of strong atomic or ionic bonds. The IFSS of the fiber may also increase as a result of strong ionic interfacial bonding. Mechanical interlocking occurs when the polymer penetrates irregularities of bamboo fibers. Due to chemical treatment. The surface roughness of bamboo fiber was increased, which may lead to a greater area of contact resulting in better mechanical interlocking with bio epoxy [245].

4.4 SUMMARY

Bamboo fiber has been effectively extracted from *Bambusa tulda*, and successfully chemically treated. The chemical treatment of the bamboo fiber involved utilizing five distinct NaOH concentrations (2%, 4%, 6%, 8%, and 10%).In the investigation of the impact of chemical treatment on various properties of bamboo fiber, several analysis has been conducted. These included the determination of mass loss percentage resulting from chemical treatment, assessment of fiber density, Fourier transform infrared spectroscopy (FTIR) examination, analysis of crystallinity index and crystalline size, single fiber tensile testing, measurement of surface roughness using Atomic Force Microscopy (AFM), evaluation of interfacial shear strength (IFSS), thermogravimetric analysis (TGA), and morphological analysis utilizing Field Emission Scanning Electron Microscopy (FESEM). The outcomes of the characterizations leads to following conclusion:

(i) As a consequence of the chemical treatment, the elimination of lignin and hemicellulose from bamboo fiber occurred, leading to a decrease in the fiber's mass.

(ii) The FTIR analysis of the treated fiber revealed that the chemical treatment resulted in removal of lignin, hemicellulose, extractives, and moisture from the fiber.

(iii) A consistent increase in both crystallinity index and crystalline size have been observed with the gradual increment in NaOH treatment concentration.

TH-3447_196103002

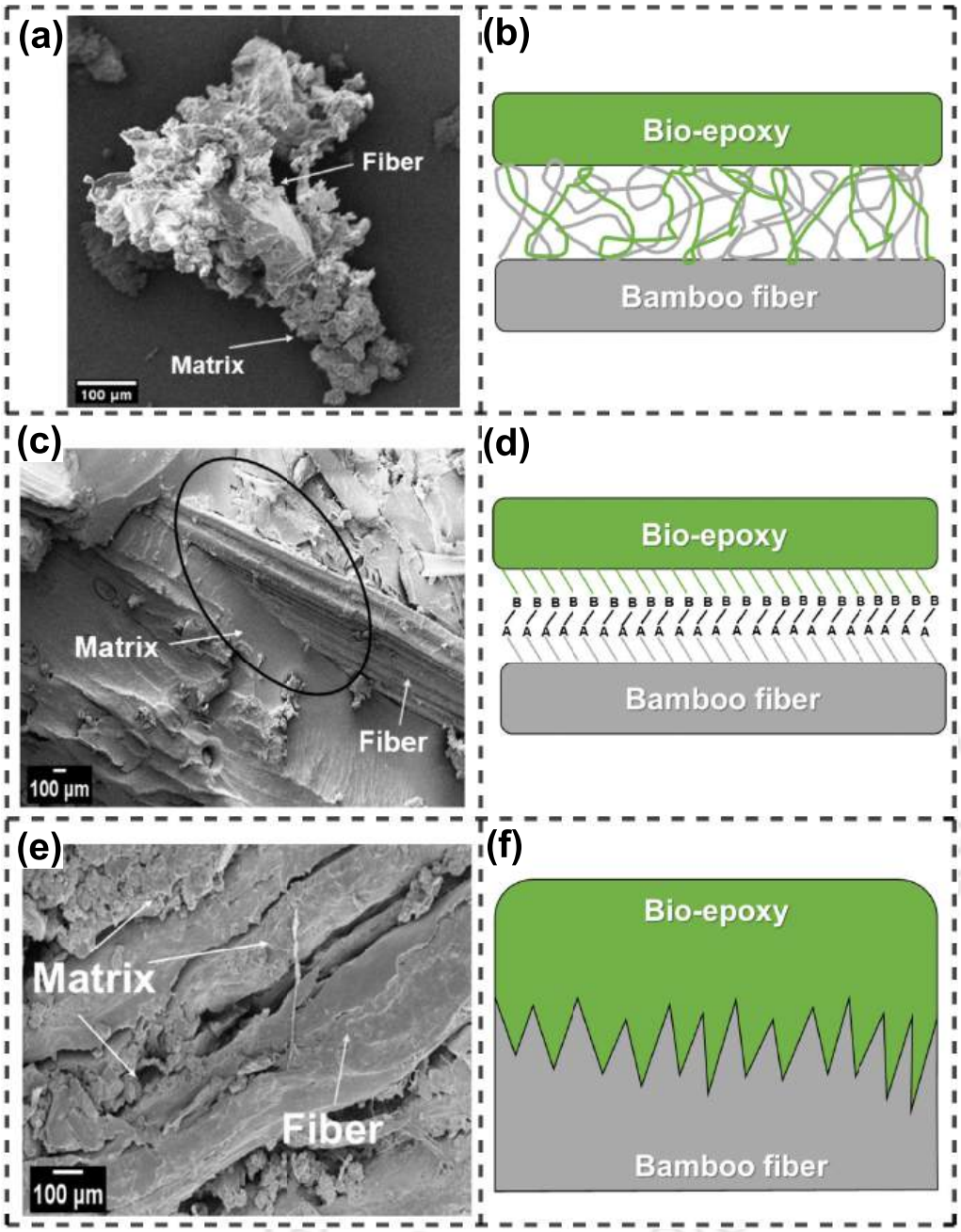

Fig. 4.15: (a), (c), (e) SEM image of different bonding, (b), (d),(f) Schamatic diagram of different bonding.

(iv) As a result of chemical treatment, there was an increase in crystallinity index, leading to higher tensile strength and tensile modulus.

(v) The chemical treatment additionally had a positive impact on the thermal stability of the fiber. An increase in both initial degradation temperature and residual mass of fiber was observed following the chemical treatment.

TH-3447_196103002

(vi) The removal of lignin, hemicellulose, and extractives from the fiber surface resulted in an increment in surface roughness for the fiber after chemical treatment.

(vii) The chemical treatment with a 6% NaOH concentration led to the degradation of the cellulose in the fiber. Consequently, all thermo-mechanical and physical properties of the fiber exhibited a decline after treatment with 8% and 10% NaOH concentrations.

TH-3447_196103002

Chapter 5

Development and characterization of bamboo based bio-composite

5.1 INTRODUCTION

Alternative environment friendly materials have gained popularity due to global concerns over fossil fuel depletion, plastic waste, and the increasing carbon footprints of products. Petrochemicals derived from fossil fuels are used in manufacturing most plastics [276]. In 2021, global plastic consumption was valued at USD 568.9 billion and is expected to grow annually by 3.2% for the next seven years [277]. Despite being inexpensive and possessing desirable long-lasting properties, plastic products are not biodegradable and accumulate as waste in landfills and oceans after reaching the end of their useful lives [278]. Environmental scientists predict that by 2050, there will be approximately 12,000 million tons of plastic waste in landfills worldwide. It is estimated that 400 million tons of plastic waste are generated annually, almost half of which comes from packaging [3]. Approximately 150 million tons out of the 400 million tons end up in oceans around the world [279]. In this chapter, the initial focus was on the development of biocomposite plates featuring varying weight fractions (10%, 20%, 30%, and 40%) of untreated bamboo fiber. A comprehensive mechanical characterization, encompassing tensile, flexural, impact, hardness, and natural frequency analysis, has been conducted for these biocomposites. The findings indicated a decline in mechanical properties beyond a 30% fiber weight fraction (specifically, at 40% fiber loading). Subsequent efforts involved refining the biocomposites using a 30% fiber load and bamboo fiber treated with different concentrations of NaOH. To elucidate the impact of NaOH treatment on diverse biocomposite properties, an array of static, dynamic mechanical, thermogravimetric, physical, dielectric,

TH-3447_196103002

and morphological characterizations was performed. **Sec. 5.2.1** provides an in-depth overview of the materials utilized in this experimental investigation. The fiber extraction and chemical treatment processes are detailed in **Sec. 5.2.2**, while **Sec. 5.2.3** outlines the meticulous procedure for biocomposite development. **Sec. 5.2.4** delves into the various characterization processes and the corresponding machinery employed, and **Sec. 5.3** comprehensively presents the results obtained from these characterizations. The results disclosed that the introduction of fiber into the polymer matrix led to a notable enhancement in mechanical strength. The highest tensile strength has been recorded as 88.57 ± 5.56 MPa for untreated bamboo biocomposites with a 30% fiber load. Furthermore, chemical treatment with up to 6% NaOH concentration resulted in increased static and dynamic mechanical properties. Specifically, 30% fiber weight fraction biocomposite treated with 6% NaOH exhibited superior mechanical performance, boasting the highest tensile strength (132.916 MPa), tensile modulus (6.983 GPa), flexural strength (154.8 MPa), modulus (8.243 GPa), and impact strength (44.06 kJ/m^2), coupled with reduced moisture absorption. Additionally, the crystallinity index and glass transition temperature of the biocomposite showed an upward trend with higher NaOH treatment concentrations. Moreover, chemical treatment up to 6% NaOH concentration resulted in a reduction in the dielectric constant, dielectric loss, and ac conductivity of the biocomposites. Conversely, treatment with 8% and 10% NaOH concentrations led to a rapid increase in dielectric and conductivity values. The developed biocomposites exhibit promising potential for advanced engineering applications, surpassing the performance of previously reported biocomposites.

5.2 MATERIALS and METHODOLOGY

This section describes the materials used in the present study, as well as the methodology and experimental processes employed for various material characterizations.

5.2.1 Materials

The bamboo (*Bambusa tulda*) is a native species in the northeast India region. It was purchased from a neighbourhood nursery in Guwahati between the age group of three to four years.

TH-3447_196103002

The acetone and sodium hydroxide pellet (NaOH) has been purchased from Merck Life Science Pvt. Ltd. The bio-epoxy resin (matrix), the FormuLITE series, is provided by Cardolite India Pvt. Ltd. (Mangaluru, Karnataka, India). The FormuLITE is composed of a thermoset polymer resin (2501A) derived from Cashew nutshell liquids (CNSL) without harming the food chain and an amine-based curing agent (2002B). The chemical composition of the epoxy resin is Poly (Bisphenol A-co-epichlorohydrin) and Cashew nutshell liquid polymer with epichlorohydrin. The chemical composition of the curing agent is m-Phenylenebis(methylamine) and 3,6,9-Triazaundecamethylenediamine. The bio content of the epoxy-curing agent mixture is about 45.4% by weight [280].

5.2.2 Fiber Extraction and Chemical Treatment

The fiber from Bambusa tulda culm has been extended by retting process. A bamboo culm has been split into four pieces and placed into water for three days. The microbial degradation of the bamboo culm makes it easier to extract fiber from the culm using a comb and a sharp knife. As per the investigation of Muhammad et al. [102] this process is one of the best processes to extract continuous or long bamboo fiber. After extracting fiber, it was placed in an oven at 80°C for 4 to 6 hours. These fibers are named as untreated bamboo fiber. Thereafter extracted fiber has been treated with NaOH solution of different concentrations of 2, 4, 6, 8 and 10%. The fiber has been merged into NaOH solutions and the beakers have been stirred on a magnetic stirrer for 8 hours at 48°C with 430 revolutions per minute [111]. The fibers were taken out of the solution after 8 hours and washed with acetone and distilled water. Thereafter the treated fibers were placed into a hot air oven at 80°C for 6hrs.

5.2.3 Development of Biocomposites

The bio-composite plate has been developed using a modified hand lay-up technique. First, bio-epoxy (2501A) and curing agent (2002B) were mixed in a weight ratio of 100:52. For homogeneous mixing of solution the mixture was stirred with a glass rod for 10 to 15 mins and thereafter put into a desiccator for 15 to 20 minutes to degas. The composite development setup consists of three parts: parts A and B are the upper and lower part of the mould (size- 250×250 mm^2), and part C is for

TH-3447_196103002

guiding the distribution of bamboo fiber. Firstly, on both the top and bottom layers of the mould, a laminated sheet was applied. After that, the homogeneous mixture of liquid polymer and curing agent was poured on the laminated sheet (the material of the laminated sheet is polypropylene, thickness-200 microns), and a roller was used for homogeneous distribution of liquid epoxy. The bamboo fibers were then placed on this liquid polymer layer by hand on the lower mould. As soon as the fibers were distributed homogeneously, a more liquid polymer mixture was poured over them. After that, the upper mould was placed on the epoxy-embedded fiber. Using four M8 nuts and bolts arranged at four corners, moulds were clamped together (the approximate amount of load used in compressing the mould is 0.5 to 0.8 kN) and left for 24 hours to cure the liquid polymer. As soon as the composite plates were solidify, they were demoulded and cut according to ASTM standards for different tests. A schematic diagram of the process has been represented in **Fig. 5.1**. The bio-composite plates were made with different weight fractions of fiber and with different treatment conditions. The details of developed biocomposites with different fiber weight fractions and treatment conditions have been tabulated in **Table 5.1**.

Table 5.1: Weight and volume fraction of bamboo fiber and bio epoxy matrix.

Sample	F(w%)	M(w%)	F(v%)	M(v%)	NaOH(%)	B(%)*
BFBC_10	10	90	11.45	88.55	—	50.86
BFBC_20	20	80	22.54	77.46	—	56.32
BFBC_30	30	70	33.28	66.72	—	61.78
BFBC_40	40	60	43.69	56.31	—	67.24
BFBC_30_0	30	70	33.28	66.72	—	61.78
BFBC_30_2	30	70	32.80	67.20	2	61.78
BFBC_30_4	30	70	32.01	67.99	4	61.78
BFBC_30_6	30	70	30.87	69.13	6	61.78
BFBC_30_8	30	70	34.00	66.00	8	61.78
BFBC_30_10	30	70	34.63	65.37	10	61.78

F(w%)= fiber weight fraction, M(w%)= matrix weight fraction, F(v%)= fiber volume fraction, M(v%)= matrix volume fraction, NaOH(%)= treatment concentration, B(%)=bio content (Bio content of the epoxy is calculated as per the data sheet.

TH-3447_196103002

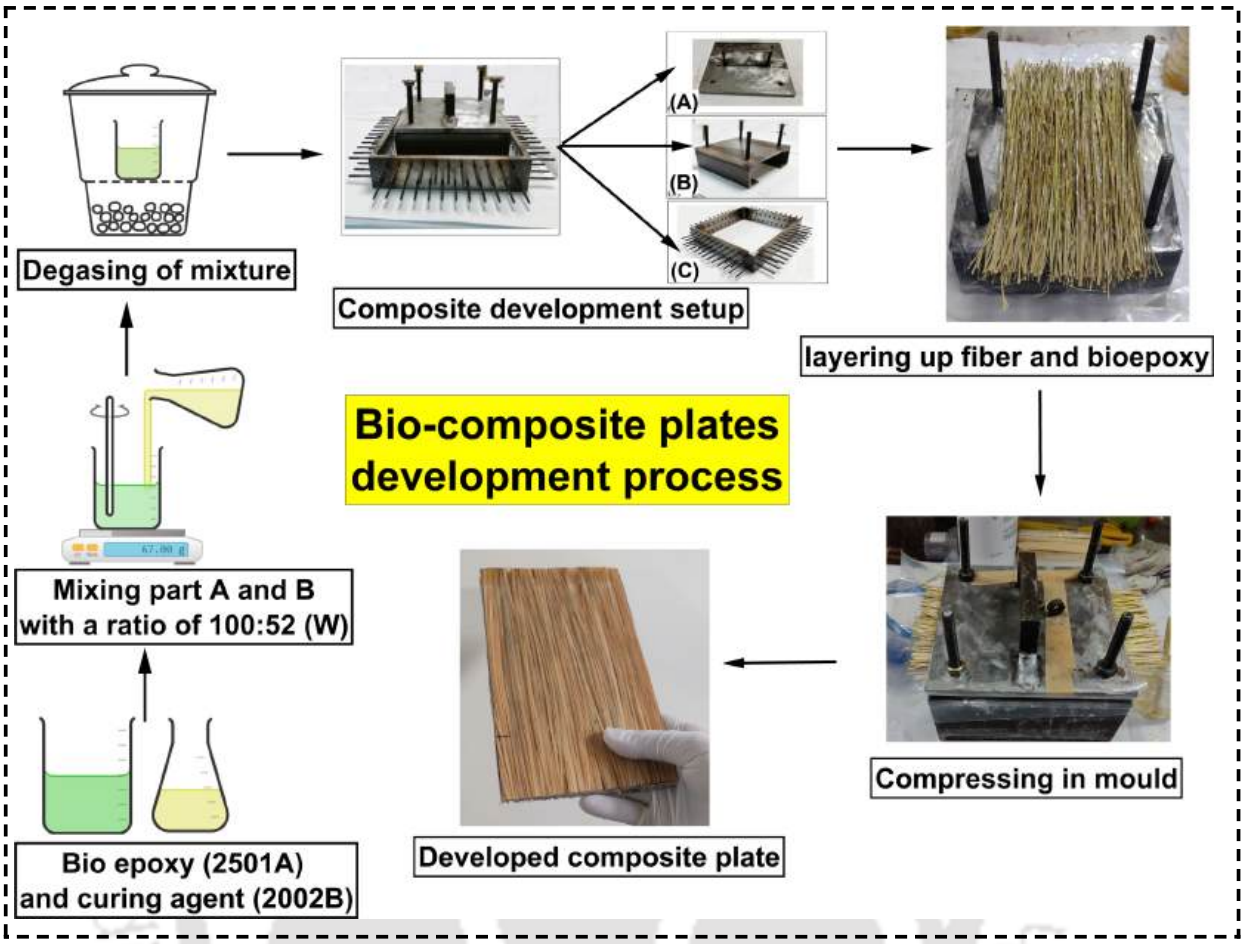

Fig. 5.1: Composite development process.

5.2.4 Characterization of Developed Biocomposites

Bio-composite plates are characterized physically, mechanically, thermally, dielectrically and biodegradabily. The details of the investigation process are presented in this section.

5.2.4.1 Density and Void Content

The theoretical density of the developed biocomposites has been investigated using the rule of mixture. The experimental density of the biocomposites is measured using Archimedes' principle. For experimental density, the samples are prepared according to ASTM-D-792-13 ($20\times20\times3mm^3$) [281]. The difference between theoretical and experimental density is referred to as the void content of the biocomposites.

TH-3447_196103002

5.2.4.2 Mechanical Characterization

The different mechanical tests, such as tensile testing, 3-point bending testing, Charpy impact testing, surface roughness, and natural frequency of the developed biocomposites, have been characterized for mechanical properties. The detailed mechanical characterization process is presented below:

Tensile Testing- Tensile testing was conducted on five samples from each group with a gauge length of 50 mm and a crosshead speed of 1 mm/min. The samples were prepared according to ASTM-D-638-3 ($160\times14\times3mm^3$) [282]. Tensile strength, modulus, and elongation at break values of the biocomposites has been measured using a Shimadzu UTM Load Cell-100 KN (model: AGX-V) machine.

3-Point Bending Test-The flexural testing was conducted on five samples from each composite group, with a span length of 70 mm and a crosshead speed of 1 mm/min. The samples were prepared according to ASTM-D-790-3 ($130\times14\times3mm^3$) [141]. Flexural strength and flexural modulus of the biocomposites were measured using a Shimadzu UTM Load Cell-100 KN (model: AGX-V).

Charpy Impact Test- The impact strength of the developed biocomposites has been measured by conducting Charpy impact testing with five samples from each batch, and mean values are reported with standard deviation. The samples were prepared according to ASTM-D-6110 ($64\times12.7\times3.2mm^3$) [283], and an IT-30 impact testing machine (maker: FIE) was used.

Surface Hardness-The surface hardness of the developed composite was measured using a 1/4" aluminum ball with an L scale by applying a 60 Kgf load of a Digital Rockwell hardness tester (maker: FIE). Samples were prepared according to ASTM-D-785 ($20\times20\times3mm^3$) [221], and hardness readings are presented as average values of five with standard deviation.

Natural Frequency- The natural frequency of the test sample has been determined using RFDA-MF-based non-distortion testing equipment (maker: IMCE), and the average value has been reported. The samples are made according to ASTM-E-1876-15 ($60\times20\times3mm^3$) [284].

TH-3447_196103002

5.2.4.3 Dynamic Mechanical Analysis

The dynamic mechanical properties of the developed biocomposites have been investigated with the help of the dynamic mechanical analyser of Anton Paar (Maker: Physica MCR, Model; 702). The samples have been prepared as per dimensions of 50 X 13 X 3 mm^3 [167] and a double cantilever fixture has been used for holding the samples inside the machine. The test condition was at a sinusoidal frequency of 1Hz and the temperature was swapped from room temperature (25°C) to 150°C with a temperature ramp of 5°C/min [285].

5.2.4.4 Structural Characterization of Biocomposites

Various structural analyses, including XRD and FTIR, have been conducted to assess the impact of chemical treatment on the developed biocomposite. The detailed process of structural characterization is outlined below:

X-ray Diffraction (XRD) Analysis- An X-ray diffraction machine (BRUKER; model: D8 advance; USA) has been used to study the influence of chemical treatment on the crystallinity index and the crystalline structure of the developed biocomposites. The machine uses Cu as the target material operated at 15 mA/ 30 kV (λ=1.542Å). A scan speed of 2°/min and a step size of 0.02° were used to record the X-ray intensity from 10° to 60°. The Ruland-Vonk method was used to calculate the crystallinity index of the composite, **Eq.5.1** [286, 287].

$$Cr\% = \frac{(A_T - A_{Am})}{A_T} \times 100\% \tag{5.1}$$

where A_T is the total area under the XRD graph, and A_{Am} is the area of the amorphous zone.

Fourier Transmission Infrared (FTIR) Analysis- Developed biocomposites have been subjected to an FTIR analysis on a PerkinElmer device to see how chemical processing affected their functional groups. The testing has been done in ATR mode with the composite film in a range of 400 to 4000 cm^{-1} spectrum at a scanning speed of 2 cm^{-1}.

5.2.4.5 Dielectric Characterization of Biocomposites

An HIOKI LCR meter, model number IM3536, was employed to assess the dielectrical characteristics of the prepared composites, including dielectric constant, dielectric loss, AC conductivity,

TH-3447_196103002

impedance, and modulus. For testing with LCR meter, following steps were followed. Firstly, ensure the LCR meter is properly calibrated according to the manufacturer's instructions. Then, select the appropriate test fixtures for the sample to ensure good electrical contact. Thereafter, prepare the sample, making sure it is clean and free of contaminants that could affect the measurement. The samples were cut to the required size of the fixture (9 mm in length and 3 mm in width). Both ends of the samples were polished with a polishing machine, and silver paste was applied to the polished ends to make contact electrodes. Connect the sample to the LCR meter using the test fixtures, ensuring the connections are secure and that there is good contact with the sample. The meter will apply an AC signal to the sample and measure the resulting impedance. The LCR meter will calculate the capacitance (C), inductance (L), or resistance (R) based on the impedance measurements. For dielectric constant measurements, the focus is usually on the capacitance. The dielectric constant of the samples was determined using **Eq.5.2**.

$$\varepsilon' = \frac{C}{C_0} \tag{5.2}$$

Where $C\_0 = \frac{\varepsilon\_0 A}{d}$. here ε_0 is the dielectric permittivity of air = 8.85×10^{-12} F/m, A stands for cross-sectional area of the sample and d is the length of the sample (distance between electrodes) [286]. The loss factor has been calculated by using **Eq.5.3**.

$$\text{Loss factor}(tan\delta) = \frac{\varepsilon^{"}}{\varepsilon'} \tag{5.3}$$

$\varepsilon^{"}$ and ε' are imaginary and real dielectric constants. The alternative current conductivity (σ_{ac}) has been calculated by using **Eq.5.4** [288].

$$\sigma_{ac} = \omega \varepsilon \varepsilon_0 tan\delta \tag{5.4}$$

where ω is frequency. The complex Impedance can be written as **Eq.5.5**.

$$Z^* = Z' - i\ Z^{"} \tag{5.5}$$

where $Z^{"} = Z\ sin(\phi)$ and $Z' = Z\ cos(\phi)$. The complex Modulus is represented as **Eq.5.6**.

$$M^* = M' + i\ M^{"} \tag{5.6}$$

TH-3447_196103002

where $M^{"} = \omega \times C_0 \times Z'$ and $M' = \omega \times C_0 \times Z^{"}$. Z is the complex impedance, Z' and $Z^{"}$ are the real and imaginary impedance as well M' and $M^{"}$ are the real and imaginary modulus. ϕ is the phase angle [289].

5.2.4.6 Moisture Absorption Characterization

To comprehend the moisture absorption characteristics of the test samples, the specimens have been immersed in distilled water, and their weights have been monitored at regular intervals of 48 hours up to 720 hours [237, 290, 291, 292]. The average of five samples was analyzed, and the reported results include the average weight gain and thickness swelling. The samples were prepared as per ASTM-D-570 ($20\times20\times3mm^3$) [293].

5.2.4.7 Biodegradability Behavior Characterization

The test samples underwent soil burial on agricultural land for 180 days at a depth of 10 cm from the surface, and weight loss was measured at regular intervals of 15 days. The samples were prepared according to ASTM-G-160-12 ($50\times50\times3mm^3$) [294].

5.2.4.8 Thermogravimetric Analysis (TGA)

The thermal degradation of the composite samples were measured by using Perkin Elmer Instrument machine. The grounded samples were used for the testing. Thermal degradation of the sample has been measured from room temperature to 800°C at the N_2 environment with a constant heating rate of 10°C/min.

5.2.4.9 Morphological Analysis

The fracture surface of different test specimen has been investigated through a field emission scanning electron microscope. The interfacial interaction of fiber and matrix at the fracture surface has been investigated using Zeiss (model: Sigma) FESEM machine.

5.3 RESULTS AND DISCUSSIONS

This section of the thesis illustrates various outcomes pertaining to the characterization of the developed biocomposites.

TH-3447_196103002

5.3.1 Static Mechanical Characterization

Tensile Testing- The biocomposites developed with different fiber weight fractions have been tested with UTM, and typical stress-strain curves have been shown in **Fig. 5.2** (a). The typical tensile stress-strain curve for all samples has been presented in **Fig. 5.3**.

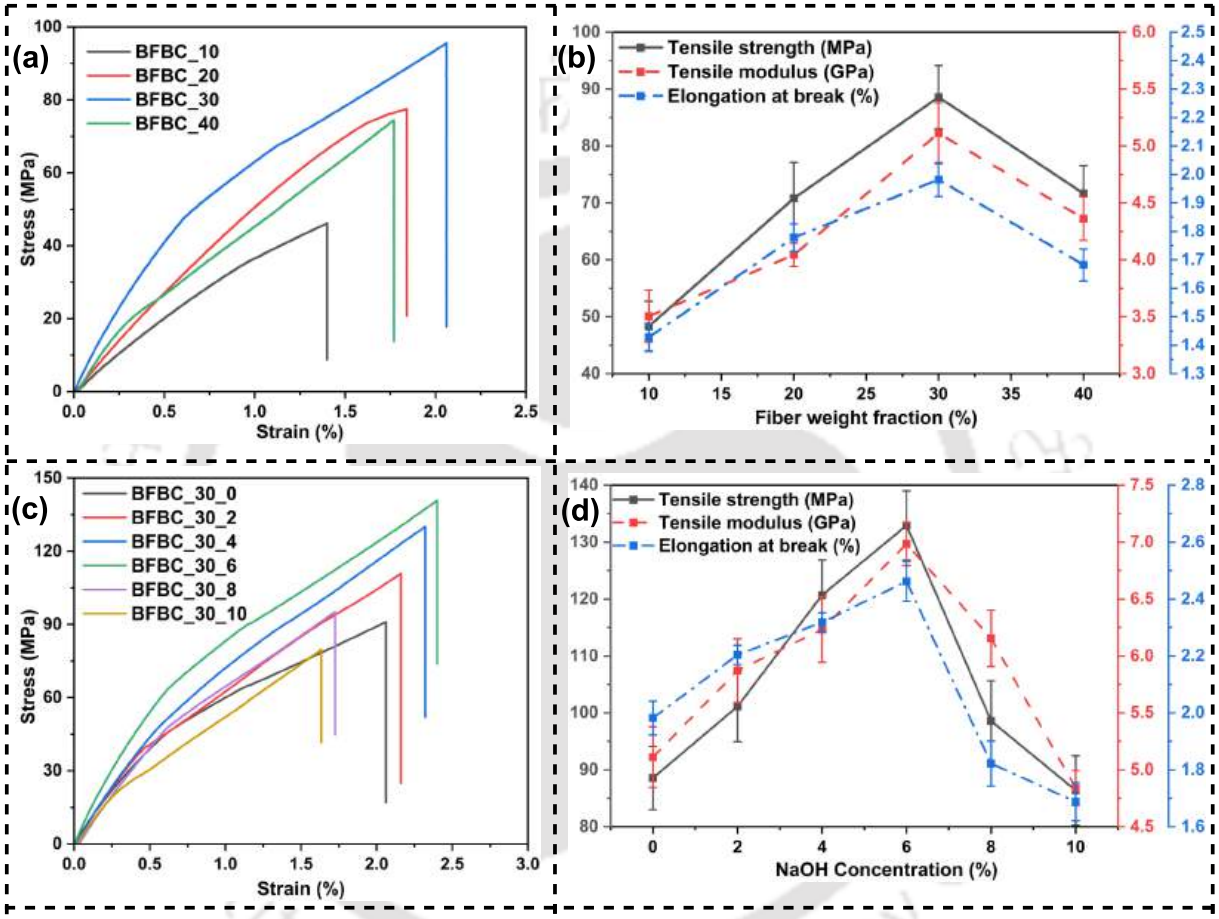

Fig. 5.2: Tensile stress-strain graph for (a) different fiber loaded composites, (c) different treated fiber loaded composites, variation of tensile properties with (b) fiber weight fraction (d) NaOH concentration.

With an increment in fiber weight fraction up to 30%, the strength and Young's modulus of the developed bio-composite also increase. But when fiber weight fraction exceeded 30%, aggrumolation occurred, which may increase the sudden stress concentration faction of the bio-composite, resulting in a reduction in strength and Young's modulus. **Fig. 5.2** (b) depicts different strengths, Young's modulus, and elongation before break values for bio-composite with different weight fractions of fiber. To understand the effect of chemical treatment on biocomposites, further analysis was carried

TH-3447_196103002

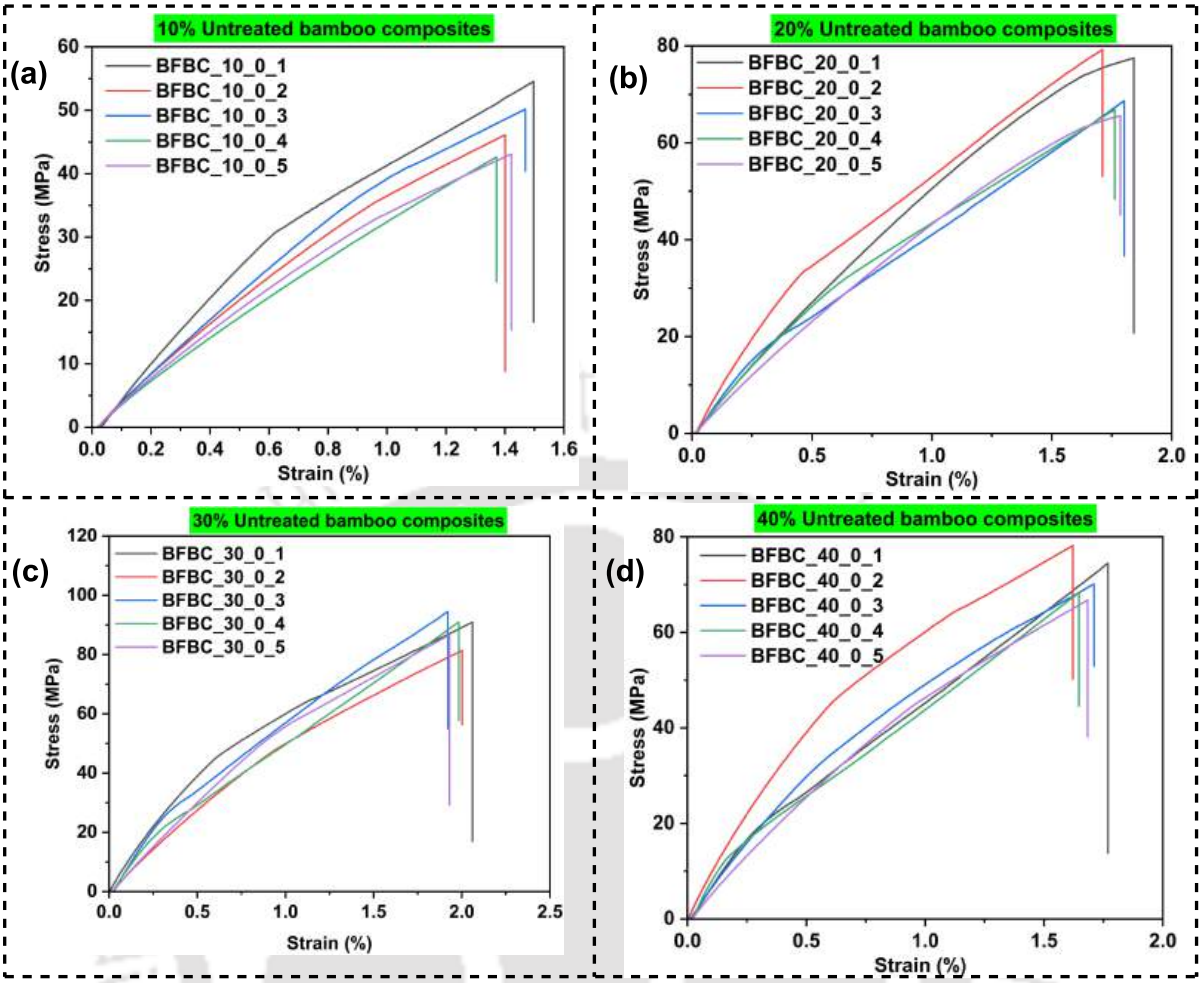

Fig. 5.3: Tensile stress-strain curve of all five samples for (a) 10%, (b) 20%, (c) 30% and (d) 40% fiber weight fraction untreated bamboo biocomposites.

out with 30% fiber loading samples treated with different concentrations of NaOH. Treatments with up to 6% NaOH concentrations affect the tensile properties positively. The maximum tensile strength and Young's modulus have been observed for the BFBC_30_6 type of bio-composite. These values are 50.06% and 36.62% higher than BFBC_30_0 type of composite. Increasing the interfacial interaction of reinforcing fiber and bio-epoxy resulted in high strength values for biocomposites, while chemical treatment also increased the crystallinity of the fiber, which resulted in an increase in the tensile modulus of biocomposites. Tensile stress-strain curves for biocomposites with different NaOH concentrations and variation in tensile properties with different NaOH concentrations are shown in **Fig. 5.2** (c) and (d), respectively. The typical stress-strain curve for all samples of differntly treated and untreated fiber reinforced biocomposite has been presented in **Fig. 5.4**.

TH-3447_196103002

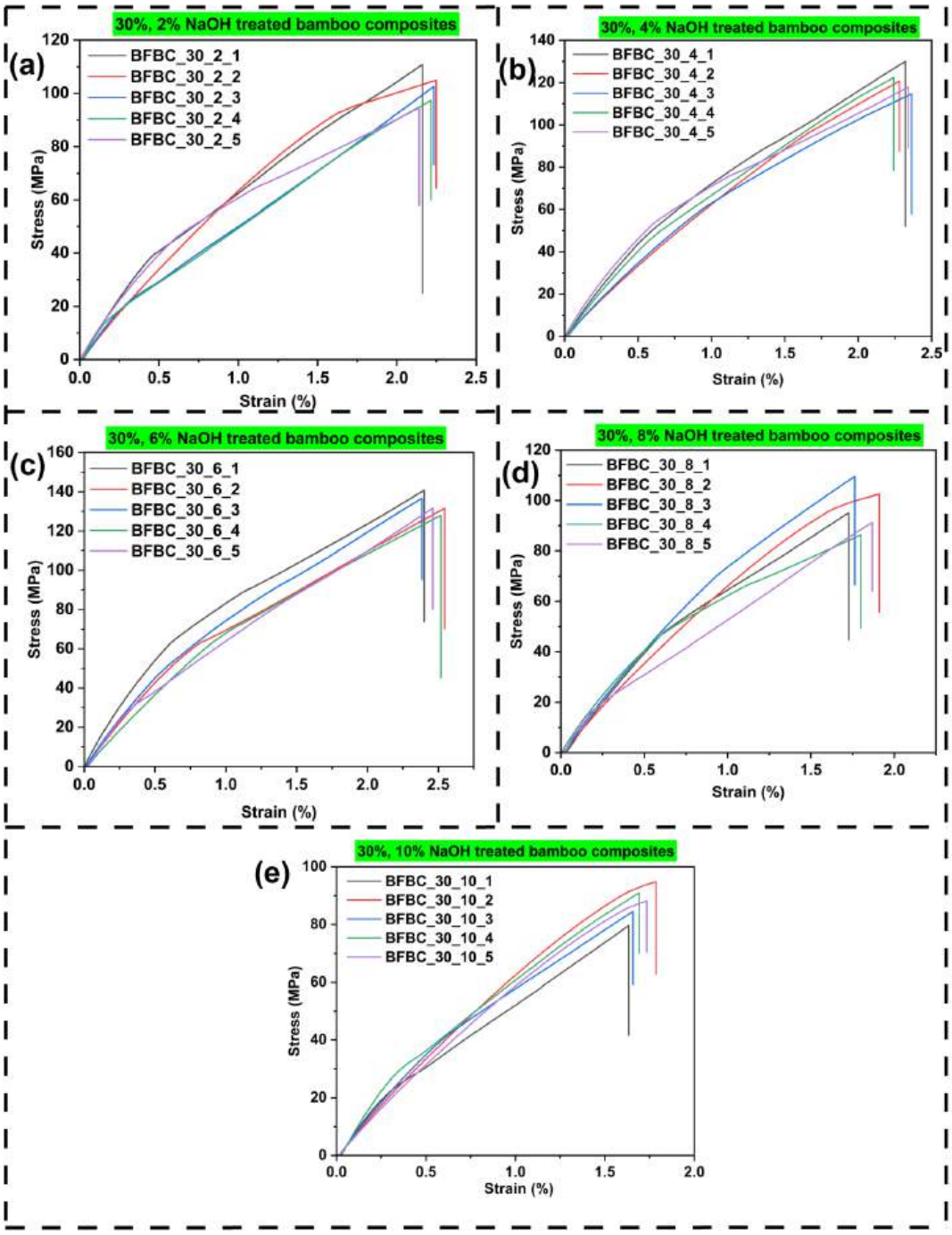

Fig. 5.4: Tensile stress-strain curve of all five samples for 30% fiber loaded treated with (a) 2%, (b) 4%, (c) 6%, (d) 8% and (e) 10% NaOH treated bamboo biocomposites.

This parameter measures the deformation the composite can withstand before breaking. A higher strain to fracture suggests that the composite can absorb more energy and undergo greater deformation, making it more resilient to dynamic loads and impacts. Thermosetting polymers are inherently brittle due to the presence of cross-links. However, the addition of bamboo fiber

TH-3447_196103002

increases the ductility of the polymer composite. Elongation at break values were recorded as 1.428 ± 0.047%, 1.778 ± 0.048%, 1.982 ± 0.059%, and 1.68 ± 0.055% for BFBC_10, BFBC_20, BFBC_30, and BFBC_40 types of bio-composites, respectively. Chemical treatment enhances the interfacial interaction between bamboo fiber and bio-epoxy, resulting in further increases in elongation at break values for the bio-composites, up to 6% NaOH-treated fiber-reinforced composite. The maximum elongation at break value was reported as 2.462 ± 0.069% for BFBC_30_6 types of composites. However, further increases in treatment concentration led to degradation in fiber-matrix interfacial bonding, resulting in lower elongation at break values.

In Ashby charts, interdependent material properties are plotted along each axis on a two-dimensional plane. Each material family is illustrated as a separate domain, which represents its range of properties in the charts. The Ashby chart also provides guidelines with different slopes depending on the loading condition, which is useful for selecting a material [295]. Materials lying on the same guideline perform equally well, while materials appearing above the guideline perform better than those below. In the Ashby chart, all types of bio-composites have been plotted between maximum tensile strength and density, as well as between elastic modulus and density. **Fig. 5.5** (a) represents the Ashby chart between maximum tensile strength with density and **Fig. 5.5** represents the elastic modulus with density. The slope has been calculated for each type of biocomposite from the Ashby charts. The dotted line in **Fig. 5.5** (a) and **Fig. 5.5** (b) is representing the slope for BFBC_30_6 types of composites. From the guideline [296], for any uniaxial loading condition, yield the maximum tensile strength for the minimum weight design is represented by $\frac{\sigma_y}{\rho}$ and maximum elastic modulus for minimum designed weight is represented by $\frac{E}{\rho}$. Maximum tensile strength and specific elastic modulus qualities constantly rise as NaOH concentration increases up to 6%, while specific properties quickly decrease as concentration grows beyond 6%. For the BFBC_30_6 kinds of composites, the maximum specific tensile strength and specific elastic modulus have been noted. The specific properties of developed composites with respect to NaOH concentration have been presented in **Fig. 5.5** (c).

3-point Bending Testing- Like tensile properties increment in fiber weight fraction resulted in an increment in flexural strength and modulus value. For untreated fiber reinforcement, the maximum

TH-3447_196103002

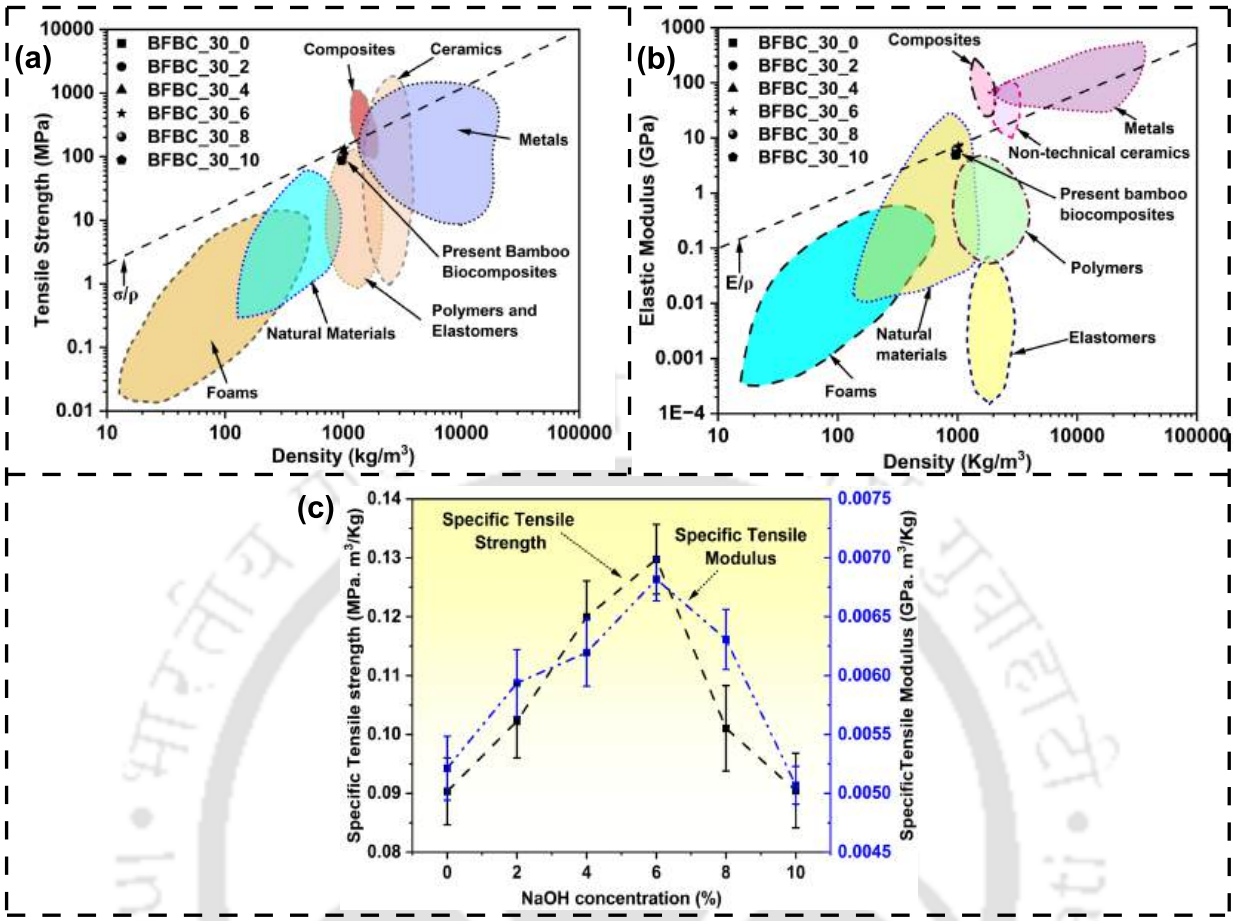

Fig. 5.5: (a) Ashby chart for ultimate tensile strength [256], (b) Ashby chart for elastic modulus [257] and (c) representation of specific mechanical properties for different developed biocomposites.

flexural strength and flexural modulus have been observed for 30% fiber weight fractions. Further increment in fiber weight fraction may be caused by the agglomeration of fiber inside bio-composite and resulted in a sudden decrement in strength and modulus value. **Fig. 5.6** (a) and (b) represent the typical flexural stress-strain curves and variation of flexural properties with different fiber weight fractions. The typical flexural stress-strain curve for all samples has been presented in **Fig. 5.7**.

The NaOH treatment increased the flexural strength and flexural modulus of bio-composite. The maximum flexural strength and flexural modulus have been observed for BFBC_30_6 type of bio-composite which are 58.28% and 36.65% higher than the flexural strength and modulus value of BFBC_30_0 type composite. Beyond 6% chemical treatment concentration, the fiber surface becomes burned, resulting in ineffective bonding between reinforcement fiber and bio-epoxy, resulting in lower tensile and flexural strength values. **Fig. 5.6** (c) and (d) illustrate the flexural stress-strain

TH-3447_196103002

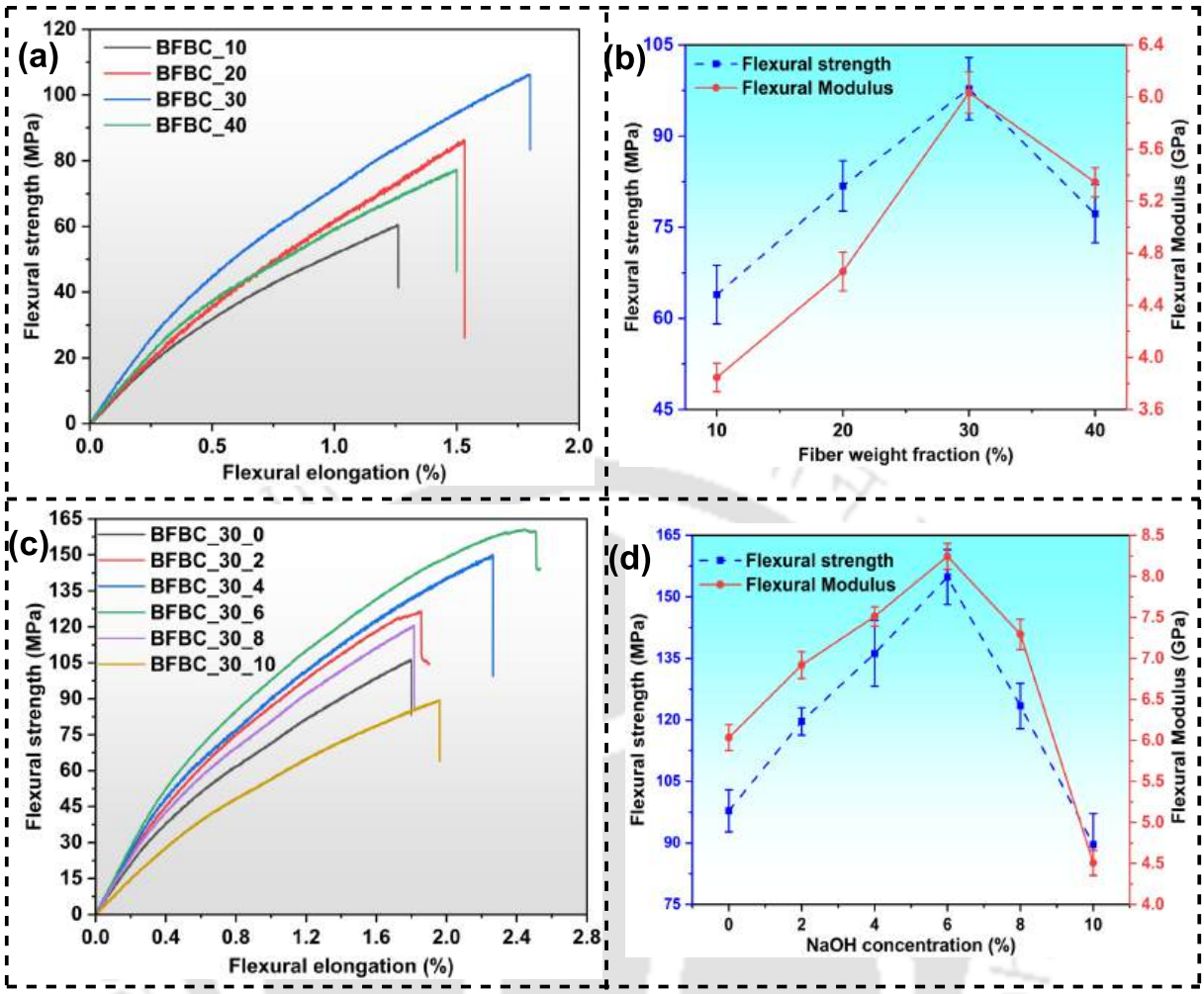

Fig. 5.6: Flexural stress-strain graph for (a) different fiber loaded composites, (c) different treated fiber loaded composites, variation of flexural properties with (b) fiber weight fraction (d) NaOH concentration.

curve and the effect of NaOH concentration on the flexural properties of biocomposites respectively. The typical flexural stress-strain curve for differntly treated and untreated fiber reinforced biocomposite has been presented in **Fig. 5.8**.

Charpy Impact Test- Impact strength/energy is the measure of a material's ability to absorb energy or shock before break. The maximum impact strength among untreated fiber reinforced composite has been observed with the BFBC_30 type of composite. Further increment in fiber weight fraction resulted in a decrement in impact strength. Impact strength may correlate with elongation before the break in tensile testing. The thermosetting bio-epoxy is brittle in nature due to the presence of a high crosslink inside it. The addition of bamboo fiber increases the ductility and

TH-3447_196103002

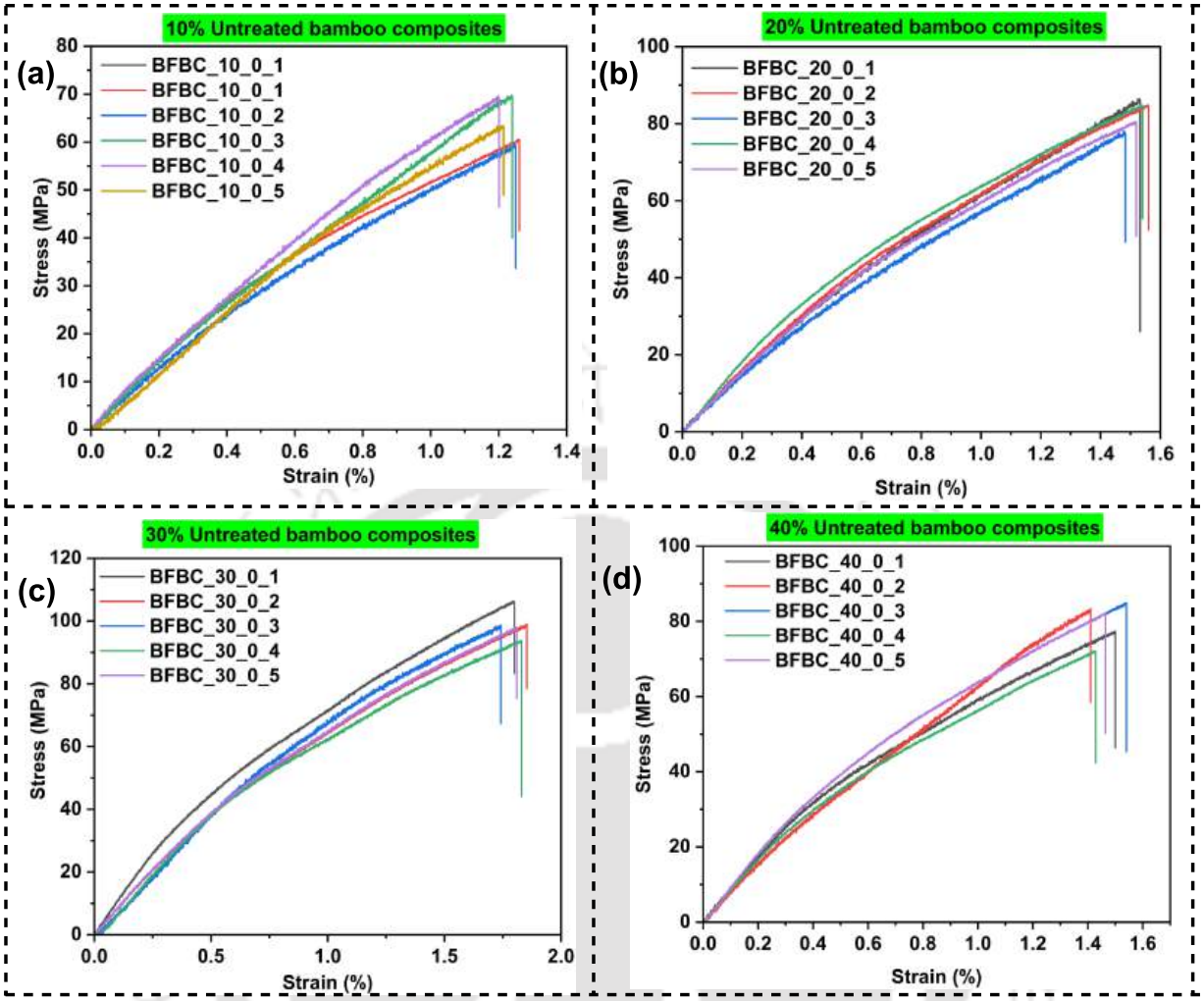

Fig. 5.7: Flexural stress-strain curve of all five samples for (a) 10%, (b) 20%, (c) 30% and (d) 40% fiber weight fraction untreated bamboo biocomposites .

toughness of composites, and as a result, the impact strength may also be enhanced. In the case of fiber weight fractions exceeding 30%, agglomeration occurs, which may make the composite brittle, and thus the impact strength also decline. Due to the same reason, the elongation before break value of the tensile testing is also decreased with 40% fiber-reinforced bio-composite. The chemical modification of fiber resulted in a further increment in impact strength value. The maximum impact strength with treated fiber has been reported as 44.064 ± 1.41 kJ/m^2 for BFBC_30_6 type of bio-composite. This value is 32.56% higher than the BFBC_30_0 type of composite. **Fig. 5.9** (a) and (b) represented the impact strength of different composites.

Surface Hardness- The addition of fiber into bio-epoxy resulted in an increment in hardness

TH-3447_196103002

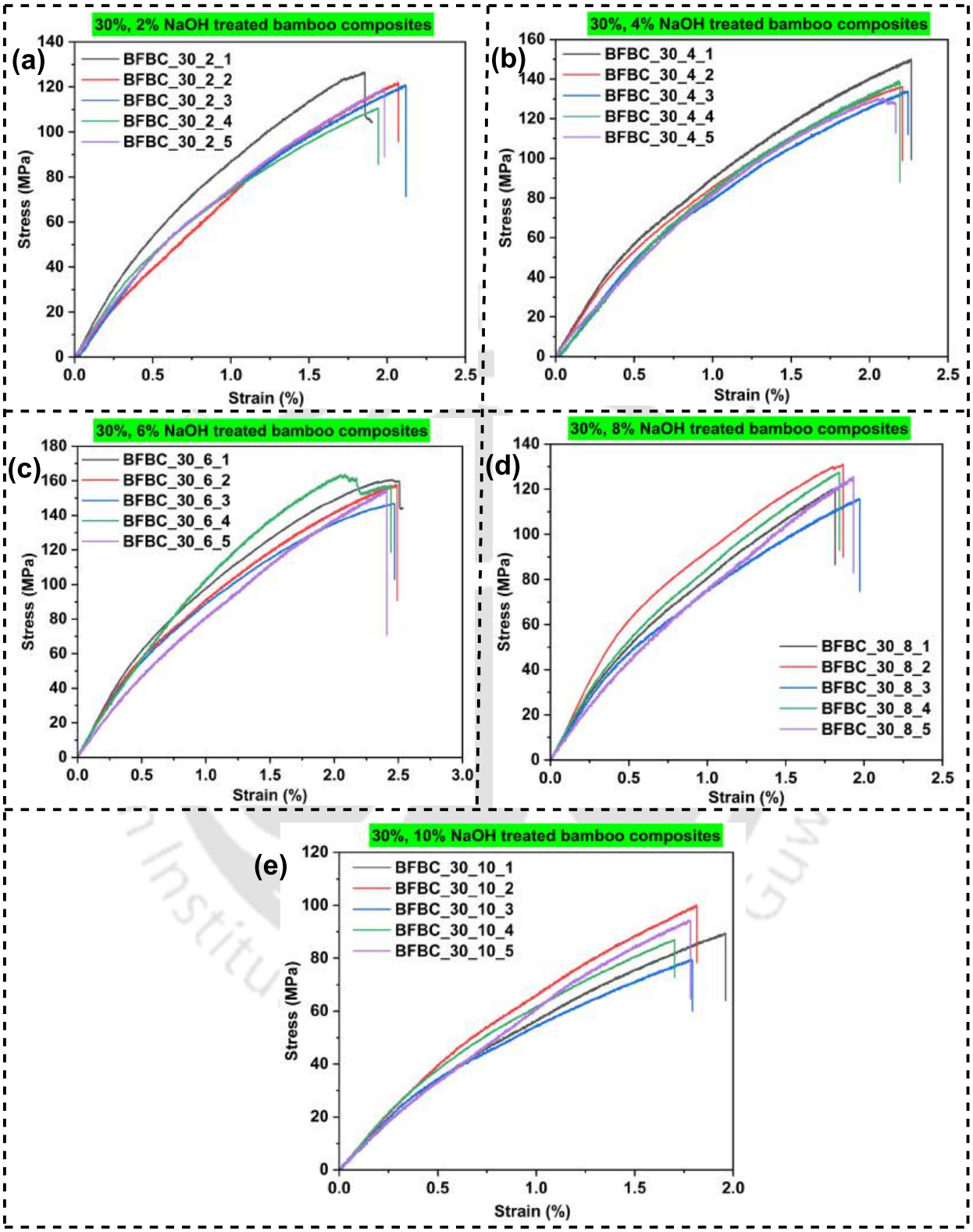

Fig. 5.8: Flexural stress-strain curve of all five samples for 30% fiber loaded treated with (a) 2%, (b) 4%, (c) 6%, (d) 8% and (e) 10% NaOH treated bamboo biocomposites.

TH-3447_196103002

value of the biocomposites. The maximum hardness value has been recorded as 62.791 ± 3.561 HRC with BFBC_30_0 types of biocomposite. Chemical treatment of fiber further increases this hardness value to a maximum of 82.31 ± 4.169 HRC for BFBC_30_6 type of bio-composite. This value is 31.08% higher than the BFBC_30_0 type of composite. The chemical treatment of fiber has modified the interfacial interaction between the matrix and fiber, which facilitates easy transmission of localized load from matrix body to reinforcement fiber, resulting in higher resistance to localized plastic deformation. **Fig. 5.9** (a) and (b) represent the different hardness values with respect to different fiber weight percentages and different NaOH concentrations of fiber treatment.

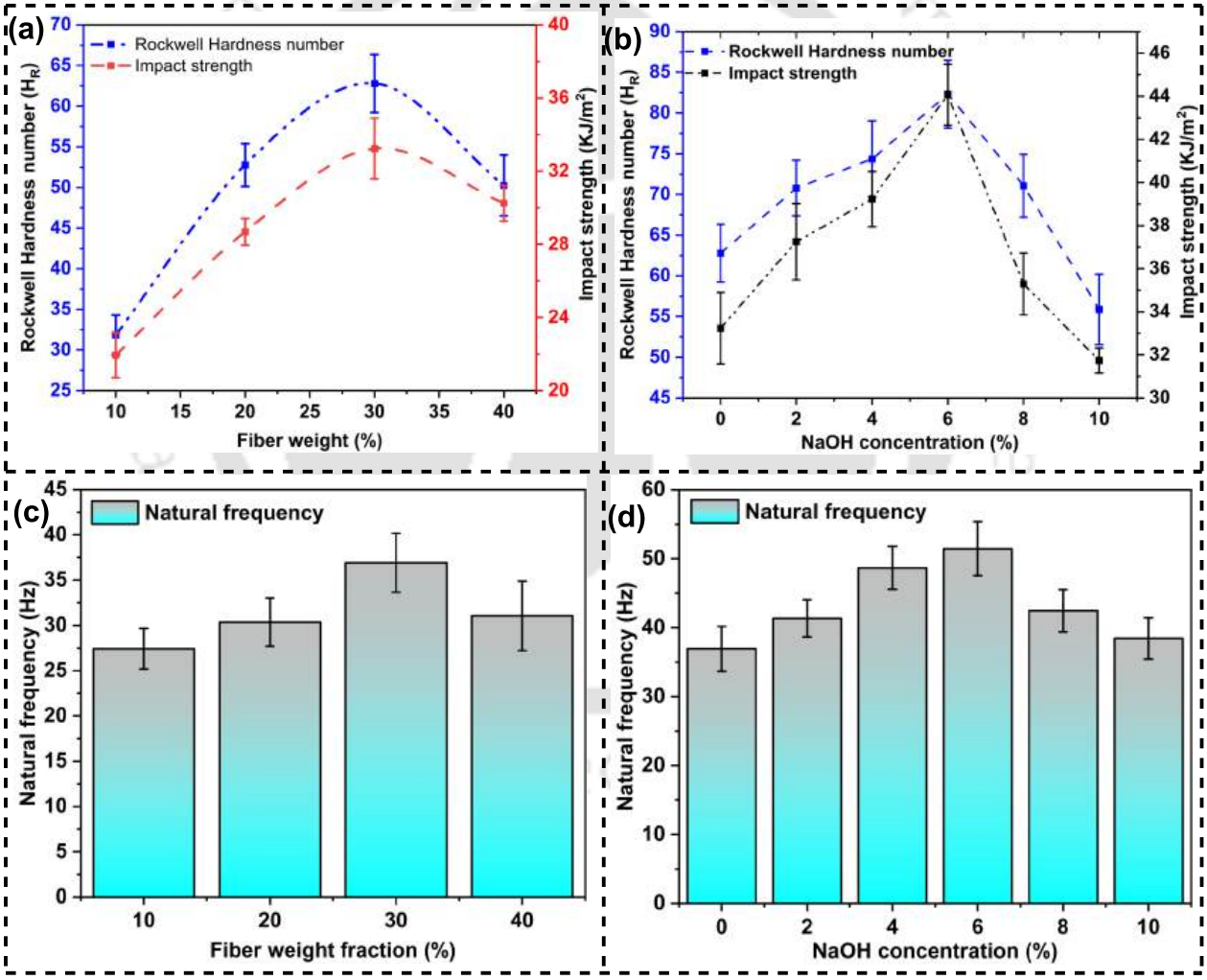

Fig. 5.9: Variation of impact and hardness with (a) fiber weight fraction, (b) NaOH concentration, variation of natural frequency with (c) fiber weight fraction, (d) NaOH concentration.

Natural Frequency- In order to utilize composites for dynamic applications, it is crucial to under-

TH-3447_196103002

stand their vibration behaviours. From the frequency response function curve, the first three modes and their corresponding frequencies have been determined in this study. Due to the similar characteristics of all the modes, the Mode I frequency has been considered for further discussion. Based on the results, the natural frequency of the biocomposites increased with an increase in fiber weight fraction. Adding fiber to bio-epoxy increases the stiffness of the composite, which may increase its natural frequency. Fiber weight fractions greater than 30% show agglomeration, and therefore stiffness, as well as natural frequency, are decreased. As a result of further chemical treatment of bamboo fiber, the interfacial interaction increased, resulting in an increment in stiffness of the composite, and, consequently, an increment in natural frequency has been observed. The maximum natural frequency has been obtained as 51.454 ± 3.930 Hz with BFBC_30_6 types of biocomposites. This value is 39.37% higher than untreated fiber reinforced composites. **Fig. 5.9** (c) and (d) represent the mode-I frequencies with respect to different fiber weight fractions and different NaOH weight concentrations. To comprehend the potential of recently developed composites for diverse structural applications, a comparative analysis is conducted to assess their mechanical properties in relation to those documented in existing literature. **Table 5.2** presents the comparative study of the composites.

5.3.2 Dynamic Mechanical Analysis (DMA)

To understand the effect of NaOH treatment on the dynamic mechanical properties of biocomposites, including storage modulus (E'), loss modulus ($E"$), and damping factor ($tan\delta$), dynamic mechanical testing have been performed in tensile mode as a function of temperature at 1 Hz constant frequency. **Fig. 5.10** represents different dynamic mechanical properties and glass transition

TH-3447_196103002

Table 5.2: Comparative study of mechanical characteristics in newly developed bioComposite against biocomposites presented in literatures.

Reference	Matrix	Reinforcement	Tensile strength (MPa)	Tensile Modulus (GPa)	Flexural strength (MPa)	Flexural modulus (GPa)	Impact Strength/ energy	Natural frequency (Hz)	Applications
Present work	FormuLITE (2501A+2002B)	Bambusa tulda	132.916	6.983	154.8	8.243	44.06 kJ/m^2	51.45	Construction, automotive section,household application
Fiore et al. [297]	epoxy	kenaf	106.1	10.7	177.6	18.8	—	—	Packaging industry
Loganathan et al. [191]	Phenolic resin PH-4055	Cyrtostachys renda	34.27	3.97	65.26	—	3.29 kJ/m^2	—	Household product
Kumar et al. [285]	FormuLITE (2501A+2401B)	Ramie and flax	108	5.63	119	12.5	—	—	Biomedical application
Sanchez et al. [111]	Veg. based polyurethane	Macana bamboo	46.83	9.16	70.94	—	—	—	Automotive section
Huang et al. [167]	Epoxy	Bamboo	222.71	13.1	182.29	17.3	—	—	Construction section
Kumar et al. [298]	Polyester	Banana	30.5	1.4	46.7	58	215.3 kJ/m^2	32.3	Electrical equipment
Ismail et al. [299]	Kenaf /Bamboo	Epoxy	68.47	5.3	—	—	—	68.3	—
Zindani et al. [189]	FormuLITE (2501A+2401B)	Punica Granatum	29.93	3.20	54.86	4.46	8.73 kJ/m^2	—	Automotive section
Senthilkumar et al. [264]	Greenpoxy-56	Sisal Granatum	33.30	2.89	55.54	2.81	16.96 kJ/m^2	—	—
Kumar et al. [26]	FormuLITE (2501A+2401B)	kenaf/ pineapple	86.47	5.01	116.43	4.88	33.84 kJ/m^2	—	Biomedical application

TH-3447_196103002

temperatures for treated and untreated bamboo fiber reinforced biocomposites.

Influence of Temperature on Viscoelastic Properties- A material's viscoelastic characteristics are strongly influenced by temperature, frequency, and time. **Fig. 5.10** (a), (b), and (c) show the impact of temperature on the storage modulus, loss modulus, and damping factor, respectively. For each type of bio composite, three different regions of storage modulus and loss modulus have been observed. The first region is the glassy region. This region exhibits the maximum value of storage modulus and the minimum value of loss modulus as well as damping factor at room temperature. As temperature increases from room temperature to high temperature, loss modulus and damping factor increase significantly. Whereas storage modulus gradually decreased with temperature, and finally decreased completely after the glassy region ended.

The second zone is called transition zone. In this zone, the viscoelastic materials change their state from glassy to rubbery. The storage modulus of the biocomposite was significantly reduced at this stage, and a maximum loss modulus and damping factor were also noted. The glass transition temperature of a viscoelastic material is the temperature at which the highest loss modulus or damping factor has been reported.

The third and last zone is the rubbery region, also known as the entropy elastics region. All viscoelastic properties of the materials reach their lowest value in this region and vary gradually with temperature increase [300].

Storage Modulus ($\mathbf{E'}$)**-** An indication of the stiffness of composite materials is the storage modulus, which is the energy-absorbing capacity of the material per cycle of oscillation. **Fig. 5.10** (a) represents the storage modulus of all types of developed biocomposites. Initially, all composites showed a higher storage modulus value in the glassy region than in the other two. The molecules of bio epoxy and bamboo fiber are tightly packed at low temperatures, which provides high resistance to the movement of molecules in the glassy region [301]. As the temperature rises from 75 to 110°C, tightly packed molecule chains lose their tight arrangement and begin to move freely. The sudden drop in storage modulus has therefore been observed in transition regions. In rubbery regions, the molecules attached to each other are free to move, therefore, the storage modulus trend is parallel to the x-axis. At room temperature, chemical treatment up to 6 weight percentages of

TH-3447_196103002

NaOH shows an incremental trend in storage modulus value. The maximum storage modulus has been observed as 8378 MPa with BFBC_30_6 type of biocomposites at room temperature. There is a 28.49% increment in storage modulus value for BFBC_30_6 compare to BFBC_30_0. The chemical treatment might improve the interfacial interlocking of bio-epoxy with bamboo fiber. Better interfacial contact allows for more effective stress transfer from matrix to fiber reinforcement, perhaps resulting in a larger storage modulus value. In contrast, chemical treatment of bio fibers with more than 6% concentration destroyed their surface, possibly resulting in inefficient bonding between fiber and epoxy, which ultimately led to a lower storage modulus [302].

Loss Modulus (E")- The term "viscous modulus," also known as "loss modulus," refers to a measurement of the amount of energy released as heat per cycle during deformation that results in a viscous response in the material and is influenced by the molecular mobility of composites [303]. **Fig. 5.10** (b) shows the viscous modulus of different biocomposites. For glassy region, the loss modulus value remains constant with the increment of temperature. In transition region, the value of loss modulus began to rise. All types of biocomposites reached their maximum loss modulus value at the glass transition temperature, and thereafter the value dropped dramatically at rubbery region. The order of maximum loss modulus value is- BFBC_30_6 >BFBC_30_8 >BFBC_30_4 >BFBC_30_2 >BFBC_30_10 >BFBC_30_0. The bio-epoxy is viscoelastic in nature and chemical treatment increased the crystallinity index as well as the elastic nature of the fiber. Fibers with higher elastic properties can absorb more energy at higher temperatures while dissipating heat more efficiently. The maximum loss modulus at peak temperature is marked as glass transition temperature (T_g). The glass transition temperature of BFBC_30_0 types of composites has been observed as 85.93°C. Treatment of fiber increased the energy dissipation value and reached the glass transition temperature of the composite to a maximum value of 105.16°C with BFBC_30_6 type of sample. **Fig. 5.10** (d) shows the glass transition temperature for different type of composite with respect to the NaOH treatment concentration.

Damping Factor (tan δ)- The damping factor is the ratio between the loss modulus and the storage modulus [304, 305]. The damping factor or loss factor in polymer composites depends on the adherence of the reinforcing fiber to the polymer matrix, at a constant frequency it is

TH-3447_196103002

temperature dependent [285]. It has been observed that BFBC_30_10 type of composite show the highest (2.775) and BFBC_30_0 type of composite show the second highest damping factor value (2.464). Whereas the minimum damping factor value was observed for BFBC_30_6 with a numeric value of 1.416. When fiber is treated with NaOH concentrations up to 6%, the damping factor value continuously decreases, whereas when NaOH concentrations of 8 and 10% are used, the value increases. The chemical treatment of fiber makes it more elastic. When the load is applied to the treated fiber reinforced composite, elastic deformation occurs, resulting in low viscous flow, which shows a lower tan δ value. Treatment with high concentrations, reduces the elastic properties of fiber and increases the viscous flow as well as the damping factor. **Fig. 5.10** (c) shows the tan delta values of different biocomposites.

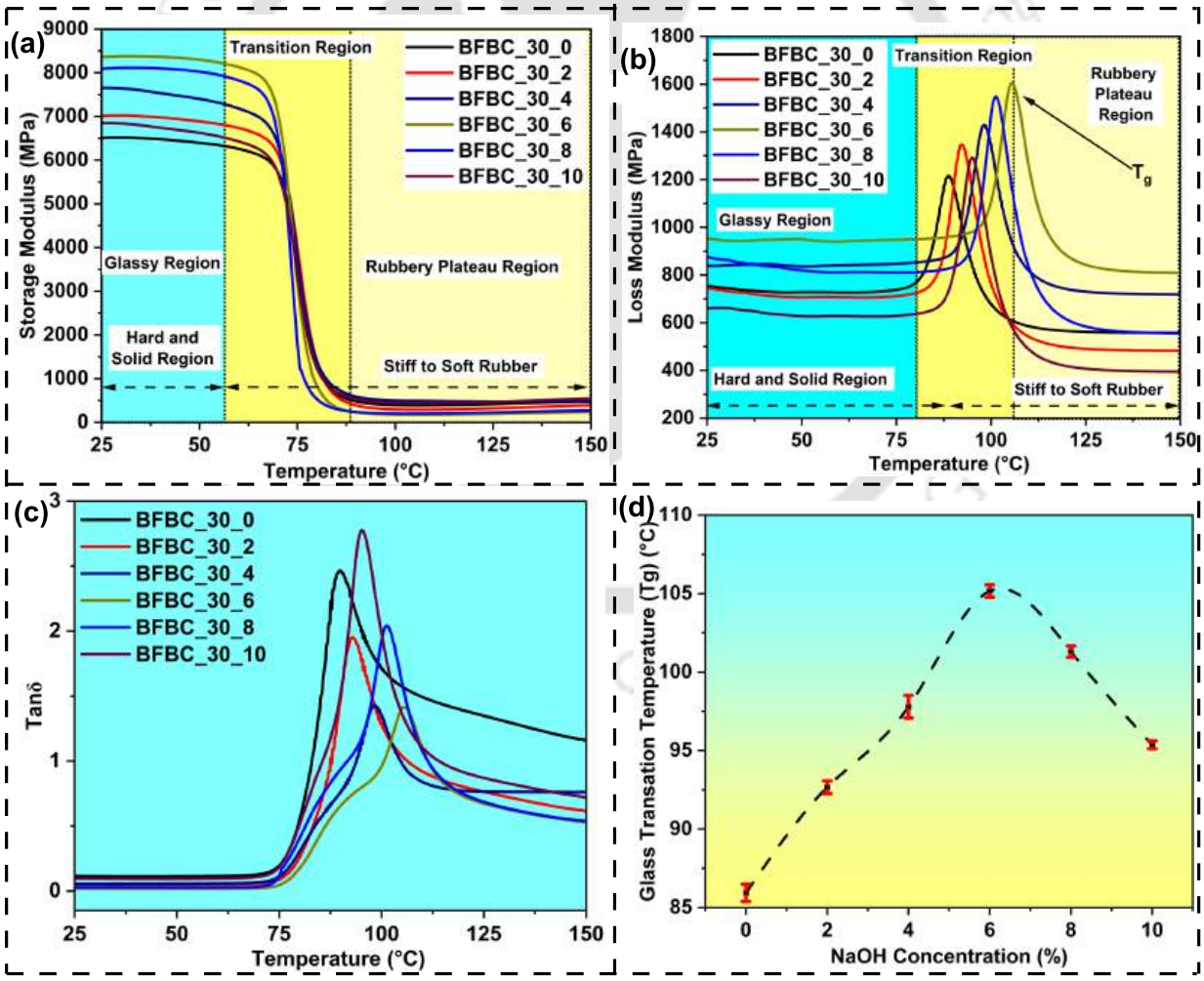

Fig. 5.10: (a) Storage modulus; (b) loss modulus, (c) Tan δ and (d) glass transition temperature of different treated and untreated bamboo fiber reinforced biocomposites.

TH-3447_196103002

5.3.3 Result for Structural Characterization of Biocomposites

XRD analysis of developed biocomposites- Crystallinity plays a major role in the properties of biocomposites. Biocomposites have been analysed using XRD to determine their crystallinity after NaOH treatment. **Fig. 5.11** (a) shows the XRD spectra of different biocomposites. In the XRD spectrum of neat epoxy, no significant peak has been observed, indicating that thermoset bio-epoxy is non-crystalline. Bamboo fiber reinforced biocomposites show two major and one minor peaks at around 15.53°, 22.2° and 34.8° corresponding to the crystalline plane (1 1 0), (0 0 2) and (0 0 4), respectively [306]. Because of the presence of crystalline cellulose in the bio-composite samples, these peaks were observed. Untreated biocomposite sample show a crystallinity of 37.46%, while biocomposites treated with NaOH show continuous increments in crystallinity. The maximum crystallinity has been observed for 6% NaOH treatment biocomposites samples (BFBC_30_6). The

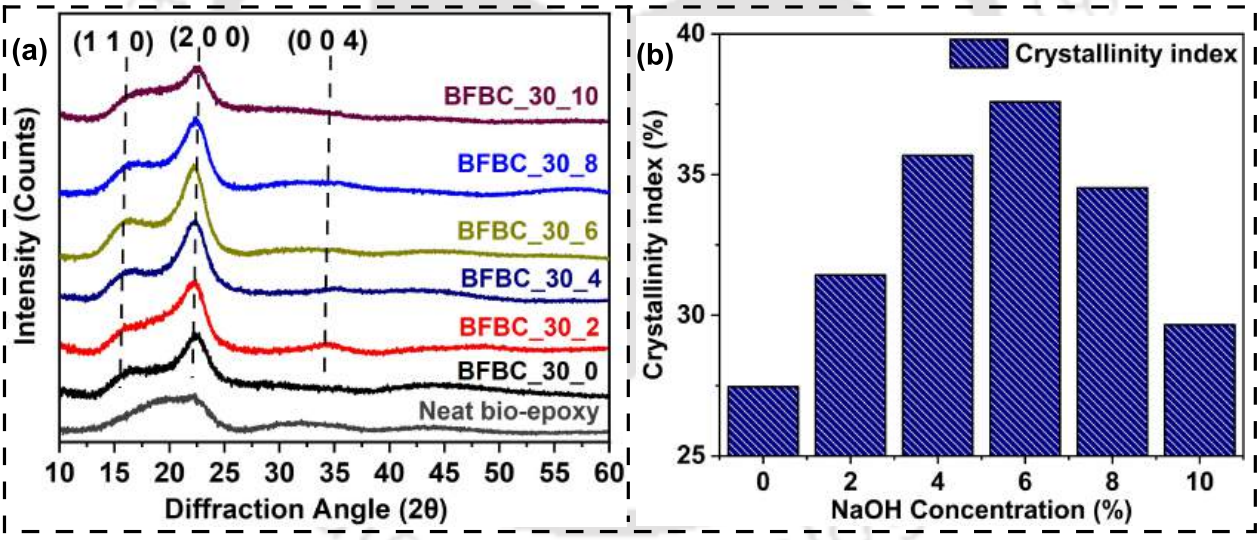

Fig. 5.11: (a) XRD spectra of different bio composites, (b) crystallinity index of different biocomposites.

crystallinity value for these type of biocomposite is 51.73%, which is 14.27% higher than untreated fiber-reinforced biocomposite. Based on the analysis presented in **Chapter-4** (Sec.4.3.2), it has been reported that NaOH treatments increase the crystallinity index of fiber, which in turn increases the crystallinity index of bio-composites. Chemical treatment with concentration greater than 6% NaOH (8% and 10%) destroys the crystalline cellulose form the fiber, resulting in a drop in crystalline index value. BFBC_30_8 and BFBC_30_10 type of sample show crystallinity index of

TH-3447_196103002

48.62% and 39.66%, respectively. In comparison to BFBC_30_6, these values are 9.11% and 12.07% lower. **Fig. 5.11** (b) shows the bar diagram for the crystallinity of different types of developed biocomposites.

FTIR analysis- FTIR analysis has been performed on the biocomposites to investigate the interfacial interactions and presence of functional groups. **Fig. 5.12** represents the FTIR spectra of different developed biocomposites. The stretching vibration of O-H group has caused a peak at 3388 cm^{-1}. The peaks at 2925 cm^{-1} and 2856 cm^{-1} are corresponding to stretching vibration of

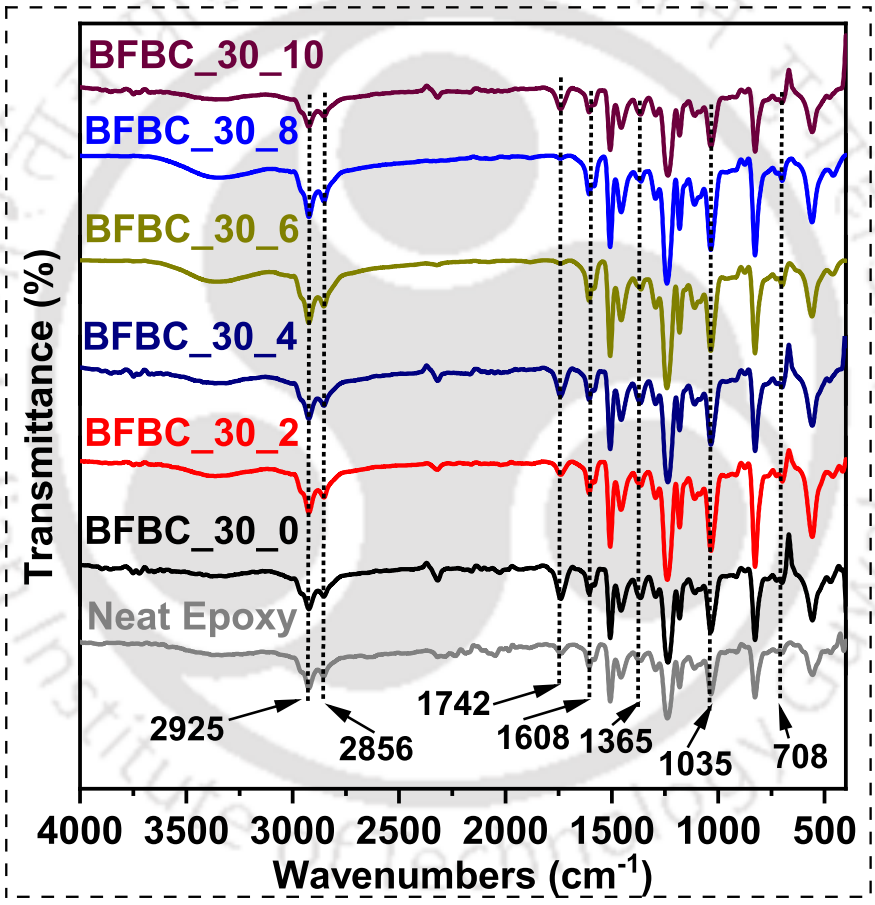

Fig. 5.12: FTIR spectra of different developed bio composites.

C-H bond and the symmetric-asymmetric stretching vibration of C-H_3, C-H_2 and C-H groups. Due to the stretching of C=O group of carboxylic acid a peak has been observed at 1742 cm^{-1} [307]. The two peaks have been seen at 1605 and 1508 cm^{-1}, which are due to the stretching vibration of C=C groups of aromatic rings. The vibration of -CH_2 and -CH_3 functional groups, two prominent peaks have been observed at 1457 and 1365 cm^{-1} wavelength [308]. The stretching vibration of C-O

TH-3447_196103002

inside epoxide groups caused intensity peaks at 1295, 1240 and 1181 cm^{-1}. The stretching of C-O-C group of ether caused a peak at 1035 cm^{-1}. A peak at 827 cm^{-1} wavelengths has been observed due to the Stretching vibration of C-O-C inside oxide groups. Finally, due to the vibration of -CH_2 groups a peak has been observed at 718 cm^{-1} [174]. According to the FTIR spectra of bio-epoxy and various bio-epoxy composites, the only difference is the intensity of the peaks, which implies that even when untreated or differently treated bamboo fibers are incorporated into biocomposites, the functional groups present in biocomposites remain the same as in bio-epoxy. A similar type of observation has been reported by Lekrine et al. [308] with Wahingtonia filifera fiber incorporated in HDPE and Komal et al. [309] incorporated banana fiber into poly-lactic acid.

5.3.4 Dielectric Analysis of Biocomposites

The dielectric properties of treated and untreated fiber reinforced biocomposites are investigated in terms of dielectric constant, loss factor, impedance, complex modulus and ac conductivity.

Dielectric Constant and Loss Factor- The dynamic response of the polymer chain towards the dielectric constant (ε') and loss factor ($\tan\delta$) in biocomposites specimens have been recorded at room temperature at a frequency range of 10^3 to 10^6 Hz. **Fig. 5.13** (a) shows the dielectric constant values for treated and untreated bamboo fiber reinforced biocomposite, while **Fig. 5.13** (b) shows their loss factor values.

It is interesting to note that both dielectric constant and loss factor show similar types of trends, in which prominence is revealed in a dispersive fashion and coalesces toward higher frequencies. As a result of interfacial and dipolar polarization, charge mobility is easier at low and medium frequencies. This resulted in a higher dielectric constant as well as a higher loss factor value. Whereas the dipole switching is difficult due to inefficient time at higher frequencies resulting in a decrement in dielectric constant and loss value [286, 310]. **Fig. 5.13** (c) and (d) present variations of dielectric constant and dielectric loss for all types of composites with respect to frequency. According to the figure, all types of composites have continuous decrement trends with respect to increments in frequency for ε' and $\tan\delta$. Alkaline treatment of bamboo fiber with NaOH solution grafts the Na^+ ion onto the cellulose structure. This makes the lignocellulose fiber hydrophobic. In

TH-3447_196103002

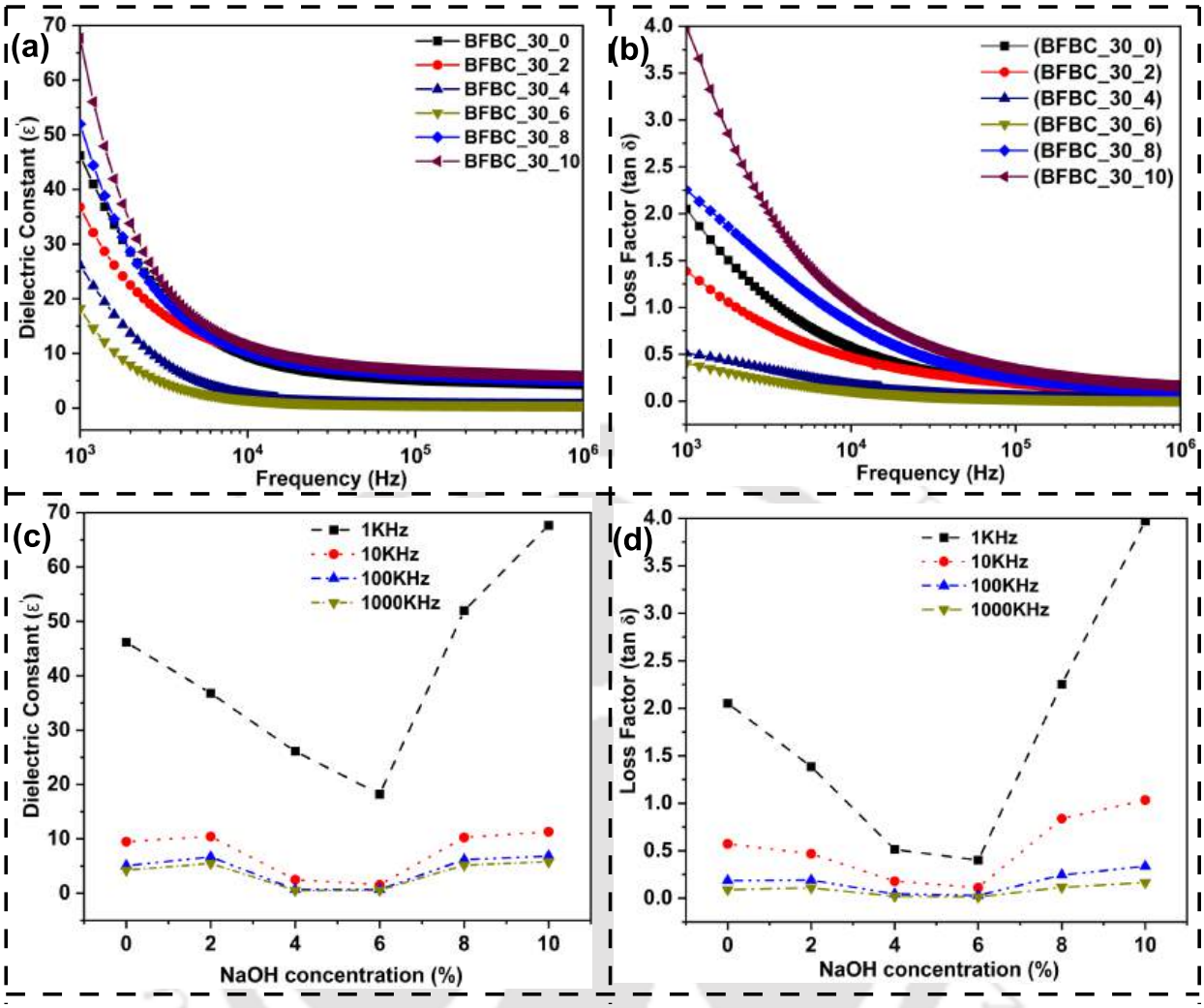

Fig. 5.13: (a) Dielectric constant, (b) Dielectric loss, (c) Variation of dielectric constant with different frequency, (d) Variation of loss factor with different frequency for different developed biocomposites.

addition, the alkaline treatment removes short-branched amorphous polymers and impurities from the fiber surface. These two analogies are also supported by the XPS results of previous chapter. The number of hydroxyl groups decreased as amorphous and impurities are removed [311]. The hydrophilicity of the fiber was decreased by removing hydroxyl groups, resulting in better interfacial bonding between bamboo fiber and bio-epoxy matrix, and decreasing in dielectric constant as well as loss factor values [289]. Due to the above mention reason, ε' and tanδ shows a decreasing trend with an increment in NaOH treatment concentrations (up to 6%). The cellulose along with non-cellulose compounds began to degrade at higher than optimal concentrations (8 or 10%) of NaOH treatment. Consequently, as a result of the treatment with a NaOH concentration of 8 or 10%, the

TH-3447_196103002

crystallinity index of the composites was also decreased. This can also be verified from the XRD result. Degradation of cellulose help to produce more polarized -OH (hydroxyl) groups leading to a higher dielectric constant and loss factor value [286, 312]. The sequence of dielectric constant values for the different developed biocomposites is- BFBC_30_10 >BFBC_30_8 >BFBC_30_0 >BFBC_30_2 >BFBC_30_4 >BFBC_30_6. For the loss factor, the biocomposites follow a similar trend.

Impedance- Impedance is the measure of a circuit's ability to withstand and store dielectric energy when current is flowing [313]. **Fig. 5.14** (a) and (b) represent the real ($Z' = Zcos\phi$) and imaginary ($Z'' = Z\ sin\phi$) impedance of the developed biocomposites materials for a frequency range from 10^3 to 10^6. Both treated and untreated fiber reinforced biocomposites show similar trends with real as well as imaginary impedance. Due to the liberation of space charge, both composites follow an equivalent trend of slowing and coalescing with rising frequency. The amorphous chain segments dominate the ionic movement of lignocellulose fiber reinforced composites. Fiber segments with non-crystalline amorphous segments act as conductive regions, while segments with crystalline cellulose chains act as resistive regions. An induced potential wall is formed by the free-charge carriers at the crystalline cellulose-amorphous interface [314]. At higher frequencies, the ac conductivity of the composite increases which reduces the interfacial barrier potential and results in a decrement of both impedance (real and imaginary) values. According to previously reported XRD data, chemical treatment eliminated the amorphous component of the lignocellulose fiber. After the chemical treatment of bamboo fiber (up to 6%), the amorphous part of the fiber was removed, in an increment in resistivity and thus both impedance (real and imaginary) values. The cellulose percentage of fibers is degraded after chemical treatment with more than 6% concentration, resulting in decreased crystallinity for fibers and composites. The reduction of cellulose reduces the resistivity of the biocomposites and results in a decrement in impedance values. At 10^3 Hz frequency, the maximum real and imaginary impedance values have been observed as $3.89\times10^7\Omega$ and $2.46\times10^7\Omega$ for BFBC_30_6 types of composites. Whereas minimum impedance at 103 Hz frequency is reported as $1.865\times10^7\Omega$ (real) and $1.295\times10^7\Omega$ (imaginary) for BFBC_30_10 types of biocomposites.

Analysis of Cole-Cole plots can provide information about relaxation mechanism behaviour, electrode effect and other microscopic effects within the material. **Fig. 5.14** (c) represents the cole-

TH-3447_196103002

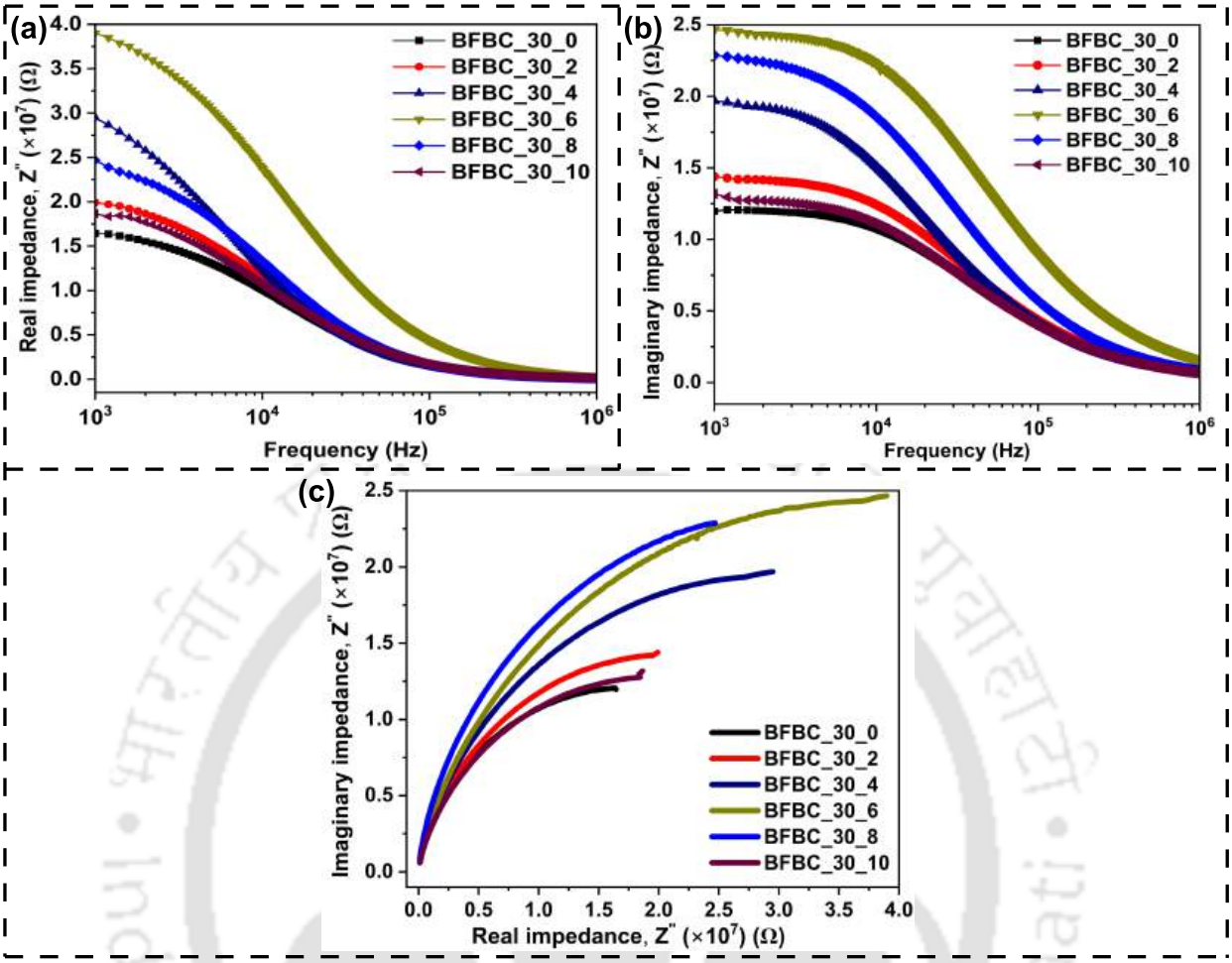

Fig. 5.14: (a) Real impedance, (b) imaginary impedance and (c) impedance cole-cole graph of developed biocomposites.

cole graph between real impedance and imaginary impedance. From linear to semicircle patterns, the plot takes on the shape of an arch, whose radii are comparatively larger and bend toward the abscissa. The linear part of the cole-cole graph is corresponding to the resistive nature of the composites due to polarization. However, the semi-circular arc indicates the conductive nature of the biocomposites due to charge transfer. The deviation of all cole-cole plots from the straight line to the complete semicircle is likely caused by the relaxation of amorphous phase and defects in nano-order inside composites.

Complex Modulus- The complex modulus ($M^* = M' + iM^{"}$) of developed biocomposites has been measured and presented in terms of real modulus ($M' = Z^{"}C_0\omega$) and imaginary modulus ($M^{"} = Z'C_0\omega$) [70] in **Fig. 5.15** (a) and (b), respectively. Real and imaginary values of the composites are very low (near zero) at lower frequencies and asymptotically increase at higher

TH-3447_196103002

frequencies. At lower frequency regimes, M' represents an insignificant contribution due to electrode effects and polarization. Whereas the spreading M' values at higher frequency regimes correspond to the conduction process, due to that the charge carriers move short distances and show higher M' values. The maximum real and imaginary complex modulus has been observed for BFBC_30_6 types of composites and minimum values have been recorded for BFBC_30_10 types of composites. **Fig. 5.14** (c) represents the modulus cole-cole graph of treated and untreated fiber reinforced biocomposites. All types of graphs showed a semi-circular pattern, indicating an ionic conduction process inside the biocomposites. The semicircle's centre is on the real modulus axis. The centre of all semicircles is on the real axis of modulus, and the intercept on the M' axis reveals the amount of total capacitance contained in the material. A dielectric relaxation process of the non-Debye type is indicated by the peak of the cole-cole graph [313].

AC-Conductivity - The AC-conductivity of the developed biocomposites has been measured and presented in **Fig. 5.15** (d). It can be seen in the figure that at low frequencies, the AC conductivity of the materials tends to zero and as the frequency increases, the AC conductivity of the materials increases. This indicates that at low frequencies, or DC, the material behaves as a non-conductor while at high frequencies, it behaves as a conductive material. In general, bio-fiber-reinforced polymers show conductivity due to their -OH bonds and amorphous structures, whereas cellulose acts as a barrier. The free charge carrier forms an internal potential wall at the interface between the crystalline and amorphous phases. At low frequencies, the conductivity is low as a result of this effect, but at higher frequencies, these potential barriers have broken and the material acts as a conductor. At 106 Hz, the maximum ac conductivity has been observed for BFBC_30_10 and the minimum has been reported for BFBC_30_6. As a result of the chemical treatment, the amorphous polymer chain is removed from the fiber, and the Na^+ ion is inserted into fiber. In this way, hydrophilic fibers become hydrophobic [315, 316]. A continuous decline in conductivity is mainly caused by the increase in hydrophobicity of biofiber. The treatment of bamboo fibers with NaOH at higher concentrations (more than 6%) degraded fiber cellulose, thus increasing polar hydroxyl groups and increasing the ac conductivity of biocomposites.

This section compares the currently developed biocomposites with previously reported biocom-

TH-3447_196103002

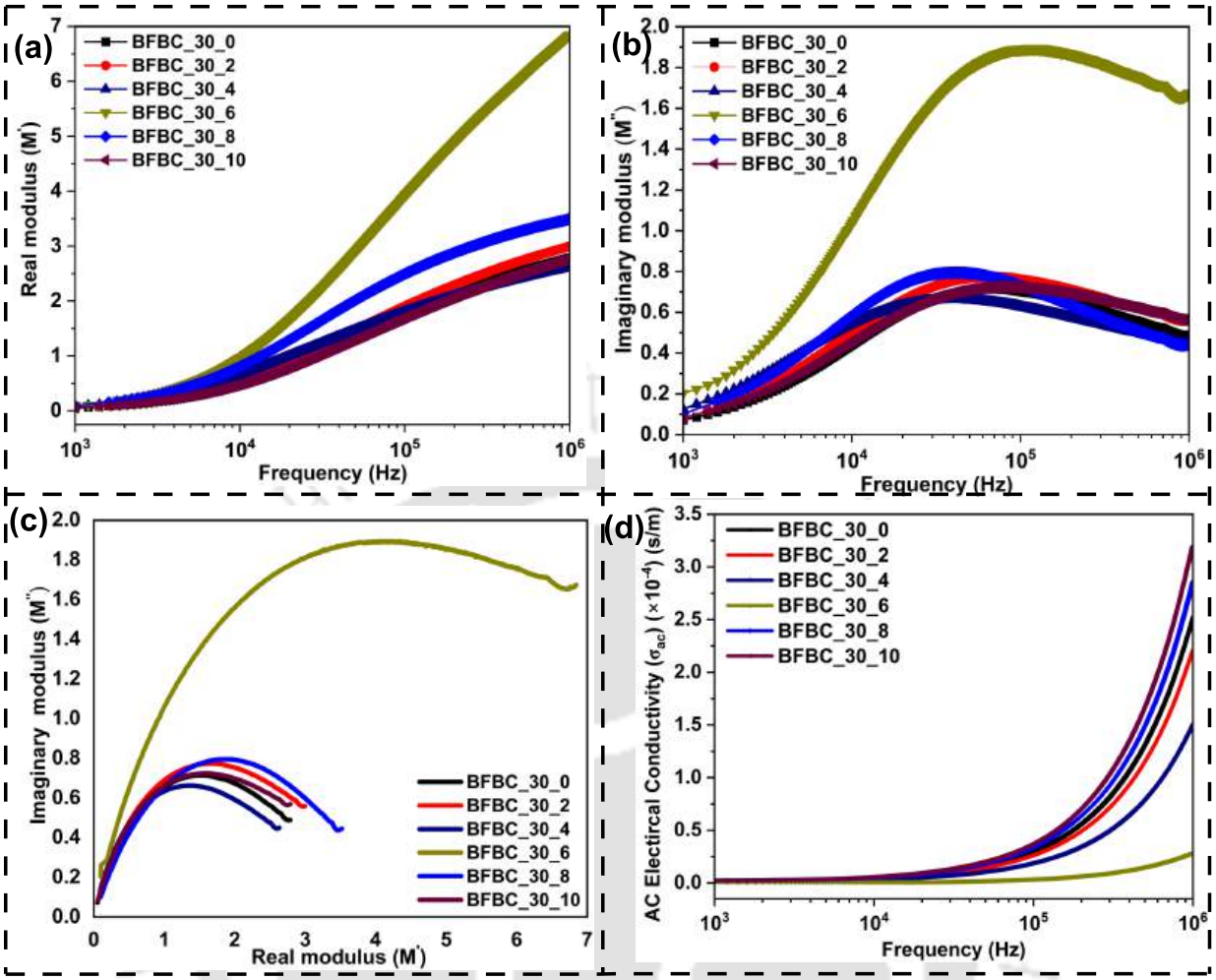

Fig. 5.15: (a) real modulus, (b) imaginary modulus, (c) modulus cole-cole graphs, (d) Ac-conductivity for all types of developed biocomposites.

posites in order to determine their potential in the electronics industry. **Table 5.3** presents the comparative studies of various properties. Materials with low density are preferable for electronics applications. So that the electronic equipment must hold a lower weight. The proposed material shows a lower density than most of the materials presented in the literature and also from the virgin polymer matrix. A material with a high dielectric constant will have a high electric breakdown voltage. It can sustain a greater voltage before failing and letting the current flow. It is desirable for insulating electronic materials, such as the casing of a laptop or a desktop, to have a higher dielectric constant. BFBC_30_10 shows a higher dielectric value compared to most of the materials presented in the comparative table. Furthermore, the ac conductivity shows extremely small values, indicating the insulation behaviour of the material. It can be concluded that developed material is

TH-3447_196103002

Table 5.3: Comparative study for dielectric properties of the biocomposites.

Composite Materials	Dielectric constant (ε')	Loss factor ($\tan\delta$)	Real Impedance ($\times 10^7$) (Ω)	Ac-conductivity($\times 10^{-4}$) (s/m)	References
BFBC_30_6	18.05	0.40	3.90	0.27	Present
BFBC_30_10	67.66	3.96	1.87	3.18	study
Coir+PP	2.54	–	–	–	[312]
Sisal+PP	4.6	0.025	–	2.65×10^{-6}	[317]
Sisal+epoxy	68.52	0.58	–	–	[318]
Alfa+ Polyester	8.7	–	–	1.32×10^{-6}	[319]
Banana+ Gluten	49.65	2.14	7.3×10^{-6}	–	[311]
Sunn Hemp+ epoxy	35.24	2.33	6.2	2.5×10^{-1}	[289, 313]
Kapok husk+ epoxy	12.42	0.116	–	–	[320]

one of the best-fit materials for the electronics industry.

In structural engineering, the dielectric constant and AC conductivity of materials are important for various applications, particularly those involving smart structures, monitoring systems, and electromagnetic shielding. Here are some specific examples where these properties are crucial [321].

Dielectric constant: High dielectric constant materials can enhance the sensitivity of sensors used in monitoring the integrity of structures, which is useful for structural health monitoring application. Materials with appropriate dielectric properties are used to insulate sensors and other electronic components embedded in structures. Ensuring that signals transmitted by embedded sensors or communication systems travel effectively through the material. High dielectric constant materials are used in capacitive sensors embedded in concrete or composite structures to monitor strain, stress, and other parameters. Applied to structures to protect embedded sensors from

TH-3447_196103002

environmental factors while maintaining their sensitivity and accuracy. Used to detect internal defects, voids, or reinforcements in structures. The dielectric constant of the material influences the penetration depth and resolution of GPR [322].

AC Conductivity: Low AC conductivity reduces energy dissipation in monitoring and communication systems, enhancing their efficiency. Proper AC conductivity ensures effective signal transmission and reduces reflection and attenuation in embedded sensors. Materials with controlled AC conductivity can be used to shield structures from electromagnetic interference. Incorporates materials with specific AC conductivity to enable the concrete itself to act as a sensor, detecting strain or cracks through changes in electrical properties. Materials with low AC conductivity are used to insulate and protect power lines and components integrated into structural elements. Materials with appropriate AC conductivity are used in walls, floors, and ceilings to shield sensitive electronic equipment from electromagnetic interference [323].

In structural engineering, many applications require careful consideration of both dielectric constant and AC conductivity to ensure optimal performance and reliability. The major applications are as follows:

(i) Smart Structures: Incorporate materials with tailored dielectric and AC conductivity properties to enable real-time monitoring and self-diagnosis of structural health. Examples include bridges, high-rise buildings, and tunnels [324].

(ii) Embedded Sensor Networks: Use materials with specific dielectric and AC conductivity properties to maintain the integrity and efficiency of sensor networks embedded in concrete, steel, and composite structures for long-term monitoring.

(iii) Wireless Communication Systems: Structures incorporating wireless communication systems for monitoring and control use materials with optimized dielectric and AC conductivity properties to ensure efficient signal transmission and minimal interference.

The dielectric constant and AC conductivity are essential properties for materials used in structural engineering applications. They play a crucial role in ensuring the efficiency and reliability

TH-3447_196103002

of monitoring systems, smart structures, electronics packaging, and EMI shielding solutions. Understanding and optimizing these properties can lead to improved structural integrity, enhanced safety, and better performance of modern engineering projects [325].

5.3.5 Water Absorption Behavior of Biocomposites

It is necessary to understand how developed biocomposites behave in a hydrated environment. Based on mechanical testing, biocomposites with 30% fiber loading exhibit the best mechanical properties, so further investigation has been conducted only on differently treated 30% fiber loaded bio-composite. The developed biocomposites were put into distilled water and the weight percentages and thickness changes were calculated using **Eq.5.7** and **Eq.5.8** with a regular interval of 48 hrs.

$$W_{\text{Water absorption}}(\%) = \frac{W_t - W_0}{W_0} \times 100 \tag{5.7}$$

Where W_t and W_0 are the weight of bio-composite samples at time = t and 0.

$$T_{\text{Thickness swelling}}(\%) \frac{T_t - T_0}{T_0} \times 100 \tag{5.8}$$

Where T_t and T_0 are the thickness of the bio-composite samples at time = t and 0 [293]. It has been observed from the testing results of all types of biocomposites that the moisture absorption and swelling percentage increase with time, and after 480 hours of submersion in water that the swelling and moisture absorption start saturation. BFBC_30_0 type of bio-composite shows moister absorption of 7.866 ± 0.364% and thickness swelling of 12.532 ± 0.364% respectively. There are many micro-level gaps presented between bamboo fiber and bio-epoxy matrix, due to the hydrophilic nature of fiber; these gaps act as capillary action and water as well as moisture are absorbed inside the composites. For biocomposites, chemical treatment with up to 6% NaOH concentration increased interfacial bonding between fiber and epoxy and the crystalline size of bio fiber, which resulted in a reduction in moisture absorption. The minimum moister absorption and thickness swelling has been recorded for BFBC_30_6 types of composites. Further increasing NaOH concentration for the chemical treatment of fiber resulted in a higher moisture absorption value for bio-composite.

TH-3447_196103002

Fig. 5.16 (a) and (b) represented the moisture absorption and thickness swelling percentage of different types of the developed composite.

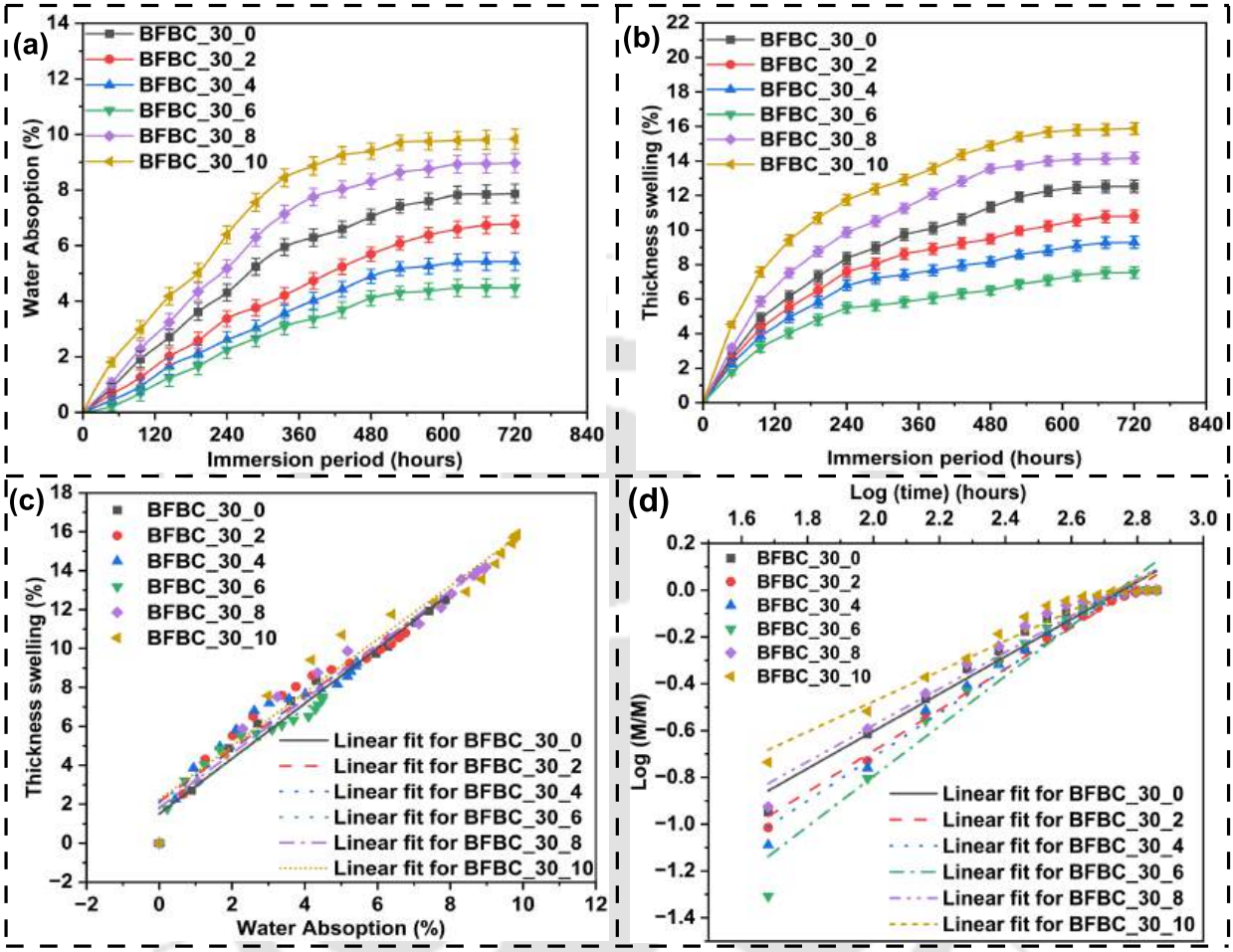

Fig. 5.16: (a) Water absorption graph; (b) thickness graph for different developed biocomposites, (c) variation of water absorption with thickness swelling, (d) diffusion mechanics fitting curve.

The graph presented in **Fig. 5.16** (c) to understand the relationship between water absorption and thickness swelling. The data points are linearly fitted and observed that the coefficient of determinations (R^2) is more than 90% for all the fits. This indicates that thickness swelling increases linearly with water absorption. The slope value and other details of the fitting have been presented in **Table 5.4**.

The water transmission kinetic equation, **Eq.5.9** has been used to analyse the behaviour of water molecules in composites.

$$\frac{M_t}{M_m} = k.t^n \tag{5.9}$$

Where M_t is the water uptake at any time t, M_m is the maximum water uptake of the sample

TH-3447_196103002

at saturation; whereas k and n are the kinetic parameters of diffusion. For n, three types of values are expected. n= 0.5 (Fickian diffusion); <0.5 (non-Fickian random diffusion) and 0.5<n<1 (anomalous diffusion, something between Fickian diffusion and random diffusion) [326, 327]. In order to identify the value of n, the straight line has been fitted with the experimental investigated data for the **Eq.5.10**.

$$log\left(\frac{M_t}{M_m}\right) = log\ (k)\ + n\ log(t) \tag{5.10}$$

The fitted graphs have been presented in **Fig. 5.16** (d) and data-related slope (n value) has been presented in **Table 5.5**. It can be seen from the table that the n-value ranges between 0.647 and 0.971, thus the biocomposites exhibit anomalous diffusion.

Table 5.4: Weight and volume fraction of bamboo fiber and bio epoxy matrix.

Sample name	Slope of the fitted straight line	R^2 value
BFBC_30_0	1.416	0.976
BFBC_30_2	1.353	0.931
BFBC_30_4	1.347	0.906
BFBC_30_6	1.277	0.903
BFBC_30_8	1.392	0.970
BFBC_30_10	1.372	0.953

Table 5.5: Weight and volume fraction of bamboo fiber and bio epoxy matrix.

Sample name	Slope of the fitted straight line	R^2 value
BFBC_30_0	0.797	0.966
BFBC_30_2	0.876	0.987
BFBC_30_4	0.935	0.976
BFBC_30_6	0.971	0.951
BFBC_30_8	0.779	0.954
BFBC_30_10	0.647	0.952

TH-3447_196103002

5.3.6 Biodegradability Behaviour of Biocomposites

The biodegradability of different NaOH-treated 30% fiber content biocomposite has been investigated in terms of mass loss. **Eq.5.11** has been used to calculated for mass loss of the composites.

$$W_{\text{loss}}(\%) = \frac{M_0 - M_t}{M_0} \times 100 \tag{5.11}$$

Where M_t is the mass of the composite samples after t days of soil buried and M_0 is the initial mass of the composite sample [67, 293].

It is possible to lose weight of developed materials during soil burial due to the moister and enzymatic action of microorganisms. **Fig. 5.17** represented the weight loss of the sample due to

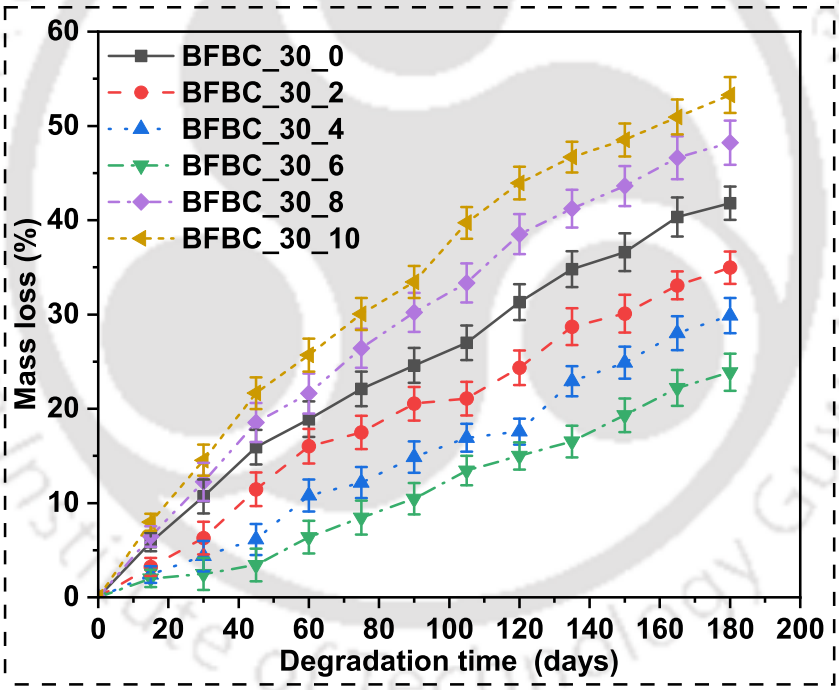

Fig. 5.17: Mass loss due to bio-degradation in composite samples.

biodegradation with respect to soil burial time. Increasing soil burial time resulted in a greater weight loss of the composites. After 180 days, maximum weight degradation was observed for BFBC_30_10, whereas minimum weight degradation was observed for BFBC_30_6 type of composites. Mechanics for biodegradation process has been presented in **Fig. 5.18** as flow diagram.

TH-3447_196103002

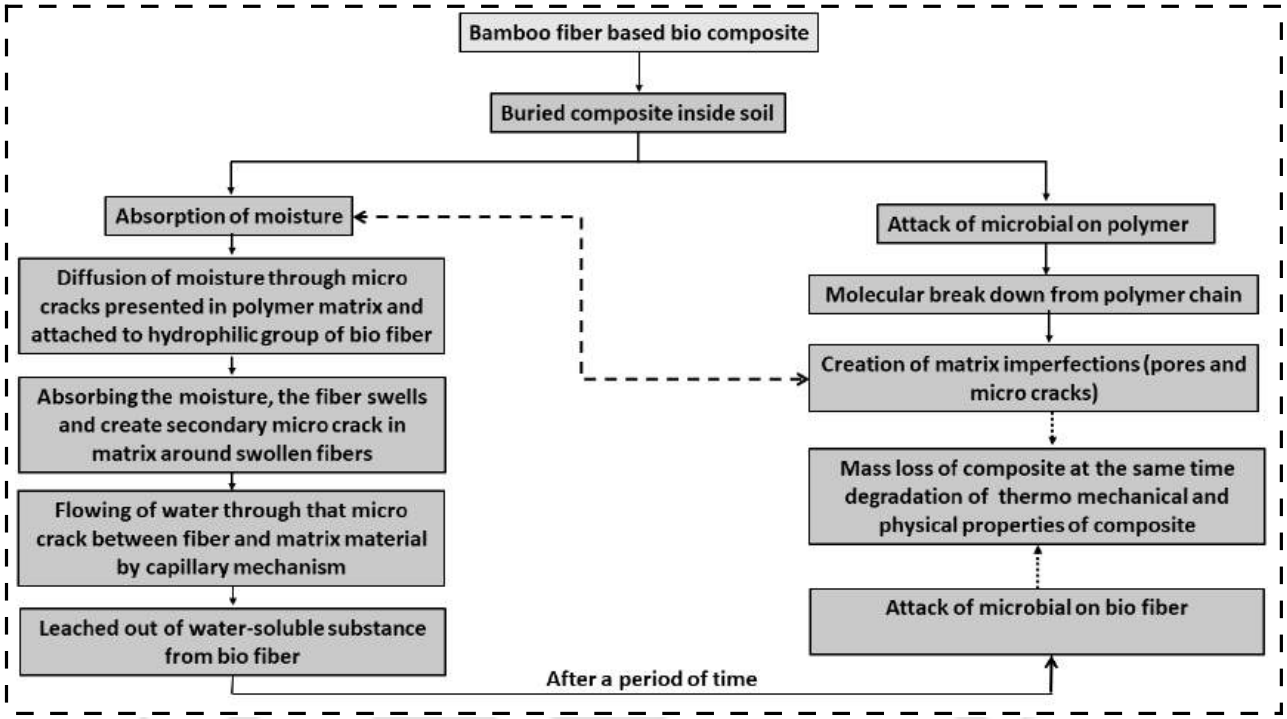

Fig. 5.18: Mechanics of biodegradation.

5.3.7 Thermal Degradation Behaviour of Biocomposites

Thermogravimetric analysis has been conducted from room temperature to 800°C in order to understand the effect of NaOH concentration on the thermal degradation behaviour of developed biocomposites. The thermogram has been presented in **Fig. 5.19**. The chemical treatment up to a concentration of 6% affects positively on the thermal stability of developed biocomposites. For initial degradation (room temperature to 150°C) minimum mass loss has been reported with BFBC_30_6 type of composite (1.85% approx.). In this temperature range generally, water is evaporated. Bamboo fiber absorbed less moisture after chemical treatment, which resulted in a lower mass loss at these temperatures. In addition to the initial loss, residual mass is also higher for BFBC_30_6 biocomposite at 800°C. The reported residual mass for the composite is 19.27%, which is much higher than the untreated fiber-reinforced composite (5.76%). The chemical treatment with more than 6% concentration resulted in a decrease in residual mass as well as an increment in initial mass loss. This may be due to inefficient bonding and greater water absorption by the bamboo fiber [174]. The activation energy for all types of developed composites has been calculated and tabulated in **Table 5.6**.

TH-3447_196103002

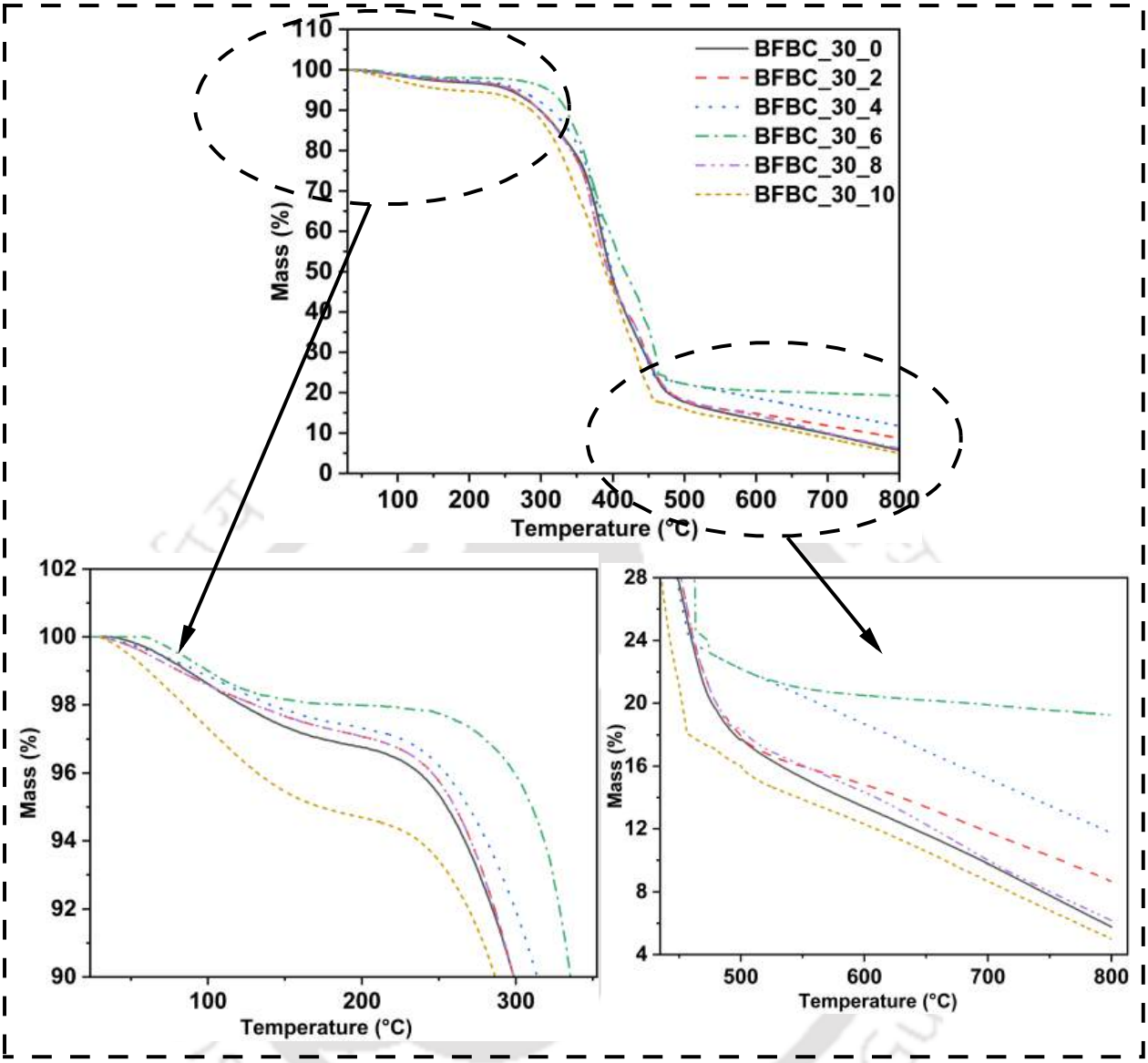

Fig. 5.19: TGA curve for different biocomposites.

5.3.8 Morphological Analysis of Biocomposites

The morphology analysis of the fracture surface has been carried out focusing on the fracture behaviour and defect analysis of the developed materials. **Fig. 5.20** (a) represents the SEM image of BFBC_30_4 type of composite. The figure indicates the shear yielding and cracks propagation in the matrix surface. A void is also observed. **Fig. 5.20** (b) is an SEM image of BFBC_40 type of composite. This composite has shown comparatively less strength with compare to BFBC_30 due to agglomerations of fiber. The SEM image is the presentation of such agglomeration of fiber inside samples. Fiber pull-out failure is a common tensile failure of untreated fiber reinforced composites.

TH-3447_196103002

Table 5.6: Activation energy of different types of developed bio-composites.

Sample name	Activation energy (kJ/mol)
BFBC_30_0	30.206
BFBC_30_2	28.862
BFBC_30_4	29.136
BFBC_30_6	31.116
BFBC_30_8	26.041
BFBC_30_10	29.120

Fig. 5.20 (c) represented an SEM image of pulling out of untreated bamboo fibers. **Fig. 5.20** (d) is the representation of tensile failure in the sample BFBC_30_6 type of composite. When fibers are subjected to tensile load, they rupture, leading to further debonding and eventually fail. **Fig. 5.20** (e) is the bending failure for BFBC_30_6 type of composite. As a result of the three-point bending test, fiber bent and delaminated. **Fig. 5.20** (f) represented the failure area of the impact test specimen. Fiber delamination and shear failure have been observed near the notch area of the sample. **Fig. 5.20** (g) is the representation of crack propagation inside a sample. In the path of the crack growth, a fiber has been observed. Initially, this fiber acts as an obstacle to crack growth. Further, when the applied load is increased, fiber debonding occurs, leading to the propagation of the crack and final failure. **Fig. 5.20** (h) shows a sample after 60 days of biodegradation. Microbial degradation and destruction of fiber surfaces and matrix parts have been observed.

5.4 SUMMARY

With the motivation to promote eco-friendly and sustainable product development practices in the field of development of composite material, the present study focuses have been done on design and development of bamboo-based biocomposites that are less detrimental to the ecosystem. The present study is an experimental investigation of the physical, mechanical, structural, and thermal properties of *Bambusa tulda* fiber-reinforced green composites. Composite sample plates have been developed with different weight fractions of fibers (i.e., 10%, 20%, 30%, and 40%). Furthermore, the

TH-3447_196103002

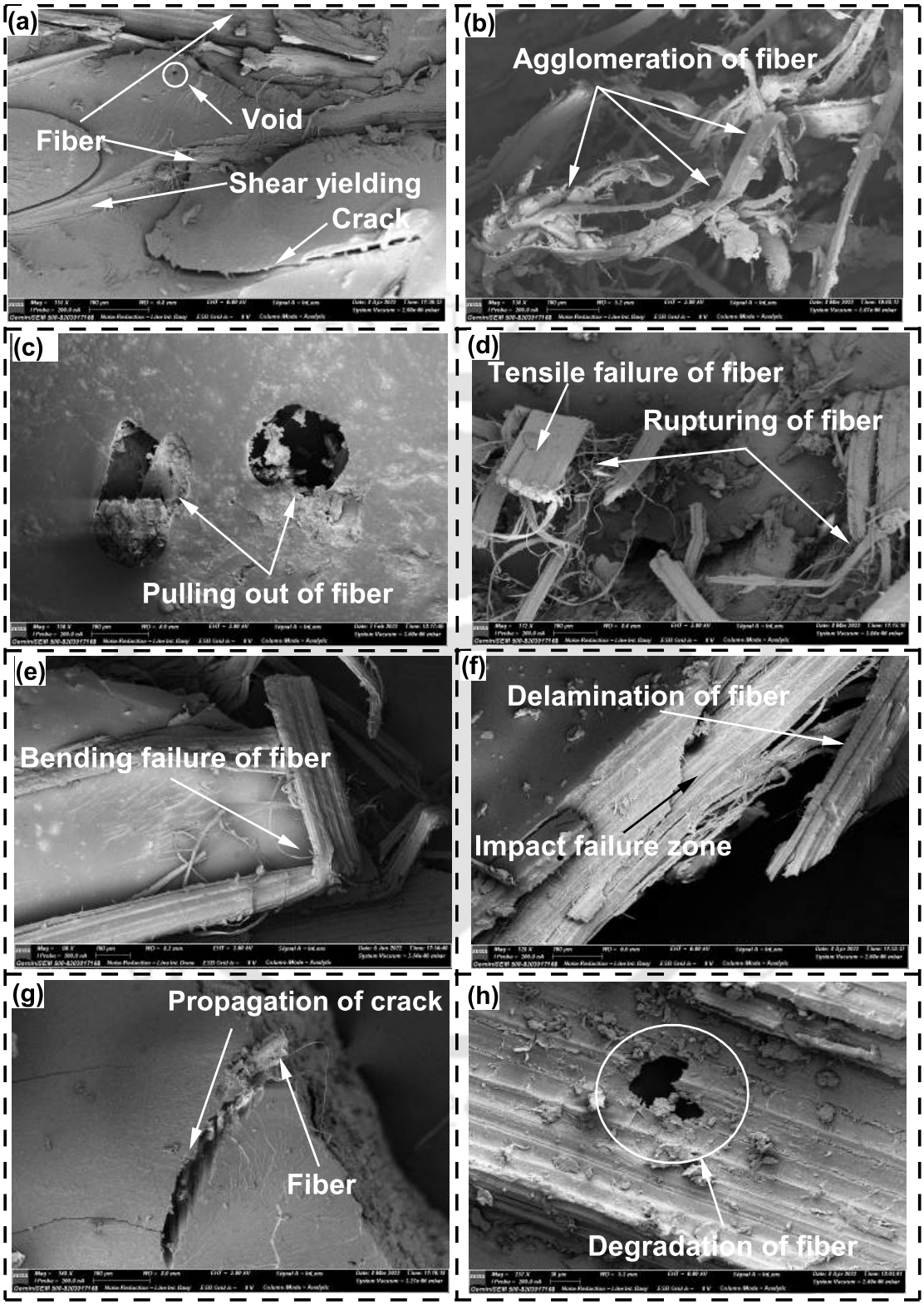

Fig. 5.20: SEM image of the different fracture surfaces of developed biocomposites.

TH-3447_196103002

composite plates have been developed with differently treated bamboo fiber, and their mechanical, thermal, physical, and morphological analyses has been performed. The investigation summarizes in following points:

(i) The addition of bamboo fiber reinforcement resulted in an increment of static mechanical properties. More than 30% fiber reinforcement resulted in decrement in mechanical properties due to agglomeration.

(ii) Up to a 6% NaOH concentration for fiber treatment also had a positive effect on the static mechanical properties of the composites.

(iii) The chemical treatment affected positively on dynamic mechanical properties of the composites. Maximum storage modulus and glass transition temperature has been observed with 6% NaOH treated 30% fiber loaded biocomposite samples.

(iv) The X-ray diffractogram shows increment in crystallinity for the developed composite with treated fiber compare to untreated one.

(v) The FTIR spectra exhibit similar patterns across all developed composites, justifying the presence of a consistent chemical bonding and functional groups within these composite materials.

(vi) Due to chemical treatment the dielectric properties of the composites are reduced. The composite made up with treated fiber of 8 and 10% concentration shows greater dielectric and Ac-conductivity values.

(vii) The chemical treatment reduced moisture absorption, thickness swelling and biodegradability behavior of the biocomposites.

(viii) The greater thermal stability has been observed with treated fiber reinforced biocomposite. Not only that biocomposites made up of treated fiber shows higher residual mass at 800°C temperature.

TH-3447_196103002

Chapter 6

Effect of Different Epoxy Matrix on Properties of Bio-Composites

6.1 INTRODUCTION

Plastics are used in many industries, including construction, packaging, automotive manufacturing, electronics, and agricultural production, due to their strength, flexibility, and affordability. The widespread usage of traditional polymers such as polyethene (PE), polyethene terephthalate (PET) and thermoset resins (like-commercial epoxy) pollute our environment. More significantly, because of their resistance to microbes, humidity, and temperature, non-degradable plastic has a severe negative effect on the survival of both plants and wildlife. Additionally, the scientific community is becoming increasingly concerned about hazardous compounds used in the manufacturing of plastics, such as bisphenol A, polychlorinated biphenyls, and phthalates, which are harmful to human health. Therefore, the decomposition of plastic waste poses an environmental issue. Growing quantities of hazardous waste and non-biodegradable plastics represent a dual threat to the environment of the twenty-first century and future generations. In 2015, more than 6,000 million tonnes of plastic trash were disposed of in landfills or the environment. Petrochemicals obtained from fossil fuels are primarily organic solids used to develop plastics. Global plastics consumption was anticipated to be worth USD 568.9 billion in 2019 and is expected to rise by 3.2% annually over the following seven years. The increasing carbon footprint of products due to plastic waste, as well as concern about depleting fossil fuels, have increased interest in alternative environmentally friendly materials. The development of polymeric materials or polymer composites using petroleum-based polymers and synthetic materials is said to be environmentally detrimental. Therefore, it is constitutive to use

TH-3447_196103002

bio-based polymers as well as bio-based reinforcement materials for developing sustainable materials. The initiative led to the development of biocomposites made from natural fibers. Typically, natural fiber reinforced biopolymer composites are subsets of fiber reinforced polymer (FRP), where the reinforcement (fibers) and matrix material (biopolymer) both derive from biological or plant-based resources. Compared to other natural fibers, bamboo fiber has a lower density. This property enables bamboo-based biocomposites to have greater specific characteristics. According to studies, any type of commercial vehicle will have a 6-8% increase in fuel economy with a 10% weight decrease. Therefore, the interior components of a commercial vehicle may be designed and developed using a green composite made from bamboo fiber. The integration of natural fiber composites in automotive applications brings forth new opportunities. The present study focuses on developing bamboo-based biocomposites that are environmentally friendly and less harmful to the ecosystem to promote eco-friendly and sustainable practices in composite material development. As such, in the present study, the biocomposites have been developed using four different types of polymers and Bambusa tulda fiber. Out of these four polymers, three are bio-based epoxy (easily available at Indian markets) and one is commercially available epoxy LY-556. Furthermore, the developed composites have been characterized physically, static, dynamic mechanically, and thermally. Following that, a multi-attributes decision-making approach (MADM), VIKOR has been utilised to select the most suitable material among these four, for automobile applications. **Sec. 6.2.1** describe about the materials used in the present study. **Sec. 6.2.2** presents fiber extraction and chemical treatment of bamboo fiber. The development process of biocomposite plate is presented in **Sec. 6.2.3**. The different characterization technique use on the developed composite is presented in **Sec. 6.2.4**. The material selection technique using multi attribute decision making approach for automobile interior is described in **Sec. 6.2.5**. **Sec. 6.3** presents detailed result of different characterization process of bio and green composites. Lastly, in **Sec. 6.4**, the optimal material selection for automobile interior applications is presented, accompanied by a comparative study of materials previously reported in the literature.

TH-3447_196103002

6.2 MATERIALS AND METHODOLOGY

This section describes the materials used in the present study, as well as the methodology and experimental processes employed for various material characterizations.

6.2.1 Materials

A local nursery in Guwahati provided 3 to 4-year-old native bamboo (*Bambusa tulda*). Acetone and sodium hydroxide were purchased from Merck Life Science Private Limited in India. Cardolite India Pvt. Ltd. (Mangaluru, Karnataka, India) provided the bio-epoxy resin (matrix) FormuLITE series. One bio epoxy polymer combination was developed using thermoset polymer 2501A obtained from Cashew nutshell liquids (CNSL) without hurting the food chain and an amine-based curing agent (2002B), while another combination was made with 2501A polymer and 2401B hardener. The BioPoxy36 liquid polymer is procured from M/s Kamal Trading and Co., Goa, India (maker: ecopoxy, Canada). The commercial epoxy (LY-556 with hardener HY-951) was purchased from Herenba Instruments and Engineers, Chennai, India. The biobased Content of 2501A+2002B is 45.4%, and for 2501A+2401B the bio-content is 34% [328]. BioPoxy36 has a 32% biobased content and commercial epoxy is a non-biobased polymer. The reason behind choosing these four types of epoxies is they are easily available in the Indian market at a comparatively cheaper rate and have better thermo-mechanical properties.

6.2.2 Fiber Extraction and Its Chemical Treatment

The bamboo fiber has been extracted using the retting process. The detailed process of extraction has been reported in **Chapter 3**. After the fiber extraction, fibers are treated with a 6% NaOH solution. That treatment increases the interfacial properties while removing lignin and other extractive components. Therefore, in this study, 6% NaOH-treated bamboo fiber has been considered for developing composite samples and other characterization of biocomposite samples.

6.2.3 Development of Biocomposite Plates

In order to develop the bio-composite plate, a modified hand lay-up approach was used. According to the study of **Chapter 5**, a 30% weight ratio of the bamboo fiber to polymer composites is

TH-3447_196103002

ideal for the construction of sustainable composites. Over 30% of the fiber reinforcement in composites exhibited fiber agglomeration, which reduced the material's overall stiffness and strength. Therefore, the constant weight fraction of fiber (30% by weight) has been considered for the current investigation. The mixing ratio for liquid epoxy with curing agent by weight is 100:52 for 2501A and 2002B, 100:31 for 2501A and 2401B, 100:40 for Biopoxy36, and 100:10 for LY556 and HY-951. After the mixing, the mixture was agitated with a glass rod for 10 to 15 minutes to ensure homogenous mixing, and it was then placed in a desiccator for 15 to 20 minutes to degass. The composite development setup consists of three parts: parts A and B are the top and bottom halves of the mould (size 250×250 mm^2). A laminated sheet (made of polypropylene; thickness 200μm) was then placed on the mould's top and bottom layers. After that, a roller was used to evenly distribute the liquid epoxy over the laminated sheet, which was then filled with a homogenous combination of liquid polymer-curing agent mixture. On the lower mould, the liquid polymer layer was then manually covered with bamboo fibers. An additional liquid polymer mixture was poured over the fibers. Once they were evenly dispersed, the top mould was then positioned over the epoxy-embedded fiber. Moulds were held together with four M8 nuts and bolts placed at each corner (the load used to compress the mould is approximately 0.5 to 0.8 kN) and left for 24 hours to cure the composite. The composite plates were demoulded and cut following ASTM guidelines for various testing. **Fig. 6.1** represents the schematic diagram of the process and **Table 6.1** represents the details of the prepared samples.

6.2.4 Characterization of Developed Composites

6.2.4.1 Physical Characterization

Density and Void Content- The theoretical density of the composite was calculated by using the rule of mixture and experimental density was measured by following Archimedes' principle with ASTM-D-792-13 (20×20×3mm^3) standard. The density of the treated bamboo fiber was previously measured as 1.025 gm/cm^3 in **Chapter 4**. As per the data sheet provided by the manufacturing company, the densities of FormuLite (2501A+2002B), FormuLite (2501A+2401B), Biopoxy36 and commercial epoxy (LY-556+HY-951) are 1.068, 1.081, 1.11, and 1.13 gm/cm^3, respectively. **Eq.6.1**

TH-3447_196103002

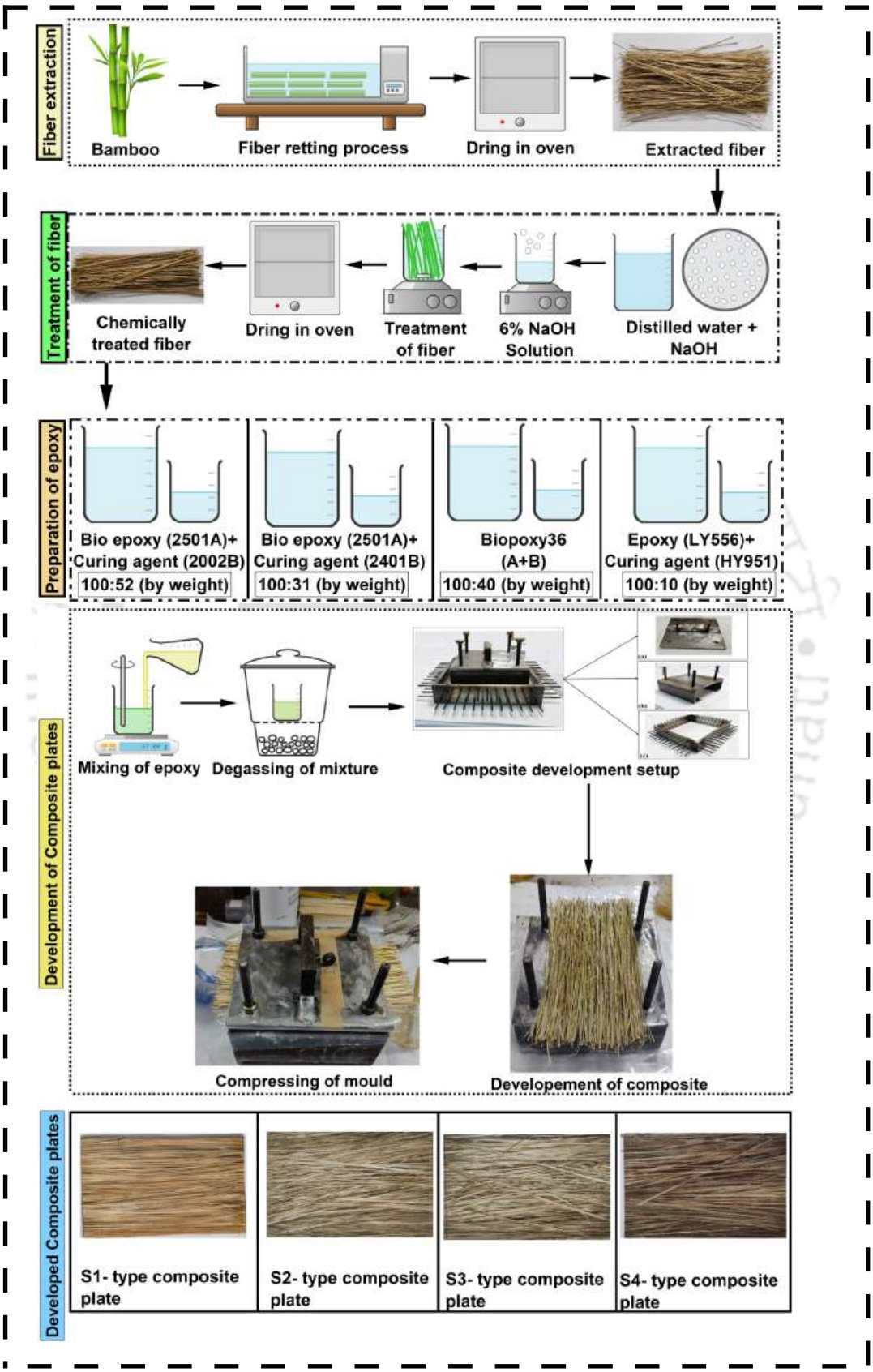

Fig. 6.1: Composite development process.

TH-3447_196103002

Table 6.1: Weight and volume fraction of bamboo fiber and bio epoxy matrix.

Sample code	Polymer matrix	Matrix weight fraction (%)	Fiber weight fraction (%)	Bio-content in composites (%)
S1	FormuLite (2501A+2002B)*	70	30	61.78
S2	FormuLite (2501A+2401B)*	70	30	53.80
S3	Biopoxy36 (A+B)*	70	30	52.40
S4	Epoxy-LY-556(A) + HY951 (B)*	70	30	30.00

*A is liquid epoxy and B is curing agent/ hardener

has been used to compute the theoretical density of the composites.

$$\frac{1}{\rho_{c(theo)}} = \frac{w_f}{\rho_f} + \frac{w_m}{\rho_m} \tag{6.1}$$

Where $\rho_{c(theo)}$ is the theoretical density of composite, w_f and w_m are the weight fraction of fiber and matrix materials, ρ_f and ρ_m are the density of fiber and matrix materials respectively.

The void content of composite materials is an important factor. Void content will greatly affect the composite's mechanical and physical characteristics. Cracks begin in composites where the voids form. There is a possibility that this could further propagate into another zone of the material, leading to catastrophic failure. For this reason, it is crucial to determine the void content in the composite in order to ensure its quality. The void content of the composite has been measured by using **Eq.6.2**.

$$V_c = \frac{\rho_{c(theo)} - \rho_{c(exp)}}{\rho_{c(theo)}} \times 100 \tag{6.2}$$

where V_c is void content of composites and $\rho_{c(exp)}$ is the experimental density of composites.

Water Absorption Test- Natural fibers are hydrophilic, so the water absorption test of the developed composites was performed at room temperature as per ASTM-D-570-98 ($20\times20\times3$ mm^3) [329]. In distilled water, test samples were submerged for 48 hours to 720 hours, and their weight and thickness were measured periodically. The weight gain and thickness swelling due to water

TH-3447_196103002

uptake are calculated by using **Eq.6.3** and **Eq.6.4**.

$$W_{\text{Water absorption}}(\%) = \frac{W_t - W_0}{W_0} \times 100 \tag{6.3}$$

Where W_t and W_0 are the weight of bio-composite samples at time = t and 0.

$$T_{\text{Thickness swelling}}(\%) \frac{T_t - T_0}{T_0} \times 100 \tag{6.4}$$

Where T_t and T_0 are the thickness of the bio-composite samples at time = t and 0.

6.2.4.2 Mechanical Characterization

Tensile Testing- The tensile properties of the developed biocomposites have been analysed using a Shimadzu Universal Testing Machine (UTM). The load cell used for the testing was 100KN. The specimens were cut into a rectangular cross-section as per ASTM-D-638-3 [330] with a dimension of 160×14×3 mm^3. A gauge length of 50 mm and a crosshead speed of 1 mm/min were used for the testing of the samples. Five samples of each type of biocomposites were tested and average results are presented with standard deviations.

Flexural Testing- The three-point bending testing has been done to comprehend the flexural properties of created materials with the Shimadzu UTM machine. The samples for the testing were prepared as per ASTM-D-790-3 [331] with a dimension of 130×14×3 mm3. The span length and cross-head speed for the testing were fixed as 50 mm and 1mm/min, respectively. **Eq.6.5**, **Eq.6.6** and, **Eq.6.7** were used to compute the flexural strength, flexural modulus, and flexural strain based on the load-displacement graphs that were produced from the tests.

$$\sigma_{fl} = \frac{3P_f L}{2bt^3} \tag{6.5}$$

$$E_{fl} = \frac{\frac{P}{\delta} L^3}{4bt^3} \tag{6.6}$$

$$\varepsilon_{fl} = \frac{6\delta t}{L^2} \tag{6.7}$$

Here σ_{fl}, E_{fl} and ε_{fl} are flexural strength, flexural modulus and flexural strain. P_f is flexural load, L is span length, t is the thickness of the sample, b= the width of the sample, δ is deflection and $\frac{P}{\delta}$ is the slope of the load-deflection curve.

TH-3447_196103002

Impact Testing- The Charpy impact testing of the developed composites has been done with an IT-30 impact testing machine (maker: FIE, India). The notched test samples have been prepared as per ASTM-D-6110 [332] with a dimension of 64×12.7×3.2 mm^3. Each type of biocomposite has been evaluated on five samples, and the average findings are shown with standard deviations.

Surface Hardness- The surface hardness of the developed composites has been measured at ten different places of each sample with a digital Rockwell hardness tester (maker: FIE, India). Surface penetration was performed using a 1/4" aluminium ball with an L scale that provided a 60Kgf force. The test samples were prepared as per ASTM-D-785 with a dimension of 20×20×3 mm^3 [333] and the average test result has been presented with standard deviation.

6.2.4.3 Dynamical Mechanical Characterization

The dynamic mechanical analyser of Anton Paar (Maker: Physica MCR, Model; 702) was used to evaluate the dynamic mechanical characteristics of the developed composites. The samples were developed with dimensions of 50×13×3 mm^3 [285] and were held within the machine using a double cantilever fixture. The test condition was at a sinusoidal frequency of 1Hz, and the temperature was swapped from 25°C to 150°C using a temperature ramp of 5°C/min.

6.2.4.4 Thermogravimetric Analysis -

The thermal stability of the developed composites has been analysed with Perkin Elmer Instruments. The mass loss of the samples has been determined in an N_2 environment as a function of temperature from room temperature to 800°C with a constant heating rate of 10°C/min. The activation energy for the composite has been calculated using **Eq.6.8**.

$$\ln\left[\ln\left(\frac{1}{y}\right)\right] = -\left(\frac{E_a}{R}\right)\left[\left(\frac{1}{T} + K\right)\right] \tag{6.8}$$

Here y is denoted as normalized weight (w_t/w_i), where wt is the weight of the sample at time t and wi is the initial weight. T is the representation of temperature in Kelvin. E_a is the activation energy. The graph has been plotted between $\ln\left[\ln\left(\frac{1}{y}\right)\right]$ and $\left(\frac{1}{T}\right)$ and the Slope of the graph has been found by a fitting straight line between the data points of the plot. The activation energy has been calculated by multiplying the slope value with the universal gas constant value (R=8.32

TH-3447_196103002

J/mol-K) as of **Eq.6.9**.

$$\frac{d\ln\left[\ln\left(\frac{1}{y}\right)\right]}{d\left(\frac{1}{T}\right)} = -\left(\frac{E_a}{R}\right) \tag{6.9}$$

6.2.4.5 Microscopic Analysis

The fracture surface of the developed composite has been examined under a field-emitted screening electron microscope (Zeiss, model: Sigma). The samples are first gold coated with a sputter coater and then examined under the FESEM machine.

6.2.5 Material Selection Using Multi-Attribute Decision-Making Approach (MADM)

When there are at least two materials available for a particular application, selecting the best one necessitates careful consideration. Approaches for multi-attribute decision-making (MADM) can help with this process [334, 335]. MADM tools are used in a variety of fields such as retail, logistics networks, engineering, and so on to offer real results [336]. Among the present four types of developed composites, the multi-attributes decision-making approach, VIKOR was employed to identify the best material for automobile interiors. The weightage of different criteria has been done with the Shannon entropy method.

6.2.5.1 Shannon Entropy Method

Entropy weights are determined based on steps that have been developed and tested by a variety of scientists in order to determine the weight of certain criteria. The weighting findings show that the top value is preferable to the lower value [337]. The weight-calculating process used in this essay is as follows [338]:

Step-1: Creating the decision matrix, A, $[a_{ic}]_{n\times m}$ as of **Eq.6.10**.

$$A = [a_{ij}]_{m\times n} = \begin{bmatrix} a_{11} & a_{12} & .... & a_{1n} \\ a_{21} & a_{22} & .... & a_{2n} \\ .... & .... & .... & .... \\ a_{m1} & a_{m2} & .... & a_{mn} \end{bmatrix} \tag{6.10}$$

Where $i = 1, 2, ...m$; $j = 1, 2, ...n$

Step-2: Normalizing the decision matrix's order for data outcome, P_{ij} as per **Eq.6.11**.

$$Pij = \frac{a_{ij}}{\sum_{i=1}^{m} a_{ij}} \tag{6.11}$$

TH-3447_196103002

Step-3: Computation of entropy using the following equation from the collected data by using **Eq.6.12**.

$$E_j = -k \sum_{i=1}^{m} P_{ij} \ \ln P_{ij} \ , \tag{6.12}$$

where $k = \frac{1}{\ln(m)}$ here m is number of alternatives

Step-4: Finally find the weightage (W_j) of different criteria has been found by using **Eq.6.13**.

$$W_j = \frac{1 - E_j}{\sum_{j=1}^{n} (1 - E_j)} \tag{6.13}$$

6.2.5.2 VIKOR Method

The VIKOR approach has been used by several researchers to resolve complex problems with numerous conflicting criteria [339, 340]. This technique analyses the closeness measure from the ideal option to the alternatives in order to rank the alternatives and find a compromise solution for a problem with competing needs. The steps for the VIKOR method are given below [341]:

Step-1: The normalization of the decision matrix has been done with the help of **Eq.6.14**.

$$n_{ij} = \frac{a_{ij}}{\sqrt{\sum_{i=1}^{m} {a_{ij}}^2}} \tag{6.14}$$

Here $i = 1, 2, 3 \ldots\ldots\ldots.., m$ *and* $j = 1, 2, 3 \ldots\ldots\ldots.., n$

Step-2: After that the standardized value of weightage has been calculated by using **Eq.6.15**.

$$v_{ij} = w_j n_{ij} \tag{6.15}$$

Here $i = 1, 2, 3 \ldots\ldots\ldots.., m$ *and* $j = 1, 2, 3 \ldots\ldots\ldots.., n$

Step-3: Thereafter, to find out the positive and negative ideal solution, **Eq.6.16**, **Eq.6.17**, **Eq.6.18**, and **Eq.6.19** are used.

$$A^+ = \{max \ v_{ij}\} = v_1^+, v_2^+, \ \ldots\ldots\ldots\ldots v_n^+ \text{ (for problems which are maximization in nature)} \tag{6.16}$$

$$A^+ = \{min \ v_{ij}\} = v_1^+, v_2^+, \ \ldots\ldots\ldots\ldots v_n^+ \text{ (for problems which are minimised in nature)} \tag{6.17}$$

$$A^- = \{min \ v_{ij}\} = v_1^-, v_2^-, \ \ldots\ldots\ldots\ldots v_n^- \text{ (for problems which are maximization in nature)} \tag{6.18}$$

$$A^- = \{max \ v_{ij}\} = v_1^-, v_2^-, \ \ldots\ldots\ldots\ldots v_n^- \text{ (for problems which are minimised in nature)} \tag{6.19}$$

TH-3447_196103002

Step-4: After that, the **Eq.6.20** and **Eq.6.21** were used to calculate regret measurement and utility calculation for each solution which is non dominated

$$R_i = \ max \ \left[\frac{w_j \left(v_j^+ - v_{ij} \right)}{\left(v_j^+ - v_j^- \right)} \right] \tag{6.20}$$

$$S_i = \sum_{j=1}^{n} \frac{w_j \left(v_j^+ - v_{ij} \right)}{\left(v_j^+ - v_j^- \right)} \tag{6.21}$$

Here S_i and R_i are $\in$ [0,1].

Step-5: Eq.6.22 was further used to calculate the VIKOR index. The lower the VIKOR index, prefer the alternative.

$$Q_i = \alpha \left[\frac{S_i - S^-}{S^+ - S^-} \right] + (1 - \alpha) \ \left[\frac{R_i - R^-}{R^+ - R^-} \right] \tag{6.22}$$

Here α is the weighting factor varied between [0 and 1].

Step-6: The sensitivity analysis has been done by putting difference α value starting from 0 to 1 with an interval of 0.1 in to **Eq.6.22**.

6.3 RESULTS AND DISCUSSIONS

6.3.1 Density and Void Content

A major advantage of biomass-reinforced plastics is that they are lightweight and environmentally friendly. Biocomposites with a low density have better specific properties and are more sustainable [159]. The experimental and theoretical density of the composites has been measured. The experimental and theoretical densities are shown in **Fig. 6.2** (a). The maximum experimental density has been observed for S4 and minimum was observed for S1 types of biocomposites with numeric values of 1.051 ± 0.124 gm/cm^3 and 1.024 ± 0.111 gm/cm^3, respectively. The variation in the density of developed composites may be attributed to the different densities of different epoxy matrices. To ensure the quality of the composites, the void content inside them has been assessed. The difference between the theoretical and experimental density is spotted as void content. The maximum void content has been observed with S4 (4.102 ± 0.202%) types of composites and minimum void

TH-3447_196103002

content has been sported for S3 (1.201 ± 0.104%) types of composites. The void content of all developed composites is shown in **Fig. 6.2** (b). The reason behind void content is the presence of hydrophilic fiber and the trapping of an air bubble inside the epoxy at the time of mixing of epoxy polymer with hardener. Air bubbles can also become trapped during the composite preparation or development process, creating a void inside the composite [215].

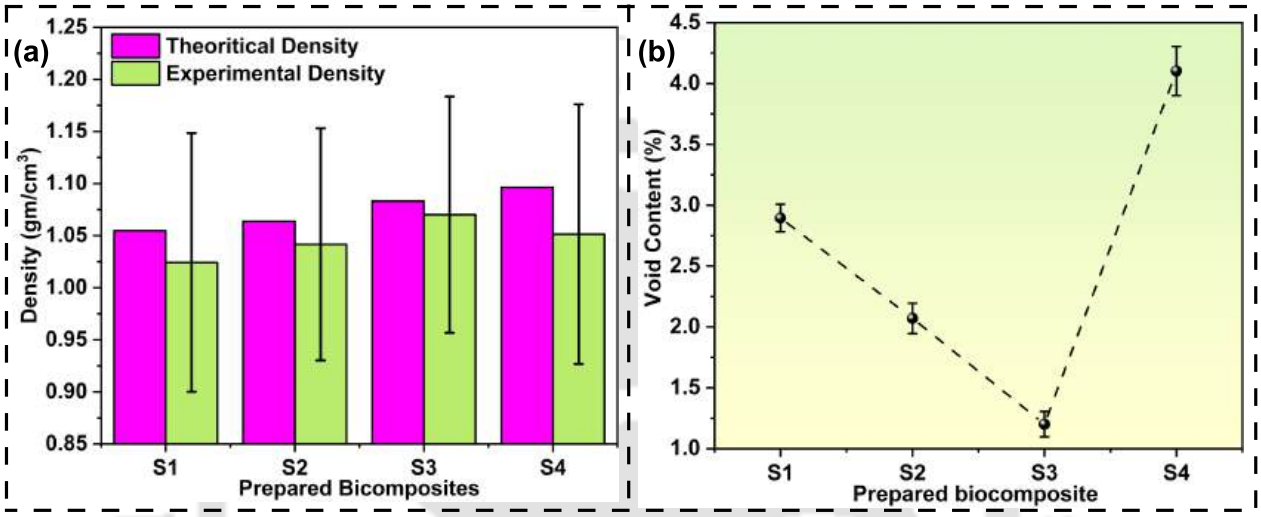

Fig. 6.2: (a) Density (b) void content of developed composites.

6.3.2 Moisture Absorption and Thickness Swelling

The polymer matrices are hydrophobic in nature, but the bio-fibers are hydrophilic. The presence of natural fibre and the formation of micro and macro cavities between the epoxy matrix and reinforcing fibre are the main causes of moisture absorption for currently developed composites. The moisture absorption for all developed composites is presented in **Fig. 6.3** (a). The moisture absorption behaviour of the composites can be divided into three phases [342]. The first or initial phase of moisture abortion is an initial 240 hrs. As a result of the micro and macro pores present in composites, the water is absorbed in the first phase. The S4 (9.66 ± 0.29%) composites absorbed the most moisture over this period, whereas the S1(5.50 ± 0.31%) composites absorbed the least. The sequence for moisture absorption in this period is S4>S3>S2>S1. Bamboo fibre and commercial epoxy may not interact well at the interface, which might lead to the formation of micro holes between the reinforcement fiber and matrix, that function as capillaries and absorb moisture.

TH-3447_196103002

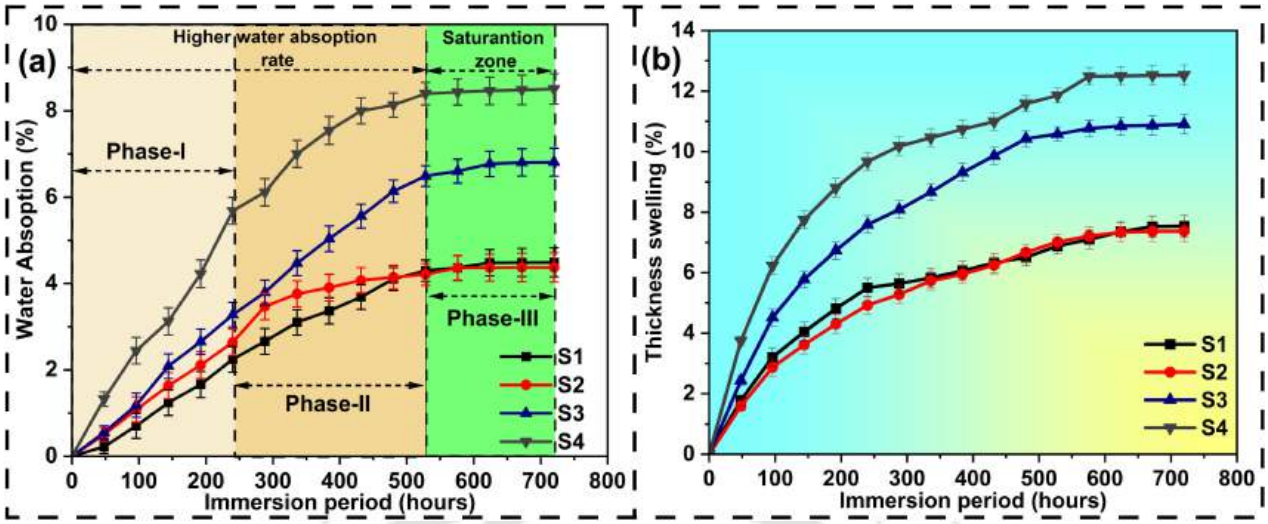

Fig. 6.3: (a) Water absorption and (b) thickness swelling for all types of composites.

Whereas the lesser moisture absorption for S1 types of composites is attributed to better fiber-matrix interaction. For the second phase of moisture absorption, the moisture has been absorbed due to the hydrophilic nature of fiber. The range of this phase is from 240 hrs to 528 hrs. The sequence of moisture absorption in this period is S4>S3>S2>S1. As a result of fibers absorbing water, certain fibers swell, which leads to cracks forming in the matrix during the third phase. Therefore, due to the micro-cracks in the matrix, in the third phase, water is absorbed. This phase is generally the saturation phase of absorption. The range of this phase is 528 hrs to 720 hrs. The sequence of moisture intake in this phase is S4>S3>S1>S2. Upon saturation, maximum moisture was absorbed by S4 types of composites (12.58 ± 0.33%), while minimum moisture was absorbed by S2 types of composites (7.37 ± 0.33%). Due to the poor adhesion between fibers and matrix, there are more crevices at the interface, which enables greater water absorption for S4 composites. Whereas better interfacial bonding between bio-epoxy and fiber for S2 types of composites has resulted in less moist absorption [343]. The thickness swelling of various developed composites caused by water absorption is depicted in **Fig. 6.3** (b). The thickness swelling of the developed composites increased as the water absorption percentage increased and after 528 hrs it started to saturate. The maximum thickness swelling is observed for S4 types of composites with the numeric value of 12.58 ± 0.33%. the reason behind the thickness swelling is the moisture absorption of the composites. Water is absorbed by hydrophilic fibers, causing them to swell. As a

TH-3447_196103002

result of swelling, fibers are debonding from matrix materials, resulting in the thickness swelling of composites [343]. The thickness swelling reduced the tensile strength as well as other mechanical properties of developed biocomposites. Due to better interfacial bonding between the bio-epoxy and bamboo fiber, S2 types of composites show lesser thickness swelling. The sequence of thickness swelling for all developed composites is S4>S3>S1>S2.

6.3.3 Tensile Testing

An engineering tensile test was widely used to determine the basic strength of materials for design and material selection purposes. The tensile testing has been performed with all four different types of developed composites and their load-displacement as well as stress-strain curve has been recorded. **Fig. 6.4** (a) represents the typical load-displacement curve of the composites and **Fig. 6.4** (b) represents the typical stress-strain curves of the materials. The load-displacement and stress-strain graph for all samples have been presented in **Fig. 6.5**. The samples' load-displacement curves exhibit linear behaviour initially, followed by non-linear behaviour till failure. The maximum tensile load-bearing capacity has been recorded for S2 types of composites. FormuLite (2501A+2401B) epoxy contains ether groups and hydroxyl polar groups, which result in better molecular adhesion between bamboo fiber and matrix. As fiber and epoxy are better bonded, the surface contact between fiber and epoxy is proper, which results in better and homogeneous stress transmission from the matrix to reinforcing fiber, resulting in better load-bearing capacity and tensile strength. The sequence of maximum load-bearing capacity for different developed composites is S2>S1>S3>S4. For the displacement curve, the maximum displacement has been also noted for S2 types of samples. The tensile strength and maximum load-bearing capacity of the developed composites follow the same sequence. The maximum tensile strength has been reported as 144.759 ± 4.402 MPa for S2 types of composites. The viscosity of matrix materials plays a very vital role here. The viscosity of the Biopoxy36 (1030 cPs), FormuLite (2501A+2002B) (1100 cPs) and Epoxy-LY-556(A)+ HY951 (B) (1350 cPs) matrix is greater than that of the FormuLite (2501A+2401B) (905 cPs), suggesting that the flow rate of resin to infiltrate the spaces between the fibers may be lowered throughout the processing and curing phase [174]. As a result, the slippage between the fibre and matrix

TH-3447_196103002

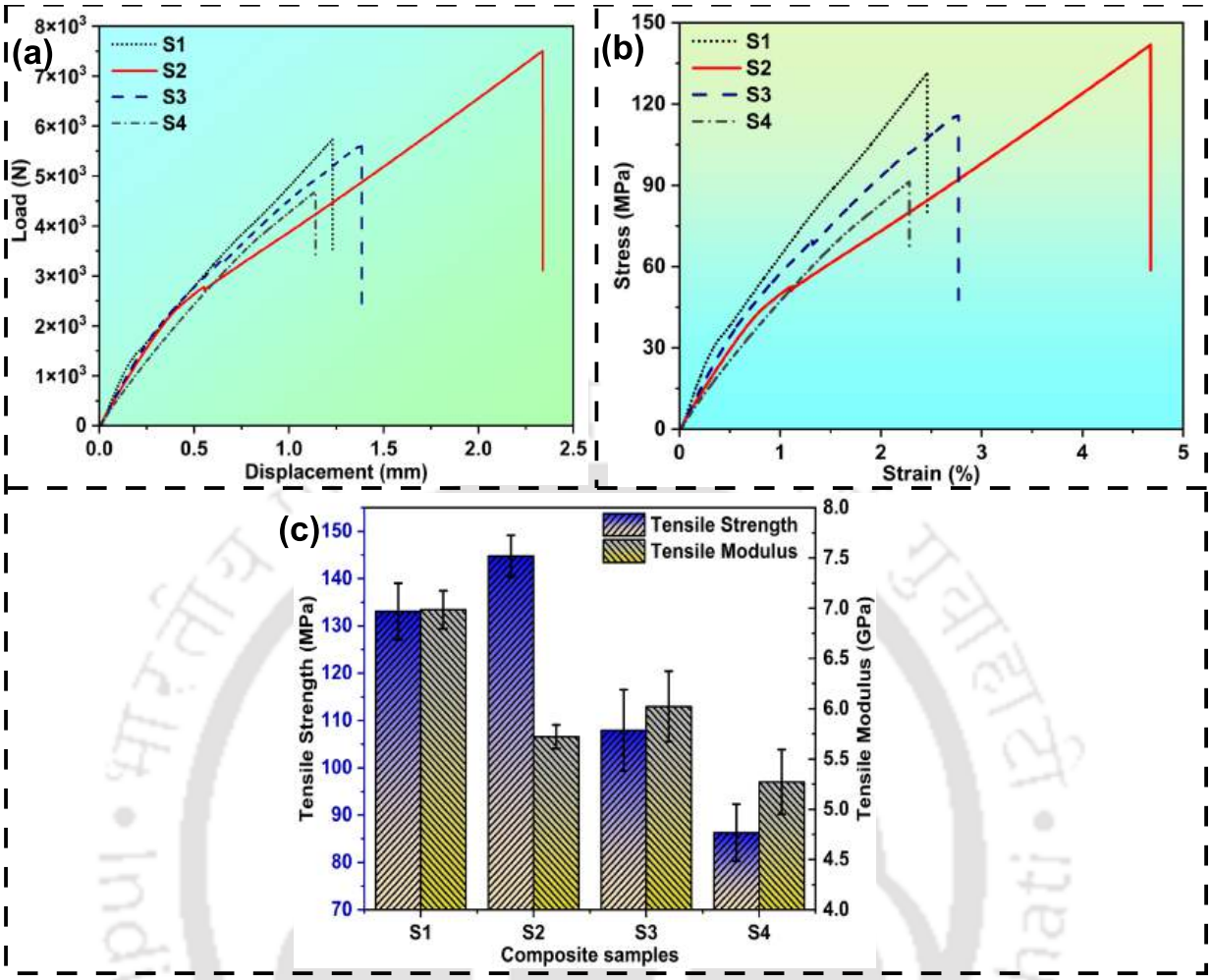

Fig. 6.4: (a) Tensile Load-displacement, (b) tensile Stress-strain graph, and (c) variation of different tensile properties of developed composites.

occurred, making it impossible for the stress to be adequately transmitted. Due to lesser viscosity, the FormuLite (2501A+2401B) matrix may be able to penetrate the surface defects of bamboo fiber and make better interfacial bonding which improves load transmission. Similarly, the elongation before the break value of the S2 types is also higher. The maximum elongation before break value is 4.71%. The sequence for elongation before the break is S2>S3>S1>S4. As the elastic modulus is defined as the ratio of stress over strain, the higher tensile modulus is attributed to a lower strain value. The maximum tensile modulus value is reported for S1 types of composites with a numeric value of 6.983 ± 0.189 GPa. Young's modulus and maximum tensile strength for all types of composites are presented in **Fig. 6.4** (c).

TH-3447_196103002

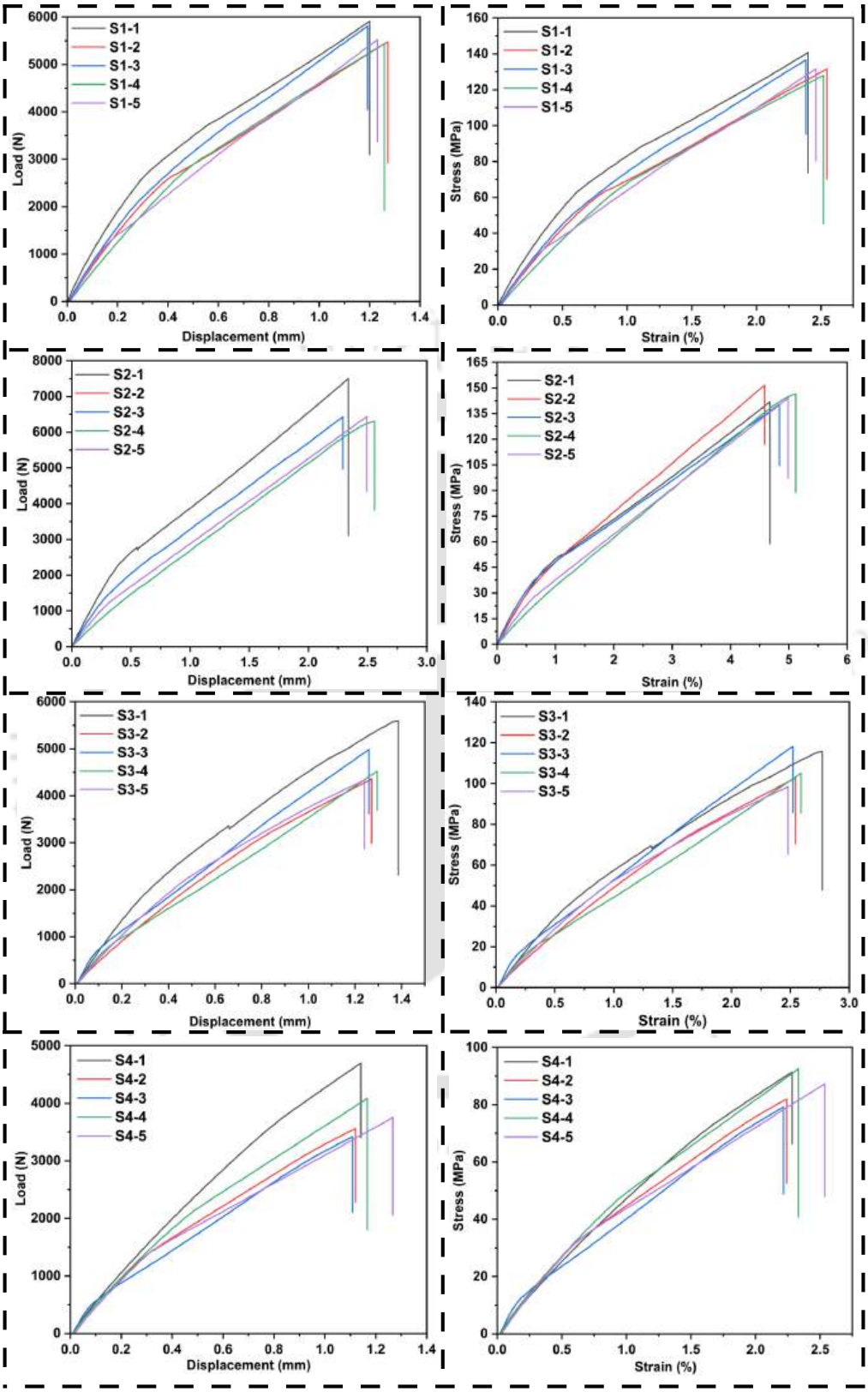

Fig. 6.5: Tensile load-displacement and stress-strain curve for all types of developed composites.

TH-3447_196103002

6.3.4 Flexural Testing

A three-point bending test has been performed to determine the flexural properties of the developed composites. The load-displacement curve was recorded, and the stress-strain curve was computed based on it. The typical load-displacement curve for the composites has been presented in **Fig. 6.6** (a). The flexural load-displacement and stress-strain graph for all samples have been presented in **Fig. 6.7**. The behaviour of composite laminates is initially linear, with a slow load rise followed by a stage in which the load stabilises with an increase in deflection before failure. The maximum flexural load-bearing capacity has been observed for S1 types of composites. The sequence of maximum load-bearing capacity for the developed composite is S1>S2>S3>S4. The flexural deformation is higher for S2 types of composites. The typical flexural stress-strain diagram is presented in **Fig. 6.6** (b). The flexural load displacement and stress-strain graph for all developed samples has been presented in supplementary document. The maximum flexural strength and flexural modulus have been observed for S1 types of composites with the values of 154.8 ± 5.97 MPa and 8.24 ± 0.15 GPa, respectively. The flexural strength value for S1 types of composites is 28.35%, 49.70% and 86.05% higher than S2, S3 and S4 types of composites respectively. The sequence for flexural strength and flexural modulus value for the composites is S1>S2>S3>S4. The maximum flexural strength is reported as 8.24 ± 0.158 GPa. This value is 31.42%, 32.68% and 71.66% higher than S2, S3 and S4 types of composites. The flexural strength and flexural modulus for different composites are presented in **Fig. 6.6** (c).

6.3.5 Impact Testing

The impact strength of a material refers to its capacity to absorb shock and energy. Various developed composites have been tested to determine their energy absorbent capacity using the Izod impact method. The maximum impact strength has been observed for S2 types of composites with a numeric value of 57.57 ± 5.93 kJ/m^2. This value is 30.65%, 90.73% and 134.01% higher than S1, S3 and S4.The sequence for Impact strength of developed composites is as follows S2>S1>S3>S4.

The impact strength may be attributed to elongation before the break value of the tensile testing. The higher value of elongation before the break value is corresponding to the higher toughness.

TH-3447_196103002

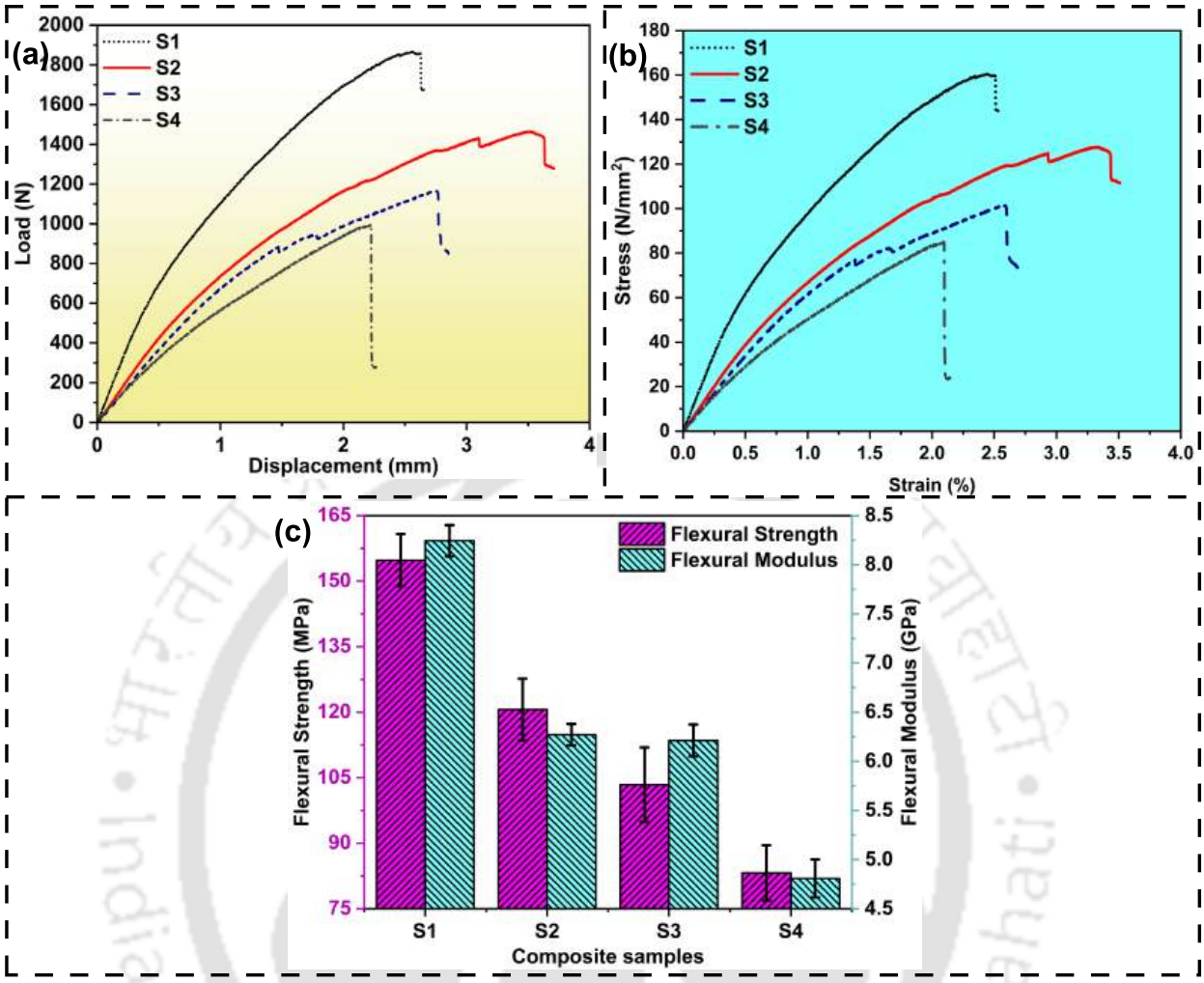

Fig. 6.6: (a) Load-displacement, (b) Flexural stress-strain diagram and (c) variation of different tensile properties of developed composites.

High-impact strength is a result of greater toughness. The matrix, FormuLite (2501A+2401B) has better wettability with bamboo fiber, which improves better stress transmission and results in higher impact strength [307]. The minimum impact strength is observed for S4 types of composites. The bar diagram for all types of composites is represented in **Fig. 6.8**.

6.3.6 Surface Hardness

The material's hardness determines how easily it can be deformed by localized plastic deformation [215]. The maximum hardness has been observed with S3 types of composites with a value of 97.59 ± 6.98 HRC. The HRC number for the S3 composite is 18.56%, 13.41% and 55.89% higher than S1, S2 and S4 types of composites respectively. The lowest value of hardness has been recorded for

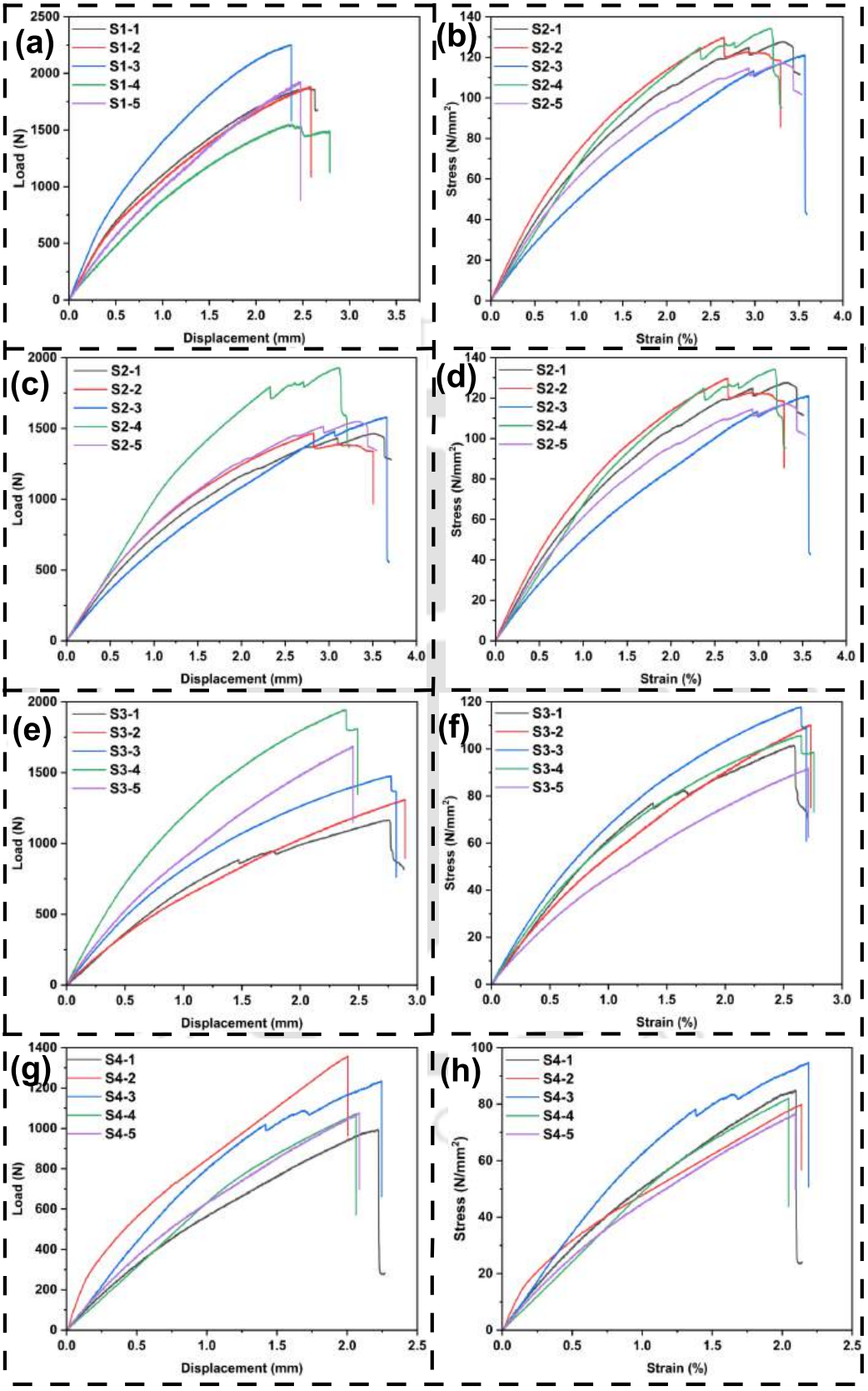

Fig. 6.7: Flexural load-displacement and stress-strain curve for all types of developed composites.

TH-3447_196103002

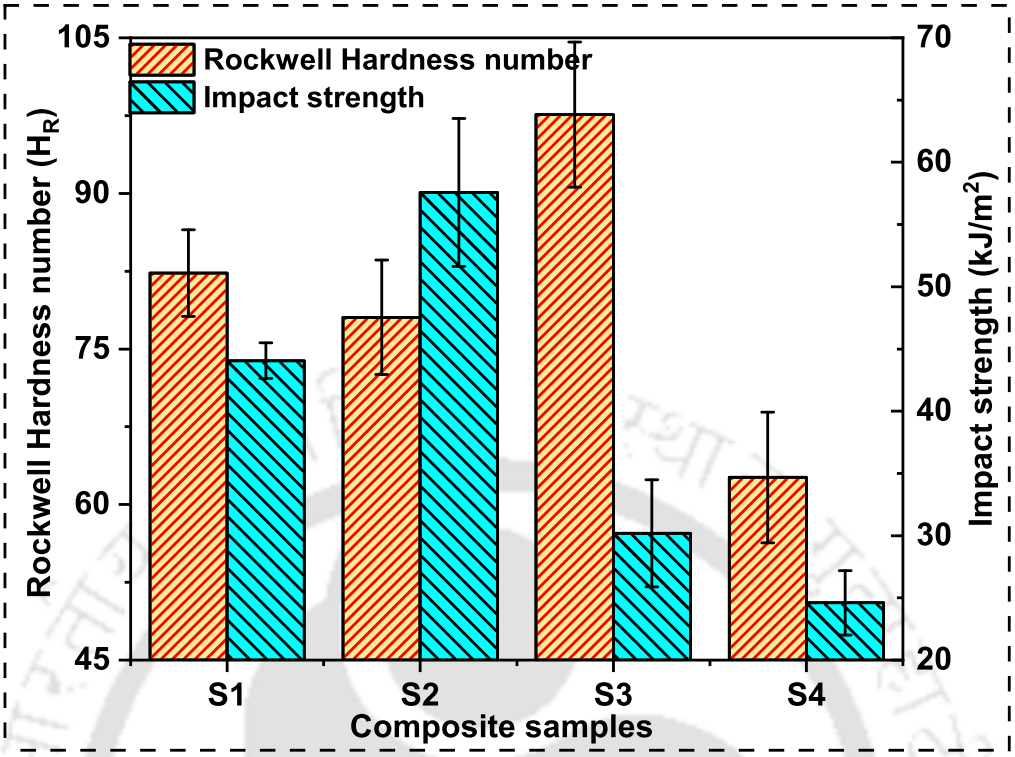

Fig. 6.8: Impact and hardness of different developed composites.

S4 types of composites with the value of 62.60 ± 6.29 HRC. The sequence for the surface hardness of different composites is observed as S3>S2>S1>S4. The hardness value of all types of samples has been presented in **Fig. 6.8**.

6.3.7 Dynamic Mechanical Analysis (DMA)

The dynamic mechanical study has been carried out to examine the impact of various viscoelastic matrix materials on storage (E') and loss modulus ($E^{"}$), damping factor ($tan\delta$), and glass transition temperature (T_g) of developed different bio-composites. In composite materials under the influence of frequency, time, and temperature, such investigations are very effective in determining molecular mobility and its arrangements.

Effect of Temperature on DMA- The temperature has a significant impact on the developed composites' viscoelastic properties. For viscoelastic composites, three regions are typically seen. The first section is known as the glassy region. Typically, this area ranges from ambient to 60°C. In this region, the highest storage modulus and the smallest loss modulus are seen. The storage modulus decreases as the temperature rises, while the loss modulus and damping factor begin to

TH-3447_196103002

rise. However, both the increase in damping factor and the decrease in storage modulus are very small in this region. The second zone is the transition region when viscoelastic materials transform from their glassy to their rubbery states. Temperature increments have been accompanied by quick decreases in storage modulus and increases in loss modulus as well as a rapid decrease in damping factor. The Plateau region is the last or third zone. In this region the composite becomes rubbery. The modulus of storage and loss, as well as the damping factor, reach their lowest values in this region and are inflated in a straight line parallel to the x-axis with the increase in temperature.

Storage Modulus- The amount of energy that a material can hold during one oscillation cycle is indicated by the storage modulus [285]. It demonstrates the load-bearing capacity and temperature-dependent stiffness behaviour of developed composites. **Fig. 6.9** (a) shows the storage modulus curve of the developed composites. The maximum storage modulus has been observed for S2 types of composites with a numeric value of 8816 MPa. The sequence for the storage modulus value is S2 (8816 MPa)>S1 (8328 MPa)>S3 (6780 MPa)>S4 (5514 MPa). The reason behind higher storage modulus may be better interfacial interaction between fiber and matrix.

Due to the low viscosity of polymer matrix used in S2 type of composites, the matrix is penetrated homogeneously into fiber and makes better fiber matrix bonding. Due to better bonding, the stiffer fiber easily reduces the mobility of molecules inside the composite. It increases the rigidity of the materials, allowing them to store more energy before failure and exhibit greater storage modulus values.

Loss Modulus- Composites dissipate thermal energy under applied energy as their loss modulus. **Fig. 6.9** (b) shows the loss modulus of different composites with respect to temperature. The maximum loss modulus is observed for S2 types of composites with the numeric value of 1782 MPa. Due to better interfacial interaction between fiber and matrix, the composites of S2 types may dissipate more energy while increasing temperature. Meanwhile, the lower loss modulus for S4-type composites indicates that less heat is dissipated due to inefficient bonding, resulting in a lower loss modulus. The sequence for loss modulus is S2>S1>S3>S4. The loss modulus is rising along with the temperature. Glass transition temperature (T_g) is defined as the temperature at which the loss modulus is maximum. Glass transition temperatures of S1, S2, S3 and S4 composites

TH-3447_196103002

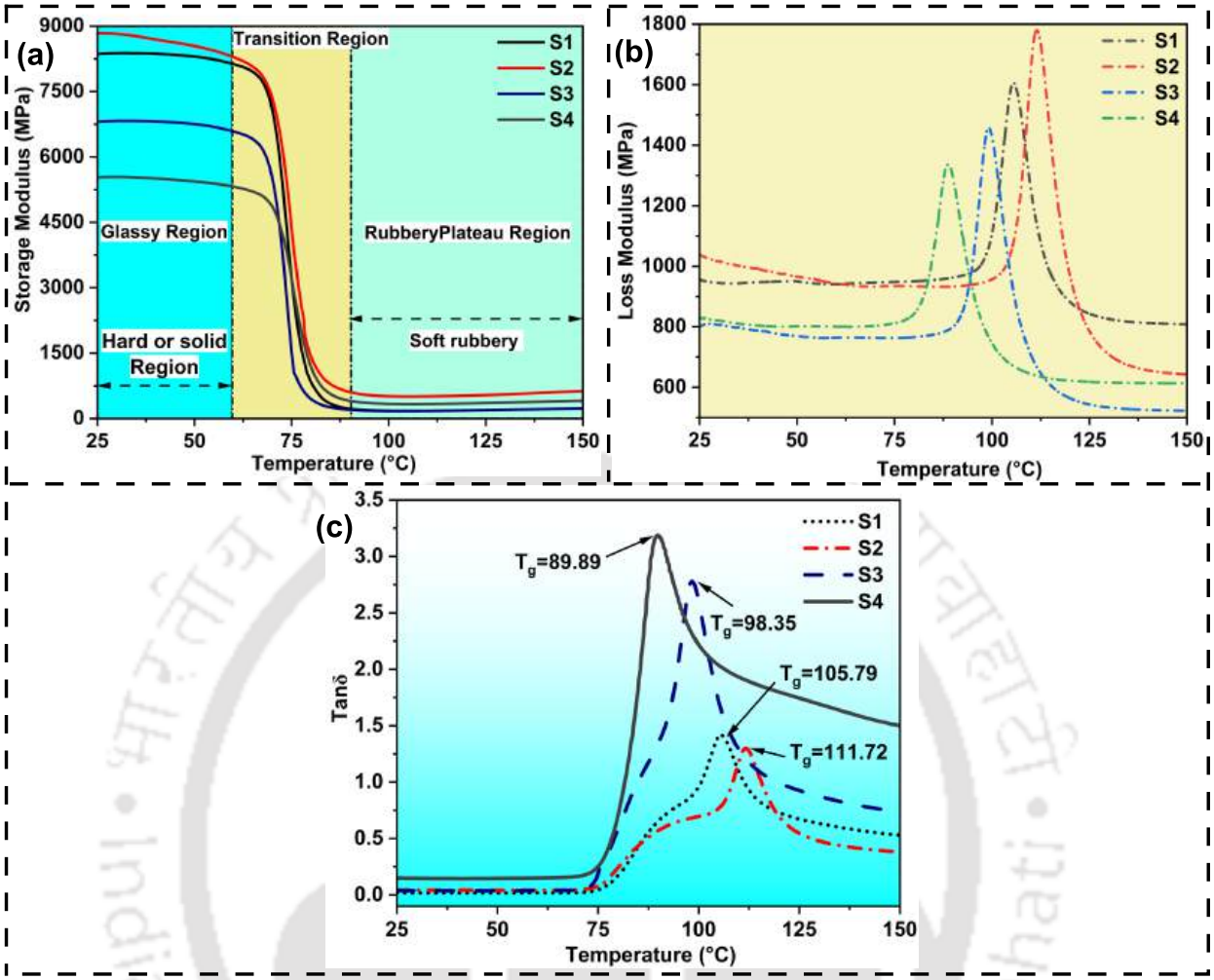

Fig. 6.9: (a) storage modulus, (b) loss modulus and (c) damping factor for developed composites.

are observed to be 105.79°C, 111.72°C, 98.35°C and 89.89°C respectively.

Tan (δ)- The molecular mobility of polymers and the frictional behaviour of fiber has been measured in terms of the damping factor (Tan δ). **Fig. 6.9** (c) presented the damping factor of different developed composites. The maximum and minimum damping factor value has been observed for S4 and S2 types of composites. The sequence for the damping factor is- S4>S3>S1>S2. Higher damping in the polymeric chain occurred due to inefficient bonding between epoxy LY-556 and bamboo fibre, which increased mobility and internal friction between fibre and matrix, resulting in a higher damping factor value. For S2 types of composites due to better interfacial bonding, this internal friction is reduced and shows a lower damping factor value.

TH-3447_196103002

6.3.8 Thermogravimetric Analysis (TGA)

The thermal stability of the developed composites has been examined with thermogravimetric analysis. **Fig. 6.10** (a) represents the thermogram for the samples. The pattern of mass loss with respect to temperature is following a similar trend for all types of composites. Generally, major three stages of mass loss have been observed for the composites [174]. The first stage is starting from 40°C to 150°C. This is corresponding to loss of mass due to the evaporation of moisture and some extractives. The second stage is from 151°C to 500°C. In this stage generally hemicellulose, some amount of lignin and cellulose has been decomposed. Decomposition of lignin generally occurred from 160°C to 650°C. The third or last stage of decomposition has been observed between 501°C to 800°C. This degradation is due to the decomposition of residual lignin and epoxy polymer. The stagewise decomposition percentage has been presented in **Table 6.2**. The initial maximum and minimum degradation have been observed for S4 and S2 types of composite corresponding to maximum and minimum moisture absorption phenomena of composites. At 800°C the maximum residual has been observed for S2 types of composites which is 21.65% and minimum residual mass has been reported for 8.82%. From this result, it can be concluded that the S2 type of composite has higher thermal stability.

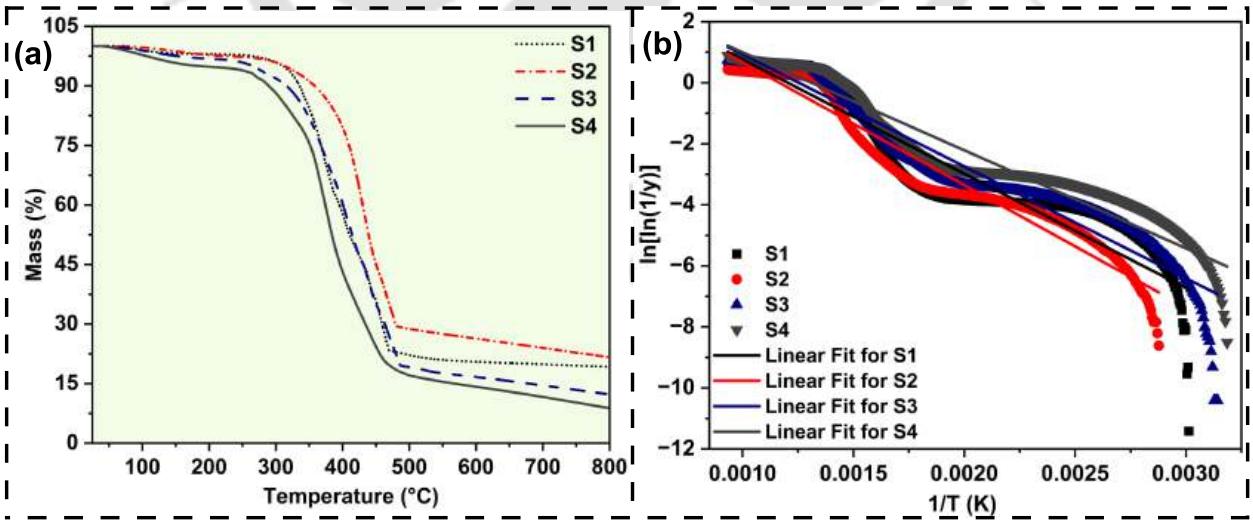

Fig. 6.10: (a) Thermogram for developed composites, (b) activation energy graph for developed composites.

The sequence for the residual mass of the composite is S2>S1>S3>S4. Another factor which

TH-3447_196103002

justifies the suitability of reinforcement at high temperatures is the kinetic activation energy. Further, the activation energy has been calculated for all types of composites. **Fig. 6.10** (b) represents the fitted graph for activation energy. The maximum activation energy has been reported for S2 types, with a value of 33.402 kJ/mol. The sequence for activation energy is S2>S1>S3>S4. The details of activation energy are also tabulated in **Table 6.2**.

Table 6.2: Mass loss in thermogravimetric analysis.

Composite sample	Stage-I weight loss (%)	Stage-II weight loss (%)	Stage-III weight loss (%)	Residual mass (%)	Activation energy (kJ/mol)
S1	1.85	77.41	13.08	19.27	31.16
S2	1.30	70.87	24.69	21.65	33.40
S3	2.45	80.36	35.72	12.31	30.53
S4	4.26	82.18	48.21	8.835	26.67

The different behaviors of the epoxy reinforced composites with 30% bamboo fiber loading can be attributed to variations in the chemical composition, curing processes, and mechanical properties of the different epoxy systems. The following may be the reasons:

1. **Cross-Link Density and Network Structure:** The chemical structure of the polymer and hardener determines the cross-link density and network structure of the cured epoxy. Different epoxies and hardeners lead to variations in the cross-link density, affecting the rigidity and toughness of the composites. A higher cross-link density generally increases stiffness but can reduce toughness.

2. **Curing Kinetics:** The curing kinetics and the extent of reaction affect the final properties. A different hardener can change the curing time, temperature, and degree of cure. The rate and extent of curing reactions vary with different formulations, influencing the thermal and mechanical properties of the final composite. Faster or more complete curing can enhance mechanical properties but might affect thermal stability.

3. **Fiber-Matrix Interaction:** The chemical compatibility between the bamboo fibers and the

TH-3447_196103002

epoxy matrix influences the adhesion and load transfer efficiency. Better adhesion leads to higher strength and stiffness.

4. **Thermal Stability:** Different epoxies have varying thermal stability, affecting the composite's performance at elevated temperatures. This is critical for applications requiring heat resistance.

5. **Mechanical Properties:** Variations in tensile strength, modulus, and impact resistance arise from differences in the chemical structure and curing process of the epoxy systems.

Understanding these factors helps in selecting the appropriate epoxy system for specific applications, ensuring optimal performance of the bamboo fiber-reinforced composites.

6.3.9 Microstructural Analysis

The failure of different composites has been characterized by observing the microstructural image of failure samples. Pulling out of fibre, fibre breakage, and matrix cracking have been identified as the leading causes of composite failure. **Fig. 6.11** represents the SEM image of fracture for different developed composites. These SEM images described the approximate failure pattern of the materials. The fiber pullout due to inefficient fiber-matrix bonding, debonding of fiber along with matrix crack, and brittle fracture of the fiber are the crucial observation from the SEM image. **Fig. 6.11** (a) is an SEM image of S1 types of composite. The pulling out of fiber from matrix material may be due to weaker interfacial bonding between them. As a result, the composites may not reach their expected strength. **Fig. 6.11** (b) represents the failure diagram for S2 type of composite. The composite fails first due to matrix failure, followed by fiber debonding and fracture. The reported damage processes are typical of brittle fractures. In the case of the S2 type of composites, stress-strain curves indicate that they are brittle in nature. **Fig. 6.11** (c) is the representation of very good fiber-matrix interfacial bonding for S2 sample. Good bonding will help the matrix to transmit load as well as stress from the matrix body to the reinforcement fiber. When the matrix fails, the fibres act as crack stoppers or arrestors to maintain the material's ductility. **Fig. 6.11** (d) is the representation of some good fiber-matrix interfacial bonding. The weak primary

TH-3447_196103002

cell wall collapses as the applied stress increases, causing cell cohesion and fiber failure. The failure of fiber inside the composite is presented in **Fig. 6.11** (e) for S3 type of material. **Fig. 6.11** (f) shows the failure of fiber. The gap between the fiber and the matrix can be used to determine the level of poor adhesion between fibers and the matrix for S3. Crack propagation and fiber-matrix inefficient bonding for S4 type of composite can be observed in **Fig. 6.11** (g) and (h). For S4, the poor interface may be responsible for the poor mechanical properties.

6.3.10 Cost Analysis

For any material, it is essential to estimate its development cost. The cost analysis has been done for all developed composites as per the Indian market and is presented in **Table 6.3**. The different costs like cost of materials, development cost, equipment cost and labour cost for the development of composites are considered and the total cost has been estimated. The maximum cost has been estimated for S3 types of composites with a value of Rs. 5140 per kg and the minimum cost is estimated for S4 types of composites with a value of Rs. 2340 per kg. The sequence for the materials from cheaper to expensive is S4<S2<S1<S3.

Table 6.3: Weight and volume fraction of bamboo fiber and bio epoxy matrix.

Sl. No.	Materials	S1	S2	S3	S4
1.	Material cost (Matrix)	3150	2800	3640	840
2.	Material cost (Fiber)	150	150	150	150
3.	Machinery and equipment cost	500	500	500	500
4.	Labour cost	800	800	800	800
5.	Consumable cost	50	50	50	50
	Total Cost (per Kg in Rs.*)	4650	4300	5140	2340

*1Rs.= 0.012 USD and 1Rs.= 0.011 EUR

6.4 MATERIAL SELECTION AND OPTIMIZATION FOR AUTOMOBILE APPLICATION

VIKOR's multi-attribute decision-making (MADM) method was used to select the best materials from these four for automobile applications. **Table 6.4** represents the performance-defining criteria

TH-3447_196103002

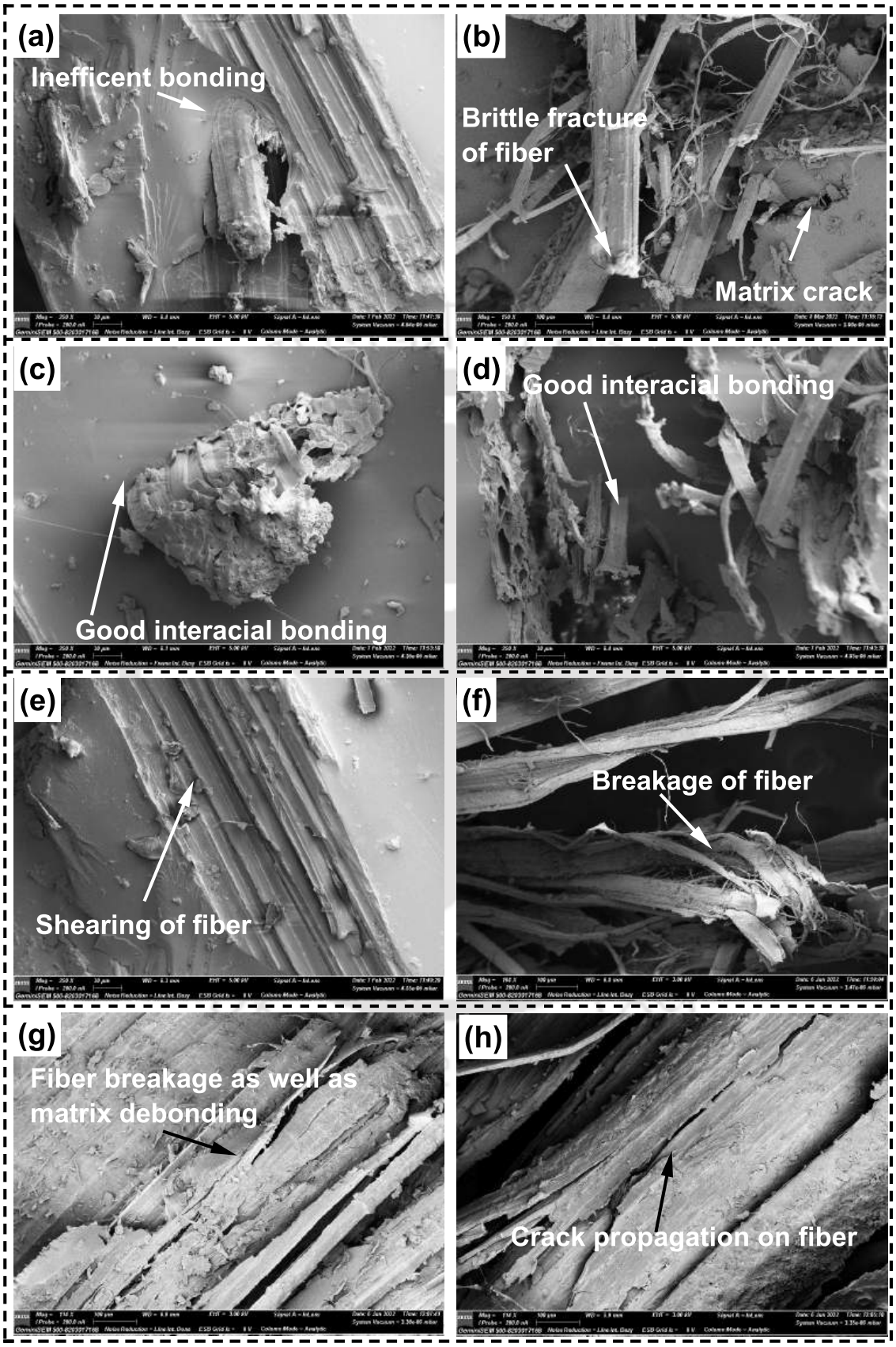

Fig. 6.11: SEM image of different failed composites.

TH-3447_196103002

and their implications.

Table 6.4: Weight and volume fraction of bamboo fiber and bio epoxy matrix.

Sl. No.	Performance-defining attributes (PDAs)	Implication
1.	Density (gm/cm_3)	↓ is better
2.	Void content (%)	↓ is better
3.	Bio-content (%)	↑ is better
4.	Water or moisture absorption (%)	↓ is better
5.	Thickness Swelling (%)	↓ is better
6.	Tensile Strength (MPa)	↑ is better
7.	Tensile Modulus (GPa)	↑ is better
8.	Flexural Strength (MPa)	↑ is better
9.	Flexural Modulus (GPa)	↑ is better
10.	Impact Strength (kJ/m^2)	↑ is better
11.	Hardness (HRC)	↑ is better
12.	Storage Modulus (MPa)	↑ is better
13.	Glass transition temperature (°C)	↑ is better
14.	Initial degradation temperature of TGA (°C)	↑ is better
15.	Residual mass of TGA (%)	↑ is better
16.	Activation energy (kJ/mol)	↑ is better
17.	Cost (Rs.)	↓ is better

↑ is stand for higher value is better and ↓ is stand for lower value

6.4.1 Shannon Entropy Method

The decision matrix has been presented in **Table 6.5**. The Shannon entropy method has been used for the ranking of different attributes. **Table 6.6** and **Table 6.7** display the computed weight using the entropy approach.

6.4.2 VIKOR Material Selection Method

The steps details have been presented in supplementary details. **Table 6.8** and **Table 6.9** presents the S_i and R_i values calculated by the VIKOR method for different materials alternatives. And thereafter the possibilities are ranked as per the VIKOR index (Q_i). More oven the S_i and R_i

TH-3447_196103002

values are also calculated for different α values and presented in **Table 6.8** and **Table6.9**. The choice with the lowest VIKOR index earns the lowest rank, which is 1.

6.4.3 Sensitivity Analysis

Further, the sensitivity of the optimization process has been analysed by using different values of α. α is often assumed to have a value of 0.5 [341]. But α can have any value between 0 and 1. Consequently, it is essential to perform a sensitivity analysis on the parameter α to verify the findings that were obtained. **Fig. 6.12** depicts the relevant outcomes based on the different values of α. As can be observed, the α value had no impact on the ranking orders of materials S2 and S3. This indicates that both materials have similar risk preferences in terms of maximal group utility and minimal individual regret. This outcome demonstrates the robustness and reliability of the outcomes produced by the suggested methodology [344]. On the other side, an increase in α value led to an improvement in S2's ranking. This result indicates that when one concentrates on maximal group utility, S2 has a greater level of risk. Additionally, S3 had a high ranking when the α value was low, indicating that its ranking increased as the significance of the minimum individual regret increased. In other words, S3 scored high on the risk scale when the minimum level of individual regret was taken into consideration. When the α value is greater than or equal to 2, no changes occur for the ranking of any materials, concluding that the process is robust over this domain.

6.4.4 Sustainable Application in the Automobile Sectors

Heavy materials such as magnesium, copper, and steel are being replaced by plastics in the locomotive industry in order to have lighter cars for higher efficiency. Additionally, automakers are focusing on choosing the most resource-efficient plastics (i.e., biobased plastics) to reduce environmental impact [345]. The result was a reduction in greenhouse gas emissions and an increase in energy efficiency. Furthermore, it is estimated that several million automobiles will reach the end of their useful life this year. Even though some components can be recycled, approximately 25 to 40% of the automotive weight (fiber and plastic) is disposed of as landfill waste. Most of the components of an automobile were made of non-biodegradable materials, including polypropylene

TH-3447_196103002

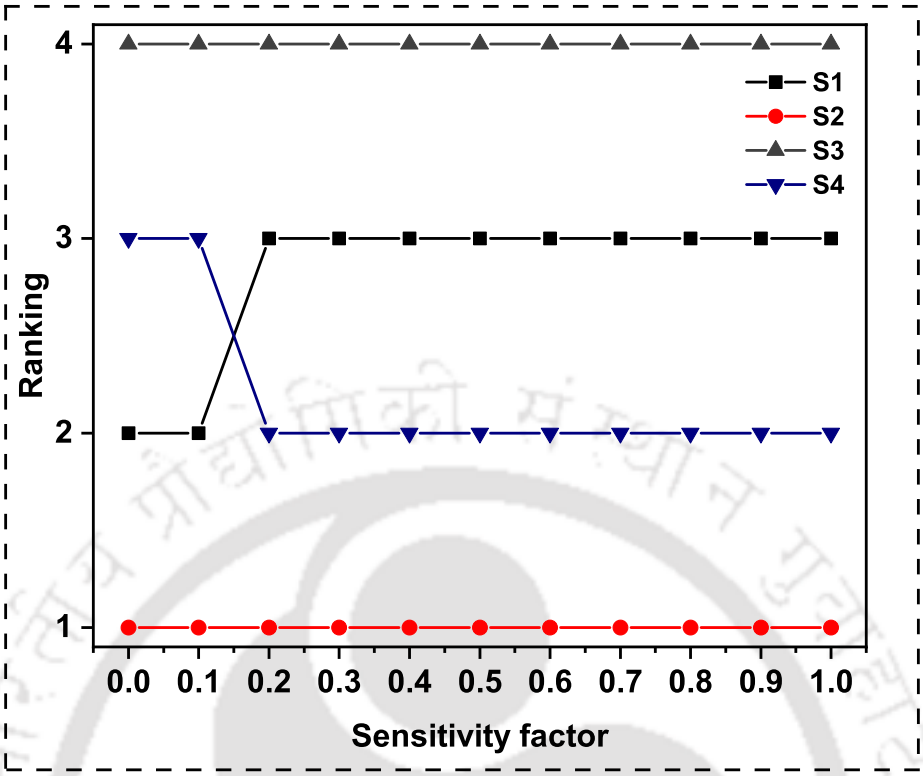

Fig. 6.12: Result for Sensitivity analysis.

(PP), polystyrene, glass fibre and polyethene (PE), making them difficult to reuse. Therefore, applying bio-based materials to automotive structural and semi-structural applications can reduce the manufacturing's environmental impact. Using bio-based materials reduces the ecological consequences as well as the emission of greenhouse gases throughout its life cycle. Not only that, natural fiber-based biocomposites are a suitable example of renewable resources. It is estimated that a modern car's body is made up of about 100-150 kg of polymer materials [346]. So, automobile manufacturers like Audi, Ford, BMW, Nissan, and Mercedes are adopting natural fiber composites for various internal as well as exterior parts of their automobiles [17]. **Table 6.10** [80, 347] presents various automobile manufacturer and their adopted biocomposites for different automobile parts.

In addition, a comparative study of present optimized materials with previously published materials has been done and is presented in **Table 6.11**. Based on the comparative study, the present material, S2, has a great deal of potential for automobile applications.

Most interior parts of a typical automobile are made of materials like Polypropylene (PP, tensile strength 20-40 MPa, flexural strength 30-45 MPa), Acrylonitrile Butadiene Styrene (ABS, tensile

TH-3447_196103002

TH-3447_196103002

Table 6.5: Decision matrix.

Materials	ρ	V_c	B_c	W_c	T_S	σ_T	E_T	σ_F	E_F	IS	H_c	SM	T_g	IDT	A_{energy}	R_{mass}	cost
	C1	C2	C3	C4	C5	C6	C7	C8	C9	C10	C11	C12	C13	C14	C15	C16	C17
S1	1.02	2.89	61.78	5.91	7.53	133.06	6.98	154.80	8.24	44.06	82.31	8.32	105.79	58.42	31.15	19.27	3950
S2	1.04	2.07	53.80	4.49	7.37	144.76	5.72	120.42	6.27	57.57	86.05	8.82	111.72	73.75	33.40	21.66	3600
S3	1.07	1.20	52.4	6.81	10.90	107.95	6.02	104.87	6.62	48.18	97.60	6.78	98.35	44.58	30.52	12.31	4400
S4	1.05	4.10	30	8.51	12.52	86.31	5.27	98.42	5.17	24.60	62.61	5.51	89.89	40.20	26.69	8.83	1640

*Standard deviation is not taken into account for making decision matrix

Density=ρ (gm/cm^3); Void content=V_c (%), Bio content=B_c (%); Water absorption= W_c (%); Thickness swelling= T_S (%); Tensile strength=σ_T (MPa); Tensile Modulus= E_T (GPa); Flexural Strength= σ_F (MPa); Flexural modulus= E_F (GPa); Impact Strength= IS (kJ/mm^2); Hardness=H_c (HRC); Storage modulus=SM (MPa); Glass trinsition temperature= T_g (^{o}C); Initial degradation temperature= IDT (^{o}C); Activation energy=A_{energy} (kJ/mol); Residual mass= R_{mass} (%); cost (Rs.)

Table 6.6: Weightage of different criteria (C1 to C8).

Criteria	C1	C2	C3	C4	C5	C6	C7	C8
Weightage	0.0003	0.2005	0.0701	0.0583	0.0595	0.0424	0.0121	0.0362

Table 6.7: Weightage of different criteria (C8 to C17).

Criteria	C9	C10	C11	C12	C13	C14	C15	C16	C17
Weightage	0.0312	0.0929	0.0274	0.0363	0.0074	0.0647	0.0072	0.1296	0.1239

Table 6.8: VIKOR Index and Ranking for α=0 to 0.4.

S_i	R_i	Q_i	Rank	Q_i	Rank	Q_i	Rank	Q_i	Rank	Q_i	Rank
		α=0		α=0.1		α=0.2		α=0.3		α=0.4	
0.3527	0.0960	0.311	2	0.357	2	0.404	3	0.450	3	0.497	3
-0.6473	-0.0003	0.000	1	0.000	1	0.000	1	0.000	1	0.000	1
0.6428	0.3094	1.000	4	1.000	4	1.000	4	1.000	4	1.000	4
-0.3572	0.1159	0.375	3	0.360	3	0.345	2	0.330	2	0.315	2

TH-3447_196103002

Table 6.9: VIKOR Index and Ranking for α=0.5 to 1.

S_i	R_i	Q_i	Rank	Q_i	Rank	Q_i	Rank	Q_i	Rank	Q_i	Rank
		α=0		α=0.1		α=0.2		α=0.3		α=0.4	
0.543	3	0.589	3	0.636	3	0.682	3	0.729	3	0.775	3
0.000	1	0.000	1	0.000	1	0.000	1	0.000	1	0.000	1
1.000	4	1.000	4	1.000	4	1.000	4	1.000	4	1.000	4
0.300	2	0.285	2	0.270	2	0.255	2	0.240	2	0.225	2

Table 6.10: Application of natural fiber composites by different automobile industries [81],[303].

Sl. No.	Company Name	Car Model	Polymer used	Natural fiber used	Application
1.	BMW	Series-7	Acrylic	Sisal, Flax, wood, cotton	Seat backs, Door panel, Panel with noise isolation, boot lines, headliner
2.	General Motors	–	–	Kenaf, Hemp, Flax	Cargo floors, back of seat, Inner part of door panels
3.	Ford	Fusion, Fiesta, BEV	Polyurethane	Kenaf, hemp, rice husk, soy, coir	Door panel, Front grills, Floor trays
4.	Toyota	Raun, Pruis	Sorona	Sugar cane, Kenaf	Spare and tire cover, Instrument panel, door panel
5.	Mercedes	Benz Class-A and C	Polyurethane	Flax, Banana, Abaca	Cover of engine and transmission units, Panel of underbody
6.	Nishan	Leaf	Sorona	Corn	Floor mat
7.	Volvo	–	–	Jute, wood, hemp	Padding of seat, Ceiling, Dashboard
8.	Mitsubishi	–	–	Bamboo, cotton, hemp	Door panel, floor mats, Floor area of the cargo mat

TH-3447_196103002

Table 6.11: Comparative study of present result with previously reported result.

Fiber	Polymer	Reference	Density (gm/cm^3)	Tensile Strength (MPa)	Tensile Modulus (GPa)	Flexural Strength (MPa)	Flexural Modulus (GPa)	Hardness (HRC)	Impact Strength	T_g (°C)
Bambusa tulda	FormuLite (2501A+2002B)	Present work (S2)	1.04	144.76	5.72	120.42	6.27	86.05	57.57 kJ/m^2	111.72
Bamboo (Taiwan origin)	Polypropylene	[80]	–	109.42	15.07	111.53	7.18	–	–	–
Rattan Fiber	Epoxy	[348]	–	46.94	3.20	113.11	7.35	26	30.67 J/m	89.22
Bamboo	Epoxy HM-533	[44, 107]	–	208	23	310	21.1	–	–	–
Sisal and Kenaf	Epoxy	[349]	– –	42.346	–	–	–	84.6	1.88 J	–
Sugarcane bagasse fiber and palm	Epoxy	[345]	–	19.80	0.953		0.2879	38.02	2 kJ/m^2	–
Bamboo	Epoxy	[110]	1.16	275.29	–	16.98	–	–	–	–
Punica Granatum	CSNLbased epoxy	[189]	–	29.93	3.20	54.86	4.46	–	8.73 kJ/m^2	–
Kenaf and Bamboo	Epoxy	[299]	–	68.47	5.3	–	–	–	–	–
Flax and Ramie	FormuLite (2501A+2401B)	[285]	–	108	5.63	119	12.5	–	–	110
Kenaf	rubber cramb	[341]	1.19	38.13	–	68.52	–	–	27.41 kJ/m^2	–
Gigantochlea scotechini	Epoxy	[174]	–	119.39	–	161.58	–	–	–	–

strength 30-50 MPa, flexural strength 60-85 MPa), Polycarbonate (PC, tensile strength 55-75 MPa, flexural strength 90-100 MPa), Nylon (Polyamide, PA, tensile strength 60-80 MPa, flexural strength 80-120 MPa), and Polyethylene Terephthalate (PET, tensile strength 50-100 MPa, flexural strength 80-120 MPa) [80, 347]. To replace all these materials with green composites, the targeted tensile strength and flexural strength of the green composites should exceed 100 MPa and 120 MPa, respectively.

6.5 SUMMARY

Four different biocomposites have been successfully developed using bamboo fiber and four different epoxy matrices, including three bio-based polymers and one commercial epoxy. The developed composites underwent comprehensive physical characterizations, encompassing density, void content, moisture absorption, and thickness swelling. Mechanical characterization involved tensile, flexural, impact, and surface hardness testing, while dynamic mechanical analysis included measurements of storage modulus, loss modulus, glass transition temperature, and tan delta. Subsequent to these analyses, thermogravimetric analysis, cost estimation, and microstructural characterization of the developed samples were conducted. To discern the optimal material for automobile interior applications among the four, the VIKOR multicriteria decision-making technique was employed. The sensitivity of the material selection process was explored by varying sensitivity factors from 0 to 1. In summary, the investigation yielded the following key points:

(i) Choosing lightweight materials hinges on the critical parameter of material density. Among the developed materials, S1 and S3 composites exhibited the lowest and highest densities, respectively.

(ii) The void content plays a crucial role in the properties of biocomposites. Minimum and maximum void content have been observed for S3 (1.2%) and S4 (4.1%) types of composites, respectively.

(iii) Moisture absorption stands as a drawback in natural fiber-reinforced biocomposites. The capillary action within the interfacial gap between fiber and matrix contributes to moisture

TH-3447_196103002

absorption. Notably, S4 composites exhibit the maximum moisture absorption, while S2 composites show the minimum moisture absorption and thickness swelling.

(iv) The S2 types of composites exhibit the highest tensile strength, measured at 144.75 ± 4.40 MPa. On the other hand, the maximum Young's modulus is observed in S1 types of composites, with a value of 6.98 ± 0.19 GPa.

(v) The S1 types of composites demonstrate the highest flexural strength, following the sequence S1>S2>S3>S4.

(vi) Additionally, the maximum hardness and impact strength are observed in S3 and S2 composites, respectively.

(vii) The highest values for storage modulus and loss modulus were reported for S2 types of composites, while these composites exhibited the lowest tan delta value.

(viii) The glass transition temperature for S2 types of composites was reported as 111.72 ^{o}C.

(ix) In the thermal analysis of the developed composites, S2 types exhibited the highest thermal stability, while S4 types experienced rapid mass degradation with increasing temperature.

(x) In the context of the Indian market, S4 composites have the lowest development cost at Rs. 2340, while S1 composites have the highest development cost at Rs. 4650 among all four types of composites.

(xi) The VIKOR material selection procedure identified S2 types of composites as the optimal materials, while S3 types of composites were deemed the least favorable. Furthermore, a sensitivity analysis of the process highlighted its robustness.

(xii) Hence, S2 composites emerge as the appropriate material for applications in the automobile industry, particularly for semi-structural and interior uses.

TH-3447_196103002

Chapter 7

Effect of Reinforcement Hybridization on Bamboo-Based Green Composites

7.1 INTRODUCTION

Natural fibers exhibit poor interfacial interaction with the polymer matrix. One of the most common and effective methods to enhance the interfacial interaction between natural fibers and the polymer matrix is the alkalization of fibers. Another approach involves the hybridization of reinforcement fibers with micro-particles. This chapter presents the design, development, and characterization of waste bamboo micro particles and bamboo fiber reinforced hybrid bio composites. The hybrid green composites are fabricated using 6% chemically treated Bambusa tulda fibers, bamboo micro-particles, and bioepoxy matrix. The bamboo micro-particles, obtained as waste from nearby bamboo industries, are cleaned with acetone and treated with a NaOH solution before being utilized as reinforcement materials. For the development of green composites, the weight fraction of bamboo fibers is kept constant at 30%, while the weight fraction of micro-particles varies from 0 to 10% at intervals of 2.5. The physical properties, such as moisture absorption, density, and void content of the developed composites, have been investigated. Mechanical characterization includes tensile, flexural, impact, and surface hardness testing have been done. Thermogravimetric analysis has been also performed to study the impact of dual reinforcement on thermal degradation properties of biocomposite. The investigation revealed that hybridization with up to 5% particle reinforcement has a positive effect on the thermomechanical properties of green composites. However, when the reinforcement exceeds 5% by weight, due to agglomeration, properties lead to a decrease. The maximum tensile modulus is observed as 7.65 $\pm$ 1.26 GPa, while the maximum

TH-3447_196103002

tensile strength is observed for BFHC_5 composites as 163.17 ± 6.44 MPa. The maximum flexural strength and flexural modulus are observed for BFHC_5 composites as 144.26 ± 4.44 MPa and 7.33 ± 1.064 GPa, respectively. **Sec. 7.2.1** describing about the materials used in the present study. **Sec. 7.2.2** discusses the development of bamboo micro-particles from bamboo biomass waste. The fiber extraction and its chemical treatment of fiber has been described in **Sec. 7.2.3**. **Sec. 7.2.4** presents the development of hybrid composite, while **Sec. 7.2.5** describes different characteristic techniques to characterized the BMP. **Sec. 7.2.6** is about characterization technique to characterize the hybrid green composites. Whereas **Sec. 7.3** discusses the results obtained from characterization, **Sec. 7.4** provides a comparative study of present study with the study presented in literature and **Sec. 7.5** provieds a summary of the present experimental work.

7.2 MATERIALS AND METHODOLOGY

This section describes the materials used in the present study, as well as the methodology and experimental processes employed for various material characterizations.

7.2.1 Materials

The FormuLITE series, a bio-epoxy resin utilized as matrix materials, is derived from natural phenolic sources obtained through the distillation of Cashew nutshell liquids (CNSL). Supplied by Cardolite India Pvt. Ltd. from Mangalore, India, these resins are recognized for their 34% bio content. Characterized by low density (1.081 gm/cm^3) and viscosity (905 cPs), the FormuLITE resin exhibits a high glass transition temperature (>95 °C) and flash point (>150°C). As investigated in the previous **Chapter 6**, the best-fit bio-based thermosetting matrix for automobile interior applications is the combination of the liquid polymer, and the matrix is Formulite 2501A+ 2401B. Therefore, in the further study in this chapter, this combination is used. The FormuLITE polymer consists of a blend of modified thermoset epoxy (2501A) and amine hardener (2401B), mixed in a proper ratio of 10:3, serving as the matrix material for the development of bio-composites. Bamboo biomass is collected from local bamboo industries. This bamboo biomass is the waste product of the bamboo industry after cutting and shaping of the bamboo. The local nursery of Guwahati, India,

TH-3447_196103002

is the source of native bamboo (*Bambusa tulda*) aged between 3 to 5 years, specifically acquired for the extraction of fibers. The sodium hydroxide pallet and ethanol are procured from Sigma-Aldrich Pvt. Ltd., India.

7.2.2 Bamboo Micro Particle (BMP) Synthesis and Chemical Treatment

Bamboo Micro Particle (BMP) is a byproduct generated during the cutting and shaping of bamboo. Using a powerful magnet, bamboo particle underwent additional screening to eliminate small iron particle. The primary challenge involved extracting minute non-ferrous metal pieces, soil particles, and grease, achieved through a multi-step cleaning process, including multiple washes with water and acetone, culminating in magnetic stirring. Following washing, the sample was dried in a hot furnace for 8 hours at 60°C. Subsequently, the ball milling process was conducted after a 30-minute drying period, followed by a sieving process in descending order (from 300 to 25 μm sieve size) to achieve the desired dimensions. The particle used in this study is less than 25 μm.

The inherent poor interfacial properties between natural particles and a polymer matrix necessitate enhancement. To address this, micro particles are meticulously treated with a 6% NaOH solution to augment the interfacial interlocking with the epoxy matrix. This treatment serves a dual purpose: it ameliorates the interfacial properties of bamboo particle and concurrently eliminates lignin and hemicellulose from them.

The chemical treatment involves immersing the particles in a 6 wt.% aqueous NaOH solution in a beaker. This solution undergoes magnetic stirring at 48 degrees Celsius for approximately 8 hours, with a stirring speed of 800 rpm. Subsequently, the solution is washed with acetone, followed by distilled water until reaching a neutral pH value of 7. After treatment, the bamboo particles undergo drying in a muffle furnace at 60°C for about 6 hours. The transformation of bamboo biomass into usable bamboo micro particle is elucidated in **Fig. 7.1**.

7.2.3 Fiber Extraction and Its Chemical Treatment

The retting process was employed to extract bamboo fiber, as detailed in **Chapter 3**. Following the fiber extraction, a treatment with a 6% NaOH solution was administered. This treatment not only increased the crystallinity index and interfacial properties but also effectively removed lignin

TH-3447_196103002

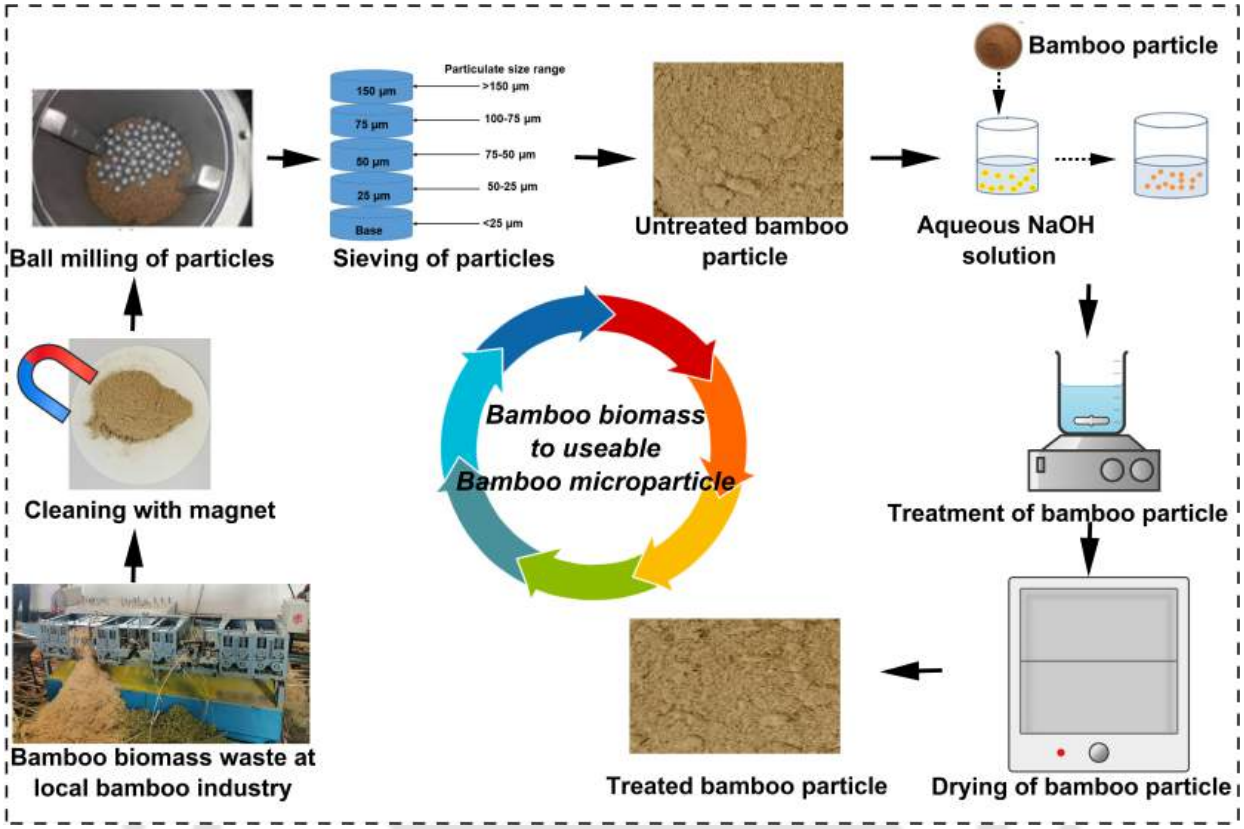

Fig. 7.1: Flow diagram of BMP recycling, processing, and its chemical treatment.

and others noncrystalline components. As detailed in **Chapter 4**, the chemical treatment resulted in significant improvements, enhancing the crystallinity index, tensile strength, tensile modulus, and interfacial shear strength of the fiber by 27.41%, 42.22%, 75.80%, and 81.09%, respectively, compared to untreated fiber. In light of these findings, the current study focuses on the utilization of 6% NaOH-treated bamboo fiber for the development of hybrid composite samples and other characterizations of hybrid biocomposite samples.

7.2.4 Development of Hybrid Biocomposite Plate

The production of biocomposite samples utilized the manual compression hand layup method, and the fabrication process is illustrated in **Fig. 7.2**. Initially, bioepoxy resin (2501A) was measured and placed in a glass container at an appropriate weight. Treated bamboo micro particles were then incorporated at various weight fractions (2.5%, 5.0%, 7.5%, and 10.0%). The mixture underwent thorough mechanical stirring for 10 minutes, followed by the addition of amine hardener at the standard ratio with bio-epoxy resin (10:3). Proper mixing ensued through mechanical processes,

TH-3447_196103002

and degassing eliminated air bubbles from the final solution.

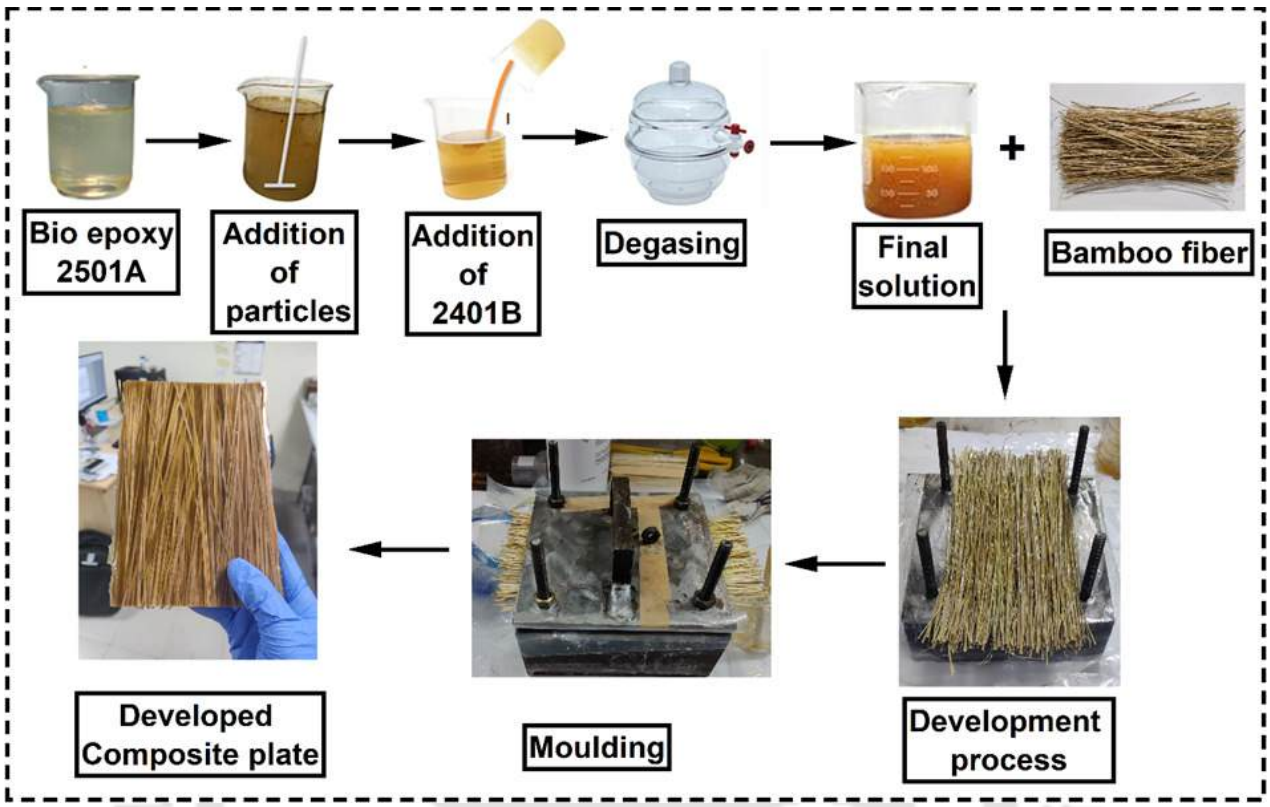

Fig. 7.2: Hybrid composite development process.

Next, bamboo fibers were evenly spread over the lower mold at a constant weight of 30%, and the final solution mixture was poured onto the fibers (According to the study of **Chapter 5**, a 30% weight ratio of the bamboo fiber to polymer composites is ideal for the construction of sustainable composites. Over 30% of the fiber reinforcement in composites exhibited fiber agglomeration, which reduced the material's overall stiffness and strength. Therefore, the constant weight fraction of fiber (30% by weight) has been considered for the current investigation.). A roller and brush were employed to ensure a uniform coating of the matrix on the fiber layer and to detect voids during sample preparation. Subsequently, the upper mold was placed over the prepared samples, and an external load of 50 kg was applied for even distribution of matrix materials within the fiber reinforcements.

The prepared samples were left to cure at room temperature for 24 hours, after which they were removed from the mold and subjected to the pre-curing and post-curing processes inside an oven. Finally, the samples were cut in accordance with ASTM standards for subsequent experimental

TH-3447_196103002

testing. Detailed information on all five types of hybrid composites is provided in **Table 7.1**.

Table 7.1: Weight fraction of bamboo fiber, BMP and bio epoxy matrix.

Sample code	Epoxy weight fraction (%)	Fiber weight fraction (%)	Particle weight fraction (%)	Bio-content in composites (%)
BFHC_0	70	30	0	53.80
BFHC_2.5	67.5	30	2.5	55.45
BFHC_5	70	30	5	57.10
BFHC_7.5	62.5	30	7.5	58.75
BFHC_10	60	30	10	60.40

7.2.5 Characterization of Bamboo Micro Particle

The scanning electron microscopy (SEM), X-ray diffraction (XRD), and thermogravimetric analyzer (TGA), along with the density assessment of bamboo micro particles, were employed to scrutinize the physical, thermal, and structural properties of prepared bamboo particles. These analytical methods facilitated the examination of the impact of chemical treatments on molecular bonding, thermal stability, phase transformation, surface modification, and interfacial structure within bamboo biomass.

Density- Using a Pycnometer, the density of bamboo micro particles was determined, employing solid and toluene as the respective mediums. The micro particles underwent a drying process in a hot air oven at 70°C for 4 hours to eliminate moisture content. The density of the fiber bundles was computed using equation **Eq.7.1**.

$$\rho_{\text{micro particle}} = \frac{(m_3 - m_1)}{(m_2 - m_1) - (m_4 - m_3)} \rho_{liq} \tag{7.1}$$

where, $\rho_{\text{micro particle}}$ is the density of bamboo micro particles,ρ_{liq} is the density of liquid used (here it is toluene,0.8623 gm/cm^3 at 25°C). m_1 is the mass of pycnometer at empty condition, m_2 is the mass of pycnometer filled with toluene, m_3 is the pycnometer's mass filled with bamboo micro particles and m_4 is the mass of the pycnometer filled with both toluene and bamboo micro

TH-3447_196103002

particles. The electronic precise weighing balance of Sartorius (Model: Cubis®, Germany) with an accuracy of ±0.1mg was used to measure the weight of the sample. Five bundles from each sample have been taken for density measurement and the average density is reported with standard deviation.

XRD- A powder X-ray diffraction analysis was performed using BRUKER (model: D8 advance, United States) to determine the crystallographic information of bamboo micro particles under Cu-Kα radiation ($\lambda = 1.542\mathring{A}$) operated at 30 kV/15 mA. The intensity count has been recorded between $2\theta = 10$ to 50° with a speed of 2°/min and step size of 0.02°. The crystallinity index of the fiber samples was determined with the help of the Ruland-Vonk method as per **Eq. 7.2**, and the crystalline size of the micro particle was determined with the help of Scherrer's formula as per **Eq. 7.3** [215].

$$Cr\% = \frac{(A_T - A_{Am})}{A_T} \times 100\% \tag{7.2}$$

$$CS = \frac{K \times \lambda}{\beta \times Cos\theta} \tag{7.3}$$

where A_T is the total area under the XRD graph, and A_{Am} is the area of the amorphous zone. where K, β, λ and θ are denoted as Scherrer's constant, full-width half maximum of the peak, the wavelength of radiation and Bragg angle, respectively.

SEM- The structural morphology of bamboo biomass and bamboo micro particles is examined using Sigma Field Emission Microscopy (Make: Zeiss, Germany). Since the natural microfibrils are non-conductive or less conductive [209], a thin film of gold was coated on the samples to enhance conductivity. The Sputter Coater (model: BALTEC-SCD-005, USA) was employed for the delicate gold coating on the fiber samples. To investigate the diameter of the original micro particles, the Field Emission Scanning Electron Microscopy (FESEM) image was analyzed with the assistance of ImageJ software (open-source software). The particle size distribution of the bamboo micro particles (BMP) is analyzed using a distribution curve.

TGA- The thermal stability of the micro particles has been investigated using a Perkin Elmer

TH-3447_196103002

Instrument (model: STA 800, USA) thermogravimetric analyser. 5 mg to 8 mg of micro particle samples were heated from room temperature (25°C) to 600°C with a heating rate of 10°C/min in a nitrogen atmosphere and weight loss curves have been recorded.The activation energy for BMP has been calculated using **Eq.7.4**.

$$\ln\left[\ln\left(\frac{1}{y}\right)\right] = -\left(\frac{E_a}{R}\right)\left[\left(\frac{1}{T} + K\right)\right] \tag{7.4}$$

Here y is denoted as normalized weight (w_t/w_i), where w_t is the weight of the sample at time t and w_i is the initial weight. T is the representation of temperature in Kelvin. E_a is the activation energy. The graph has been plotted between $\ln\left[\ln\left(\frac{1}{y}\right)\right]$ and $\left(\frac{1}{T}\right)$ and the Slope of the graph has been found by a fitting straight line between the data points of the plot. The activation energy has been calculated by multiplying the slope value with the universal gas constant value (R=8.32 J/mol-K) as of **Eq.7.5**.

$$\frac{d\ln\left[\ln\left(\frac{1}{y}\right)\right]}{d\left(\frac{1}{T}\right)} = -\left(\frac{E_a}{R}\right) \tag{7.5}$$

7.2.6 Characterization of Hybrid Composite

The developed hybrid green composite plates are characterized physically, mechanically and thermally. The details of investigation process are presented in this section.

7.2.6.1 Physical Characterization

Density and Void Content- The theoretical density of the composite was calculated using the rule of mixture, while the experimental density was measured following Archimedes' principle with ASTM-D-792-13 (20×20×3 mm^3) samples. The density of the treated bamboo fiber was previously measured as 1.025 gm/cm^3 in **Chapter 4**. According to the data sheet provided by the manufacturing company, the density of FormuLite (2501A+2401B) is 1.081 gm/cm^3. **Eq. 7.6** has been used to compute the theoretical density of the composites.

$$\frac{1}{\rho_{c(theo)}} = \frac{w_f}{\rho_f} + \frac{w_p}{\rho_p} + \frac{w_m}{\rho_m} \tag{7.6}$$

Where $\rho_{c(theo)}$ is the theoretical density of composite, w_f, w_p and w_m are the weight fraction of fiber, particulate and matrix materials, ρ_f, ρ_p and ρ_m are the density of fiber, micro particle and

TH-3447_196103002

matrix materials respectively.

The presence of voids in composite materials holds significant importance as it substantially influences the mechanical and physical properties of the composite. Cracks typically initiate in regions where voids are present, and there's a potential for these cracks to extend into other areas of the material, resulting in catastrophic failure. Therefore, assessing the void content in the composite is crucial for ensuring its quality. The void content was quantified using **Eq.7.7**.

$$V_c = \frac{\rho_{c(theo)} - \rho_{c(exp)}}{\rho_{c(theo)}} \times 100 \tag{7.7}$$

where V_c is void content of composites and $\rho_{c(exp)}$ is the experimental density of composites.

Water Absorption Test- Natural fibers micro particles exhibit hydrophilic properties. Consequently, the water absorption test for the developed hybrid composites was conducted at room temperature following ASTM-D-570 standards with samples of dimensions 20×20×3 mm^3 [329]. The test samples were immersed in distilled water for durations ranging from 48 to 720 hours, with periodic measurements of their weight and thickness. The weight gain and thickness swelling resulting from water uptake are computed using **Eq.7.8** and **Eq.7.9**.

$$W_{\text{Water absorption}}(\%) = \frac{W_t - W_0}{W_0} \times 100 \tag{7.8}$$

Where W_t and W_0 are the weight of bio-composite samples at time = t and 0.

$$T_{\text{Thickness swelling}}(\%) \frac{T_t - T_0}{T_0} \times 100 \tag{7.9}$$

Where T_t and T_0 are the thickness of the bio-composite samples at time = t and 0.

7.2.6.2 Mechanical Characterization

Tensile Testing- The tensile properties of the developed hybrid green composites were assessed using a Shimadzu Universal Testing Machine (UTM) equipped with a 100 kN load cell. Specimens were prepared with a rectangular cross-section following ASTM-D-638-3 standards [330], with dimensions of 160×14×3 mm^3. Testing utilized a gauge length of 50 mm and a crosshead speed of 1 mm/min. Each type of green composite underwent testing with five samples, and the average results, along with standard deviations, are presented.

TH-3447_196103002

Flexural Testing- To understand the flexural properties of hybrid composites, three-point bending tests were conducted using the Shimadzu Universal Testing Machine (UTM). Test samples were prepared in accordance with ASTM-D-790-3 standards [331], featuring dimensions of 130×14×3 mm^3. The testing configuration included a fixed span length of 50 mm and a cross-head speed set at 1 mm/min.

Impact Testing- The Charpy impact testing for the developed hybrid composites was conducted using an IT-30 impact testing machine (manufacturer: FIE, India). Notched test samples were prepared following ASTM-D-6110 standards [332], with dimensions of 64×12.7×3.2 mm^3. Each type of hybrid green composite underwent evaluation on five samples, and the average results, along with standard deviations, are presented.

Surface Hardness- Surface hardness measurements for the developed hybrid green composites were conducted at ten different locations on each sample using a digital Rockwell hardness tester (manufacturer: FIE, India). Surface penetration was executed with a 1/4" aluminum ball under a 60Kgf force on an L scale. Test samples were prepared in accordance with ASTM-D-785, featuring dimensions of 20×20×3 mm^3 [333]. The average test results, along with standard deviation, are provided in the results and discussion section.

Dynamical Mechanical Analysis (DMA)- The dynamic mechanical characteristics of the developed hybrid green composites were assessed using the Anton Paar Dynamic Mechanical Analyzer (Maker: Physica MCR, Model: 702). Test samples, with dimensions of 50×13×3 mm^3 [285], were secured within the machine using a double cantilever fixture. The testing was conducted under a sinusoidal frequency of 1 Hz, with the temperature ranging from 25°C to 150°C and a temperature ramp of 5°C/min.

7.2.6.3 Thermogravimetric Analysis -

The thermal stability of the developed green hybrid composites has been analysed with Perkin Elmer Instruments. The mass loss of the samples has been determined in an N_2 environment as a function of temperature from room temperature to 800°C with a constant heating rate of 10°C/min.

TH-3447_196103002

7.2.6.4 Microscopic Analysis

The fracture surface of the developed hybrid composite was scrutinized using a field-emitted scanning electron microscope (Zeiss, model: Sigma). Prior to examination, the samples underwent gold coating using a sputter coater and were subsequently observed under the FESEM machine.

7.3 RESULTS AND DISCUSSIONS

This section of the thesis illustrates various outcomes pertaining to the characterization of the developed hybrid green composites.

7.3.1 Bamboo Micro Particle Characterization

Density- The density of bamboo biomass as measured as 0.201 gm/cm^3. After the bamboo biomass was converted into bamboo micro particles, the density was measured as 0.245 gm/cm^3. A study by Cai et al. [263] reveals that natural particles/fiber contain non-cellulose substance polysaccharides that are low-molecular-weight and form amorphous, random, and breached structures; removing these nanocellulose components could result in a higher particle density.

Morphological Analysis- The thermo-mechanical properties of the developed composites were primarily influenced by two key factors: the particle size and morphology of the reinforcing material. An examination of the morphology of treated bamboo micro particles was conducted using a scanning electron microscope (SEM), and **Fig. 7.3** (a) illustrates the observed morphology. Natural biofillers often face challenges in achieving effective interfacial interaction with the matrix. However, chemical treatment appears to enhance interfacial interaction by creating a rougher surface for the biofiller. To assess the size distribution of the prepared particles, the SEM image was imported into ImageJ software, enabling the measurement of particle sizes. **Fig. 7.3** (b) depicts the particle size distribution and normal distribution curve for treated bamboo micro particles. The average particle size was determined to be 18.50 μm, with a standard deviation of 10.097 and a median value of 16.67 μm. The range of particle sizes varied, with maximum and minimum values observed at 43.63 μm and 3.90 μm, respectively.

XRD-The effects of alkaline treatments on the crystalline properties of extracted bamboo micro

TH-3447_196103002

particles were examined using X-ray diffractometry (XRD). The XRD pattern of both bamboo biomass and treated bamboo micro particles is illustrated in **Fig. 7.3** (c). Analysis of the XRD pattern revealed three prominent peaks for both treated and untreated particles, located at 2θ = 15.8°, 22.3°, and 35.8°, corresponding to the crystalline planes of (1 1 0), (2 0 0), and (0 0 4), respectively [221, 230] These peaks are attributed to the presence of cellulose within bamboo micro particles in the β phase. The untreated biomass exhibited a crystalline index of 50.17%, whereas the treated particles demonstrated a higher crystalline index of 61.53%. Furthermore, alkaline treatment for surface modification increased the crystalline size of the particles from 3.22 to 3.74 nm.

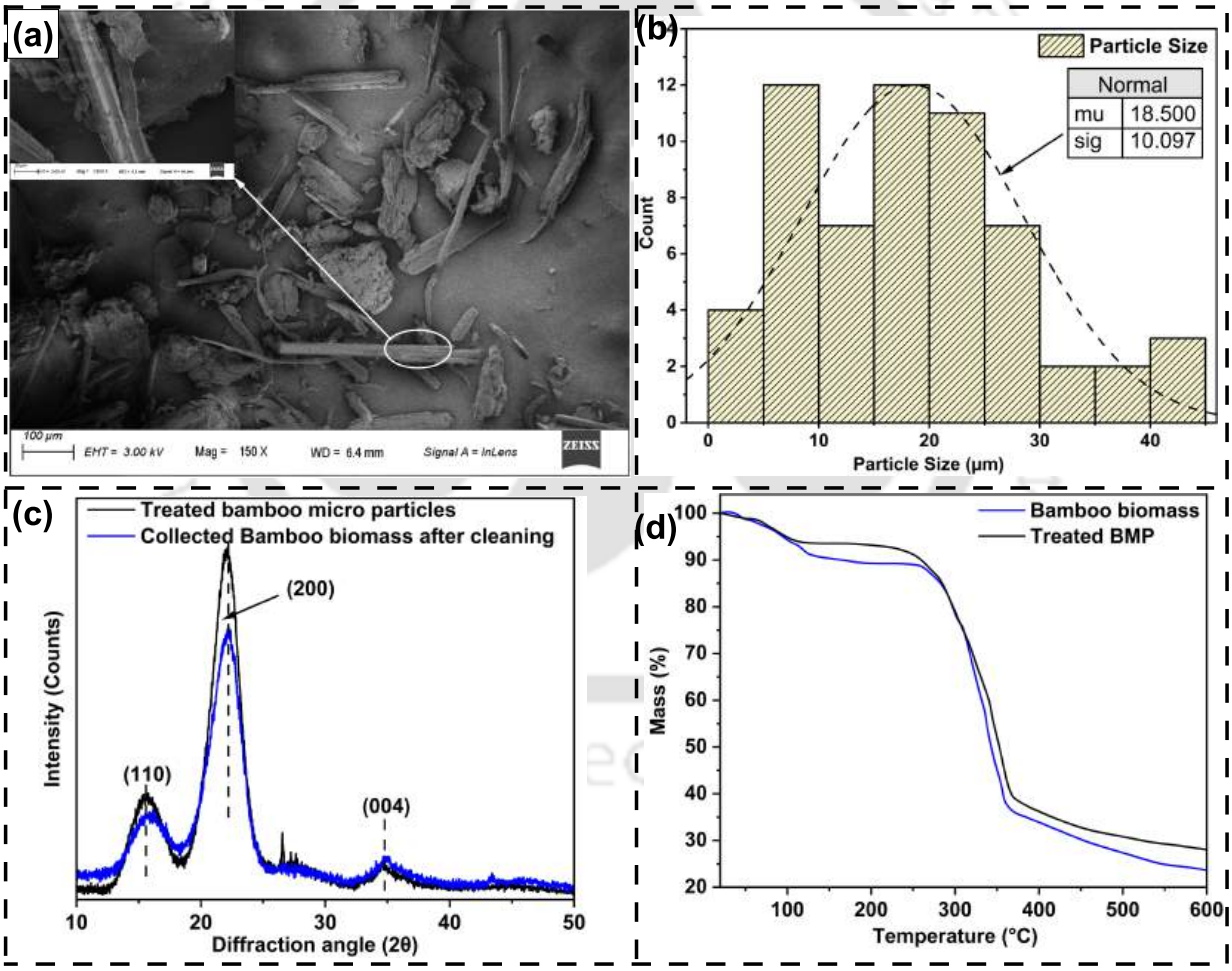

Fig. 7.3: (a) SEM image of treated BMP; (b) particle size distribution for treated BMP; (c) XRD pattern; (d) TGA thermogram for bamboo biomass and treated BMP.

TH-3447_196103002

TGA- Thermo-gravimetric analysis (TGA) was conducted to assess the impact of alkalization on the thermal stability and degradation of bamboo particles. **Fig. 7.3** (d) displays the thermogram for both treated and untreated bamboo particles. The thermal stability was evaluated by analyzing weight loss at four different temperature stages. The degradation temperature details for untreated and treated particles are presented in **Table 7.2**.

The initial stage of weight loss occurred between 25° and 150°C, reflecting the loss of moisture present in the bamboo particles. Subsequently, the second stage of weight loss was observed between 151°C and 250°C, attributed to the evaporation of extractives, wax, and other impurities. Following this, the temperature range of 251°C to 380°C corresponded to the weight loss due to cellulose degradation, while the fourth stage, occurring between 381°C and 600°C, indicated the degradation of major lignin and high crystalline cellulose. The alkaline treatment of extracted bamboo particles led to the conversion of cellulose-I into a more thermally stable and higher crystalline structure known as cellulose-II [230, 309]. Consequently, treated particles exhibited enhanced thermal stability and reduced weight loss at elevated temperatures. The chemical treatment also affected positively on activation energy of micro particles. The bamboo biomass shows activation energy of 21.316 J/mol-K , whereas BMP shows acitivation energy of 22.574 J/mol-K. This increment of 5.56% is due to cellulose modification during chemical treatment.

Table 7.2: Mass loss in thermogravimetric analysis for bamboo micro particle.

Composite sample	Stage-I weight loss (%)	Stage-II weight loss (%)	Stage-III weight loss (%)	Stage-IV weight loss (%)	Residual mass (%)
*BB	9.55	1.746	60.56	32.83	23.54
**BMP	6.56	2.48	59.45	28.13	28.03

*BB- Bamboo biomass,**BMP- Bamboo micro particle

7.3.2 Characteristic Analysis of Hybrid Green Composite

Density and Void Content- The analysis of density and void content in the developed hybrid composite has been conducted. Both the theoretical and experimental density of the developed hybrid green composites have been explored and are presented in **Table 7.3**. The investigation re-

TH-3447_196103002

vealed a consistent reduction in the overall density of the hybrid green composite with an increasing addition of bamboo micro particles. This phenomenon is likely attributed to the lower density of bamboo micro particles compared to the bio-epoxy matrix. The BFHC_0 green composite exhibited the maximum experimental density at 1.064 gm/cm^3, while the BFHC_10 green hybrid composite demonstrated the minimum experimental density at 0.796 gm/cm^3. Discrepancies between theoretical and experimental densities in the developed green composite were observed, and this disparity is manifested as the void content in the developed green composites [221].

Table 7.3: Density and void contents of developed hybrid green composites.

Sample code	Theoretical density gm/cm^3	Theoretical density gm/cm^3	Void content (%)
BFHC_0	1.064	1.042	2.070
BFHC_2.5	0.981	0.962	1.984
BFHC_5	0.911	0.895	1.754
BFHC_7.5	0.850	0.830	2.265
BFHC_10	0.796	0.772	3.021

The presence of voids within the material poses a critical challenge. Consequently, these voids serve as points for crack nucleation, leading to a decline in the performance of the developed biocomposites. A relationship of inverse proportionality has been identified between void content and the weight fraction of bamboo micro particles in the developed green composites. The BFHC_0 green composite exhibited the maximum void content, while the BFHC_5 biocomposite reported the minimum void content. The incorporation of bamboo particles improved the interfacial bonding among fibers, fillers, and the matrix, thereby reducing void content. However, BFHC_7.5 and BFHC_10 biocomposites displayed a higher void percentage due to particle agglomeration and cauterization at higher filler loading percentages with the matrix, as detailed in references [220].

Water Absorption Test- In **Fig. 7.4**, the water absorption behavior of the developed green composites is depicted. The analysis indicates that with an increase in the number of immersion days, the percentage of water absorption also increases, eventually reaching saturation after 600

TH-3447_196103002

hrs.

The BFHC_5 green composite demonstrated the least water absorption behavior. The introduction of bamboo micro particles up to 5% weight fraction decrease the water absorption tendencies of the biocomposites. Addition of micro particle resulted better interfacial interaction between bamboo fiber and bio-epoxy results less moister absoption. The BFHC_10 hybrid green composite exhibited the maximum water absorption, primarily due to the elevated bamboo particle content (more than 5 wt.%) and suboptimal interfacial bonding between the matrix and reinforcement. The occurrence of agglomeration and insufficient bonding between reinforcements and the matrix led to the formation of micro-level gaps, fostering capillary action and resulting in heightened water absorption.

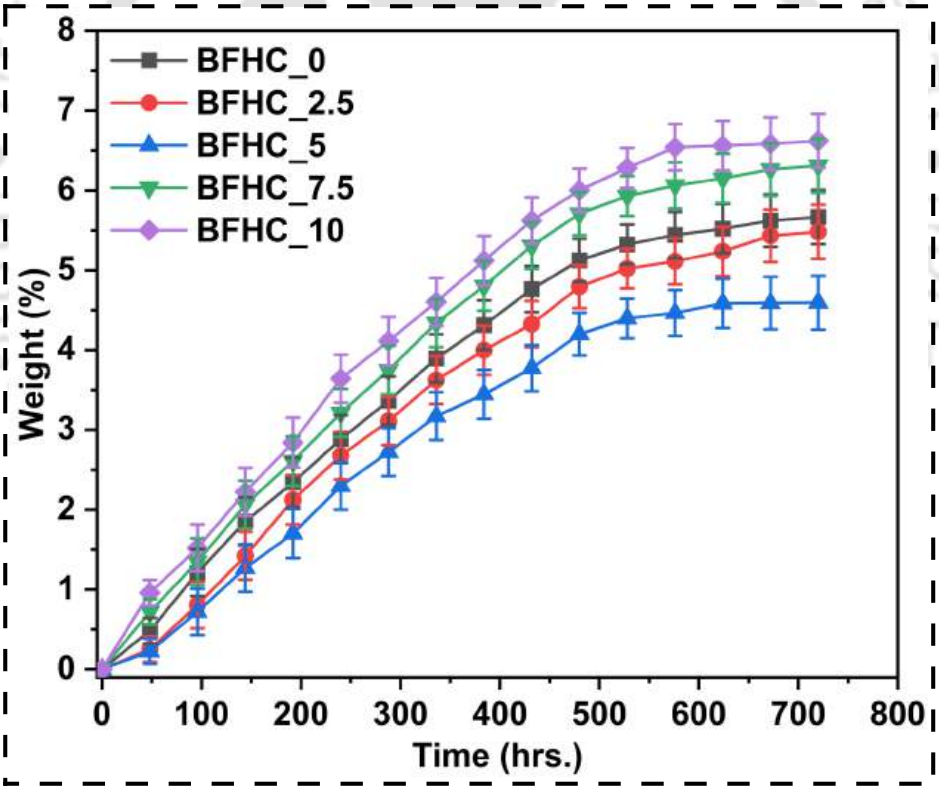

Fig. 7.4: Result for moisture absorption properties of hybrid green composites.

Tensile Properties- In order to assess the strength and stiffness of the developed hybrid green composites, a tensile test was conducted. **Fig. 7.5** (a) illustrates the tensile stress–strain curve of the developed green composites, which exhibited linear behavior up to failure without any plastic deformation. The tensile properties, including strength, and modulus are presented in **Fig. 7.5** (b).

TH-3447_196103002

The incorporation of bamboo micro particles up to a 5% weight fraction enhanced tensile strength and tensile modulus compared to BFHC_0 green composites. This improvement is attributed to the addition of particles into fiber-reinforced composites, resulting in an increase in the crystalline index of the polymeric green composite. The crystalline index of green composite showing a directly proportional relation with the bamboo particle weight fraction. The maximum tensile strength was observed in the BFHC_5 hybrid green composite (163.17 ± 6.44 MPa), which is 12.72% higher than BFHC_0 green composite. The highest tensile modulus was examined in BFHC_5 hybrid green composites (7.65 ± 1.264 GPa), representing a 33.74% increase over BFHC_0 green composite. However, a further increase in particle reinforcement percentage (for 7.5 and 10 wt.%) led to a decrease in tensile strength and modulus due to agglomeration and inefficient bonding between reinforcement and the bioepoxy matrix [217, 221, 293].

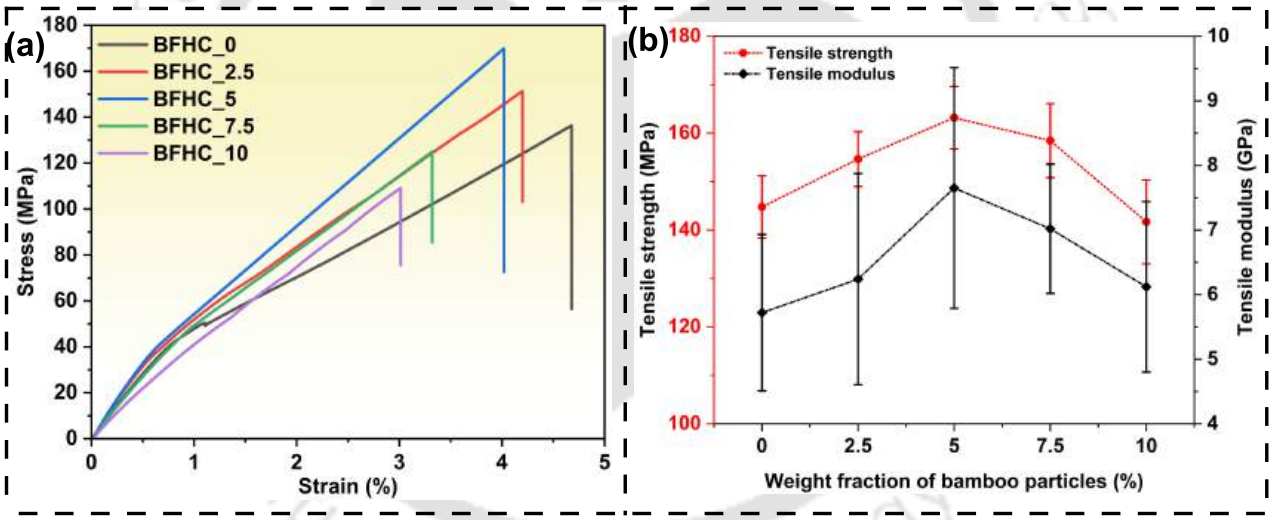

Fig. 7.5: (a) Tensile stress-strain curve, (b) variation of tensile properties with weight fraction of bamboo micro particles.

Flexural Properties- The flexural properties of the hybrid green composites were determined through the utilization of the three-point bending test. In **Fig. 7.6** (a), the flexural stress–strain curves of the developed green composites depict a linear behavior leading up to failure, characterized by level buckling and an absence of plastic deformations. In contrast to the tensile strength and tensile modulus, the flexural strength and flexural modulus exhibit a direct correlation with the weight percentage of bamboo particles.

TH-3447_196103002

Fig. 7.6 (b) illustrates the flexural strength and flexural modulus of the developed green composites under the influence of varying bamboo particle concentrations. The BFHC_5 hybrid green composites exhibit the highest reported flexural strength at 144.26 ± 4.44 MPa, and the maximum flexural modulus is observed at 7.33 ± 1.06 GPa. These values surpass those of the nonhybrid BFHC_0 green composites by 19.79% and 16.9%, respectively.

The introduction of bamboo micro-particles, in conjunction with fibers, enhances the interfacial interaction between the reinforcing materials and the bio-epoxy matrix. This improved interaction results in enhanced stress transfer mechanisms, leading to an overall increase in the strength and modulus of the green composites. However, when bamboo particles exceed 5 wt.%, excessive clustering occurs between the particles and the bio-epoxy, leading to agglomeration and an increased stress concentration factor. Consequently, this excessive particle addition contributes to a decrement in the flexural properties of the developed green composites.

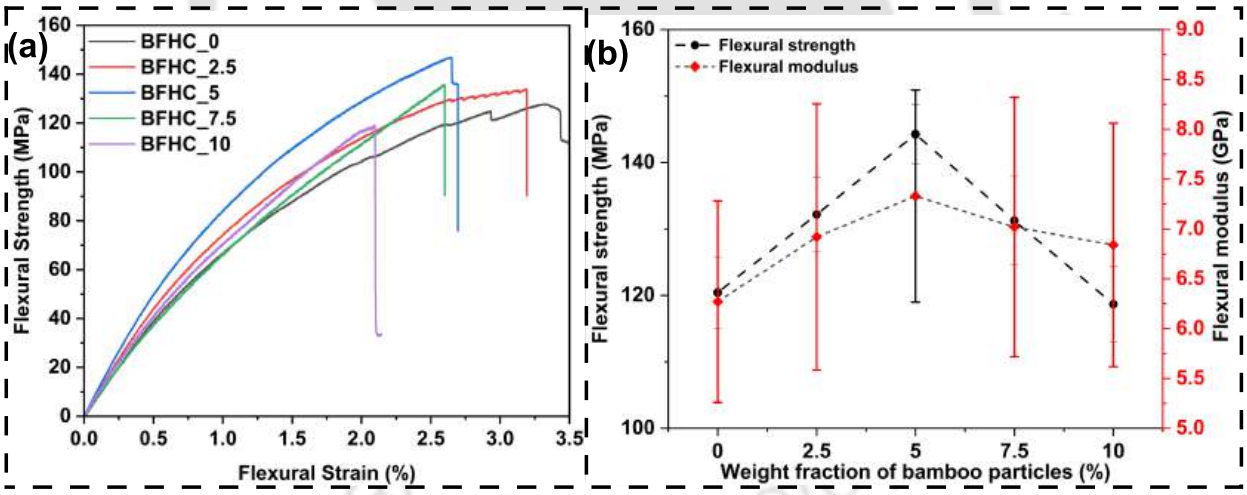

Fig. 7.6: (a) Flexural stress-strain curve, (b) variation of flexural properties with weight fraction of bamboo micro particles.

Impact Strength- The impact strength or energy absorption capability of a material is a crucial attribute [215]. In this study, the impact strength of the developed green composite was assessed through the Charpy impact test, as illustrated in **Fig. 7.7**. The BFHC_5 hybrid green composite exhibited the highest reported impact strength at 64.52 ± 5.97 kJ/m^2, representing a 12.07% increase compared to the non-hybrid BFHC_0 green composite. The incorporation of micro-particles into the green composite improved the wettability between the matrix and reinforcement, facilitat-

TH-3447_196103002

ing efficient stress transmission within the hybrid composite. Consequently, the shock absorption capacity of the green composite was enhanced.

However, when the weight fraction of bamboo particles exceeded 5 wt.%, the clustering of bamboo particles occurred [221],leading to a reduction in the impact strength of the developed green composites.

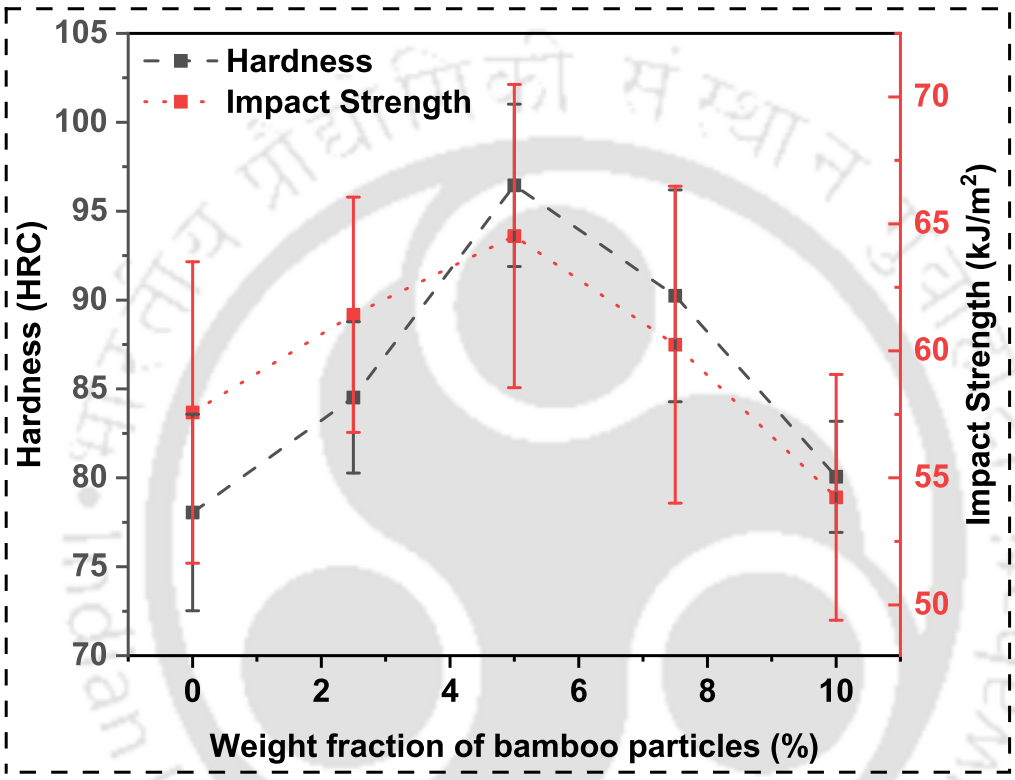

Fig. 7.7: Variation of impact strength and hadrness with weight fraction of bamboo weight fraction.

Hardness- Hardness refers to a material's resistance to localized plastic deformation. The surface hardness of the developed hybrid green composite was examined and is depicted in **Fig. 7.7**. The incorporation of bamboo micro-particles, up to 5% by weight, augmented the resistance to localized plastic deformation in the developed hybrid green composites. This enhancement can be attributed to improved interfacial bonding among fibers, particles, and the bio-epoxy matrix. The maximum hardness value was recorded for BFHC_5 hybrid green composites at 78.05, surpassing the non-hybrid BFHC_0 green composites by 23.57%. The addition of micro-bamboo particles in the bamboo fiber–reinforced bio-epoxy green composite contributed to increased indentation resistance, thereby enhancing the Shore-D hardness value. However, in the cases of BFHC_7.5 and

TH-3447_196103002

BFHC_10 hybrid green composites, excessive particle loading led to a reduction in hardness due to decreased in binding strength between the matrix and reinforcing materials.

DMA- The dynamic characteristics of both developed hybrid and non-hybrid composites were examined to elucidate their viscoelastic response under oscillatory deformations. Such investigations prove highly effective in discerning the molecular arrangements and the mobility of molecular distributions within composite materials, particularly concerning the impact of time, frequency, and temperatures. As the BFHC_5 type of green composite exhibited superior mechanical properties, the storage modulus (E'), viscous modulus (G'), and damping factor ($\tan\delta$) were analyzed under the influence of temperature for the BFHC_5 type of green hybrid composite and BFHC_0 type of green non-hybrid composite.

The storage modulus (E') measures the elastic deformation and stiffness during each cycle of oscillation for the developed hybrid composites. In **Fig. 7.8** (a), the storage modulus variation with temperature (25–150°C) is illustrated for both hybrid and non-hybrid composites. The introduction of particulates elevated the modulus values within the epoxy matrix, demonstrating that incorporating bamboo particles into bamboo fiber-reinforced biocomposites resulted in a higher storage modulus compared to non-hybrid bamboo fiber polymer composites. This enhancement is attributed to the larger contact surfaces of bamboo particles, potentially enhancing bonding with the matrix materials [350]. The storage modulus for BFHC_5 type of hybrid composites was recored as 9.29 GPa, which is 5.38% higher than non-hybrid BFHC_0 composite (8.81 GPa).

Initially, at lower temperatures (ambient temperature), both composites exhibited higher storage modulus values, attributed to a closely packed structure between the reinforcement and matrix materials. As the temperature transitions from the glassy region to the transition region, the storage modulus experiences a significant decrease due to temperature-induced effects on molecular chains, leading to a reduction in the stiffness of the developed composites. Conversely, no substantial changes were recorded in the rubbery region, where accelerated polymeric chain mobility occurs at higher temperatures [351]. The observation clearly indicates that the incorporation of bamboo micro-particles induces significant changes in the storage modulus (E') within the glassy and transition regions, while no discernible change is observed in the rubbery region [352].

TH-3447_196103002

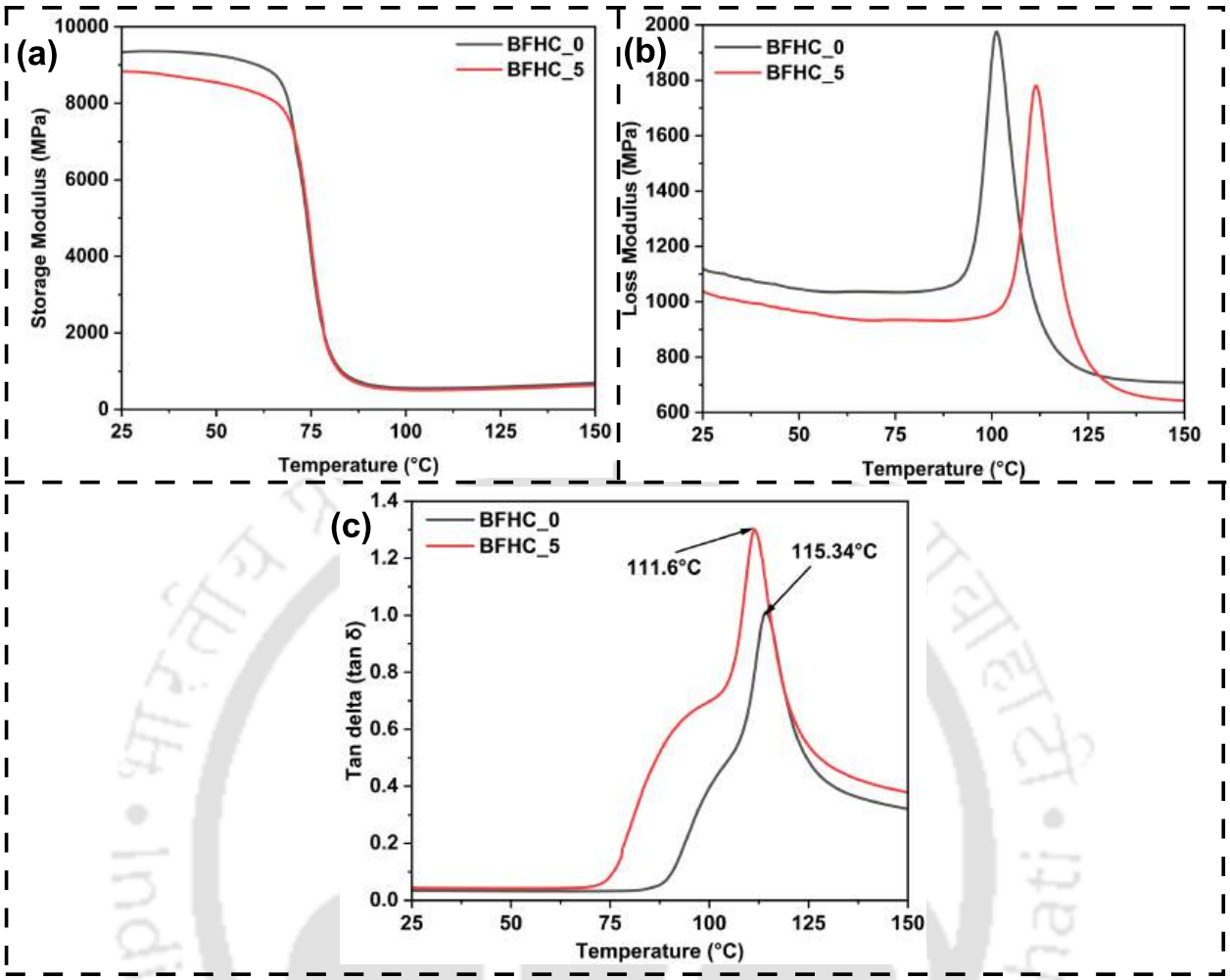

Fig. 7.8: (a) Storage modulus, (b) loss modulus and (c) damping factor for hybrid and non-hybrid composites.

The viscous modulus (G''), also known as the loss modulus, quantifies the released heat energy per cycle, typically associated with the viscous response and internal friction of the materials [353]. **Fig. 7.8** (b) shows viscous modulus with the variation of temperature (25–150°C) for both hybrid and non-hybrid composites.

The increase in temperature is linked to the viscous response of the materials, characterized by observed molecular motion and structural heterogeneity. With rising temperature, the loss modulus exhibits a consistent trend in the glassy region. The maximum value is attained in the glass transition region for both composites, followed by a significant decline to the lowest values in the rubbery region. The recorded loss moduli for BFHC_5 and BFHC_0 were 1.12 GPa and 1.04 GPa, respectively. The even distribution of bamboo filler augmented the friction among particles

TH-3447_196103002

within the bio-epoxy matrix [300], resulting in an enhanced loss modulus for the hybrid composite compared to the non-hybrid bamboo fiber-reinforced polymer (BFHC_0).

The damping factor ($\tan\delta$) is calculated as the ratio of the viscous modulus to the storage modulus and depends on the adhesion between reinforcements and matrix [354]. **Fig. 7.8** (c) presents the damping factor and glass transition temperature (T_g) for the developed hybrid and no-hybrid composites, showcasing variations in temperature (20–150°C).

The dynamic characteristics of composites are contingent on the mobility of polymer chains and the interaction between fillers and polymer chains. Restrictions on polymer chain movement enhance the storage modulus at lower temperatures, whereas the viscous movement of polymer chains at the glass transition temperature leads to an increase in the viscous modulus [355]. The glass transition temperature (T_g) was determined from the $\tan\delta$ curve, representing the transition between the glassy state and the rubbery state [352]. The findings indicate that an increase in T_g corresponds to a decrease in the peak height of the $\tan\delta$ curve, indicating a reduction in the mobility of polymer chains. The hybrid composite BFHC_5 exhibited a lower damping factor (1.00) coupled with a maximum glass transition temperature (T_g) of 115.34°C. In contrast, BFHC_0 displayed a higher damping factor (1.29) with a minimum Tg of 111.6°C. This disparity can be attributed to the interaction between polymer and filler, which restricts polymer chain mobility, leading to an increase in the glass transition temperature and a reduction in the damping factor of the developed composites.

TGA- Thermogravimetric analysis (TGA) was conducted to assess the thermal stability of both the developed hybrid and non-hybrid green composites. BFHC_0 represents the non-hybrid material, and BFHC_5 given the superior mechanical properties, TGA was specifically performed on BFHC_0 and BFHC_5 types of green composites.

In **Fig. 7.9**, the mass loss of green composite is depicted at elevated temperatures. Additional mass loss properties have been analyzed and are presented in **Table 7.4**. The incorporation of particulates alongside bamboo fiber had a beneficial impact on the thermal stability of biocomposite. Notably, the BFHC_5 hybrid green composite exhibited reduce weight loss and higher residuals at 800°C, attributed to the impediment of heat passage, resulted delaying mass loss.

TH-3447_196103002

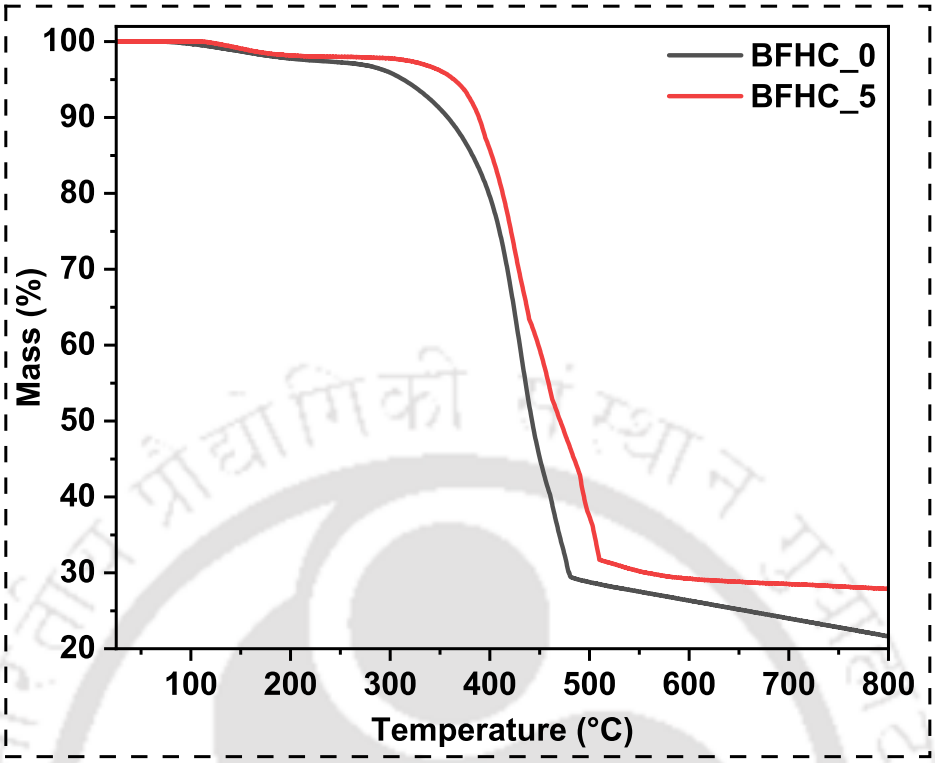

Fig. 7.9: Thermogram for hybrid and non-hybrid green composites.

Table 7.4: Thermogravimetric analysis of non-hybrid and hybrid green composite.

Sample code	IDT (°C)	MRDT (°C)	T_{50} (°C)	Final residue (%)
BFHC_0	73.75	432.56	441.25	21.65
BFHC_5	111.92	451.67	467.92	27.88

Analysis of Surface Morphology- Field emission scanning electron microscopy (FESEM) was employed to examine the distribution of bamboo particles and the fracture morphology of the newly developed hybrid green composite. The primary objective of the analysis was to ascertain the surface morphology, distribution, and scattering characteristics of bamboo particles within the developed hybrid green composites, as illustrated in **Fig. 7.10**.

Fig. 7.10 (a) depicts the representation of the BFHC_2.5 green composite type, showcasing the arrangement of bamboo micro particles within the polymer matrix. A uniform distribution of micro particles is evident in the green composite sample. Moving on to **Fig. 7.10** (b), it illustrates the

TH-3447_196103002

BFHC_5 composite type, emphasizing the interfacial interaction between micro particles and the bio matrix. **Fig. 7.10** (c) displays the fracture surface of the BFHC_5 composite resulting from tensile failure, while **Fig. 7.10** (d) presents the fractural morphology of bending failure for BFHC_5.

All analyzed biocomposites exhibit brittle fracture without plastic deformation of fibers, displaying a linear stress behavior. Failures primarily stem from breakage, pull-out, crushing, debonding, and level buckling of bamboo fibers. **Fig. 7.10** (e) captures a failure sample from impact testing, while **Fig. 7.10** (f) represents the agglomeration of particles at a higher weight fraction (10 wt.%) in the BFHC_10 composite.

7.4 COMPARATIVE STUDY

In contemporary times, the widespread utilization of naturally derived biocomposites and green composites have gained prominence across diverse industrial and engineering applications. This popularity is attributed to their abundant availability, lighter weight, lower cost, renewability, compatibility, and eco-friendliness. Such composites offer not only economically viable alternatives but also versatile and pragmatic solutions for diminishing reliance on petroleum-based products, substituting them with cost-effective bio-products. **Table 7.5** presents a comparative analysis of naturally derived green composites, outlining their mechanical and physical properties.

7.5 SUMMERY

Hybrid green composites were developed through the reinforcement of bamboo fiber and bamboo micro particles with a bio-epoxy matrix, employing the compression molding technique. Initially, the chemico-physical characterization of the extracted bio-filler was conducted. Subsequently, five distinct types of green composites were developed, with variations in the weight fraction of bamboo particles. The physical, mechanical, and thermal properties of the resultant green composites were systematically examined, leading to the following conclusions:

TH-3447_196103002

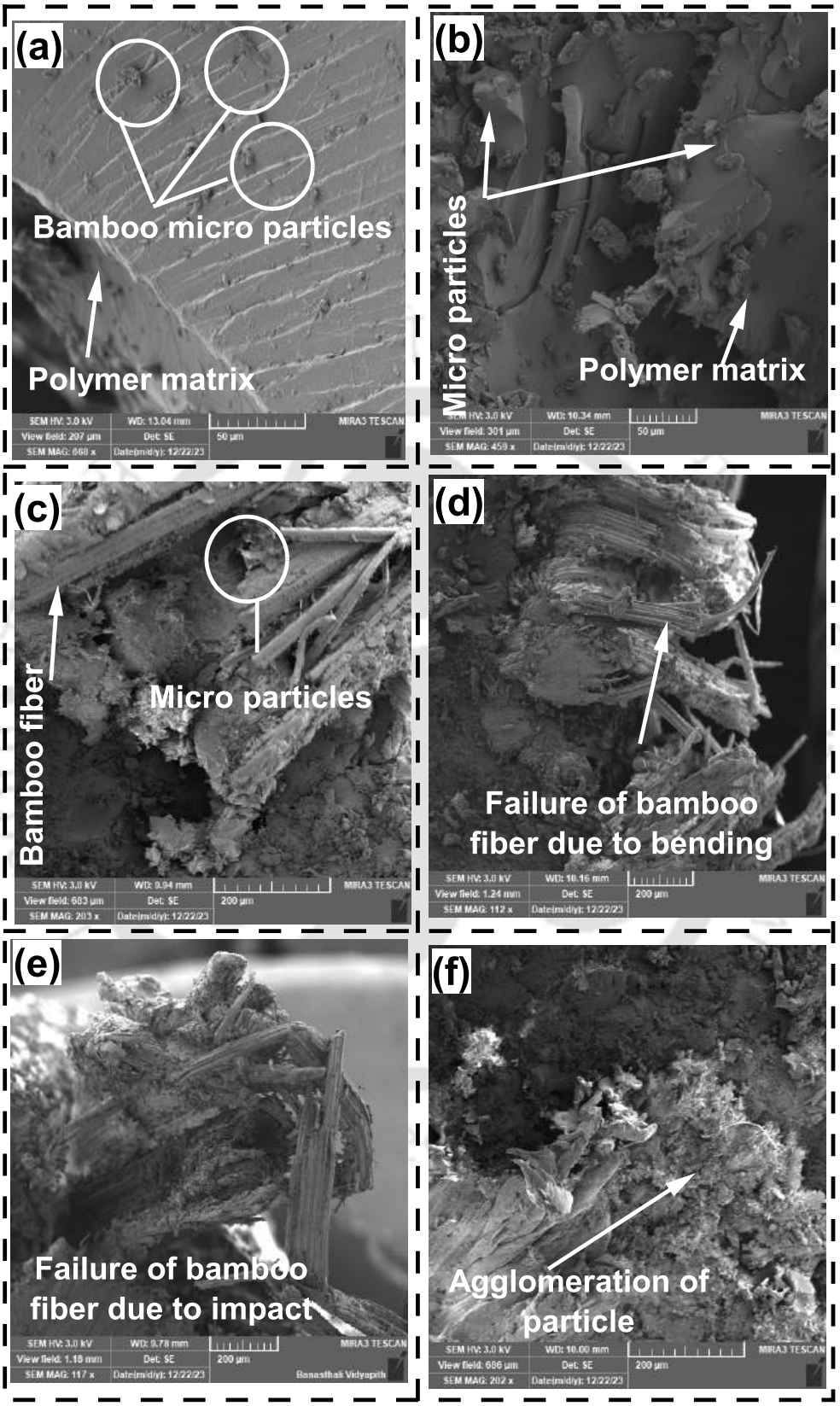

Fig. 7.10: SEM image of different hybrid green composites.

TH-3447_196103002

TH-3447_196103002

Table 7.5: Comparative study of mechanical characteristics in newly developed green Composite with composites presented in literature.

Matrix	Reinforcement-I	Reinforcement-II	Tensile strength (MPa)	Tensile Modulus (GPa)	Flexural strength (MPa)	Flexural modulus (GPa)	Impact Strength/ energy	Moister absorption (%)	Reference
Formulite 2501A+ 2401B	Bamboo fiber	Bamboo particle	163.17	7.65	144	7.33	64.52kJ/m^2	4.59	Present study
Vinyl esters	Coconut particles	nano clay	72.6	3.8	186.42	—	2.7 kJ/m^2	11.62	[356]
SR greenpoxy 56	Hemp fiber	Sisal fiber	30.76	1.095	—	—	—	11.86	[357]
Epoxy resin	Sisal fiber	—	43.32	1.64	86.6	1.78	10 kJ/m^2	—	[358]
SR green poxy 56	Hemp fiber	–	33.30	2.893	60.56	2.860	19.19 kJ/m^2	–	[264]
Epoxy	Bamboo fiber	Coconut particle	62.42	2.685	58.79	3.624	—	—	[359]
Epoxy	Flax fiber	Hemp fiber	46.41	—	134.28	—	21.107 J/m	4.48	[360]
Polyvinyl chloride	coconut fiber	corn cub ash	51.42	3.12	48.96	3.8	98.42J/m^2	—	[361]
Epoxamite 100	Flax	glass	241.2	10.5	140.8	0.364	—	—	[362]
Epoxy LY-556	Hemp fiber	flax fiber	84.67	4.4	11.413	134.663	—	5.06	[293]
Polyester	Flax	—	74.61	—	18.35	—	6.7 J	2.43	[363]
Epoxy LY556	PALF	PALF particles	89.432	3.032	103.521	4.521	87.56 J/m	70	[221]
Formulite 2501A +2401B	Coconut fiber	Coir particle	142.46	5.366	151.451	7.451	88.41 J/m	6.25	[364]

1. Successful conversion of bamboo biomass into valuable bamboo micro particles for reinforcing the polymer matrix has been achieved.

2. The chemical treatment process has led to an increased density of bamboo micro particles compared to bamboo biomass.

3. Chemical treatment has effectively removed lignin and other impurities from bamboo biomass, resulting in an elevated crystallinity index.

4. Thermal stability of bamboo micro particles has been improved through chemical treatment.

5. The incorporation of bamboo micro particles into bamboo fiber-reinforced polymer composites has resulted in a reduction in overall density and moisture absorption.

6. The addition of micro particles has positively influenced the mechanical properties of green hybrid composites.

7. The BFHC_5 type of green hybrid composites exhibited the maximum mechanical properties.

8. Bio filler additions exceeding 5wt.% caused agglomeration, leading to increased stress concentration factors and subsequently lower mechanical properties.

9. Hybridization has raised the glass transition temperature of the composite.

10. The storage modulus, loss modulus, and tan delta values have experienced positive effects through hybridization with bamboo micro particles.

11. The comparative study of the results highlights the significant potential of the developed materials for various engineering applications.

TH-3447_196103002

Chapter 8

Conclusions

8.1 CHAPTERWISE SYNOPTIC CONCLUSIONS FROM THE PRESENT WORK

This research successfully extracted bamboo fibers from the inner, middle, and outer parts of the Bambusa tulda bamboo culm and investigated their potential as reinforcing materials in bio-composites. The external technical fibers (ETF) were found to be more compact, stronger, and larger in diameter compared to middle (MTF) and internal technical fibers (ITF), making ETF more suitable for reinforcement. Chemical treatment with NaOH revealed that a 6% concentration optimized the physical, mechanical, and thermal properties of the fibers. These treated fibers exhibited higher tensile strength, modulus, and thermal stability while reducing water absorption due to increased crystallinity. Bio-composites developed with these treated fibers showed significant improvements in mechanical and thermal properties, particularly at a 30% fiber weight fraction. The composites exhibited enhanced tensile strength, flexural strength, hardness, impact strength, and thermal stability compared to untreated composites. Additionally, the developed bio-composites demonstrated lower moisture absorption and higher crystallinity, indicating better performance for practical applications. The study also explored the use of hybrid bio-composites with bamboo fibers and particles, finding that a 5% particle addition positively impacted mechanical performance. The research concludes that the developed bio-composites, especially those with treated fibers, are promising materials for various industrial applications, including automobile interiors, packaging, and construction, potentially boosting the rural agro-based economy in India. The major outcomes of this research work are encapsulated below:

1. Bamboo fiber has been successfully extracted from the internal, middle and outer parts of

TH-3447_196103002

the bamboo culm of *Bambusa tulda* bamboo and their potential as reinforcing materials in bio-composite has been investigated. The following conclusion has been drawn from the above experimental investigation.

- As a result of the structural investigation and FESEM micro graphs, it was observed that the external technical fibers (ETF) were made of finer single fibers compared to the middle and internal technical fibers. This helped to make ETF more compact and stronger.
- Due to compact structure, the diameter of ETF is also greater than internal technical fiber (ITF) and middle technical fiber (MTF). ETF showed a larger technical fiber diameter compared to the other two types of fibers.
- According to FTIR results, all three types of technical fibers exhibited similar bonding, but from an analysis of the chemical composition, ETF had higher amount of lignin and cellulose, whereas the lower amount of moisture, extractive, and hemicellulose content compare to MTF and ITF.
- Due to higher cellulose content ETF also shows higher crystalline index, about 7.5% and 18.78% higher than MTF and ITF. In comparison of other two kinds of technical fibers, ETF also has larger crystalline size.
- The mechanical properties of ETF were found more superior to ITF and MTF. The tensile strength of ETF was found 31.46% and 59.47% higher than ITF and MTF fiber. Additionally, ETF showed 24.35% and 41.52% higher tensile modulus than ITF and MTF.
- Due to higher crystalline size ETFs exhibit lower water absorption properties and higher thermal stability compared to other technical fibers.

The *Bambusa tulda* is one of the major natural resources and agricultural products available in northeast India (especially in the Assam region). The extraction and use of bamboo fiber as a reinforcing material of bio-composite may motivate micro and small industries

TH-3447_196103002

to develop a bio-based economy and boost up Indian rural agro-based economy. Moreover, it is concluded that due to higher cellulose content, higher crystallinity index, crystalline size, better mechanical strength and stiffness, lower water absorption properties and higher thermal stability, the external technical fibers are more suitable reinforcing material compare to middle and internal technical fibers. However, MTF and ITF are suitable for use in home decoration and textile industries.

2. The bamboo fiber has been successfully extracted from *Bambusa tulda* and chemical treatment of the fiber has been done successfully. The different characterizations have been performed on treated as well as untreated bamboo fiber. Based on the results of the characterization, the following conclusions can be drawn:

    - The chemical treatment of bamboo fiber has been carried out with five different NaOH concentrations (2, 4, 6, 8 and 10%) and 6% was found to provide the best physical, mechanical, and thermal properties.
    - FTIR results confirm that non-crystalline materials like hemicellulose and lignin have been removed by chemical treatment. Due to the removal of non-crystalline materials, the overall crystallinity index has been increased. (BF_6)
    - Chemical treatment affected the mechanical properties of the fiber positively. In comparison with the untreated fiber (BF_0), the 6% NaOH treated fiber (BF_6) exhibited 42.09% higher tensile strength and 75.71% modulus. The chemical treatment increases the surface roughness of the fiber, which further increases the interfacial bonding strength between bio-epoxy and the fiber.
    - However, treatments with more than 6% NaOH concentration removed cellulose from fiber surfaces, reducing the crystallinity index and mechanical properties of the fiber.
    - Chemical treatment up to 6% NaOH concentration successfully removed the lignin and hemicellulose from bamboo fibers as observed through XPS analyses (X-ray Photoelectron Spectroscopy). Hydrophilic fibers became hydrophobic after amorphous (lignin, and hemicellulose) has been removed.

TH-3447_196103002

Since the fibers treated with 6% NaOH concentration showed higher thermomechanical properties, they are further used to develop bio-composites.

3. Bio-composites have been developed with untreated and differently treated bamboo fibers, and different characterizations have been performed on developed composites. Based on the results of the characterization, the following conclusions can be drawn:

   - The bio-composites have been developed with fiber weight fractions of 10, 20, 30, and 40% and different mechanical tests were conducted on each. The mechanical properties of bio-composites with fiber fractions exceeding 30% were degraded. So, further studies have been conducted with fiber weight fractions of 30%.
   - Chemical treatments with NaOH concentrations of up to 6% had a positive effect on bio-composites' mechanical properties. As compared to BFBC_30_0 composites, BFBC_30_6 composites have a 50% increase in tensile strength, 36.6% increase in tensile modulus, 58.28% increase in flexural strength, 36.63% increase in flexural modulus, 31.08% increase in hardness value, and 32.56% increase in impact strength.
   - As NaOH concentration increased (up to 6%), not only mechanical properties but also thermal stability of the bio-composites increased. Bio-composites reinforced with chemically treated fibers have a lower moisture absorption capacity and mass loss due to biodegradability.
   - The developed bio-composites with treated fiber showed a higher crystallinity index compared to untreated fiber reinforced composites. The maximum crystallinity index has been recorded as 51.73% with BFBC_30_6 types of bio-composites. The treatment with more than 6%, i.e., 8 and 10% NaOH concentration degraded the crystalline cellulose from the fiber and resulted in a decrement in the crystallinity index.
   - A similar types of bonding peaks are observed for all types of developed bio-composites, which indicated that the functional groups present in the bio-epoxy and the bio-composites are similar.

TH-3447_196103002

- The maximum increment in tensile strength and modulus values are observed for BFBC_30_6 types of composites. The fiber with 8 and 10% NaOH treatment shows a decrement in dynamic mechanical values. The maximum storage modulus and glass transition temperature have been observed as 8378 MPa and 105.16 °C for BFBC_30_6 types of composites.
- The chemical treatment made the fiber hydrophobic, resulting in lower dielectric constants, loss factor, and AC conductivity values. The treatment with more than 6% NaOH concentration degraded the cellulose from fiber surface and makes the fiber hydrophilic again. Therefore, fiber reinforced bio-composites treated with NaOH at 8 and 10% exhibit increased dielectric properties and AC conductivity. The maximum dielectric constant and loss factor has been recorded as 67.89 and 3.79, respectively.

Compared to the previously reported bio-composites in the literature, the developed composites are better in terms of thermal, mechanical, dielectric and physical properties. In future, a production line will be set up to manufacture bio-composites by using *Bambusa tulda* and bio-epoxy for commercial purposes. As a result, micro and small industries based on the agro-economy will be developed in rural India.

4. Bamboo fiber-based bio-composite with four different epoxy matrices has been successfully developed and their static, dynamic mechanical, physical and thermal properties have been analysed. Moreover, a multicritical decision-making technique called VIKOR has been employed to determine the best material for automobile interior applications within the developed four kinds of bio-composites. The major findings of the study are summarised below:

   - The density of the material is the crucial parameter for choosing lightweight material. S1 and S3 types of composites showed the lowest and highest densities respectively among the developed materials, whereas minimum and maximum void content has been reported for S3 (1.2 %) and S4 (4.1 %) types of composites, respectively.
   - Moisture absorption is one of the drawbacks for natural fiber reinforced bio-composites.

TH-3447_196103002

The interfacial gap between fiber and matrix acts as capillary action and absorbs moisture. The maximum and minimum moisture absorption, as well as thickness swelling, have been observed for S4 and S2 types of composites respectively.

- The maximum tensile strength has been reported for S2 types of composites with a numeric value of 144.75 ± 4.40 MPa whereas the maximum Young's modulus is reported for S1 (6.98 ± 0.19 GPa) types of composites.
- The maximum flexural strength has been observed for S1 types of composites. The sequence for flexural strength is S1>S2>S3>S4. The maximum hardness and maximum impact strength has been noted for S3 and S2 kinds of composites.
- For storage modulus and loss modulus value, the maximum was reported for S2 types of composites whereas S2 types of composites showed the lowest tan δ value. The glass transition temperature for the S2 types of composites was reported as 111.72 °C.
- In the thermal analysis of developed composites, S2 types are showed maximum thermal stability and S4 types degraded their mass rapidly with temperature. Based on the Indian market, S4 types of composites have the lowest development cost of Rs. 2340 and S1 composites have the highest development cost of Rs. 4650 among all four types of composites.
- The best materials in the VIKOR material selection procedure were chosen as S2 types of composites, and the poorest materials were chosen as S3 types of composites. Additionally, a sensitivity analysis of the process revealed its robustness.

Therefore, the S2 types of composite is the suitable material for automobile industry applications, especially for semi-structural and interior application.

5. Bio-composites reinforced with bamboo fibers and bamboo particles has been developed and their thermo-mechanical and physical characteristics have been examined. The following conclusion has been drawn from the above experimental investigation.

   - The addition of bamboo particles up to 5% impacted positively on the mechanical per-

TH-3447_196103002

formances of the developed bio-composites. BFHC_5 bio-composite observed maximum tensile strength (163.17 MPa) and flexural strength (144.26 MPa) tensile modulus (7.65 GPa) and flexural modulus (7.33 GPa). The maximum degradation temperature has been recorded at 350.47 °C for BFHC_5 bio-composites with better thermal stability.

- The addition of particles restricted the elongation before the break and improved the brittleness of the bio-composites. Therefore, BFHC_2.5 bio-composites exhibits higher impact strength (88.41 J/m). The developed bio-composites showed comparatively less water absorption behavior as compared to other natural fiber composites due to the presence of high ligno-cellulose contents.
- The excessive addition of bamboo particles (more than 5% by weight) resulted in the agglomeration and clusterization with the bio-epoxy matrix. This resulted in a decrement in thermo-mechanical behaviours.

Thus, the utilization of waste from bamboo particles has great potential to develop sustainable and eco-friendly bio-composites and could lead to the development of a bio-based economy and boost the agro-based rural Indian economy. Furthermore, the developed bio-composites are also capable and suitable for industrial applications like automobile interior parts, packaging industries to develop delivery boxes, construction industry, and development of wind turbine blades and solar cell back sheets.

8.2 CONTRIBUTIONS OF THE THESIS

The noteworthy contributions of the doctoral thesis in addressing challenges associated with the use of sustainable green composites for structural applications hold considerable engineering significance. The experimental investigation of bamboo fiber and its reinforced green composite plates has encountered obstacles attributable to influential factors like the fiber extraction process, chemical treatment parameters for the fiber, fiber loading, and others. The significant and novel contributions of the thesis are as follows:

1. The present work employed *Bambusa tulda* bamboo for fiber extraction process. This partic-

TH-3447_196103002

ular bamboo species is abundant in North East India, representing an underexplored resource with notably higher cellulose content.

2. A significant challenge associated with natural fibers is their inherent variability in properties. Functional gradation of bamboo may be the one of the major reasons for this deviation for bamboo fiber. In addressing this issue, the current research employed a classified extraction technique and compellingly identified external technical fibers as the most suitable candidates for reinforcing biocomposites.

3. Natural fibers exhibit bad interfacial interaction with polymers. Alkalization with different NaOH concentrated solution increase this interfacial interaction. The present study focused on optimizing the concentration of NaOH solution to achieve the best thermomechanical properties for *Bambusa tulda* fiber as well as its reinforced biocomposites

4. In this research, the loading percentage of *Bambusa tulda* fiber in the biocomposite was systematically optimized to attain superior thermo-mechanical and physical properties for the biocomposite.

5. The green composites has been developed with optimized chemically treated *Bambusa tulda* fiber reinforcement loading. This study presents the benchmark thermo-mechanical results of the developed green composites.

6. In this research, the impact of NaOH treatment concentration on the physical, mechanical, structural, thermal, and dielectric properties of biocomposites was systematically explored and presented.

7. This research investigated the influence of various bio based and commercial matrix materials on diverse properties of biocomposites.

8. The present study a Multiple Attribute Decision Making (MADM) technique, VIKOR, was utilized to choose the optimal materials among the developed bio and green composites intended for automobile interior applications.

TH-3447_196103002

9. The current experimental analysis introduces a green composite with an impressive 61.78% bio content, marking one of the highest levels of bio content reported in the existing literature on green composites.

10. This study introduced a hybrid green composite incorporating continuous bamboo fiber and bamboo micro particles, exhibiting improved thermo-mechanical properties and achieving a remarkable bio content of 54.67%.

8.3 FUTURE SCOPE OF WORK

The future studies based on this work can be in following aspects:

- The present experimental investigation can be extended to develop bigger samples like: beam or plate structure for household and real life structural application.
- To obtain analytical solution for the bamboo based bio composites under static load condition
- To obtain low cycle fatigue life of bamboo based green composites.
- The present bamboo fiber and epoxy based material can be developed by employed by different composites manufacturing technique, like- VARTM etc.
- To develop short bamboo fiber and PLA based composites using 3-D printing for complex geometry.
- To develop bamboo mat based epoxy composites and investigate their thermo-mechanical and dynamic mechanical properties.

TH-3447_196103002

Bibliography

[1] Wang Wenfeng, Ge Jing, Yu Xiangyang, and Li Hui. Environmental fate and impacts of microplastics in soil ecosystems: Progress and perspective. *Science of the total environment*, **708**:134841, 2020.

[2] Arif Zia Ullah, Khalid Muhammad Yasir, Sheikh Muhammad Fahad, Zolfagharian Ali, and Bodaghi Mahdi. Biopolymeric sustainable materials and their emerging applications. *Journal of Environmental Chemical Engineering*, **10**(4):108159, 2022.

[3] Kopparthy Sripathi Dev Sharma and Netravali Anil N. Green composites for structural applications. *Composites Part C: Open Access*, **6**:100169, 2021.

[4] Moharir Rucha V and Kumar Sunil. Challenges associated with plastic waste disposal and allied microbial routes for its effective degradation: a comprehensive review. *Journal of Cleaner Production*, **208**:65–76, 2019.

[5] Dicker Michael PM, Duckworth Peter F, Baker Anna B, Francois Guillaume, Hazzard Mark K, and Weaver Paul M. Green composites: A review of material attributes and complementary applications. *Composites part A: applied science and manufacturing*, **56**:280–289, 2014.

[6] Shanmugam Vigneshwaran, Mensah Rhoda Afriyie, Försth Michael, Sas Gabriel, Restás Ágoston, Addy Cyrus, Xu Qiang, Jiang Lin, Neisiany Rasoul Esmaeely, Singha Shuvra, and others . Circular economy in biocomposite development: State-of-the-art, challenges and emerging trends. *Composites Part C: Open Access*, **5**:100138, 2021.

TH-3447_196103002

[7] Mensah Rhoda Afriyie, Shanmugam Vigneshwaran, Narayanan Sreenivasan, Razavi Nima, Ulfberg Adrian, Blanksvärd Thomas, Sayahi Faez, Simonsson Peter, Reinke Benjamin, Försth Michael, and others . Biochar-added cementitious materials—a review on mechanical, thermal, and environmental properties. *Sustainability*, **13**(16):9336, 2021.

[8] Guru Kumar Manjappara Subramanian M. Balasubramanian and Kumar A. Arul Jeya. A review on the mechanical properties of natural fiber reinforced compressed earth blocks. *Journal of Natural Fibers*, **19**(14):7687–7701, 2022.

[9] Li Haibin, Liu Songjiang, Yang Fan, He Siyu, Jing Hongjun, Zou Xiaolong, Li Zhigang, and Sheng Yanping. Review of utilization of bamboo fiber in asphalt modification: insights into preparation, performance, reinforcement, and challenges. *Journal of Cleaner Production*, **19**: 143010, 2024.

[10] Gao Xun, Zhu Deju, Fan Shutong, Rahman Md Zillur, Guo Shuaicheng, and Chen Feng. Structural and mechanical properties of bamboo fiber bundle and fiber/bundle reinforced composites: A review. *Journal of Materials Research and Technology*, **19**:1162–1190, 2022.

[11] Mohammed Khalid, Zulkifli Rozli, Tahir Mohd Faizal Mat, and Gaaz Tayser Sumer. A study of mechanical properties and performance of bamboo fiber/polymer composites. *Results in Engineering*, **19**:102396, 2024.

[12] Faruk Omar, Bledzki Andrzej K, Fink Hans-Peter, and Sain Mohini. Biocomposites reinforced with natural fibers: 2000–2010. *Progress in polymer science*, **37**(11):1552–1596, 2012.

[13] Rangappa Sanjay Mavinkere and Siengchin Suchart. Natural fibers as perspective materials. *Applied Science and Engineering Progress*, **11**(4), 2018.

[14] Sanjay MR, Arpitha GR, Naik L Laxmana, Gopalakrishna K, and Yogesha BJNR. Applications of natural fibers and its composites: an overview. *Natural Resources*, **7**(3):108–114, 2016.

TH-3447_196103002

[15] Komuraiah A, Kumar N Shyam, and Prasad B Durga. Chemical composition of natural fibers and its influence on their mechanical properties. *Mechanics of composite materials*, **50**:359–376, 2014.

[16] Thyavihalli Girijappa Yashas Gowda, Mavinkere Rangappa Sanjay, Parameswaranpillai Jyotishkumar, and Siengchin Suchart. Natural fibers as sustainable and renewable resource for development of eco-friendly composites: a comprehensive review. *Frontiers in Materials*, **6**: 226, 2019.

[17] Li Mi, Pu Yunqiao, Thomas Valerie M, Yoo Chang Geun, Ozcan Soydan, Deng Yulin, Nelson Kim, and Ragauskas Arthur J. Recent advancements of plant-based natural fiber–reinforced composites and their applications. *Composites Part B: Engineering*, **200**:108254, 2020.

[18] Rangappa Sanjay Mavinkere, Siengchin Suchart, Parameswaranpillai Jyotishkumar, Jawaid Mohammad, and Ozbakkaloglu Togay. Lignocellulosic fiber reinforced composites: Progress, performance, properties, applications, and future perspectives. *Polymer Composites*, **43**(2): 645–691, 2022.

[19] Graupner Nina and Müssig J. Technical applications of natural fibres: An overview. *Industrial applications of natural fibres: structure, properties and technical applications*, **1**:73–86, 2010.

[20] Zakikhani P, Zahari R, Sultan MTH, and Majid DL. Bamboo fibre extraction and its reinforced polymer composite material. *Int. J. Chem. Biomol. Metall. Mater. Sci. Eng*, **8**(4): 271–274, 2014.

[21] Bahari Shahril Anuar and Krause Andreas. Utilizing malaysian bamboo for use in thermoplastic composites. *Journal of Cleaner Production*, **110**:16–24, 2016.

[22] Qin Li, Wen-Ji Yu, and Yang-lun Yu. Research on properties of reconstituted bamboo lumber made by thermo-treated bamboo bundle curtains. *Forest Products Journal*, **62**(7-8):545–550, 2012.

TH-3447_196103002

[23] Lobovikov Maxim, Ball Lynn, and Guardia María. *World bamboo resources: a thematic study prepared in the framework of the global forest resources assessment 2005*. Number 18. Food and Agriculture Org., 2007.

[24] Khalil HPS Abdul, Bhat IUH, Jawaid M, Zaidon A, Hermawan D, and Hadi YS. Bamboo fibre reinforced biocomposites: A review. *Materials and Design*, **42**:353–368, 2012.

[25] Liu Dagang, Song Jianwei, Anderson Debbie P, Chang Peter R, and Hua Yan. Bamboo fiber and its reinforced composites: structure and properties. *Cellulose*, **19**:1449–1480, 2012.

[26] Mousavi Seyed Rasoul, Zamani Mohammad Hossein, Estaji Sara, Tayouri Mohammad Iman, Arjmand Mohammad, Jafari Seyed Hassan, Nouranian Sasan, and Khonakdar Hossein Ali. Mechanical properties of bamboo fiber-reinforced polymer composites: a review of recent case studies. *Journal of Materials Science*, **57**(5):3143–3167, 2022.

[27] Imadi Sameen Ruqia, Mahmood Isra, and Kazi Alvina Gul. Bamboo fiber processing, properties, and applications. *Biomass and Bioenergy: Processing and Properties*, **14**:27–46, 2014.

[28] Prang Rocky Bahrum and Thompson Amanda J. Investigation and comparison of antibacterial property of bamboo plants, natural bamboo fibers and commercial bamboo viscose textiles. *The Journal of The Textile Institute*, **112**(7):1159–1170, 2021.

[29] Prasad Vemu Vara and Kumar Mattam Lava. Chemical resistance and tensile properties of bamboo and glass fibres reinforced epoxy hybrid composites. *Int J Mater Biomat Appl*, **1**: 17–20, 2011.

[30] Schulgasser K and Witztum A. On the strength, stiffness and stability of tubular plant stems and leaves. *Journal of theoretical biology*, **155**(4):497–515, 1992.

[31] Amada Shigeyasu, Munekata Tamotsu, Nagase Yukito, Ichikawa Yoshinobu, Kirigai Atsushi,

TH-3447_196103002

and Zhifei Yang. The mechanical structures of bamboos in viewpoint of functionally gradient and composite materials. *Journal of Composite Materials*, **30**(7):800–819, 1996.

[32] Wegst Ulrike GK, Bai Hao, Saiz Eduardo, Tomsia Antoni P, and Ritchie Robert O. Bioinspired structural materials. *Nature materials*, **14**(1):23–36, 2015.

[33] Mannan Sayyad, Paul Knox J, and Basu Sumit. Correlations between axial stiffness and microstructure of a species of bamboo. *Royal Society open science*, **4**(1):160412, 2017.

[34] Dixon Patrick G and Gibson Lorna J. The structure and mechanics of moso bamboo material. *Journal of the Royal Society Interface*, **11**(99):20140321, 2014.

[35] Gibson Lorna J. The hierarchical structure and mechanics of plant materials. *Journal of the royal society interface*, **9**(76):2749–2766, 2012.

[36] Suzuki Kiyoshi and Itoh Takao. The changes in cell wall architecture during lignification of bamboo, phyllostachys aurea carr. *Trees*, **15**:137–147, 2001.

[37] Gritsch Cristina Sanchis and Murphy Richard J. Ultrastructure of fibre and parenchyma cell walls during early stages of culm development in dendrocalamus asper. *Annals of botany*, **95**(4):619–629, 2005.

[38] Cousins WJ. Elastic modulus of lignin as related to moisture content. *Wood science and technology*, **10**(1):9–17, 1976.

[39] Cousins WJ. Young's modulus of hemicellulose as related to moisture content. *Wood science and technology*, **12**(3):161–167, 1978.

[40] Xie Jiulong, Hse Chung-Yun, Shupe Todd F, Pan Hui, and Hu Tingxing. Extraction and characterization of holocellulose fibers by microwave-assisted selective liquefaction of bamboo. *Journal of Applied Polymer Science*, **133**(18), 2016.

TH-3447_196103002

[41] IR HUNTER. Bamboo resources, uses and trade: the future? *J Bamboo Rattan*, **2**:1–19, 2002.

[42] Biswas Subhankar, Ahsan Qumrul, Cenna Ahmed, Hasan Mahbub, and Hassan Azman. Physical and mechanical properties of jute, bamboo and coir natural fiber. *Fibers and Polymers*, **14**:1762–1767, 2013.

[43] Nayak Lopamudra and Mishra Siba Prasad. Prospect of bamboo as a renewable textile fiber, historical overview, labeling, controversies and regulation. *Fashion and Textiles*, **3**(1):2, 2016.

[44] Osorio Lina, Trujillo E, Van Vuure Aart Willem, and Verpoest Ignace. Morphological aspects and mechanical properties of single bamboo fibers and flexural characterization of bamboo/epoxy composites. *Journal of reinforced plastics and composites*, **30**(5):396–408, 2011.

[45] Sugesty Susi, Kardiansyah Teddy, and Hardiani Henggar. Bamboo as raw materials for dissolving pulp with environmental friendly technology for rayon fiber. *Procedia Chemistry*, **17**:194–199, 2015.

[46] Pinho Eva, Henriques Mariana, Oliveira Rosário, Dias Alberto, and Soares Graça. Development of biofunctional textiles by the application of resveratrol to cotton, bamboo, and silk. *Fibers and Polymers*, **11**:271–276, 2010.

[47] Yao Jian, Bastiaansen Cees WM, and Peijs Ton. High strength and high modulus electrospun nanofibers. *Fibers*, **2**(2):158–187, 2014.

[48] Zou Linhua, Jin Helena, Lu Wei-Yang, and Li Xiaodong. Nanoscale structural and mechanical characterization of the cell wall of bamboo fibers. *Materials Science and Engineering: C*, **29**(4):1375–1379, 2009.

[49] Kang Jun Tae and Kim Seong Hun. Improvement in the mechanical properties of polylactide

TH-3447_196103002

and bamboo fiber biocomposites by fiber surface modification. *Macromolecular Research*, **19**: 789–796, 2011.

[50] Kuromi Yosuke, Sato Taku, Ando Hitoshi, Matsumoto Yuka, Oda Keiko, Ito Eiji, Ichikawa Masahiro, Watanabe Tadashi, Sakuma Jun, and Saito Kiyoshi. Removal of bamboo fragments transorbitally penetrated into the cerebellum and temporal lobe 30 years after the injury. *No Shinkei geka. Neurological Surgery*, **40**(11):979–983, 2012.

[51] Yu Hongqin and Yu Chongwen. Study on microbe retting of kenaf fiber. *Enzyme and microbial technology*, **40**(7):1806–1809, 2007.

[52] Lin JS, Wang X, and Lu G. Crushing characteristics of fiber reinforced conical tubes with foam-filler. *Composite Structures*, **116**:18–28, 2014.

[53] Yu Yanglun, Huang Xianai, and Yu Wenji. A novel process to improve yield and mechanical performance of bamboo fiber reinforced composite via mechanical treatments. *Composites Part B: Engineering*, **56**:48–53, 2014.

[54] Correia Viviane da Costa, Santos dos Valdemir, Sain Mohini, Santos Sergio Francisco, Leao Alcides Lopes, and Savastano Junior Holmer. Grinding process for the production of nanofibrillated cellulose based on unbleached and bleached bamboo organosolv pulp. *Cellulose*, **23**: 2971–2987, 2016.

[55] Hamdi Hédi, Zahouani Hassan, and Bergheau Jean-Michel. Residual stresses computation in a grinding process. *Journal of materials processing technology*, **147**(3):277–285, 2004.

[56] Erdumlu Nazan and Ozipek Bulent. Investigation of regenerated bamboo fibre and yarn characteristics. *Fibres and Textiles in Eastern Europe*, **16**(4):69, 2008.

[57] Li Ming-Fei, Sun Shao-Ni, Xu Feng, and Sun Run-Cang. Microwave-assisted organic acid

TH-3447_196103002

extraction of lignin from bamboo: Structure and antioxidant activity investigation. *Food chemistry*, **134**(3):1392–1398, 2012.

[58] Fu Jiajia, Yang Xuexia, and Yu Chongwen. Preliminary research on bamboo degumming with xylanase. *Biocatalysis and Biotransformation*, **26**(5):450–454, 2008.

[59] Manalo Allan C, Wani Evans, Zukarnain Noor Azwa, Karunasena Warna, and Lau Kin-tak. Effects of alkali treatment and elevated temperature on the mechanical properties of bamboo fibre–polyester composites. *Composites Part B: Engineering*, **80**:73–83, 2015.

[60] Jonoobi Mehdi, Oladi Reza, Davoudpour Yalda, Oksman Kristiina, Dufresne Alain, Hamzeh Yahya, and Davoodi Reza. Different preparation methods and properties of nanostructured cellulose from various natural resources and residues: a review. *Cellulose*, **22**:935–969, 2015.

[61] Amada Shigeyasu and Untao Sun. Fracture properties of bamboo. *Composites Part B: Engineering*, **32**(5):451–459, 2001.

[62] Castanet Erwan, Li Quanxiang, Dumee Ludovic F, Garvey Christopher, Rajkhowa Rangam, Zhang Jin, Rolfe Bernard, and Magniez Kevin. Structure–property relationships of elementary bamboo fibers. *Cellulose*, **23**:3521–3534, 2016.

[63] Okubo Kazuya, Fujii Toru, and Yamamoto Yuzo. Development of bamboo-based polymer composites and their mechanical properties. *Composites Part A: Applied science and manufacturing*, **35**(3):377–383, 2004.

[64] Phong Nguyen Tien, Fujii Toru, Chuong Bui, and Okubo Kazuya. Study on how to effectively extract bamboo fibers from raw bamboo and wastewater treatment. *Journal of Materials Science Research*, **1**(1):144, 2012.

[65] Rohit Kiran and Dixit Savita. A review-future aspect of natural fiber reinforced composite. *Polymers from Renewable Resources*, **7**(2):43–59, 2016.

TH-3447_196103002

[66] Li Xue, Tabil Lope G, and Panigrahi Satyanarayan. Chemical treatments of natural fiber for use in natural fiber-reinforced composites: a review. *Journal of Polymers and the Environment*, **15**:25–33, 2007.

[67] Hamideh Hajiha Mohini Sain and Mei Lucia H. Modification and characterization of hemp and sisal fibers. *Journal of Natural Fibers*, **11**(2):144–168, 2014.

[68] Tonoli Gustavo Henrique Denzin, Mendes Rafael F, Siqueira Gilberto, Bras Julien, Belgacem Mohamed N, and Savastano Jr Holmer. Isocyanate-treated cellulose pulp and its effect on the alkali resistance and performance of fiber cement composites. *Holzforschung*, **67**(8):853–861, 2013.

[69] Kaushik Vijay K, Kumar Anil, and Kalia Susheel. Effect of mercerization and benzoyl peroxide treatment on morphology, thermal stability and crystallinity of sisal fibers. *International Journal of Textile Science*, **1**(6):101–105, 2012.

[70] George Michael, Mussone Paolo G, Alemaskin Kirill, Chae Michael, Wolodko John, and Bressler David C. Enzymatically treated natural fibres as reinforcing agents for biocomposite material: mechanical, thermal, and moisture absorption characterization. *Journal of materials science*, **51**:2677–2686, 2016.

[71] Mesquita Ricardo Gabriel de Almeida, César Antônia Amanda da Silva, Mendes Rafael Farinassi, Mendes Lourival Marin, Marconcini José Manoel, Glenn Greg, and Tonoli Gustavo Henrique Denzin. Polyester composites reinforced with corona-treated fibers from pine, eucalyptus and sugarcane bagasse. *Journal of Polymers and the Environment*, **25**:800–811, 2017.

[72] Puchot Laura. *Cardanol: a bio-based building block for new sustainable and functional materials*. PhD thesis, Cergy-Pontoise, 2016.

TH-3447_196103002

[73] Mohammed Layth, Ansari Mohamed NM, Pua Grace, Jawaid Mohammad, Islam M Saiful, and others . A review on natural fiber reinforced polymer composite and its applications. *International journal of polymer science*, **2015**, 2015.

[74] Gholampour Aliakbar and Ozbakkaloglu Togay. A review of natural fiber composites: Properties, modification and processing techniques, characterization, applications. *Journal of Materials Science*, **55**(3):829–892, 2020.

[75] Jaafar Jamiluddin, Siregar Januar Parlaungan, Mohd Salleh Salwani, Mohd Hamdan Mohd Hazim, Cionita Tezara, and Rihayat Teuku. Important considerations in manufacturing of natural fiber composites: a review. *International Journal of Precision Engineering and Manufacturing-Green Technology*, **6**:647–664, 2019.

[76] Lotfi Amirhossein, Li Huaizhong, Dao Dzung Viet, and Prusty Gangadhara. Natural fiber–reinforced composites: A review on material, manufacturing, and machinability. *Journal of Thermoplastic Composite Materials*, **34**(2):238–284, 2021.

[77] Khan Tabrej, Hameed Sultan Mohamed Thariq Bin, and Ariffin Ahmad Hamdan. The challenges of natural fiber in manufacturing, material selection, and technology application: A review. *Journal of Reinforced Plastics and Composites*, **37**(11):770–779, 2018.

[78] Pandey Jitendra K, Ahn SH, Lee Caroline S, Mohanty Amar K, and Misra Manjusri. Recent advances in the application of natural fiber based composites. *Macromolecular materials and engineering*, **295**(11):975–989, 2010.

[79] Singh Manoj Kumar, Tewari Renu, Zafar Sunny, Rangappa Sanjay Mavinkere, and Siengchin Suchart. A comprehensive review of various factors for application feasibility of natural fiber-reinforced polymer composites. *Results in Materials*, **17**:100355, 2023.

[80] Maurya Atul Kumar and Manik Gaurav. Advances towards development of industrially

TH-3447_196103002

relevant short natural fiber reinforced and hybridized polypropylene composites for various industrial applications: a review. *Journal of Polymer Research*, **30**(1):47, 2023.

[81] Clyne Trevor William and Hull Derek. *An introduction to composite materials*. Cambridge university press, 2019.

[82] Faruk Omar, Bledzki Andrzej K, Fink Hans-Peter, and Sain Mohini. Progress report on natural fiber reinforced composites. *Macromolecular Materials and Engineering*, **299**(1): 9–26, 2014.

[83] Rajak Dipen Kumar, Pagar Durgesh D, Menezes Pradeep L, and Linul Emanoil. Fiber-reinforced polymer composites: Manufacturing, properties, and applications. *Polymers*, **11** (10):1667, 2019.

[84] Leny Mathew and Narayanankutty Sunil K. *Development of Elastomeric Hybrid Composite Based on Synthesised Manosilica and Short Nylon Fiber*. PhD thesis, Cochin University of Science and Technology, 2009.

[85] TRANSACTIONS I PHILOSOPHICAL. of the royal society of london. *Series B*, **318**:1–107, 1914.

[86] Shackelford James F. *Introduction to materials science for engineers*. Pearson Upper Saddle River, 2016.

[87] Keya Kamrun N, Kona Nasrin A, Koly Farjana A, Maraz Kazi Madina, Islam Md Naimul, and Khan Ruhul A. Natural fiber reinforced polymer composites: history, types, advantages and applications. *Materials Engineering Research*, **1**(2):69–85, 2019.

[88] Saheb D Nabi and Jog Jyoti P. Natural fiber polymer composites: a review. *Advances in Polymer Technology: Journal of the Polymer Processing Institute*, **18**(4):351–363, 1999.

TH-3447_196103002

[89] Lila Manish Kumar, Komal Ujendra Kumar, Singh Yashvir, and Singh Inderdeep. Extraction and characterization of munja fibers and its potential in the biocomposites. *Journal of Natural Fibers*, **19**(7):2675–2693, 2022.

[90] Lila Manish Kumar, Saini Gaurav Kumar, Kannan M, and Singh Inderdeep. Effect of fiber type on thermal and mechanical behavior of epoxy based composites. *Fibers and Polymers*, **18**:806–810, 2017.

[91] Chawla Krishan K. *Composite materials: science and engineering*. Springer Science and Business Media, 2012.

[92] Donald IW and McMillan PW. Ceramic-matrix composites. *Journal of materials Science*, **11**:949–972, 1976.

[93] Zheng SR, Wang RM, and Zheng Y George. Polymer matrix composites and technology, 2011.

[94] Bajpai Pramendra K and Singh Inderdeep. *Reinforced polymer composites: Processing, characterization and post life cycle assessment*. John Wiley and Sons, 2019.

[95] Fu Shao-Yun, Hu Xiao, and Yue Chee-Yoon. Effects of fiber length and orientation distributions on the mechanical properties of short-fiber-reinforced polymers a review. *Journal of the Society of Materials Science, Japan*, **48**(6Appendix):74–83, 1999.

[96] Prashanth S, Subbaya KM, Nithin K, and Sachhidananda S. Fiber reinforced composites-a review. *J. Mater. Sci. Eng*, **6**(03):2–6, 2017.

[97] Kurtyka Pawel and Rylko Natalia. Quantitative analysis of the particles distributions in reinforced composites. *Composite Structures*, **182**:412–419, 2017.

[98] Deepak Verma Kheng Lim Goh and Vimal Vrince. Interfacial studies of natural fiber-

TH-3447_196103002

reinforced particulate thermoplastic composites and their mechanical properties. *Journal of Natural Fibers*, **19**(6):2299–2326, 2022.

[99] Jawaid MHPS and Khalil HPS Abdul. Cellulosic/synthetic fibre reinforced polymer hybrid composites: A review. *Carbohydrate polymers*, **86**(1):1–18, 2011.

[100] Nunna Srinivas, Chandra P Ravi, Shrivastava Sharad, and Jalan AK. A review on mechanical behavior of natural fiber based hybrid composites. *Journal of Reinforced Plastics and Composites*, **31**(11):759–769, 2012.

[101] Zini Elisa and Scandola Mariastella. Green composites: an overview. *Polymer composites*, **32**(12):1905–1915, 2011.

[102] Muhammad Adamu, Rahman Md Rezaur, Hamdan Sinin, and Sanaullah Khairuddin. Recent developments in bamboo fiber-based composites: a review. *Polymer bulletin*, **76**:2655–2682, 2019.

[103] Liu Lifang, Wang Qianli, Cheng Longdi, Qian Jingfang, and Yu Jianyong. Modification of natural bamboo fibers for textile applications. *Fibers and Polymers*, **12**:95–103, 2011.

[104] Cao Shilin, Ma Xiaojuan, Lin Ling, Huang Fang, Huang Liulian, and Chen Lihui. Morphological and chemical characterization of green bamboo (dendrocalamopsis oldhami (munro) keng f.) for dissolving pulp production. *BioResources*, **9**(3):4528–4539, 2014.

[105] Zakikhani Parnia, Zahari Rizal, Sultan Mohamed Thariq bin Haji Hameed, and Majid Dayang Laila Abang Abdul. Morphological, mechanical, and physical properties of four bamboo species. *BioResources*, **12**(2):2479–2495, 2017.

[106] Zhang Yamei, Yu Yanglun, Yu Wenji, and others . Effects of internal structure and chemical compositions on the hygroscopic property of bamboo fiber reinforced composites. *Applied Surface Science*, **492**:936–943, 2019.

TH-3447_196103002

[107] Depuydt Delphine EC, Soete Jeroen, Asfaw Yalew D, Wevers Martine, Ivens Jan, and Van Vuure Aart W. Sorption behaviour of bamboo fibre reinforced composites, why do they retain their properties? *Composites Part A: Applied Science and Manufacturing*, **119**:48–60, 2019.

[108] Wang Fuli and Shao Zhuoping. Study on the variation law of bamboo fibers' tensile properties and the organization structure on the radial direction of bamboo stem. *Industrial crops and products*, **152**:112521, 2020.

[109] Adel Salih Abeer, Zulkifli Rozli, and Azhari Che Husna. Tensile properties and microstructure of single-cellulosic bamboo fiber strips after alkali treatment. *Fibers*, **8**(5):26, 2020.

[110] Chiu Hsuan-Hao and Young Wen-Bin. The longitudinal and transverse tensile properties of unidirectional and bidirectional bamboo fiber reinforced composites. *Fibers and Polymers*, **21**:2938–2948, 2020.

[111] Sánchez Martha L, Patino William, and Cardenas Jhon. Physical-mechanical properties of bamboo fibers-reinforced biocomposites: Influence of surface treatment of fibers. *Journal of Building Engineering*, **28**:101058, 2020.

[112] Hassan Mohamad Zaki, Roslan Siti Amni, Sapuan SM, Rasid Zainudin A, Mohd Nor Ariff Farhan, Md Daud Mohd Yusof, Dolah Rozzeta, and Mohamed Yusoff Mohd Zuhri. Mercerization optimization of bamboo (bambusa vulgaris) fiber-reinforced epoxy composite structures using a box–behnken design. *Polymers*, **12**(6):1367, 2020.

[113] Macedo Lucélia Alves, Rousset Patrick Louis Albert, and Vale Ailton Teixeira. Influência da composição da biomassa no rendimento em condensáveis da torrefação de resíduos vegetais. *Pesquisa Florestal Brasileira*, **34**(80):417–424, 2014.

[114] Hernandez-Mena Laidy E, Pécoraa AA, and Beraldob Antonio L. Slow pyrolysis of bamboo biomass: analysis of biochar properties. *Chem Eng*, **37**:115–120, 2014.

TH-3447_196103002

[115] Lin Lang-Dong, Chang Fang-Chih, Ko Chun-Han, and Wang Chieh-Ting. Bamboo-derived fuel from dendrocalamus latiflorus, phyllostachys makinoi, and phyllostachys pubescens waste. *BioResources*, **11**(4):8425–8434, 2016.

[116] Neves Daniel, Thunman Henrik, Matos Arlindo, Tarelho Luís, and Gómez-Barea Alberto. Characterization and prediction of biomass pyrolysis products. *Progress in energy and combustion Science*, **37**(5):611–630, 2011.

[117] Rusch Fernando, Wastowski Arci Dirceu, Lira de Taisa Shimosakai, Moreira Kelly Costa Cabral Salazar Ramos, and Moraes Lúcio de Danielle. Description of the component properties of species of bamboo: a review. *Biomass Conversion and Biorefinery*, **13**(3):2487–2495, 2023.

[118] Liese Walter and Tang Thi Kim Hong. Properties of the bamboo culm. *Bamboo: the plant and its uses*, **10**:227–256, 2015.

[119] Correia Viviane da Costa. *Produção e caracterização de polpa organossolve de bambu para reforço de matrizes cimentícias*. PhD thesis, Universidade de São Paulo, 2011.

[120] Wahab Razak, Mustafa Mohd Tamizi, Sudin Mahmud, Mohamed Aminuddin, Rahman Shafiqur, Samsi Hashim W, and Khalid Izyan. Extractives, holocellulose, α-cellulose, lignin and ash contents in cultivated tropical bamboo gigantochloa brang, g. levis, g. scortechinii and g. wrayi. *Current Research Journal of Biological Sciences*, **5**(6):266–272, 2013.

[121] Kerschbaumer Fernando Eduardo. Potencial energético de bambus plantados no brasil: Phyllostachys bambusoides (madake), phyllostachys nigra cv henonis (hatiku) e phyllostachys pubescens (mossô). **8**:266–272, 2014.

[122] Dam van Jan EG, Elbersen H Wolter, and Montaño Claudia M Daza. Bamboo production for industrial utilization. *Perennial grasses for bioenergy and bioproducts*, **6**:175–216, 2018.

TH-3447_196103002

[123] Ray Ashok K, Mondal S, Das Swapan K, and Ramachandrarao P. Bamboo—a functionally graded composite-correlation between microstructure and mechanical strength. *Journal of materials science*, **40**:5249–5253, 2005.

[124] Shao Zhuo-Ping, Fang Chang-Hua, Huang Sheng-Xia, and Tian Gen-Lin. Tensile properties of moso bamboo (phyllostachys pubescens) and its components with respect to its fiber-reinforced composite structure. *Wood science and technology*, **44**:655–666, 2010.

[125] Chen Hong, Yu Yan, Zhong Tuhua, Wu Yan, Li Yanjun, Wu Zhihui, and Fei Benhua. Effect of alkali treatment on microstructure and mechanical properties of individual bamboo fibers. *Cellulose*, **24**:333–347, 2017.

[126] Chen Qi, Dai Chunping, Fang Changhua, Chen Meiling, Zhang Shuqin, Liu Rong, Liu Xianmiao, and Fei Benhua. Mode i interlaminar fracture toughness behavior and mechanisms of bamboo. *Materials and Design*, **183**:108132, 2019.

[127] Chen Meiling, Ye Ling, Li Hui, Wang Ge, Chen Qi, Fang Changhua, Dai Chunping, and Fei Benhua. Flexural strength and ductility of moso bamboo. *Construction and Building Materials*, **246**:118418, 2020.

[128] Zhan Tianyi, Sun Fengze, Lyu Chao, He Qian, Xu Kang, Zhang Yaoli, Cai Liping, Huang Zhenhua, and Lyu Jianxiong. Moisture diffusion properties of graded hierarchical structure of bamboo: Longitudinal and radial variations. *Construction and Building Materials*, **259**: 119641, 2020.

[129] Azadeh Arash, Ghavami Khosrow, Junior H Savastano, Toledo Filho Romildo Dias, and Barbosa Normando Perazzo. Static flexural behavior of bamboo as a functionally graded material and the effect of heat on dynamic flexural modulus. *Journal of Building Engineering*, **34**:101949, 2021.

TH-3447_196103002

[130] Zhao Xianhui, Copenhaver Katie, Wang Lu, Korey Matthew, Gardner Douglas J, Li Kai, Lamm Meghan E, Kishore Vidya, Bhagia Samarthya, Tajvidi Mehdi, and others . Recycling of natural fiber composites: Challenges and opportunities. *Resources, Conservation and Recycling*, **177**:105962, 2022.

[131] Das Mahuya and Chakraborty Debabrata. Influence of alkali treatment on the fine structure and morphology of bamboo fibers. *Journal of Applied Polymer Science*, **102**(5):5050–5056, 2006.

[132] Das Mahuya and Chakraborty Debabrata. Evaluation of improvement of physical and mechanical properties of bamboo fibers due to alkali treatment. *Journal of applied polymer science*, **107**(1):522–527, 2008.

[133] Das Mahuya and Chakraborty Debabrata. The effect of alkalization and fiber loading on the mechanical properties of bamboo fiber composites, part 1:—polyester resin matrix. *Journal of applied polymer science*, **112**(1):489–495, 2009.

[134] Kushwaha Pradeep and Kumar Rakesh. Enhanced mechanical strength of bfrp composite using modified bamboos. *Journal of reinforced plastics and composites*, **28**(23):2851–2859, 2009.

[135] Kushwaha Pradeep K and Kumar Rakesh. Effect of silanes on mechanical properties of bamboo fiber-epoxy composites. *Journal of Reinforced Plastics and Composites*, **29**(5):718–724, 2010.

[136] Chang Fuxiang, Kwon Jin-Heon, Kim Nam-Hun, Endo Takashi, and Lee Seung-Hwan. Effect of hot-compressed water treatment of bamboo fiber on the properties of polypropylene/bamboo fiber composite. *Bioresources*, **10**(1):1366–1377, 2015.

[137] Khan Ziaullah, Yousif BF, and Islam Mainul. Fracture behaviour of bamboo fiber reinforced epoxy composites. *Composites Part B: Engineering*, **116**:186–199, 2017.

TH-3447_196103002

[138] Buson RF, Melo LFL, Oliveira MN, Rangel GAVP, and Deus EP. Physical and mechanical characterization of surface treated bamboo fibers. *Science and Technology of Materials*, **30** (2):67–73, 2018.

[139] Tong Foo Sheng, Chin Siew Choo, Mustafa Mohd Tamizi, Ong Huei Ruey, Khan Md Maksudur Rahman, Gimbun Jolius, and Doh Shu Ing. Influence of alkali treatment on physicochemical properties of malaysian bamboo fiber: A preliminary study. *Malaysian Journal of Analytical Sciences*, **22**(1):143–150, 2018.

[140] Chen Hong, Zhang Wenfu, Wang Xuehua, Wang Hankun, Wu Yan, Zhong Tuhua, and Fei Benhua. Effect of alkali treatment on wettability and thermal stability of individual bamboo fibers. *Journal of Wood Science*, **64**:398–405, 2018.

[141] Zhang Kai, Wang Fangxin, Liang Wenyan, Wang Zhenqing, Duan Zhiwei, and Yang Bin. Thermal and mechanical properties of bamboo fiber reinforced epoxy composites. *Polymers*, **10**(6):608, 2018.

[142] Chen Hong, Wu Jieyu, Shi Jiangjing, Zhang Wenfu, and Wang Hankun. Effect of alkali treatment on microstructure and thermal stability of parenchyma cell compared with bamboo fiber. *Industrial Crops and Products*, **164**:113380, 2021.

[143] Wu Jieyu, Zhong Tuhua, Zou Yanping, Li Jingjing, Zhao Wenjuan, and Chen Hong. Microstructure, chemical composition and thermal stability of alkali-treated bamboo fibers and parenchyma cells: effects of treatment time and temperature. *Cellulose*, **30**(3):1911–1925, 2023.

[144] Radzi AM, Zaki Sheikh Ahmad, Hassan Mohamad Zaki, Ilyas RA, Jamaludin Khairur Rijal, Daud Mohd Yusof Md, and Aziz Sa'ardin Abd. Bamboo-fiber-reinforced thermoset and thermoplastic polymer composites: A review of properties, fabrication, and potential applications. *Polymers*, **14**(7):1387, 2022.

TH-3447_196103002

[145] Glenn Howard Emmitt. *Bamboo reinforcement in portland cement concrete*. Engineering Experiment Station, 1950.

[146] Mehra SR, Uppal HL, and Chadda LR. Some preliminary investigations in the use of bamboo for reinforcing concrete. *Indian Concrete Journal*, **25**(1):20–21, 1951.

[147] Fang HY and Mehta HC. Sulfur-sand treated bamboo rod for reinforcing structural concrete. ACS Publications, 1978.

[148] Guthrie Bernard M and Torley Robert B. Composite materials made from plant fibers bonded with portland cement and method of producing same, September 27 1983. US Patent 4,406,703.

[149] Mansur MA and Aziz MA. Study of bamboo-mesh reinforced cement composites. *International Journal of Cement composites and lightweight concrete*, **5**(3):165–171, 1983.

[150] Chen Xiaoya, Guo Qipeng, and Mi Yongli. Bamboo fiber-reinforced polypropylene composites: A study of the mechanical properties. *Journal of applied polymer science*, **69**(10): 1891–1899, 1998.

[151] Mi Yongli, Chen Xiaoya, and Guo Qipeng. Bamboo fiber-reinforced polypropylene composites: Crystallization and interfacial morphology. *Journal of applied polymer science*, **64**(7): 1267–1273, 1997.

[152] Rajulu A Varada, Baksh S Allah, Reddy G Ramachandra, and Chary K Narasimha. Chemical resistance and tensile properties of short bamboo fiber reinforced epoxy composites. *Journal of reinforced plastics and composites*, **17**(17):1507–1511, 1998.

[153] Rajulu A Varada, Chary K Narasimha, Reddy G Ramachandra, and Meng YZ. Void content, density and weight reduction studies on short bamboo fiber–epoxy composites. *Journal of Reinforced Plastics and Composites*, **23**(2):127–130, 2004.

TH-3447_196103002

[154] Varada Rajulu A, Narasimha Chary K, Ramachandra Reddy G, and Meng YZ. Void content, density and weight reduction studies on short bamboo fiber-epoxy composites. *Journal of reinforced plastics and composites*, **23**(2):127–130, 2004.

[155] Saxena Mohini and Gowri V Sorna. Studies on bamboo polymer composites with polyester amide polyol as interfacial agent. *Polymer composites*, **24**(3):428–436, 2003.

[156] Das Mahuya and Chakraborty Debabrata. Effects of alkalization and fiber loading on the mechanical properties and morphology of bamboo fiber composites. ii. resol matrix. *Journal of applied polymer science*, **112**(1):447–453, 2009.

[157] Krishnaprasad R, Veena NR, Maria Hanna J, Rajan Rathish, Skrifvars Mikael, and Joseph Kuruvilla. Mechanical and thermal properties of bamboo microfibril reinforced polyhydroxybutyrate biocomposites. *Journal of Polymers and the Environment*, **17**:109–114, 2009.

[158] Gupta Anu. Synthesis, chemical resistance, and water absorption of bamboo fiber reinforced epoxy composites. *Polymer composites*, **37**(1):141–145, 2016.

[159] Kumari Sanju, Kumar Ritesh, Rai Bhuvneshwar, and Kumar Gulshan. Effect of fiber content on thermal and mechanical properties of euphorbia coagulum modified polyester and bamboo fiber composite. *Materials Research Express*, **6**(12):125341, 2019.

[160] Wang Hui, Chang Rui, Sheng Kui-chuan, Adl Mehrdad, and Qian Xiang-qun. Impact response of bamboo-plastic composites with the properties of bamboo and polyvinylchloride (pvc). *Journal of Bionic Engineering*, **5**(1):28–33, 2008.

[161] Phuong Nguyen Tri, Sollogoub Cyrille, and Guinault Alain. Relationship between fiber chemical treatment and properties of recycled pp/bamboo fiber composites. *Journal of Reinforced Plastics and Composites*, **29**(21):3244–3256, 2010.

[162] Hung Ke-Chang, Chen Yong-Long, and Wu Jyh-Horng. Natural weathering properties of

TH-3447_196103002

acetylated bamboo plastic composites. *Polymer Degradation and Stability*, **97**(9):1680–1685, 2012.

[163] Wang Chuanbao and Ying Sanjiu. A novel strategy for the preparation of bamboo fiber reinforced polypropylene composites. *Fibers and Polymers*, **15**:117–125, 2014.

[164] Zhu Rongxian, Zhang Yahui, and Yu Wenji. Outdoor exposure tests of bamboo-fiber reinforced composite: evaluation of the physical and mechanical properties after two years. *European Journal of Wood and Wood Products*, **73**:275–278, 2015.

[165] Xie Jiulong, Qi Jinqiu, Hu Tingxing, De Hoop Cornelis F, Hse Chung Yun, and Shupe Todd F. Effect of fabricated density and bamboo species on physical–mechanical properties of bamboo fiber bundle reinforced composites. *Journal of materials science*, **51**:7480–7490, 2016.

[166] Chunhong Wang, Shengkai Liu, and Zhanglong Ye. Mechanical, hygrothermal ageing and moisture absorption properties of bamboo fibers reinforced with polypropylene composites. *Journal of Reinforced Plastics and Composites*, **35**(13):1062–1074, 2016.

[167] Huang Jyun-Kai and Young Wen-Bin. The mechanical, hygral, and interfacial strength of continuous bamboo fiber reinforced epoxy composites. *Composites Part B: Engineering*, **166**: 272–283, 2019.

[168] Rao Fei, Ji Yaohui, Li Neng, Zhang Yahui, Chen Yuhe, and Yu Wenji. Outdoor bamboo-fiber-reinforced composite: Influence of resin content on water resistance and mechanical properties. *Construction and Building Materials*, **261**:120022, 2020.

[169] Wang Yunfei, Zou Miao, Gao Kezheng, Guo Wenjing, Wang Ge, and Tang Qiheng. Effects of surface modification on the physical, mechanical, and thermal properties of bamboo-polypropylene composites. *BioResources*, **15**(3):6230–6243, 2020.

[170] Kim Hyojin, Okubo Kazuya, Fujii Toru, and Takemura Kenichi. Influence of fiber extraction

TH-3447_196103002

and surface modification on mechanical properties of green composites with bamboo fiber. *Journal of Adhesion Science and Technology*, **27**(12):1348–1358, 2013.

[171] Wang Cuicui, Xian Yu, Cheng Haitao, Li Wenyan, and Zhang Shuangbao. Tensile properties of bamboo fiber-reinforced polypropylene composites modified by impregnation with calcium carbonate nanoparticles. *BioResources*, **10**(4):6783–6796, 2015.

[172] Wang Cuicui, Wang Shuo, Cheng Haitao, Xian Yu, and Zhang Shuangbao. Mechanical properties and prediction for nanocalcium carbonate-treated bamboo fiber/high-density polyethylene composites. *Journal of Materials Science*, **52**:11482–11495, 2017.

[173] Ma Hongwei and Whan Joo Chang. Influence of surface treatments on structural and mechanical properties of bamboo fiber-reinforced poly (lactic acid) biocomposites. *Journal of composite materials*, **45**(23):2455–2463, 2011.

[174] Chin Siew Choo, Tee Kong Fah, Tong Foo Sheng, Ong Huei Ruey, and Gimbun Jolius. Thermal and mechanical properties of bamboo fiber reinforced composites. *Materials Today Communications*, **23**:100876, 2020.

[175] Porras Alicia and Maranon Alejandro. Development and characterization of a laminate composite material from polylactic acid (pla) and woven bamboo fabric. *Composites Part B: Engineering*, **43**(7):2782–2788, 2012.

[176] Sánchez Martha L, Morales Luz Y, and Caicedo Juan D. Physical and mechanical properties of agglomerated panels made from bamboo fiber and vegetable resin. *Construction and Building Materials*, **156**:330–339, 2017.

[177] Lima Fajardo Cabrera de Lety del Pilar, Santana Ruth Marlene Campomanes, and Chamorro Rodríguez Cristian David. Influence of coupling agent in mechanical, physical and thermal properties of polypropylene/bamboo fiber composites: under natural outdoor aging. *Polymers*, **12**(4):929, 2020.

TH-3447_196103002

[178] Inácio André LN, Nonato Renato C, and Bonse Baltus C. Mechanical and thermal behavior of aged composites of recycled pp/epdm/talc reinforced with bamboo fiber. *Polymer Testing*, **72**:357–363, 2018.

[179] Akindapo JO, Adeleke SA, and Orueri DU. Development of bamboo fiber and polyester composite for production of protective shield. *Nigerian Journal of Engineering Science and Technology Research*, **9**(2):222–242, 2023.

[180] Mebratie Berihun Abebaw, Ayele Bekalu Sintayehu, and Meku Addisu Alamirew. Investigating the tensile and flexural strength of sunflower oil treated ethiopian highland bamboo fibre reinforced polyester composites. *Advances in Bamboo Science*, **3**:100021, 2023.

[181] Daramola OO, Akinwekomi AD, Adediran AA, Akindote-White O, and Sadiku ER. Mechanical performance and water uptake behaviour of treated bamboo fibre-reinforced high-density polyethylene composites. *Heliyon*, **5**(7), 2019.

[182] Jiang Liuyun, Li Ye, Xiong Chengdong, and Su Shengpei. Preparation and characterization of a novel degradable nano-hydroxyapatite/poly (lactic-co-glycolic) composite reinforced with bamboo fiber. *Materials Science and Engineering: C*, **75**:1014–1018, 2017.

[183] Wang Fang, Yang Mengqing, Zhou Shujue, Ran Siyan, and Zhang Junqian. Effect of fiber volume fraction on the thermal and mechanical behavior of polylactide-based composites incorporating bamboo fibers. *Journal of Applied Polymer Science*, **135**(15):46148, 2018.

[184] Wang Fang, Zhou Shujue, Li Lu, and Zhang Xiaoping. Changes in the morphological–mechanical properties and thermal stability of bamboo fibers during the processing of alkaline treatment. *Polymer Composites*, **39**(S3):E1421–E1428, 2018.

[185] Yang Mengqing, Wang Fang, Zhou Shujue, Lu Zhisong, Ran Siyan, Li Lu, and Shao Jiaxing. Thermal and mechanical performance of unidirectional composites from bamboo fibers with varying volume fractions. *Polymer Composites*, **40**(10):3929–3937, 2019.

TH-3447_196103002

[186] Long Haibo, Wu Zhiqiang, Dong Qianqian, Shen Yuting, Zhou Wuyi, Luo Ying, Zhang Chaoqun, and Dong Xianming. Mechanical and thermal properties of bamboo fiber reinforced polypropylene/polylactic acid composites for 3d printing. *Polymer Engineering and Science*, **59**(s2):E247–E260, 2019.

[187] Long Haibo, Wu Zhiqiang, Dong Qianqian, Shen Yuting, Zhou Wuyi, Luo Ying, Zhang Chaoqun, and Dong Xianming. Effect of polyethylene glycol on mechanical properties of bamboo fiber-reinforced polylactic acid composites. *Journal of Applied Polymer Science*, **136**(26):47709, 2019.

[188] Yang Feiwen, Long Haibo, Xie Baojun, Zhou Wuyi, Luo Ying, Zhang Chaoqun, and Dong Xianming. Mechanical and biodegradation properties of bamboo fiber-reinforced starch/polypropylene biodegradable composites. *Journal of Applied Polymer Science*, **137** (20):48694, 2020.

[189] Zindani Divya, Kumar Santosh, Maity Saikat Ranjan, and Bhowmik Sumit. Punica granatum fibers as potential reinforcement of composite structures. *Fibers and Polymers*, **21**:1535–1549, 2020.

[190] Cortat Lucas Ornellas, Zanini Noelle C, Barbosa Rennan FS, Souza de Alana G, Rosa Derval S, and Mulinari Daniella R. A sustainable perspective for macadamia nutshell residues revalorization by green composites development. *Journal of Polymers and the Environment*, **29**:3210–3226, 2021.

[191] Loganathan Tamil Moli, Sultan Mohamed Thariq Hameed, Ahsan Qumrul, Shah Ain Umaira Md, Jawaid Mohammad, Talib Abd Rahim Abu, and Basri Adi Azriff. Physico-mechanical and flammability properties of cyrtostachys renda fibers reinforced phenolic resin bio-composites. *Journal of Polymers and the Environment*, **29**:3703–3720, 2021.

[192] Kumar Santosh, Saha Abir, and Bhowmik Sumit. Accelerated weathering effects on mechan-

TH-3447_196103002

ical, thermal and viscoelastic properties of kenaf/pineapple biocomposite laminates for load bearing structural applications. *Journal of Applied Polymer Science*, **139**(2):51465, 2022.

[193] Thwe Moe Moe and Liao Kin. Durability of bamboo-glass fiber reinforced polymer matrix hybrid composites. *Composites science and technology*, **63**(3-4):375–387, 2003.

[194] Han G, Lei Y, Wu Q, Kojima Y, and Suzuki S. Bamboo–fiber filled high density polyethylene composites: effect of coupling treatment and nanoclay. *Journal of Polymers and the Environment*, **16**:123–130, 2008.

[195] Okubo Kazuya, Fujii Toru, and Thostenson Erik T. Multi-scale hybrid biocomposite: processing and mechanical characterization of bamboo fiber reinforced pla with microfibrillated cellulose. *Composites Part A: Applied Science and Manufacturing*, **40**(4):469–475, 2009.

[196] Wang Cuicui, Xian Yu, Smith Lee M, Wang Ge, Cheng Haitao, and Zhang Shuangbao. Interfacial properties of bamboo fiber-reinforced high-density polyethylene composites by different methods for adding nano calcium carbonate. *Polymers*, **9**(11):587, 2017.

[197] Chee Siew Sand, Jawaid Mohammad, Sultan MTH, Alothman Othman Y, and Abdullah Luqman Chuah. Evaluation of the hybridization effect on the thermal and thermo-oxidative stability of bamboo/kenaf/epoxy hybrid composites. *Journal of Thermal Analysis and Calorimetry*, **137**:55–63, 2019.

[198] Wang Qianting, Zhang Yu, Liang Weikang, Wang Jianjie, and Chen Youxin. Improved mechanical properties of the graphene oxide modified bamboo-fiber-reinforced polypropylene composites. *Polymer Composites*, **41**(9):3615–3626, 2020.

[199] Gouda Krushna, Bhowmik Sumit, and Das Biplab. Synergetic effect of micro-bamboo filler and graphene nanoplatelets on thermomechanical properties of epoxy-based hybrid composite. *JOM*, **72**:4466–4476, 2020.

TH-3447_196103002

[200] Gupta Anu. Effect of industrial waste on chemical and water absorption of bamboo fiber reinforced composites. *Silicon*, **12**(1):139–146, 2020.

[201] Adediran Adeolu A, Akinwande Abayomi A, Balogun Oluwatosin A, Olasoju OS, and Adesina Olanrewaju S. Experimental evaluation of bamboo fiber/particulate coconut shell hybrid pvc composite. *Scientific reports*, **11**(1):5465, 2021.

[202] Ramu S, Senthilkumar N, Rajendran Saravanan, Deepanraj B, and Abdeta Dereje Bayisa. Physical and mechanical characterization of bamboo fiber/groundnut shell/copper particle/mwcnt-filled epoxy hybrid polymer nanocomposites. *Journal of Nanomaterials*, **2022**, 2022.

[203] Ramu S, Senthilkumar N, Rajendran Saravanan, Deepanraj B, and Paramasivam Prabhu. Thermal conductivity and mechanical characterization of bamboo fiber and rice husk/mwcnt filler epoxy hybrid composite. *Journal of Nanomaterials*, **2022**, 2022.

[204] Sarmin Siti Noorbaini, Jawaid Mohammad, Mahmoud Mohamed H, Saba Naheed, Fouad Hassan, Alothman Othman Y, and Santulli Carlo. Mechanical and physical properties analysis of olive biomass and bamboo reinforced epoxy-based hybrid composites. *Biomass Conversion and Biorefinery*, **6**:1–11, 2022.

[205] S. Sharar Alam Abu Shufian M. Merajul Haque Mohammad Rejaul Haque Mahbub Hasan M. A. Gafur, Md. Rezwan Munshi and Rahman Fazlar. Influence of alkalisation and eggshell particles on mechanical, thermal and physical properties of rattan-bamboo fibre reinforced hybrid polyester laminated composite. *Advances in Materials and Processing Technologies*, **0**(0):1–20, 2022.

[206] Kumar Roopesh, Ganguly Abhijeet, and Purohit Rajesh. Optimization of mechanical properties of bamboo fiber reinforced epoxy hybrid nano composites by response surface methodology. *International Journal on Interactive Design and Manufacturing (IJIDeM)*, **53**.

TH-3447_196103002

[207] Chakkour Mouad, Ould Moussa Mohamed, Khay Ismail, Balli Mohamed, and Ben Zineb Tarak. Effects of moist ageing on composites of bamboo fiber and montmorillonite/eggshell powder. *Cellulose*, **30**(10):6349–6363, 2023.

[208] Rocky Bahrum Prang and Thompson Amanda J. Production of natural bamboo fibers-1: Experimental approaches to different processes and analyses. *The Journal of the Textile Institute*, **109**(10):1381–1391, 2018.

[209] Zhao Xiaoyu, Tu Wenqiong, Chen Qiang, and Wang Guannan. Progressive modeling of transverse thermal conductivity of unidirectional natural fiber composites. *International Journal of Thermal Sciences*, **162**:106782, 2021.

[210] Bakari Ramadhani, Kivevele Thomas, Masawa Salma Maneno, Huang Xiao, and Jande Yusufu AC. Assessment of rice husk biomass from different agro-ecological zones of tanzania for biofuels feasibility via supercritical water gasification. *Biomass and Bioenergy*, **173**:106771, 2023.

[211] Sadiku Nusirat A, Oluyege Amos O, and Sadiku Isiaka B. Analysis of the calorific and fuel value index of bamboo as a source of renewable biomass feedstock for energy generation in nigeria. *Lignocellulose*, **5**(1):34–49, 2016.

[212] Li Shiguang, Xu Shaoping, Liu Shuqin, Yang Chen, and Lu Qinghua. Fast pyrolysis of biomass in free-fall reactor for hydrogen-rich gas. *Fuel Processing Technology*, **85**(8-10):1201–1211, 2004.

[213] Varma Anil Kumar and Mondal Prasenjit. Physicochemical characterization and pyrolysis kinetic study of sugarcane bagasse using thermogravimetric analysis. *Journal of Energy Resources Technology*, **138**(5):052205, 2016.

[214] Maache Mabrouk, Bezazi Abderrezak, Amroune Salah, Scarpa Fabrizio, and Dufresne Alain.

TH-3447_196103002

Characterization of a novel natural cellulosic fiber from juncus effusus l. *Carbohydrate polymers*, **171**:163–172, 2017.

[215] Kumar Santosh and Saha Abir. Graphene nanoplatelets/organic wood dust hybrid composites: physical, mechanical and thermal characterization. *Iranian Polymer Journal*, **30**(9): 935–951, 2021.

[216] Kumar Rahul, Kumar Kaushik, Bhowmik Sumit, and Sarkhel Gautam. Tailoring the performance of bamboo filler reinforced epoxy composite: insights into fracture properties and fracture mechanism. *Journal of Polymer Research*, **26**:1–15, 2019.

[217] Saha Abir, Kumar Santosh, Zindani Divya, and Bhowmik Sumit. Micro-mechanical analysis of the pineapple-reinforced polymeric composite by the inclusion of pineapple leaf particulates. *Proceedings of the Institution of Mechanical Engineers, Part L: Journal of Materials: Design and Applications*, **235**(5):1112–1127, 2021.

[218] Hu Min, Wang Chunhong, Lu Chao, Anuar Noor Intan Saffinaz, Yousfani Sheraz Hussain Siddique, Jing Miaolei, Chen Zhen, Zakaria Sarani, and Zuo Hengfeng. Investigation on the classified extraction of the bamboo fiber and its properties. *Journal of Natural Fibers*, **17** (12):1798–1808, 2020.

[219] Aisyah HA, Paridah MT, Sapuan SM, Ilyas RA, Khalina A, Nurazzi NM, Lee SH, and Lee CH. A comprehensive review on advanced sustainable woven natural fibre polymer composites. *Polymers*, **13**(3):471, 2021.

[220] Kumar Santosh and Saha Abir. Effects of stacking sequence of pineapple leaf-flax reinforced hybrid composite laminates on mechanical characterization and moisture resistant properties. *Proceedings of the Institution of Mechanical Engineers, Part C: Journal of Mechanical Engineering Science*, **236**(3):1733–1750, 2022.

TH-3447_196103002

[221] Saha Abir, Kumar Santosh, and Kumar Avinash. Influence of pineapple leaf particulate on mechanical, thermal and biodegradation characteristics of pineapple leaf fiber reinforced polymer composite. *Journal of Polymer Research*, **28**:1–23, 2021.

[222] Rao Jiuping, Bao Lingxiang, Wang Baowen, Fan Mizi, and Feo Luciano. Plasma surface modification and bonding enhancement for bamboo composites. *Composites Part B: Engineering*, **138**:157–167, 2018.

[223] Sánchez ML, Aperador WA, and Capote G. Influence of the delignification process on the properties of panels made with guadua fibers and plant resin. *Industrial Crops and Products*, **125**:33–40, 2018.

[224] Rasheed Masrat, Jawaid Mohammad, Karim Zoheb, and Abdullah Luqman Chuah. Morphological, physiochemical and thermal properties of microcrystalline cellulose (mcc) extracted from bamboo fiber. *Molecules*, **25**(12):2824, 2020.

[225] Chee Siew Sand, Jawaid Mohammad, Sultan MTH, Alothman Othman Y, and Abdullah Luqman Chuah. Thermomechanical and dynamic mechanical properties of bamboo/woven kenaf mat reinforced epoxy hybrid composites. *Composites Part B: Engineering*, **163**:165–174, 2019.

[226] Vinod A, Sanjay MR, Siengchin Suchart, and Fischer Steffen. Fully bio-based agro-waste soy stem fiber reinforced bio-epoxy composites for lightweight structural applications: influence of surface modification techniques. *Construction and Building Materials*, **303**:124509, 2021.

[227] Benhamou Anass Ait, Kassab Zineb, Boussetta Abdelghani, Salim Mohamed Hamid, Ablouh El-Houssaine, Nadifiyine Mehdi, Moubarik Amine, El Achaby Mounir, and others . Beneficiation of cactus fruit waste seeds for the production of cellulose nanostructures: extraction and properties. *International Journal of Biological Macromolecules*, **203**:302–311, 2022.

TH-3447_196103002

[228] Vijay R, Singaravelu D Lenin, Vinod A, Sanjay MR, Siengchin Suchart, Jawaid Mohammad, Khan Anish, and Parameswaranpillai Jyotishkumar. Characterization of raw and alkali treated new natural cellulosic fibers from tridax procumbens. *International journal of biological macromolecules*, **125**:99–108, 2019.

[229] Kalia Susheel, Kaith BS, and Kaur Inderjeet. *Cellulose fibers: bio-and nano-polymer composites: green chemistry and technology*. Springer Science and Business Media, 2011.

[230] Basu Gautam, Mishra Leena, and Samanta Ashis Kumar. Investigation of structure and property of indian cocos nucifera l. fibre. *Journal of The Institution of Engineers (India): Series E*, **98**:135–140, 2017.

[231] Behazin Ehsan, Misra Manjusri, and Mohanty Amar K. Sustainable biocarbon from pyrolyzed perennial grasses and their effects on impact modified polypropylene biocomposites. *Composites Part B: Engineering*, **118**:116–124, 2017.

[232] Belaadi Ahmed, Bezazi Abderrezak, Bourchak Mostefa, Scarpa Fabrizio, and Zhu Chenchen. Thermochemical and statistical mechanical properties of natural sisal fibres. *Composites Part B: Engineering*, **67**:481–489, 2014.

[233] Amroune Salah, Bezazi Abderrezak, Dufresne Alain, Scarpa Fabrizio, and Imad Abdellatif. Investigation of the date palm fiber for green composites reinforcement: thermo-physical and mechanical properties of the fiber. *Journal of Natural Fibers*, **18**(5):717–734, 2021.

[234] Zhang Xiaoping, Wang Fang, and Keer Leon M. Influence of surface modification on the microstructure and thermo-mechanical properties of bamboo fibers. *Materials*, **8**(10):6597–6608, 2015.

[235] Devireddy Siva Bhaskara Rao and Biswas Sandhyarani. Physical and thermal properties of unidirectional banana–jute hybrid fiber-reinforced epoxy composites. *Journal of Reinforced Plastics and Composites*, **35**(15):1157–1172, 2016.

TH-3447_196103002

[236] Bollino Flavia, Giannella Venanzio, Armentani Enrico, and Sepe Raffaele. Mechanical behavior of chemically-treated hemp fibers reinforced composites subjected to moisture absorption. *Journal of Materials Research and Technology*, **22**:762–775, 2023.

[237] Mohammed Mohammed, Jawad Anwar Ja'afar Mohamad, Mohammed Aeshah M, Oleiwi Jawad K, Adam Tijjani, Osman Azlin F, Dahham Omar S, Betar Bashir O, Gopinath Subash CB, and Jaafar Mustafa. Challenges and advancement in water absorption of natural fiber-reinforced polymer composites. *Polymer Testing*, **124**:108083, 2023.

[238] Mahalingam Jayaraj. Mechanical, thermal, and water absorption properties of hybrid short coconut tree primary flower leaf stalk fiber/glass fiber-reinforced unsaturated polyester composites for biomedical applications. *Biomass Conversion and Biorefinery*, **14**(6):7543–7554, 2024.

[239] Balaji A, Kannan S, Purushothaman R, Mohanakannan S, Maideen A Haja, Swaminathan J, Karthikeyan B, and Premkumar P. Banana fiber and particle-reinforced epoxy biocomposites: mechanical, water absorption, and thermal properties investigation. *Biomass Conversion and Biorefinery*, **14**(6):7835–7845, 2024.

[240] Manickam Tamilselvan, Iyyadurai Jenish, Jaganathan Maniraj, Babuchellam Ashokkumar, Mayakrishnan Muthukrishnan, and Arockiasamy Felix Sahayaraj. Effect of stacking sequence on mechanical, water absorption, and biodegradable properties of novel hybrid composites for structural applications. *International Polymer Processing*, **38**(1):88–96, 2023.

[241] Kumar Avinash, Saha Abir, and Kumar Santosh. Structural analysis of sol-gel derived tio 2 nanoparticles: a critical impact of tio 2 nanoparticles on thermo-mechanical mechanism of glass fiber polymer composites. *Journal of Polymer Research*, **28**:1–16, 2021.

[242] Seki Yoldas, Sarikanat Mehmet, Sever Kutlay, and Durmuşkahya Cenk. Extraction and prop-

TH-3447_196103002

erties of ferula communis (chakshir) fibers as novel reinforcement for composites materials. *Composites Part B: Engineering*, **44**(1):517–523, 2013.

[243] Nurazzi NM, Asyraf MRM, Rayung M, Norrrahim MNF, Shazleen SS, Rani MSA, Shafi AR, Aisyah HA, Radzi MHM, Sabaruddin FA, and others . Thermogravimetric analysis properties of cellulosic natural fiber polymer composites: A review on influence of chemical treatments. *Polymers*, **13**(16):2710, 2021.

[244] Saw Sudhir Kumar, Akhtar Khurshid, Yadav Narendra, and Singh Ashwini Kumar. Hybrid composites made from jute/coir fibers: Water absorption, thickness swelling, density, morphology, and mechanical properties. *Journal of Natural Fibers*, **11**(1):39–53, 2014.

[245] Moshi A Arul Marcel, Ravindran D, Bharathi SR Sundara, Indran S, Saravanakumar SS, and Liu Yucheng. Characterization of a new cellulosic natural fiber extracted from the root of ficus religiosa tree. *International Journal of Biological Macromolecules*, **142**:212–221, 2020.

[246] Tomczak Fábio, Sydenstricker Thais Helena Demétrio, and Satyanarayana Kestur Gundappa. Studies on lignocellulosic fibers of brazil. part ii: Morphology and properties of brazilian coconut fibers. *Composites Part A: Applied Science and Manufacturing*, **38**(7):1710–1721, 2007.

[247] Hajiha Hamideh, Sain Mohini, and Mei Lucia H. Modification and characterization of hemp and sisal fibers. *Journal of Natural Fibers*, **11**(2):144–168, 2014.

[248] Abbas Al-Ghazali Noor, Aziz Farah Nora Aznieta Abdul, Abdan Khalina, Mohd Nasir Noor Azline, and Norizan Mohd Nurazzi. Kenaf fibre reinforced cementitious composites. *Fibers*, **10**(1):3, 2022.

[249] Kathirselvam M, Kumaravel A, Arthanarieswaran VP, and Saravanakumar SS. Isolation and characterization of cellulose fibers from thespesia populnea barks: A study on physicochemical

TH-3447_196103002

and structural properties. *International Journal of Biological Macromolecules*, **129**:396–406, 2019.

[250] Balaji AN and Nagarajan KJ. Characterization of alkali treated and untreated new cellulosic fiber from saharan aloe vera cactus leaves. *Carbohydrate Polymers*, **174**:200–208, 2017.

[251] Li Rongji, Fei Jianming, Cai Yurong, Li Yufeng, Feng Jianqin, and Yao Juming. Cellulose whiskers extracted from mulberry: A novel biomass production. *Carbohydrate polymers*, **76** (1):94–99, 2009.

[252] P. Manimaran P. Senthamaraikannan Mohammad Jawaid S. S. Saravanakumar, M. R. Sanjay and George Raji. Synthesis and characterization of cellulosic fiber from red banana peduncle as reinforcement for potential applications. *Journal of Natural Fibers*, **16**(5):768–780, 2019.

[253] Jebadurai S Garette, Raj R Edwin, Sreenivasan VS, and Binoj JS. Comprehensive characterization of natural cellulosic fiber from coccinia grandis stem. *Carbohydrate polymers*, **207**: 675–683, 2019.

[254] P. Manimaran S.S. Saravanakumar V.P. Arthanarieswaran, M. Prithiviraj and Senthamaraikannan P. Physicochemical, tensile, and thermal characterization of new natural cellulosic fibers from the stems of sida cordifolia. *Journal of Natural Fibers*, **15**(6):860–869, 2018.

[255] Shanmugasundaram N, Rajendran I, and Ramkumar T. Characterization of untreated and alkali treated new cellulosic fiber from an areca palm leaf stalk as potential reinforcement in polymer composites. *Carbohydrate Polymers*, **195**:566–575, 2018.

[256] Ganapathy T, Sathiskumar R, Senthamaraikannan P, Saravanakumar SS, and Khan Anish. Characterization of raw and alkali treated new natural cellulosic fibres extracted from the aerial roots of banyan tree. *International Journal of Biological Macromolecules*, **138**:573–581, 2019.

TH-3447_196103002

[257] Kumar Rahul, Kumar Kaushik, and Bhowmik Sumit. Assessment and response of treated cocos nucifera reinforced toughened epoxy composite towards fracture and viscoelastic properties. *Journal of Polymers and the Environment*, **26**:2522–2535, 2018.

[258] Kinloch AJ, Taylor AC, Techapaitoon M, Teo WS, and Sprenger S. Tough, natural-fibre composites based upon epoxy matrices. *Journal of materials science*, **50**:6947–6960, 2015.

[259] Harzallah Omar, Benzina H, and Drean Jean-Yves. Physical and mechanical properties of cotton fibers: Single-fiber failure. *Textile Research Journal*, **80**(11):1093–1102, 2010.

[260] Chen Xiaohan, Wang Xianke, Luo Xun, Chen Lin, Li Yuquan, Xu Jiarui, Liu Zengqian, Dai Chunping, Miao Hu, and Liu Huanrong. Bamboo as a naturally-optimized fiber-reinforced composite: Interfacial mechanical properties and failure mechanisms. *Composites Part B: Engineering*, **279**:111458, 2024.

[261] Cai Ming, Takagi Hitoshi, Nakagaito Antonio N, Li Yan, and Waterhouse Geoffrey IN. Effect of alkali treatment on interfacial bonding in abaca fiber-reinforced composites. *Composites Part A: Applied Science and Manufacturing*, **90**:589–597, 2016.

[262] Ahmad Jawad, Zhou Zhiguang, and Deifalla Ahmed Farouk. Structural properties of concrete reinforced with bamboo fibers: a review. *Journal of Materials Research and Technology*, **24**: 844–865, 2023.

[263] Cai Ming, Takagi Hitoshi, Nakagaito Antonio N, Katoh Masahiro, Ueki Tomoyuki, Waterhouse Geoffrey IN, and Li Yan. Influence of alkali treatment on internal microstructure and tensile properties of abaca fibers. *Industrial Crops and Products*, **65**:27–35, 2015.

[264] Senthilkumar K, Ungtrakul Thitinun, Chandrasekar M, Senthil Muthu Kumar T, Rajini N, Siengchin Suchart, Pulikkalparambil Harikrishnan, Parameswaranpillai Jyotishkumar, and Ayrilmis Nadir. Performance of sisal/hemp bio-based epoxy composites under accelerated weathering. *Journal of Polymers and the Environment*, **29**:624–636, 2021.

TH-3447_196103002

[265] Liu Yanping and Hu Hong. X-ray diffraction study of bamboo fibers treated with naoh. *Fibers and Polymers*, **9**:735–739, 2008.

[266] Fang Xiaoyang, Xu Jianuo, Guo Hongwu, and Liu Yi. The effect of alkali treatment on the crystallinity, thermal stability, and surface roughness of bamboo fibers. *Fibers and Polymers*, **24**(2):505–514, 2023.

[267] Sawangrat Choncharoen, Thipchai Parichat, Kaewapai Kannikar, Jantanasakulwong Kittisak, Suhr Jonghwan, Wattanachai Pitiwat, and Rachtanapun Pornchai. Surface modification and mechanical properties improvement of bamboo fibers using dielectric barrier discharge plasma treatment. *Polymers*, **15**(7):1711, 2023.

[268] Lobregas Michaela Olisha S, Buniao Emmanuel Victor D, and Leaño Jr Julius L. Alkali-enzymatic treatment of bambusa blumeana textile fibers for natural fiber-based textile material production. *Industrial Crops and Products*, **194**:116268, 2023.

[269] Wu Jieyu, Zhong Tuhua, Zhang Wenfu, Shi Jiangjing, Fei Benhua, and Chen Hong. Comparison of colors, microstructure, chemical composition and thermal properties of bamboo fibers and parenchyma cells with heat treatment. *Journal of Wood Science*, **67**:1–11, 2021.

[270] Ren Wenting, Guo Fei, Zhu Jiawei, Cao Mengdan, Wang Hankun, and Yu Yan. A comparative study on the crystalline structure of cellulose isolated from bamboo fibers and parenchyma cells. *Cellulose*, **28**(10):5993–6005, 2021.

[271] Chen Zhenghao, Du Keke, Yin Hongnian, Zhang Dongyan, Gao Jian, Song Wei, and Zhang Shuangbao. Surface modification of bamboo fiber with dopamine associated by laccase for poly (3-hydroxylbutyrate) biocomposites. *Journal of Cleaner Production*, **389**:135996, 2023.

[272] Hu Fu, Li Lifen, Wu Zhigang, Yu Liping, Liu Baoyu, Cao Yan, and Xu Hailong. Surface characteristics of thermally modified bamboo fibers and its utilization potential for bamboo plastic composites. *Materials*, **15**(13):4481, 2022.

TH-3447_196103002

[273] Shrivastava Rahul and Parashar Vishal. Effect of alkali treatment on tensile strength of epoxy composite reinforced with coir fiber. *Polymer Bulletin*, **80**(1):541–553, 2023.

[274] George Michael, Mussone Paolo G, and Bressler David C. Modification of the cellulosic component of hemp fibers using sulfonic acid derivatives: surface and thermal characterization. *Carbohydrate polymers*, **134**:230–239, 2015.

[275] Zhuo Guangming, Zhang Xiaolin, Jin Xiao, Wang Mei, Yang Xiongnan, and Li Shaoge. Effect of different enzymatic treatment on mechanical, water absorption and thermal properties of bamboo fibers reinforced poly (hydroxybutyrate-co-valerate) biocomposites. *Journal of Polymers and the Environment*, **28**:2377–2385, 2020.

[276] Chang Boon Peng, Mohanty Amar K, and Misra Manjusri. Studies on durability of sustainable biobased composites: a review. *RSC advances*, **10**(31):17955–17999, 2020.

[277] Andrew J Jefferson and Dhakal HN. Sustainable biobased composites for advanced applications: recent trends and future opportunities–a critical review. *Composites Part C: Open Access*, **7**:100220, 2022.

[278] Maiti Saptarshi, Islam Md Rashedul, Uddin Mohammad Abbas, Afroj Shaila, Eichhorn Stephen J, and Karim Nazmul. Sustainable fiber-reinforced composites: a review. *Advanced Sustainable Systems*, **6**(11):2200258, 2022.

[279] La Mantia FP and Morreale Marco. Green composites: A brief review. *Composites Part A: Applied Science and Manufacturing*, **42**(6):579–588, 2011.

[280] Corigliano Pasqualino, Crupi Vincenzo, Bertagna Serena, and Marinò Alberto. Bio-based adhesives for wooden boatbuilding. *Journal of Marine Science and Engineering*, **9**(1):28, 2020.

[281] Tarique J, Zainudin ES, Sapuan SM, Ilyas RA, and Khalina A. Physical, mechanical, and

TH-3447_196103002

morphological performances of arrowroot (maranta arundinacea) fiber reinforced arrowroot starch biopolymer composites. *Polymers*, **14**(3):388, 2022.

[282] Sadasivuni Kishor Kumar, Saha Prosenjit, Adhikari Jaideep, Deshmukh Kalim, Ahamed M Basheer, and Cabibihan John-John. Recent advances in mechanical properties of biopolymer composites: A review. *Polymer Composites*, **41**(1):32–59, 2020.

[283] Hristov VN, Lach R, and Grellmann W. Impact fracture behavior of modified polypropylene/wood fiber composites. *Polymer testing*, **23**(5):581–589, 2004.

[284] Coldea Andrea, Fischer Jens, Swain Michael V, and Thiel Norbert. Damage tolerance of indirect restorative materials (including picn) after simulated bur adjustments. *Dental materials*, **31**(6):684–694, 2015.

[285] Kumar Santosh, Zindani Divya, and Bhowmik Sumit. Investigation of mechanical and viscoelastic properties of flax-and ramie-reinforced green composites for orthopedic implants. *Journal of Materials Engineering and Performance*, **29**:3161–3171, 2020.

[286] Dash Chinmayee and Bisoyi Dillip Kumar. Study on dielectric and charge transport behavior in alkali-treated randomly oriented sunn hemp fiber reinforced epoxy composite in connection with the microstructure of fiber. *Journal of Natural Fibers*, **19**(13):6214–6229, 2022.

[287] Wu Chin-San, Wu Dung-Yi, and Wang Shan-Shue. Preparation and characterization of polylactic acid/bamboo fiber composites. *ACS Applied Bio Materials*, **5**(3):1038–1046, 2022.

[288] Min Hu Chao Lu Noor Intan Saffinaz Anuar Sheraz Hussain Siddique Yousfani Miaolei Jing Zhen Chen Sarani Zakaria, Chunhong Wang and Zuo Hengfeng. Investigation on the classified extraction of the bamboo fiber and its properties. *Journal of Natural Fibers*, **17**(12):1798–1808, 2020.

[289] Dash Chinmayee, Das Ramyaranjan, Sahu Deepak K, Upreti Divyansh, Patro T Umasankar,

TH-3447_196103002

and Bisoyi Dillip K. Investigation of dielectric and mechanical properties of pretreated natural sunn hemp fiber-reinforced composite in correlation with macromolecular structure of the fiber. *Biomacromolecules*, **24**(3):1329–1344, 2023.

[290] Sathiyamoorthy Margabandu and Senthilkumar Subramaniam. Mechanical, thermal, and water absorption behaviour of jute/carbon reinforced hybrid composites. *Sādhanā*, **45**(1): 278, 2020.

[291] Sekar S, Suresh Kumar S, Vigneshwaran S, and Velmurugan G. Evaluation of mechanical and water absorption behavior of natural fiber-reinforced hybrid biocomposites. *Journal of Natural Fibers*, **19**(5):1772–1782, 2022.

[292] Prabhu P, Jayabalakrishnan D, Balaji V, Bhaskar K, Maridurai T, and Prakash VR Arun. Mechanical, tribology, dielectric, thermal conductivity, and water absorption behaviour of caryota urens woven fibre-reinforced coconut husk biochar toughened wood-plastic composite. *Biomass Conversion and Biorefinery*, **14**(1):109–116, 2024.

[293] Saha Abir, Kumar Santosh, and Zindani Divya. Investigation of the effect of water absorption on thermomechanical and viscoelastic properties of flax-hemp-reinforced hybrid composite. *Polymer Composites*, **42**(9):4497–4516, 2021.

[294] Rizzarelli P. Biodegradation of green polymer composites: Laboratory procedures and standard test methods. *Materials Research Foundations*, **68**, 2020.

[295] Fleck Norman A, Deshpande Vikram S, and Ashby Michael F. Micro-architectured materials: past, present and future. *Proceedings of the Royal Society A: Mathematical, Physical and Engineering Sciences*, **466**(2121):2495–2516, 2010.

[296] Baishya Manash Jyoti, Sahariah Bikram Jyoti, Muthu Nelson, and Khanikar Prasenjit. Composite strut-plate lattice: A high-stiffness design of cellular metamaterial having excellent strength and energy absorption ability. *Materials Today Communications*, **33**:104939, 2022.

TH-3447_196103002

[297] Fiore V, Di Bella G, and Valenza A. The effect of alkaline treatment on mechanical properties of kenaf fibers and their epoxy composites. *Composites Part B: Engineering*, **68**:14–21, 2015.

[298] Kumar K Senthil, Siva I, Jeyaraj P, Jappes JT Winowlin, Amico SC, and Rajini N. Synergy of fiber length and content on free vibration and damping behavior of natural fiber reinforced polyester composite beams. *Materials and Design (1980-2015)*, **56**:379–386, 2014.

[299] Ismail Ahmad Safwan, Jawaid Mohammad, and Naveen Jesuarockiam. Void content, tensile, vibration and acoustic properties of kenaf/bamboo fiber reinforced epoxy hybrid composites. *Materials*, **12**(13):2094, 2019.

[300] Saba Naheed, Jawaid Mohammad, Alothman Othman Y, and Paridah MT. A review on dynamic mechanical properties of natural fibre reinforced polymer composites. *Construction and Building Materials*, **106**:149–159, 2016.

[301] Arvinda Pandian CK and Siddhi Jailani H. Investigation of viscoelastic attributes and vibrational characteristics of natural fabrics-incorporated hybrid laminate beams. *Polymer Bulletin*, **75**(5):1997–2014, 2018.

[302] Ramakrishnan S, Krishnamurthy K, Rajeshkumar G, and Asim M. Dynamic mechanical properties and free vibration characteristics of surface modified jute fiber/nano-clay reinforced epoxy composites. *Journal of Polymers and the Environment*, **29**:1076–1088, 2021.

[303] Chaudhary Vijay, Bajpai Pramendra Kumar, and Maheshwari Sachin. An investigation on wear and dynamic mechanical behavior of jute/hemp/flax reinforced composites and its hybrids for tribological applications. *Fibers and Polymers*, **19**:403–415, 2018.

[304] Saw Sudhir Kumar, Sarkhel Gautam, and Choudhury Arup. Dynamic mechanical analysis of randomly oriented short bagasse/coir hybrid fibre-reinforced epoxy novolac composites. *Fibers and Polymers*, **12**:506–513, 2011.

TH-3447_196103002

[305] Jawaid M, Khalil HPS Abdul, Hassan Azman, Dungani Rudi, and Hadiyane A. Effect of jute fibre loading on tensile and dynamic mechanical properties of oil palm epoxy composites. *Composites Part B: Engineering*, **45**(1):619–624, 2013.

[306] Rajeshkumar G, Devnani GL, Maran J Prakash, Sanjay MR, Siengchin Suchart, Al-Dhabi Naif Abdullah, and Ponmurugan K. Characterization of novel natural cellulosic fibers from purple bauhinia for potential reinforcement in polymer composites. *Cellulose*, **28**(9):5373–5385, 2021.

[307] Ismail Ahmad Safwan, Jawaid Mohammad, Hamid Norul Hisham, Yahaya Ridwan, Hassan Azman, and Sarmin Siti Noorbaini. Physical, structural and thermal properties of bio-phenolic/epoxy polymers blends. *Materials Today Communications*, **34**:105455, 2023.

[308] Lekrine Abdelaziz, Belaadi Ahmed, Makhlouf Azzedine, Amroune Salah, Bourchak Mostefa, Satha Hamid, and Jawaid Mohammad. Structural, thermal, mechanical and physical properties of washingtonia filifera fibres reinforced thermoplastic biocomposites. *Materials Today Communications*, **31**:103574, 2022.

[309] Komal Ujendra Kumar, Lila Manish Kumar, and Singh Inderdeep. Pla/banana fiber based sustainable biocomposites: A manufacturing perspective. *Composites Part B: Engineering*, **180**:107535, 2020.

[310] Bhuvaneswari HB and Reddy Narendra. A review on dielectric properties of biofiber-based composites. *Advanced composites and hybrid materials*, **1**:635–648, 2018.

[311] Bhuvaneswari HB, Vinayaka DL, Ilangovan Manikandan, and Reddy Narendra. Completely biodegradable banana fiber-wheat gluten composites for dielectric applications. *Journal of Materials Science: Materials in Electronics*, **28**(17):12383–12390, 2017.

[312] Lai CY, Sapuan SM, Ahmad M, Yahya N, and Dahlan KZHM. Mechanical and electrical

TH-3447_196103002

properties of coconut coir fiber-reinforced polypropylene composites. *Polymer-Plastic Technology and Engineering*, **44**(4):619–632, 2005.

[313] Dash Chinmayee, Das Asim, and Kumar Bisoyi Dillip. Influence of pretreatment on mechanical and dielectric properties of short sunn hemp fiber-reinforced polymer composite in correlation with fine structure of the fiber. *Journal of Composite Materials*, **54**(23):3313–3327, 2020.

[314] Reddy P Venkateshwar, Reddy RV Saikumar, Reddy B Veerabhadra, Krishnudu D Mohana, Prasad P Rajendra, and Rao P Srinivasa. Enhancement of the dynamic mechanical and dielectric properties of prosopis juliflora fiber-reinforced composites by fiber modification. *Journal of Natural Fibers*, **19**(13):6780–6796, 2022.

[315] Dash Chinmayee and Bisoyi Dillip Kumar. Study on dielectric and charge transport behavior in alkali-treated randomly oriented sunn hemp fiber reinforced epoxy composite in connection with the microstructure of fiber. *Journal of Natural Fibers*, **19**(13):6214–6229, 2022.

[316] Dash Chinmayee and Bisoyi Dillip Kumar. Experimental investigation of structural stabilization in sunn hemp fiber and its influence on flexural, tensile, electrical properties of reinforced composite. *Journal of Materials Science: Materials in Electronics*, **33**(16):13075–13094, 2022.

[317] Navin Chand Archana Nigrawal and Jain Deepak. Dielectric behavior of maleic anhydride grafted polypropylene (magpp) modified sisal fiber reinforced pp composites. *Journal of Natural Fibers*, **5**(3):270–288, 2008.

[318] Patra Annapurna and Bisoyi Dillip Kumar. Investigation of the electrical and mechanical properties of short sisal fiber-reinforced epoxy composite in correlation with structural parameters of the reinforced fiber. *Journal of materials science*, **46**:7206–7213, 2011.

TH-3447_196103002

[319] Triki A, Guicha M, Ben Hassen Med, Arous M, and Fakhfakh Z. Studies of dielectric relaxation in natural fibres reinforced unsaturated polyester. *Journal of materials science*, **46**: 3698–3707, 2011.

[320] Bisoyi Dillip Kumar, Oram Sujit Kumar, and Dash Chinmayee. A mechanical and dielectric study on calcium hydroxide pre-treated kapok husk-reinforced epoxy composites. *Polymer Bulletin*, **79**(7):4923–4939, 2022.

[321] Balaji N, Natrayan L, Kaliappan S, Patil Pravin P, and Sivakumar NS. Annealed peanut shell biochar as potential reinforcement for aloe vera fiber-epoxy biocomposite: mechanical, thermal conductivity, and dielectric properties. *Biomass Conversion and Biorefinery*, **14**(3): 4155–4163, 2024.

[322] Coşkun Ramazan, Yalçın Orhan, and Okutan Mustafa. Investigation of capacitors and electrical circuit elements performance of magnetic biocomposites prepared by using the hemp biomass. *Materials Chemistry and Physics*, **296**:127171, 2023.

[323] Khouaja Asma, Koubaa Ahmed, and Daly Hachmi Ben. Study of the dielectric and chemical properties of cellulose bio-based composites. *Industrial Crops and Products*, **214**:118493, 2024.

[324] Aziz Ahmad Farid, Jamail Nor Akmal Mohd, and Kamarudin Qamarul Ezani. Electric field analysis of hdpe/nr biocomposite due to moisture content condition. *Journal of Electronic Voltage and Application*, **4**(1):21–29, 2023.

[325] Wang Hong and Yang Liang. Dielectric constant, dielectric loss, conductivity, capacitance and model analysis of electronic electroactive polymers. *Polymer Testing*, **120**:107965, 2023.

[326] Chen Ruey Shan, Ab Ghani Mohd Hafizuddin, Ahmad Sahrim, Mou'ad A Tarawneh, and Gan Sinyee. Tensile, thermal degradation and water diffusion behaviour of gamma-radiation

TH-3447_196103002

induced recycled polymer blend/rice husk composites: Experimental and statistical analysis. *Composites Science and Technology*, **207**:108748, 2021.

[327] Wang Peng, Wu Hao-liang, Leung Christopher KY, and others . Hygrothermal aging effect on the water diffusion in glass fiber reinforced polymer (gfrp) composite: Experimental study and numerical simulation. *Composites Science and Technology*, **230**:109762, 2022.

[328] Mu Mulan and Vaughan Alun. Dielectric behaviours of bio-derived epoxy resins from cashew nutshell liquid. *High Voltage*, **6**(2):255–263, 2021.

[329] Azzedine Makhlouf Messaouda Boumaaza Lakhdar Mansouri Mostefa Bourchak, Ahmed Belaadi and Jawaid Mohammad. Water absorption behavior of jute fibers reinforced hdpe biocomposites: Prediction using rsm and ann modeling. *Journal of Natural Fibers*, **19**(16): 14014–14031, 2022.

[330] Karthick L, Rathinam R, Kalam Sd Abdul, Loganathan Ganesh Babu, Sabeenian RS, Joshi SK, Ramesh L, Ali H Mohammed, and Mammo Wubishet Degife. Influence of nano-/microfiller addition on mechanical and morphological performance of kenaf/glass fibre-reinforced hybrid composites. *Journal of Nanomaterials*, **2022**, 2022.

[331] Perdana Mastariyanto, Putra Meiki Eru, Akmal Akmal, Putra Hengki, Al Ikram Murfid, and Meidianda Ardhy. Characteristics of palm kernel shell/alumina/epoxy composites as motorcycle brake pad material. *Jurnal Teknik Mesin*, **13**(1):13–18, 2023.

[332] Silva Douglas Santos, Ribeiro Maurício Maia, Silva Rodrigues da Jean, Castro Corrêa de Alessandro, Costa Denis Carlos Lima, Oliveira Costa de Heictor Alves, Silva da Fernando José Aguirre Ramos, Santos dos Alessandro José Gomes, Silva da Marcelo Henrique Prado, and Fujiyama Roberto Tetsuo. Properties of flexural and impact of matrix composites polyester reinforced with short lignocellulosic fibers. *Research, Society and Development*, **11**(3):e32511326612–e32511326612, 2022.

TH-3447_196103002

[333] Sukrawan Y, Hamdani A, and Mardani SA. Effect of bamboo weight faction on mechanical properties in non-asbestos composite of motorcycle brake pad. *Materials Physics and Mechanics*, **42**(3):367–372, 2019.

[334] Hammed Samar Hazim and Albahri AS. Unlocking the potential of autism detection: integrating traditional feature selection and machine learning techniques. *Applied Data Science and Analysis*, **2023**:42–58, 2023.

[335] Talib Hiba Mohammed, Albahri AS, and Thierry OC. Fuzzy decision-making framework for sensitively prioritizing autism patients with moderate emergency level. *Applied Data Science and Analysis*, **2023**:16–41, 2023.

[336] Opricovic Serafim and Tzeng Gwo-Hshiung. Compromise solution by mcdm methods: A comparative analysis of vikor and topsis. *European journal of operational research*, **156**(2): 445–455, 2004.

[337] Mahajan Aditi, Binaz V, Singh Inderdeep, and Arora Navneet. Selection of natural fiber for sustainable composites using hybrid multi criteria decision making techniques. *Composites Part C: Open Access*, **7**:100224, 2022.

[338] Hafezalkotob Arian and Hafezalkotob Ashkan. Extended multimoora method based on shannon entropy weight for materials selection. *Journal of Industrial Engineering International*, **12**(1):1–13, 2016.

[339] Ali Ali A, Al-Attar Tareq S, and Abbas Waleed A. A statistical model to predict the strength development of geopolymer concrete based on sio2/al2o3 ratio variation. *Civil Engineering Journal*, **8**(3):454–471, 2022.

[340] Hapsari Ika Chandra, Anandya Rayhan, Hidayanto Achmad Nizar, Budi Nur Fitriah Ayuning, and Phusavat Kongkiti. Prioritizing barriers and strategies mapping in business intel-

TH-3447_196103002

ligence projects using fuzzy ahp topsis framework in developing country. *Emerging Science Journal*, **6**(2):337–355, 2022.

[341] Mahesh Vishwas and Mahesh Vinyas. Harnessing of waste rubber crumb and development of sustainable hybrid composite using kenaf (hibiscus cannabinus) for structural applications. *Journal of Natural Fibers*, **20**(1):2126423, 2023.

[342] Gairola Sandeep, Naik Tejas Pramod, Sinha Shishir, and Singh Inderdeep. Waste biomass and recycled polypropylene based jute hybrid composites for non-structural applications. *Journal of Material Cycles and Waste Management*, **25**(1):1–14, 2023.

[343] Dinesh S, Kumaran P, Mohanamurugan S, Vijay R, Singaravelu D Lenin, Vinod A, Sanjay MR, Siengchin Suchart, and Bhat K Subrahmanya. Influence of wood dust fillers on the mechanical, thermal, water absorption and biodegradation characteristics of jute fiber epoxy composites. *Journal of Polymer Research*, **27**:1–13, 2020.

[344] Liu Hu-Chen, You Jian-Xin, You Xiao-Yue, and Shan Meng-Meng. A novel approach for failure mode and effects analysis using combination weighting and fuzzy vikor method. *Applied soft computing*, **28**:579–588, 2015.

[345] Sreenivas HT, Krishnamurthy N, and Arpitha GR. A comprehensive review on light weight kenaf fiber for automobiles. *International Journal of Lightweight Materials and Manufacture*, **3**(4):328–337, 2020.

[346] Suddell Brett C and Evans William J. Natural fiber composites in automotive applications. In *Natural fibers, biopolymers, and biocomposites*, pages 253–282. CRC Press, 2005.

[347] Chandgude Swapnil and Salunkhe Sachin. In state of art: Mechanical behavior of natural fiber-based hybrid polymeric composites for application of automobile components. *Polymer Composites*, **42**(6):2678–2703, 2021.

TH-3447_196103002

[348] Behera Susanta, Mohanty JR, Nath G, and Mahanta Tapan K. Exploring properties of short randomly oriented rattan fiber reinforced epoxy composite for automotive application. *Journal of Natural Fibers*, **20**(1):2163024, 2023.

[349] Ramasubbu Rajkumar and Madasamy Sankaranarayanan. Fabrication of automobile component using hybrid natural fiber reinforced polymer composite. *Journal of Natural Fibers*, **19**(2):736–746, 2022.

[350] Prasob PA and Sasikumar M. Viscoelastic and mechanical behaviour of reduced graphene oxide and zirconium dioxide filled jute/epoxy composites at different temperature conditions. *Materials Today Communications*, **19**:252–261, 2019.

[351] Jesuarockiam Naveen, Jawaid Mohammad, Zainudin Edi Syams, Thariq Hameed Sultan Mohamed, and Yahaya Ridwan. Enhanced thermal and dynamic mechanical properties of synthetic/natural hybrid composites with graphene nanoplateletes. *Polymers*, **11**(7):1085, 2019.

[352] Md Shah Ain U, Sultan Mohamed TH, and Jawaid Mohammad. Sandwich-structured bamboo powder/glass fibre-reinforced epoxy hybrid composites–mechanical performance in static and dynamic evaluations. *Journal of Sandwich Structures and Materials*, **23**(1):47–64, 2021.

[353] Rasana N, Jayanarayanan K, Deeraj BDS, and Joseph K. The thermal degradation and dynamic mechanical properties modeling of mwcnt/glass fiber multiscale filler reinforced polypropylene composites. *Composites Science and Technology*, **169**:249–259, 2019.

[354] Zeltmann Steven Eric, Kumar BR Bharath, Doddamani Mrityunjay, and Gupta Nikhil. Prediction of strain rate sensitivity of high density polyethylene using integral transform of dynamic mechanical analysis data. *Polymer*, **101**:1–6, 2016.

[355] Li Yageng, Jahr H, Lietaert K, Pavanram P, Yilmaz A, Fockaert LI, Leeflang MA, Pouran B, Gonzalez-Garcia Y, Weinans H, and others . Additively manufactured biodegradable porous iron. *Acta biomaterialia*, **77**:380–393, 2018.

TH-3447_196103002

[356] Balaji A, Udhayasankar R, Karthikeyan B, Swaminathan J, and Purushothaman R. Mechanical and thermal characterization of bagasse fiber/coconut shell particle hybrid biocomposites reinforced with cardanol resin. *Results in Chemistry*, **2**:100056, 2020.

[357] Thiagamani Senthil Muthu Kumar, Krishnasamy Senthilkumar, Muthukumar Chandrasekar, Tengsuthiwat Jiratti, Nagarajan Rajini, Siengchin Suchart, and Ismail Sikiru O. Investigation into mechanical, absorption and swelling behaviour of hemp/sisal fibre reinforced bioepoxy hybrid composites: Effects of stacking sequences. *International journal of biological macromolecules*, **140**:637–646, 2019.

[358] Vijay Chaudhary Pramendra Kumar Bajpai and Maheshwari Sachin. Studies on mechanical and morphological characterization of developed jute/hemp/flax reinforced hybrid composites for structural applications. *Journal of Natural Fibers*, **15**(1):80–97, 2018.

[359] Raman Velpuri Venkat, Kumar P Sathish, Sunagar Prashant, Bommanna K, Vezhavendhan R, Bhattacharya Sumanta, Prabhu S Venkatesa, Sasikumar Bashyam, and others . Investigation on mechanical properties of bamboo and coconut fiber with epoxy hybrid polymer composite. *Advances in Polymer Technology*, **2022**, 2022.

[360] Prabu krishnasamy S Aravindraj, G. Rajamurugan and Sudhagar P Edwin. Vibration and wear characteristics of aloevera/flax/hemp woven fiber epoxy composite reinforced with wire mesh and baso4. *Journal of Natural Fibers*, **19**(8):2885–2901, 2022.

[361] Isiaka Oluwole Oladele Samson Oluwagbenga Adelani, Michael Oluwatosin Olayinka and Borode Joseph Olatunde. Development of coconut fiber-corn cub ash hybrid reinforced polyvinyl chloride composites for shoe sole application. *Journal of Natural Fibers*, **19**(15): 11763–11776, 2022.

[362] Ashraf W, Ishak MR, Zuhri MYM, Yidris N, and Ya'Acob AM. Experimental investigation

TH-3447_196103002

on the mechanical properties of a sandwich structure made of flax/glass hybrid composite facesheet and honeycomb core. *International Journal of Polymer Science*, **2021**:1–10, 2021.

[363] Lalta Prasad Raj Vardhan Patel Anshul Yadav, Ashish Kumain and Winczek Jerzy. Physical and mechanical behavior of hemp and nettle fiber-reinforced polyester resin-based hybrid composites. *Journal of Natural Fibers*, **19**(7):2632–2647, 2022.

[364] Kumar Santosh and Saha Abir. Utilization of coconut shell biomass residue to develop sustainable biocomposites and characterize the physical, mechanical, thermal, and water absorption properties. *Biomass Conversion and Biorefinery*, **17**:1–17, 2022.

TH-3447_196103002